Novel Cys crosslinks and Trp side chain cleavages in proteins and peptides exposed to light

By

Jessica M. Bane

Submitted to the graduate degree program in Pharmaceutical Chemistry and the Graduate Faculty of the University of Kansas in partial fulfillment of the requirements for the degree of Doctor of Philosophy.

_____

Chairperson Christian Schöneich

_____

David B. Volkin

_____

Zhou (Michael) Wang

_____

Teruna J. Siahaan

_____

Heather Desaire

Date Defended: March 4, 2015

The Dissertation Committee for Jessica M. Bane

certifies that this is the approved version of the following dissertation:

Novel Cys crosslinks and Trp side chain cleavages in proteins and peptides exposed to light

_____

Chairperson Christian Schöneich

Date approved: March 4, 2015

Abstract

Protein pharmaceuticals, like monoclonal antibodies (mAbs), are sensitive to many degradation pathways, such as oxidation and photodegradation. Photostability testing provides essential information to characterize protein stability because mAbs are exposed to light during the production and storage process, which could lead to instability problems. Photostability testing has also become increasingly important to demonstrate likeness between biosimilars and original protein therapeutics. All amino acids are sensitive to oxidation, but only the aromatic amino acids and the disulfide bond are directly sensitive to light. The Trp residue is the most sensitive to light, and its photochemistry has been studied extensively, but the photochemistry involving both Trp and the disulfide bond in peptides and proteins has not been fully characterized, although the Trp residue is frequently located near disulfide bonds. To improve our understanding of the mechanisms of degradation and stability of protein pharmaceuticals, we have exposed disulfide-containing, Trp-containing, and disulfide and Trp-containing peptides, and an IgG1 molecule to light at $\lambda = 254$ nm and/or $\lambda_{max} = 305$ nm. By mass spectrometry, chemical derivation, and NMR analysis, we observed a novel Cys crosslinked product after photoirradiation, tentatively identified as isothiazole-3(2H)-one. By mass spectrometry, we observed cleavage of the Trp side chain to Gly and/or Gly hydroperoxide in IgG1 at three separate Trp residues located in both the heavy and light chains, all of which were within close proximity to a disulfide bond. We also detected the cleavage of the Trp side chain to Gly and/or Gly hydroperoxide in two model peptides. In a third model peptide, we observed the cleavage and trapping of the Trp side chain by nearby Lys and Tyr residues. The Cys crosslink and Trp cleavage products highlight the damage light exposure can have by not only inducing a significant amino acid modification, but also leading to protein aggregation or amino acid hydroperoxides that have the potential to induce additional protein oxidation.

To my family, for always believing in me.

Acknowledgements

I would not be where I am today without the love and support of my family, friends, and colleagues, prior to and during my graduate work. I have so many people to thank, but I will attempt to include them all in this brief acknowledgement section.

Firstly, I would like to thank my academic advisor, Christian Schöneich, for providing me with unsurpassed leadership and guidance. I will forever be grateful to him for the breadth of knowledge he has helped me acquire, the opportunity to present my research at scientific meetings, both nationally and internationally, and his support of my industrial internship. Through his mentorship, I have seen myself develop into a scientist with a deep desire to question the data, think critically and creatively to solve problems, and never underestimate the value of scientific discussion with colleagues.

I would also like to thank the other members of my dissertation committee: David Volkin, Michael Wang, Teruna Siahaan, and Heather Desaire. Thank you for your attendance at my review meetings and at my defense. Your comments and critiques helped me in the experimental and writing process. I would especially like to thank the readers of my dissertation, Christian, David, and Michael, for their helpful insights and suggestions.

I am extremely grateful to all the members of the Schöneich lab who have helped me set up experiments, analyze data, engage in helpful scientific discussion, and create such a thriving work environment by setting a great example of work ethic. I must first acknowledge Olivier Mozziconacci, for encouraging me even before my graduate work began by his enthusiasm, creativity, and passion for science. His vast scientific knowledge and leadership skills allowed me to get a head start on research early in my graduate work. Whenever I needed help or advice, he never hesitated, even when his workload was much greater than mine. Thanks to Christopher

Asmus for all his help in fixing instruments, electronics, and really anything that needed fixing, as it saved the rest of the lab group much time and effort. I also thank him for his friendship throughout our five years together, as we learned how to become better scientists together. I would like to thank Rupesh Bommana for helping me with experiments and for making the laboratory an easy place to work each day. A special thanks to Asha Hewarathna for always lending an ear for conversation, scientific and otherwise, and always encouraging me. I would also like to thank the rest of the members of the Schöneich lab for their support: Maria Feeney, Elena Dremina, Victor Sharov, Daniel Steinmann, Shuxia Zhou, Riccardo Torosantucci, Lin Zang, and Indira Prajapati.

I would like to thank all the Pharmaceutical Chemistry faculty for their great knowledge and support of my work and studies. I have learned more than I thought possible, and have been given many opportunities to grow as a scientist and communicator because of their efforts. I would like to thank the past and present faculty for helping make the Pharmaceutical Chemistry department so successful, and the industrial and academic network so vast and influential. I would especially like to thank Val Stella for providing me with connections for career opportunities and making my job hunt a very easy one.

A major part of my research was mass spectrometry, so I must thank the mass spectrometry researchers that helped me progress in my graduate work: Todd Williams, Nadya Galeva, and Bob Drake. Thanks to Todd Williams for helping me learn the fundamentals of mass spectrometry and providing some great stories while I was working in the mass spectrometry labs. I would like to thank Nadya Galeva for operating the FT-MS instrument and Bob Drake for maintaining the Q-tof Premier.

Thanks to the NMR experts Justin Douglas, Sarah Neuenswander, and Asokan Anbanandam for teaching and helping me run NMR experiments.

I am grateful to the Siahaan lab members who helped me learn how to use the peptide synthesizer and always provided assistance when I needed it: Paul Kiptoo, John Stewart, Barlas Buyuktimkin, Ahmed Alaofi, and Matt Behymer.

All the research and coursework I've completed would not have been possible without our funding sources. I would like to thank Amgen, Inc. and Genentech, Inc. for industrial support of our research. I would also like to thank the Department of Pharmaceutical Chemistry for awarding me the Howard Rytting Fellowship, and Dr. Siahaan and Dr. Volkin for selecting me as a trainee on the NIGMS Biotechnology Training Grant (T32GM008359).

I was fortunate enough to participate in a 6-month industrial internship at Genentech, Inc. that persuaded me to pursue a career in industry. I would like to thank the great scientists I learned from and worked with while I was in South San Francisco: Li Yi, Sreedhara Alavattam, Y. John Wang, and Vikas Sharma. I would also like to thank Mary Cromwell and Jamie Moore for their support of the project.

This acknowledgement section wouldn't be complete without thanking the wonderful Pharmaceutical Chemistry staff: Nancy Helm, Nicole Brooks, Ann Heptig, and Karen Hall. Without them, the department would not run nearly as smoothly or efficiently. Their helpful attitudes, knowledge of the department, and smiles in the hallway were always appreciated. A special thanks to Nancy Helm for making Lawrence feel like home, for always giving great advice, and for helping me plan my wedding.

There is no way I would have learned so much, worked so hard, and enjoyed it as much as I have without the assistance of my fellow graduate students. Thank you to the KU

Pharmaceutical Chemistry class of 2010 as we completed the difficult classwork by studying together. A special thanks goes to Shara Thati, Chris Kuehl, and John Stewart for their great friendship. Sushi dates, study sessions, and get-to-gethers were vital to my sanity and success while in the program. I would also like to thank some of the older graduate students who lead by great example: Jessica Creamer, Randy Logan, Josh Woods, and Barlas Buyuktimkin.

I was also fortunate enough to develop many more great friends in Lawrence: Andrew Riley, Chris Palmer, Dana Daugharthy, David Daugharthy, Eric Bane, Joseph Barlan, Mason Lantz, Angela Stoss, Jenna Lindsey, Kate Eshelman, and Sara Wenzel. I could not have completed my graduate work without their unwavering friendship. A special thanks goes to my past roommates Jenna and Kate for allowing me to vent and relax at home after work, and especially to Jenna for helping get through the roughest times in graduate school with movies, sweets, and great advice.

Lawrence also felt like home thanks to the spiritual support from Pastor Steve Koberlein and Lawrence Heights Christian Church. I would like to thank him for blessing my husband, Kevin Bane, and me with love and support during our tenure in Lawrence, and also being a part of the most special day in our lives, our wedding day.

I would sincerely like to thank my family for their unconditional love and support throughout my life and my academic journey. I would first like to thank my parents, Charlie and Linda Haywood, for encouraging me throughout my 23 years of education and always believing I could do anything I set my mind to. Thank you for steering me toward science, for making me attend engineering camp, for suggesting I major in biochemistry instead of going to pharmacy school, and for supporting me when I chose to attend graduate school at KU. I would also like to thank my first and best friend, my sister Nicole Haywood, for absolutely always standing by my

side and for giving me someone to set an example for. Additionally, I would like to thank my grandparents, Arvin and Carolyn Haywood and Richard and Leona Smith for their constant love and for always sending encouraging phone calls and emails my way. I would also like to thank all my aunts and uncles, cousins and friends from back home for always providing laughs and love whenever I needed it when I traveled back home. I would also like to thank the newest addition to my support system, my in-laws. Thank you to Rodney and Irene Bane for loving me as their own and giving me the greatest gift I could hope for, Kevin.

Lastly, and most importantly, I would like to thank my husband, Kevin, for loving and supporting me unconditionally, although often bearing the brunt of my frustrations and anxiety throughout my graduate work. There is no way I could have accomplished this degree without your music, smile, or lighthearted nature. Thank you for taking time to read this dissertation, and thank you for allowing me to pursue my dreams and move to California with me.

Chapter 1. Introduction to protein photochemistry 1

1.1 The Emergence of Antibodies in the Biotechnology Industry 2

1.2 Light Exposure in the Biotechnology Industry 2

1.3 Protein Photo-oxidation 3

1.4 Disulfide Photochemistry 4

1.5 Tryptophan Photochemistry 6

1.6 Tryptophan and Disulfide Interactions 7

1.7 Aim and Outline of Dissertation 8

1.8 References 10

Chapter 2. Photodegradation of valine and disulfide-containing model peptides: reactions of thiyl radicals and formation of isothiazol-3(2H)-one 16

2.1 Introduction 17

2.2 Experimental Methods 20

2.2.1 Materials. 20

2.2.2 Peptide Synthesis. 20

2.2.3 UV Irradiation of Model Peptides. 22

2.2.4 AAPH Reaction with Peptide 1d. 22

2.2.5 LTQ-FT Mass Spectrometry Analysis. 23

2.2.6 Q-tof Mass Spectrometry Analysis. 23

2.2.7 ^{1}H-NMR. 24

2.2.8 ^{1}H-^{1}H TOCSY NMR. 24

2.2.9 ^{1}H-^{13}C HSQC NMR. 25

2.2.10 Ozonolysis Reaction with Peptide 1a Photoproducts. 25

2.3 Results. 26
2.3.1 Photo-irradiation of 100 nM Peptide 1a at pH 7.0. 26
2.3.2 Derivatization of Photoproducts with N-ethylmaleimide (NEM). 31
2.3.3 Derivatization of Photoproducts from 100nM Peptide 1a at pH 7.0 with β-mercaptoethanol (BME). 34
2.3.4 Isothiazole-3(2H)-one formation in Peptides 1a, 1b, and 1c at pH 7.0. 37
2.3.5 MS^3 fragmentation of Products 2a, 9, and 10. 40
2.3.6 Reaction of Cys-Containing Peptide 1d with Carbon-Centered Radicals Derived From AAPH. 45
2.3.7 Derivatization of AAPH-Generated Products with NEM. 50
2.3.8 ^{1}H-NMR of Product 2a. 55
2.3.9 Photo-irradiation of 100 µM Peptide 1a at pH 7.0. 56
2.3.10 Derivatization of Product 6, 18, 19a, and 19b with β-mercaptoethanol (BME)....61
2.2.11 ^{1}H-^{1}H TOCSY NMR (TOtal Correlated SpectroscopY) of Irradiated Peptide 1a. 63
2.2.12 ^{1}H-^{13}C HSQC (Heteronuclear Single Quantum Coherence) NMR. 64
2.2.13 Ozonolysis of Photoproducts Generated during Photo-irradiation of 100 µM Peptide 1a at pH 7.0....66
2.3.14 Photo-irradiation of 100 µM Peptide 1a at pH 4.0. 67
2.4 Discussion 69
2.5 Conclusion....79
2.6 References 80
2.7 Appendix A 88

Chapter 3. Light-induced conversion of Trp to Gly and Gly hydroperoxide 93

3.1.1 Parts of this section have been published in a peer-reviewed journal.[1] 94

3.1 Introduction 94

3.2 Experimental Methods 95

3.2.1 Materials. 95

3.2.2 Peptide Synthesis. 95

3.2.3 UV Irradiation of IgG1. 96

3.2.4 UV Irradiation of Model Peptides. 96

3.2.5 IgG1 Enzymatic Digest. 97

3.2.6 IgG1 Reduction of Hydroperoxides. 97

3.2.7 Measurement of Alkyl Peroxides in the GGCGGL-GGCWGL Peptide by the FOX2 Assay. 98

3.2.8 LTQ-FT Mass Spectrometry Analysis. 98

3.2.9 Synapt G2 Mass Spectrometry Analysis. 99

3.3 Results 99

3.3.1 UV Irradiation of IgG1. 99

3.3.2 UV Irradiation of GGCGGL-GGCWGL. 104

3.3.3 UV Irradiation of N-acetyl-L-tryptophanamide (NATA) with Oxidized L-glutathione (GSSG) 105

3.3.4 UV Irradiation of $(LGGCWGL)_2$. 106

3.4 Discussion 111

3.5 Conclusion 113

3.6 References 115

3.6 Appendix B 119

Chapter 4. Photo-oxidation of model peptides: Formation of triply oxidized His and Trp side chain cleavage products 126

4.1 Introduction 127

4.2 Experimental Methods 129

4.2.1 Materials. 129

4.2.2 Methylation of the Lys Residues in H293W. 130

4.2.3 Acetylation of the Lys and Tyr Residues in H293W 131

4.2.4 UV Irradiation of Model Peptides. 132

4.2.5 UV Irradiation of H293W and Oxidized L-glutathione. 132

4.2.6 Glu-C Digestion of H293W and H293A. 132

4.2.7 Tryptic Digestion of H293W. 133

4.2.8 LTQ-FT Mass Spectrometry Analysis. 133

4.2.9 Q-Tof Mass Spectrometry Analysis. 133

4.3 Results 134

4.3.1 His and Trp Modifications observed in Model Peptides. 134

4.3.2 Characterization of Product 1 Formation in H293W 138

i. Glu-C Digestion of H293W and H293A. 139

ii. Kinetics of Product 1 Formation. 140

iii. Tryptic Digestion of H293W. 143

iv. Trapping 3-methyleneindolenine (3-MEI) with Oxidized L-glutathione (GSSG). 146

v. Blocking the H293W Lys Amine Reactivity by Methylation. 147

vi. Chymotryptic Digestion of $H293W_K$. 152

vii. Blocking the H293W Lys Amine and Tyr Hydroxyl group Reactivity by Acetylation. 154

4.4 Discussion 156

4.5 Conclusion 163

4.6 References 164

4.7 Appendix C 168

Chapter 5. Conclusions and future directions 171

5.1 Summary and conclusions 172

5.2 Future directions 174

5.3 References 175

List of Abbreviations

AAPH	2,2’-azobis-2-methyl-propanimidamide, dihydrochloride
ACN	acetonitrile
Ar	argon
BME	2-mercaptoethanol
BDE	bond dissociation energy
CID	collision-induced dissociation
CDR	complementarity-determining region
$CysS^{\bullet}$	Cys thiyl radical
D_2O	deuterium oxide
Dha	dehydroalanine
DMSO	dimethyl sulfoxide
DTT	dithiothreitol
ESI	electrospray ionization
FC	fragment crystallizable region
FcRn	neonatal fragment crystallizable receptor
FOX	ferrous iron oxidation xylenol orange
FT	Fourier transform
GSH	glutathione, reduced
GSSG	glutathione, oxidized
H-atom	hydrogen atom
H293A	Ac-KNAYVDGVEVHNAK-Am model peptide
H293W	Ac-KNWYVDGVEVHNAK-Am model peptide

H318A	Ac-KTVLHQDALNGK-Am model peptide
H318W	Ac-KTVLHQDWLNGK-Am model peptide
H_2O	water
H_2O_2	hydrogen peroxide
HATU	O-(7-Azabenzotriazole-1-yl)-N, N,N'N'-tetramethyluronium hexafluorophosphate
HC	heavy chain
HO-	hydroxyl anion
$HO^{\bullet}$	hydroxyl radical
$HOO^{\bullet}$	hydroperoxyl radical
HPLC	high-performance liquid chromatography
HPLC-MS	high-performance liquid chromatography- mass spectrometry
HPLC-MS/MS	high-performance liquid chromatography-tandem mass spectrometry
IAA	iodoacetamide
ICH	international conference on harmonisation
ICR	ion cyclotron resonance
ID	inner diameter
IgG1	immunoglobulin G
Ky	kynurenine
LC	light chain
LC-MS	liquid chromatography- mass spectrometry
LC-MS/MS	liquid chromatography-tandem mass spectrometry
LTQ	linear trap quadrupole (linear ion trap)

mAb	monoclonal antibody
$[M+H]^{+1}$	molecular ion
$[M+H]^{+1}$ - 17	molecular ion minus ammonia
$[M+H]^{+1}$ - 18	molecular ion minus water
m/z	mass-to-charge-ratio
MS	mass spectrometry
MS/MS	tandem mass spectrometry
MS^3	multistage mass spectrometry, where n = 3
$NaBH_4$	sodium borohydride
NEM	N-ethylmaleimide
NH_3	ammonia
NFK	N-formylkynurenine
NMR	nuclear magnetic resonance
NSA	N-succinimidyl acetate
$^1O_2$	singlet oxygen
$^3O_2$	triplet oxygen
$O_2^{\bullet-}$	superoxide
O_3	ozone
PS	polysorbate
PTM	post-translational modification
R=S	thioaldehyde
$ROO^{\bullet}$	peroxyl radical
ROS	reactive oxygen species

RP	reverse-phase
RP-HPLC	reverse-phase high-performance liquid chromatography
$RS^{\bullet}$	thiyl radical
RS^{-}	thiolate
$RS\text{-}S^{-}$	persulfide
$RS\text{-}SR^{\bullet -}$	disulfide radical anion
RSH	thiol
RSOH	sulfenic acid
RSOOH	sulfinic acid
RSO_3H	sulfonic acid
RT	room temperature
TFA	trifluoroacetic acid
Q-tof	quadrupole-time-of-flight
UPLC	ultra-performance liquid chromatography
UV	ultraviolet
XIC	extracted ion chromatograms

List of names and structures used throughout the dissertation

Name	Structure	Origin
Thiyl radical	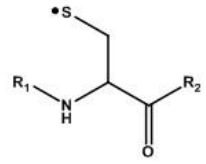	Photolysis of disulfide bond
Thiol	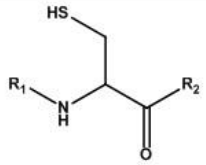	Thiyl disproportionation product
Thioaldehyde	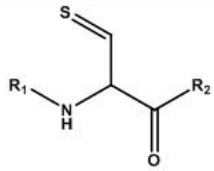	Thiyl disproportionation product
Aldehyde	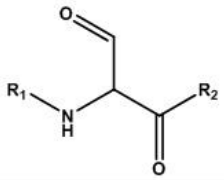	Oxidation of thioaldehyde disproportionation product
Dehydroalanine	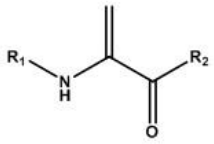	Photolysis of disulfide bond
Disulfide	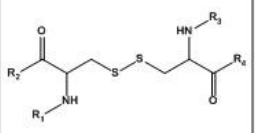	Precursor to thiyl radicals
Dithiohemiacetal	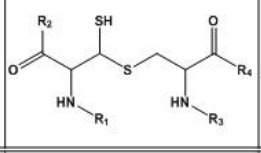	Photolysis of disulfide bond

Name	Structure	Origin
Thioether	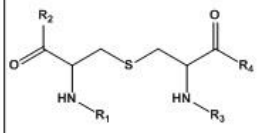	Photolysis of disulfide bond
Isothiazol-3(2H)-one	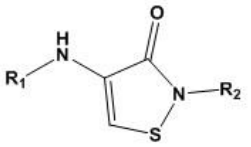	Photolysis of disulfide bond in close proximity to Val residues
Trp radical cation	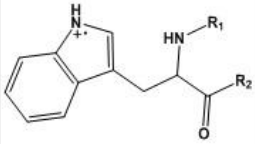	Photolysis of Trp
3-methyleneindolenine	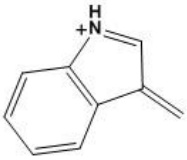	Photolysis of Trp and Trp side chain cleavage
Glycyl radical	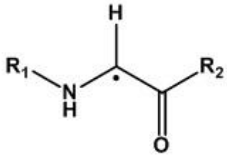	Trp side chain cleavage
Glycylperoxyl radical	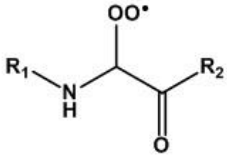	Trp side chain cleavage and oxidation
Gly hydroperoxide	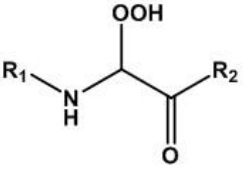	Trp side chain cleavage and oxidation

Chapter 1. Introduction to protein photochemistry

1.1 The emergence of antibodies in the biotechnology industry

The biotechnology industry is becoming increasingly interested in developing protein pharmaceuticals as therapeutic agents on a large scale, evidenced by the 47 approved antibodies in the US or Europe and over 300 molecules currently in development since the first protein therapeutic, human insulin, was approved by the Food and Drug Administration (FDA) in 1982.[1,2,3,4,5] These protein pharmaceuticals are effective against a variety of cancers,[6] autoimmune disorders,[7] and inflammatory diseases.[8] Novel antibody therapeutics and related products have emerged in recent years such as antibody-drug conjugates (ADCs), bispecific antibodies, Fc-fusion proteins, and biosimilars.[5] The advantage of using protein pharmaceuticals over small molecule drugs stems from their effectiveness at lower concentrations, reduced side effects, their affinity to bind target molecules, and their utility in combination with other therapies and radioisotopes.[9] Antibodies also show increased stability over other protein pharmaceuticals because of their disulfide-rich nature, but they are still sensitive to a number of chemical and physical instabilities: oxidation, photochemical degradation, denaturation, aggregation, etc.[9,10,11,12,13] Oxidative and photochemical damage, collectively photo-oxidation, could occur after antibodies are exposed to light during formulation or storage, and this damage could enhance immunogenicity or cause inactivation.[10,14,15,16] To increase the stability of these antibodies, an understanding of their mechanisms of degradation is necessary.

1.2 Light exposure in the biotechnology industry

In the biotechnology industry, proteins are often exposed to light during the manufacturing, purification, storage, and administration processes.[12] Small-scale (2L) culture processing is often done in glass bioreactors, where the protein is exposed to various levels of ambient light, which has been documented to cause an unwanted increase in acidic variants.[17]

UV detection at 280 and 300 nm is frequently used to monitor and subsequently separate and purify proteins, which could induce protein degradation.[18] While most protein therapeutics are now stored properly without possibility of light exposure, during administration through intravenous injection, they could be exposed to light in clear IV bags. To ensure that light exposure does not degrade protein therapeutics (or small molecule drugs) to an unacceptable level and affect safety, a set of photostability testing guidelines was reached by the International Conference on Harmonization of Technical Requirements for Registration of Pharmaceuticals for Human Use (ICH).[19] Under this regulation, Q1B, photostability testing must be carried out on the drug substance (containing only the active pharmaceutical ingredient (API) exerting pharmacological action in the buffer or vehicle it will be delivered, e.g. the protein) and on the drug product (containing the API and other non-active ingredients (such as excipients, e.g. sugars, surfactants) that will be sold commercially). To comply with the Q1B, the samples must be exposed to at least 1.2 million lux hours of visible light and 200 watt hours/m^2 of UV light using approved light sources, although revisions to this guideline have been recommended.[20,21]

1.3 Protein photo-oxidation

Photo-oxidation may lead to a change in the overall protein structure (e.g. aggregation or fragmentation)[22], however, these reactions are only targeted to a select group of amino acids. Disulfides and the aromatic amino acids tryptophan (Trp), phenylalanine (Phe), and tyrosine (Tyr), are most susceptible to UV irradiation between 250-320 nm.[23,24,25,26] Oxidation reactions mainly occur with the aforementioned amino acids, as well as histidine and methionine.[12,22] Figure 1.1 shows the absorbance spectra of the disulfide bond and the aromatic amino acids.[27] Trp has the highest extinction coefficient in the near-UV region compared to the other residues, with its absorption maxima at 280 nm, and absorbing light over 300 nm. Above ca. 290 nm is the

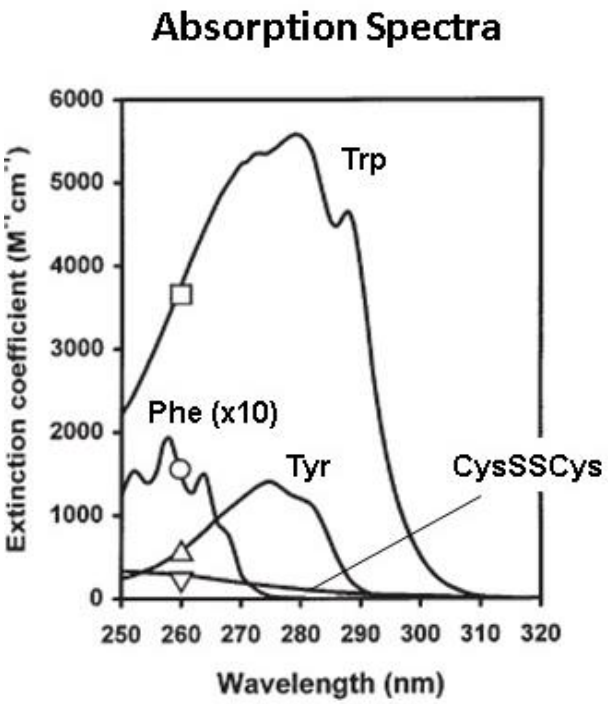

Figure 1.1. Absorbance spectra of the disulfide bond (CysSSCys), Trp, Tyr, and Phe.[27]

cutoff for Pyrex glass, allowing Trp to absorb light during conditions when a protein is stored in glass. The disulfide bond, although of much lower intensity, also absorbs light past 300 nm, with its absorption maxima at 254 nm. Tyr absorbs light at a higher intensity than the disulfide bond, with its absorption maxima at 275 nm, but not absorbing light past 290 nm. Phe, however, absorbs light with similar efficiency as the disulfide bond.

After exposure to light, photooxidation of proteins occurs by either a direct (type I) or indirect (type II) process.[28] In the type I process, UV light is directly absorbed by a protein chromophore (e.g. Trp), creating an excited state or radical species. In the type II process, an excited chromophore transfers its energy to ground state triplet oxygen ($^3O_2$), forming singlet oxygen ($^1O_2$), superoxide ($O_2^{\cdot-}$), peroxy radicals ($ROO^{\cdot}$) or hydroxyl radicals ($HO^{\cdot}$**)** which react with other residues in the protein. In the following sections, we will primarily focus on disulfide and Trp photochemistry, and on the interaction between the two moieties.

1.4 Disulfide photochemistry

Cys disulfides often play a role in the three-dimensional structure of proteins; for instance, Y-shaped antibodies usually contain at least four *inter*chain disulfides linking the two heavy chains and the heavy and light chains, along with more *intra*chain disulfides.[9] Although disulfides can stabilize proteins, they are sensitive to light, heat, and high pH, and will undergo

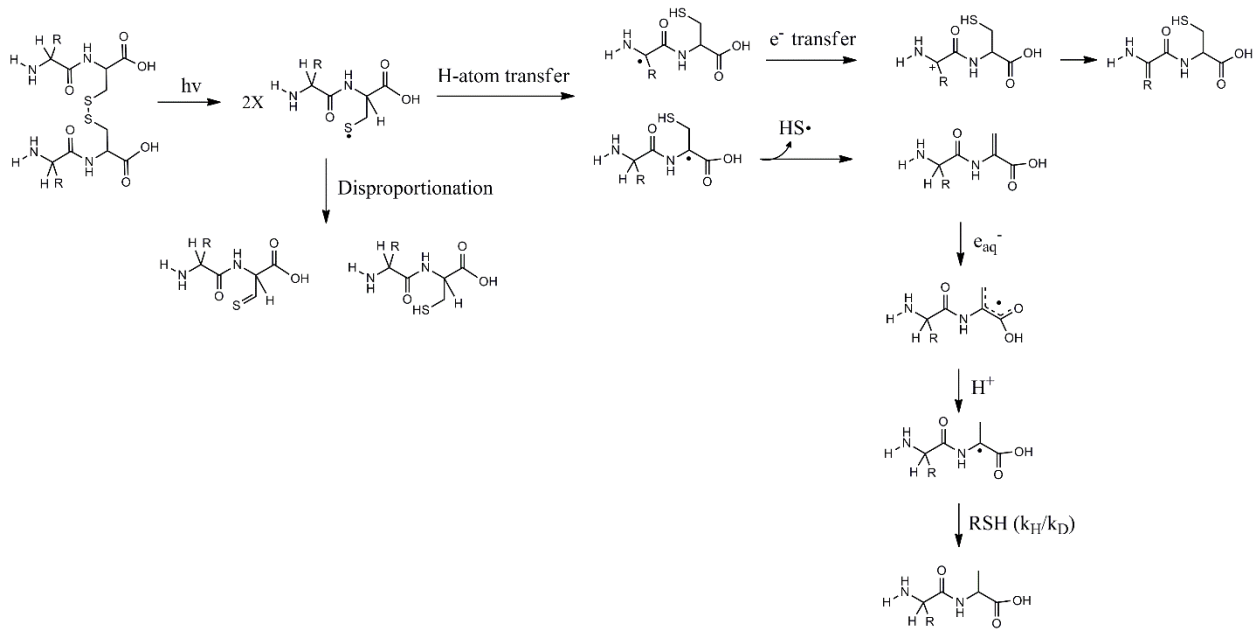

Figure 1.2. Light-induced degradation of a disulfide bond.

heterolytic cleavage to yield a thiolate (RS^-)[29], or homolytic cleavage to yield a thiyl radical pair ($RS^\cdot$).[30] For example, at high pH, cleavage of the disulfide through β-elimination results in the formation of persulfide ($RS\text{-}S^-$) and dehydroalanine, an unstable molecule that can form unnatural cross-links with nucleophilic amino acids such as lysine.[31] The persulfide can lose one sulfur to form the thiol product (RSH), which can undergo two-electron oxidation to form the disulfide again, or form sulfenic acid (RSOH), sulfinic acid (RSOOH), or sulfonic acid (RSO3H).[32]

The less studied one-electron oxidation of Cys produces thiyl radicals ($CysS^\cdot$), and the one-electron reduction of a disulfide produces disulfide radical anions ($RS\text{-}SR^{\cdot-}$), which may undergo disproportionation to yield a thiol (RSH) and thioaldehyde (R=S) (Figure 1.2).[30] Based on theoretical calculations of a relaxed model peptide, the S-H bond has higher bond dissociation energy (BDE) than the $^{\alpha}$C-H bond of other amino acids, indicating a thermodynamic preference for hydrogen-atom (H-atom) abstraction by thiyl radicals.[33] To probe H-atom abstraction reactions with thiyl radicals, Mozziconacci *et al.* used model peptides containing disulfides with

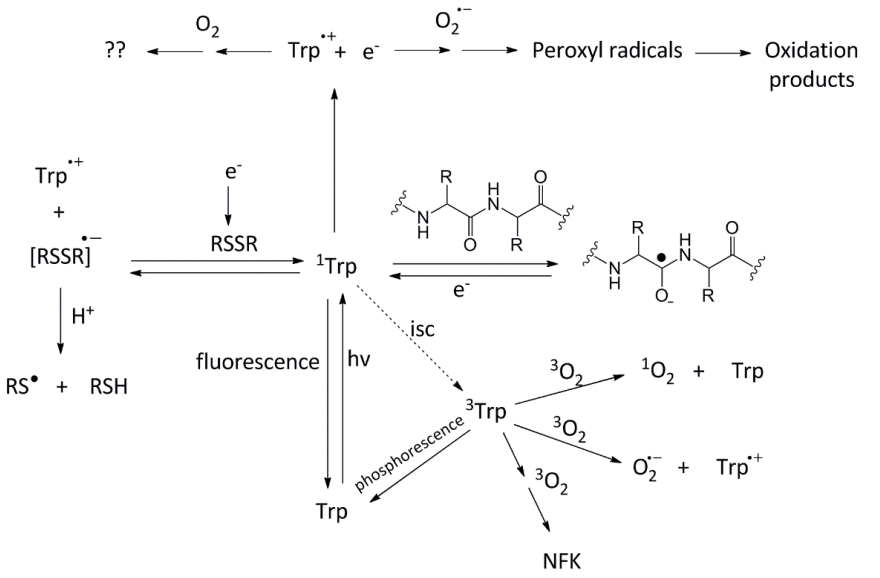

Figure 1.3. Light-induced degradation of Trp, and its reaction with disulfides, the peptide backbone, and oxygen.

flanking alanine residues. To study the H-atom abstraction between the S· and C-H bonds, the model peptide was irradiated in both water (H_2O) and deuterium oxide (D_2O), and the resultant deuterium incorporation after irradiation on C-D bonds confirmed H-atom transfer reactions (more details to follow in Chapter 2).[34] These experiments showed not only $^{\alpha}$C-H abstraction by the thiyl radicals, but $^{\beta}$C-H abstraction as well, which should have been less favorable than the $^{\alpha}$C-H abstraction since radicals are less stable on secondary carbons than on tertiary carbons. Consequently, these H-atom transfer reactions led to the transformation of Cys into Ala and dehydroalanine, and Ala into dehydroalanine.

1.5 Tryptophan photochemistry

Trp is a unique amino acid, often used as an intrinsic probe to detect conformational shifts due to environmental changes in pH, temperature, solvent, or protein interactions. Trp is useful to see such conformational changes because of its strong absorbance at 280 nm and fluorescence emission at 348 nm. However, the indole structure making Trp so useful for probing protein dynamics also makes Trp susceptible to light-induced damage; Trp residues play a major role in the activation of protein photodegradation, and their photoinduced processes are numerous (See Figure 1.3).[23,35] After photochemical excitation, Trp is excited to its singlet state

(^{1}Trp) where it can fluoresce, intersystem cross to its triplet state (^{3}Trp), or undergo photoionization to a Trp radical cation ($Trp^{\cdot+}$), while ejecting an electron (e^-_{aq}). The ^{1}Trp can reduce the nearby peptide backbone, and either the ^{1}Trp or e^-_{aq} can reduce a disulfide through a one-electron transfer. If there is a proton in the solution, the newly reduced $RSSR^{\cdot-}$ will react with it to form a thiyl radical, leading to the cascade of other photochemical reactions discussed in the previous disulfide photochemistry section. The ^{3}Trp will either phosphoresce back to the ground state Trp or react with $^3O_2$ to form N-formylkynurenine (NFK), $^1O_2$, or $O_2^{\cdot-}$.

Many studies have been aimed to identify Trp photoproducts and reaction mechanisms.[23,36,37,35,38] Some products identified after irradiation of the amino acid form of Trp at λ = 254 nm under slightly acidic, anaerobic conditions include: alanine (Ala), serine (Ser), aspartic acid (Asp), tryptamine, kynurenine (Ky), and N-formylkynurenine (NFK).[23] Under aerobic conditions at λ = 254 nm, the main Trp photoproduct was NFK, which underwent secondary photolysis to Asp, Ser, Ala, Ky, and ammonia.[23] Ky and NFK are important photoproducts because they are endogenous photosensitizers, absorbing light at 365 and 325 nm, respectively, above the cutoff for transmission through glass at ca. 290 nm.[39,40] Ky is also a well-studied degradation product, having been linked to neurodegenerative disorders like Alzheimer's and Huntington's disease.[41]

1.6 Tryptophan and disulfide interactions

In proteins, Trp is a common neighbor of disulfides, and, as seen in Figure 1.3, disulfides are common quenchers of the excited Trp residue.[42] Although much has been studied about the photochemistry of disulfides and Trp separately, our understanding of the photochemistry of their interaction is limited. The first Trp-mediated photolysis of disulfides within a protein was seen in F. solani pisi cutinase, and since then, other proteins, such as goat α-lactalbumin and bovine somatotropin, have shown similar results.[43,44,45] In goat α-lactalbumin, there has also been

evidence of a Trp-Cys crosslink after photolysis.[46] The photochemistry of disulfides and Trp separately is complex, so the photochemistry involving both residues will be much more complex, and this leaves much to be studied in this area.

1.7 Aim and outline of this dissertation

As outlined in this introduction, protein stability, and specifically photochemical stability is of immense interest to the pharmaceutical industry due to the unwanted consequences of protein structural changes, increased immunogenicity, and potential inactivation. In the biotechnology industry, proteins have the potential to be exposed to ambient light during all phases of development. The most photosensitive amino acids, Trp and Cys, have been studied thoroughly, but little is known about their combined photochemistry in proteins. It is important to study such interactions because many relevant biopharmaceuticals, like antibodies, contain multiple disulfides and Trp.

The aim of this dissertation project was to further investigate protein stability in proteins and model peptides containing Trp and/or disulfide bonds to help elucidate novel mechanisms of protein degradation to lead to a greater understanding of protein stability. With this knowledge, better formulation of antibodies can be developed, and faster progression through the drug development stages could lead to more stable antibodies on the market.

Chapter 2 investigates the extent of H-atom transfer reactions between thiyl radicals and neighboring amino acid residues using a model peptide with sterically demanding Val amino acids flanking the disulfide bond, $(LGVCVGL)_2$.

Chapter 3 aims to elucidate the mechanism of Trp side chain cleavage in the presence of a disulfide with an IgG1 molecule and several Trp and disulfide containing model peptides.

Chapter 4 evaluates His oxidation in an IgG1 molecule and model peptides, and describes a Trp side chain cleavage reaction without the presence of a disulfide in Trp-containing model peptides.

Chapter 5 summarizes the findings and conclusions of this dissertation and discusses the outlook for the future.

1.8 References

1. Dingermann, T., Recombinant therapeutic proteins: production platforms and challenges. *Biotechnol J* **2008,** *3* (1), 90-7.
2. Carter, P. J., Introduction to current and future protein therapeutics: a protein engineering perspective. *Exp Cell Res* **2011,** *317* (9), 1261-9.
3. Goeddel, D. V.; Kleid, D. G.; Bolivar, F.; Heyneker, H. L.; Yansura, D. G.; Crea, R.; Hirose, T.; Kraszewski, A.; Itakura, K.; Riggs, A. D., Expression in Escherichia coli of chemically synthesized genes for human insulin. *Proc Natl Acad Sci U S A* **1979,** *76* (1), 106-10.
4. Reichert, J. M. In *Antibodies to watch in 2015*, MAbs, Taylor & Francis: 2015; pp 1-8.
5. Ecker, D. M.; Jones, S. D.; Levine, H. L., The therapeutic monoclonal antibody market. *MAbs* **2014,** *7* (1), 9-14.
6. Sliwkowski, M. X.; Mellman, I., Antibody therapeutics in cancer. *Science* **2013,** *341* (6151), 1192-8.
7. Taylor, P. C., Pharmacology of TNF blockade in rheumatoid arthritis and other chronic inflammatory diseases. *Curr Opin Pharmacol* **2010,** *10* (3), 308-315.
8. Kotsovilis, S.; Andreakos, E., Therapeutic human monoclonal antibodies in inflammatory diseases. *Methods Mol Biol* **2014**, 586-6_3.
9. Wang, W.; Singh, S.; Zeng, D. L.; King, K.; Nema, S., Antibody structure, instability, and formulation. *J Pharm Sci* **2007,** *96* (1), 1-26.
10. Volkin, D. B.; Mach, H.; Middaugh, C. R., Degradative covalent reactions important to protein stability. *Mol Biotechnol* **1997,** *8* (2), 105-22.

11. Torosantucci, R.; Schöneich, C.; Jiskoot, W., Oxidation of therapeutic proteins and peptides: structural and biological consequences. *Pharm Res* **2014,** *31* (3), 541-53.

12. Kerwin, B. A.; Remmele, R. L., Jr., Protect from light: photodegradation and protein biologics. *J Pharm Sci* **2007,** *96* (6), 1468-79.

13. Randolph, T. W.; Schiltz, E.; Sederstrom, D.; Steinmann, D.; Mozziconacci, O.; Schöneich, C.; Freund, E.; Ricci, M. S.; Carpenter, J. F.; Lengsfeld, C. S., Do not drop: mechanical shock in vials causes cavitation, protein aggregation, and particle formation. *J Pharm Sci* **2015,** *104* (2), 602-11.

14. Fradkin, A. H.; Mozziconacci, O.; Schöneich, C.; Carpenter, J. F.; Randolph, T. W., UV photodegradation of murine growth hormone: chemical analysis and immunogenicity consequences. *European journal of pharmaceutics and biopharmaceutics : official journal of Arbeitsgemeinschaft fur Pharmazeutische Verfahrenstechnik e.V* **2014,** *87* (2), 395-402.

15. Jiskoot, W.; Randolph, T. W.; Volkin, D. B.; Middaugh, C. R.; Schöneich, C.; Winter, G.; Friess, W.; Crommelin, D. J.; Carpenter, J. F., Protein instability and immunogenicity: roadblocks to clinical application of injectable protein delivery systems for sustained release. *J Pharm Sci* **2012,** *101* (3), 946-54.

16. Wei, Z.; Feng, J.; Lin, H. Y.; Mullapudi, S.; Bishop, E.; Tous, G. I.; Casas-Finet, J.; Hakki, F.; Strouse, R.; Schenerman, M. A., Identification of a single tryptophan residue as critical for binding activity in a humanized monoclonal antibody against respiratory syncytial virus. *Anal Chem* **2007,** *79* (7), 2797-805.

17. Mallaney, M.; Wang, S. H.; Sreedhara, A., Effect of ambient light on monoclonal antibody product quality during small-scale mammalian cell culture process in clear glass bioreactors. *Biotechnol Prog* **2014,** *30* (3), 562-70.

18. Frank, J.; Braat, A.; Duine, J. A., Assessment of protein purity by chromatography and multiwavelength detection. *Anal Biochem* **1987,** *162* (1), 65-73.

19. ICH, Q. B., Stability Testing: Photostability testing of new drug substances and products. **1996**.

20. Baertschi, S. W.; Alsante, K. M.; Tonnesen, H. H., A critical assessment of the ICH guideline on photostability testing of new drug substances and products (Q1B): Recommendation for revision. *J Pharm Sci* **2010,** *99* (7), 2934-40.

21. Baertschi, S. W.; Clapham, D.; Foti, C.; Jansen, P. J.; Kristensen, S.; Reed, R. A.; Templeton, A. C.; Tonnesen, H. H., Implications of in-use photostability: proposed guidance for photostability testing and labeling to support the administration of photosensitive pharmaceutical products, part 1: drug products administered by injection. *J Pharm Sci* **2013,** *102* (11), 3888-99.

22. Pattison, D. I.; Rahmanto, A. S.; Davies, M. J., Photo-oxidation of proteins. *Photochem Photobiol Sci* **2012,** *11* (1), 38-53.

23. Creed, D., The photophysics and photochemistry of the near-UV absorbing amino-acids .I. Tryptophan and its simple derivatives. *Photochem Photobiol* **1984,** *39* (4), 537-562.

24. Creed, D., The photophysics and photochemistry of the near-UV absorbing amino-acids .II. Tyrosine and its simple derivatives. *Photochem Photobiol* **1984,** *39* (4), 563-575.

25. Creed, D., The photophysics and photochemistry of the near-UV absorbing amino-acids .III. Cystine and its simple derivatives.THE PHOTOPHYSICS AND *Photochem Photobiol* **1984,** *39* (4), 577-583.

26. Bent, D. V.; Hayon, E., Excited-state chemistry of aromatic amino-acids and related peptides .II. Phenylalanine. *J Am Chem Soc* **1975,** *97* (10), 2606-2612.

27. Martin, S. R.; Bayley, P. M., Absorption and circular dichroism spectroscopy. *Methods Mol Biol* **2002,** *173*, 43-55.

28. Igarashi, N.; Onoue, S.; Tsuda, Y., Photoreactivity of amino acids: tryptophan-induced photochemical events via reactive oxygen species generation. *Anal Sci* **2007,** *23* (8), 943-8.

29. Florence, T. M., Degradation of protein disulphide bonds in dilute alkali. *Biochem J.* **1980**,189(3):507-20.

30. Mozziconacci, O.; Sharov, V.; Williams, T. D.; Kerwin, B. A.; Schöneich, C., Peptide cysteine thiyl radicals abstract hydrogen atoms from surrounding amino acids: the photolysis of a cystine containing model peptide. *J Phys Chem B* **2008,** *112* (30), 9250-7.

31. Patchornik, A.; Sokolovsky, M., Chemical interactions between lysine and dehydroalanine in modified bovine pancreatic ribonuclease. *J Am Chem Soc* **1964,** *86* (9), 1860-1861.

32. Kosen, P., Disulfide bonds in proteins. Stability of protein pharmaceuticals. A. Chemical and physical pathways of protein degradation. *Plenum Press, New York* **1992**, 31-67.

33. Rauk, A.; Yu, D.; Taylor, J.; Shustov, G. V.; Block, D. A.; Armstrong, D. A., Effects of structure on alpha C-H bond enthalpies of amino acid residues: relevance to H transfers in enzyme mechanisms and in protein oxidation. *Biochemistry* **1999,** *38* (28), 9089-96.

34. Mozziconacci, O.; Kerwin, B. A.; Schöneich, C., Reversible hydrogen transfer reactions of cysteine thiyl radicals in peptides: the conversion of cysteine into dehydroalanine and alanine, and of alanine into dehydroalanine. *J Phys Chem B* **2011,** *115* (42), 12287-305.

35. Bent, D. V.; Hayon, E., Excited state chemistry of aromatic amino acids and related peptides. III. Tryptophan. *J Am Chem Soc* **1975,** *97* (10), 2612-9.

36. Laustriat, G.; Hasselmann, C., Photochemistry of proteins. *Photochem Photobiol* **1975,** *22* (6), 295-8.

37. Grossweiner, L. I., Photochemistry of proteins: a review. *Curr Eye Res* **1984,** *3* (1), 137-44.

38. Davies, M. J.; Truscott, R. J., Photo-oxidation of proteins and its role in cataractogenesis. *J Photochem Photobiol B* **2001,** *63* (1-3), 114-25.

39. Fukunaga, Y.; Katsuragi, Y.; Izumi, T.; Sakiyama, F., Fluorescence characteristics of kynurenine and N'-formylkynurenine. Their use as reporters of the environment of tryptophan 62 in hen egg-white lysozyme. *J Biochem* **1982,** *92* (1), 129-41.

40. Parker, N. R.; Jamie, J. F.; Davies, M. J.; Truscott, R. J., Protein-bound kynurenine is a photosensitizer of oxidative damage. *Free Radic Biol Med* **2004,** *37* (9), 1479-89.

41. Davies, N. W.; Guillemin, G.; Brew, B. J., Tryptophan, neurodegeneration and HIV-associated neurocognitive disorder. *Int J Tryptophan Res* **2010,** *3*, 121-40.

42. Marques, J. R. F.; da Fonseca, R. R.; Drury, B.; Melo, A., Amino acid patterns around disulfide bonds. *Int J Mol Sci* **2010,** *11* (11), 4673-4686.

43. Prompers, J. J.; Hilbers, C. W.; Pepermans, H. A., Tryptophan mediated photoreduction of disulfide bond causes unusual fluorescence behaviour of Fusarium solani pisi cutinase. *FEBS Lett* **1999,** *456* (3), 409-16.

44. Vanhooren, A.; De Vriendt, K.; Devreese, B.; Chedad, A.; Sterling, A.; Van Dael, H.; Van Beeumen, J.; Hanssens, I., Selectivity of tryptophan residues in mediating photolysis of disulfide bridges in goat alpha-lactalbumin. *Biochemistry* **2006,** *45* (7), 2085-93.

45. Miller, B. L.; Hageman, M. J.; Thamann, T. J.; Barron, L. B.; Schöneich, C., Solid-state photodegradation of bovine somatotropin (bovine growth hormone): evidence for tryptophan-mediated photooxidation of disulfide bonds. *J Pharm Sci* **2003,** *92* (8), 1698-709.

46. Vanhooren, A.; Devreese, B.; Vanhee, K.; Van Beeumen, J.; Hanssens, I., Photoexcitation of tryptophan groups induces reduction of two disulfide bonds in goat alpha-lactalbumin. *Biochemistry* **2002,** *41* (36), 11035-43.

Chapter 2. Photodegradation of valine and disulfide-containing model peptides: reactions of thiyl radicals and formation of isothiazol-3(2H)-one

2.1 Introduction

The superior specificity and efficiency has boosted the development of protein pharmaceuticals.[1,2] However, proteins are susceptible to chemical and physical degradation that can result in loss of potency or cause immunogenicity.[3,4,5,6,7] Therefore, the evaluation of protein stability is paramount to the development of protein pharmaceuticals. Stability studies are also becoming increasingly important to demonstrate likeness between follow-on biologics (biosimilars) and their original counterparts (innovator drugs).[8] One important area of concern is photostability, as proteins are exposed to light during production, purification, formulation and storage.[9,10]

In proteins, the amino acids most susceptible to light stress are the aromatic amino acids, Trp, Tyr, and Phe, and the disulfide bond.[9] The absorption of light by aromatic amino acids generates an excited singlet state, which can fluoresce, undergo intersystem crossing to the first excited triplet state, or eject an electron into solution, resulting in a solvated electron and an aromatic radical cation.[11,12,13,14,15] In case of Trp, Trp radicals or triplet Trp can react with oxygen to form the photosensitizing products N-formyl kynurenine and kynurenine,[16,11,12, 17,18,19] amino acid peroxy radicals,[20,21] or other reactive oxygen species. These products can promote additional oxidation reactions in the protein solution.

Triplet Trp or the solvated electron can reduce the disulfide bond to a disulfide radical anion, and following proton addition and cleavage, generate a thiol and a thiyl radical.[22,23,24] Thiyl radicals can also be generated directly by homolytic cleavage of a disulfide bond following photo-irradiation.[25] Especially in the case of Cys disulfide bonds, the homolytic cleavage generates predominantly thiyl radicals while perthiyl radicals are a major product of the homolytic cleavage of penicillamine disulfide.[26] Subsequently, thiyl radicals can recombine to

disulfide bonds,[27] native or scrambled, disproportionate into thiol and thioaldehyde,[28] and/or generate thioether and dithiohemiacetal products.[29] The later products were observed first in model peptides upon UV light exposure, and subsequently detected in IgG1 after exposure to similar light stress.[30] Under aerobic conditions, thiyl radicals reversibly add oxygen to form thiyl peroxyl radicals,[31] which ultimately convert into sulfinic, sulfenic, or sulfonic acids.[32,33] These oxidation products are also formed non-photolytically in alkaline conditions.[34,35] Additional non-photolytic disulfide degradation pathways under alkaline conditions include disulfide scrambling[36] and β-elimination.[37] β-Elimination leads to the formation of dehydroalanine, which can subsequently cross-link with nucleophiles such as thiols and amines.[38]

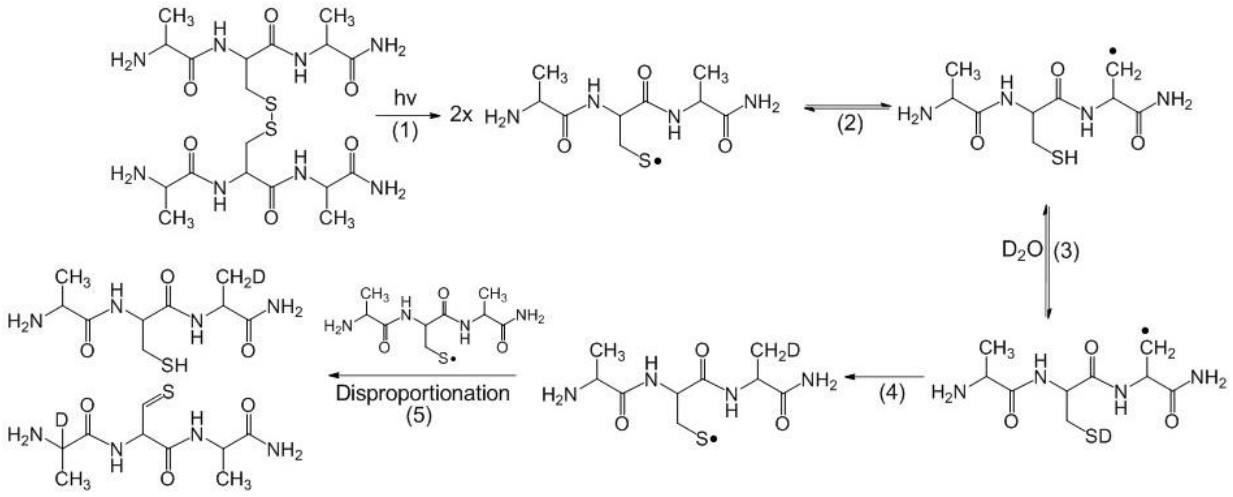

Scheme 2.1. Reaction for covalent H/D exchange between the thiyl radical and $^{\beta}$C-H.

Protein and peptide thiyl radicals may involve in reversible, *intra*molecular hydrogen atom (H-atom) abstraction reactions from nearby $^{\alpha}$C-H or side chain C-H bonds generating intermediary C-centered radicals.[28,29,39,40] Scheme 2.1 shows the pathway to form such C-centered radicals, using covalent H/D exchange to monitor where Deuterium incorporation is observed by mass spectrometry. C-centered radicals may subsequently involve in oxidation, cross-linking or fragmentation pathways.[41] Especially with $^{\alpha}$C-H bonds, such reversible H-atom transfer processes may induce epimerization.[42,43,44]

To evaluate the reactivity of Cys thiyl radicals and their propensity for reversible, *intra*molecular H-atom abstraction from nearby amino acids, Cys thiyl radicals were generated photolytically from a series of model disulfide peptides. In these peptides, various aliphatic amino acids were placed in the i+1 and i-1 position relative to the disulfide bond.[39,40,28-29] Evidence for reversible *intra*molecular H-atom transfer reactions was obtained through covalent H/D exchange (Scheme 2.1).[28] Interestingly, H-atom transfer was most efficient for reactions of Cys thiyl radicals with Gly in i-1 and i+1 in the peptide GGCGGL.[28] When Cys thiyl radicals were generated in peptides containing Ala at positions i-1 and i+1, i.e., in the peptide $(LGACAGL)_2$, H-atom transfer proceeded not only from the $^{\alpha}$C-H bond but also the side chain C-H bond from Ala. Moreover, L-Ala was efficiently converted into D-Ala and additional products were observed, such as dehydroalanine (Dha).

These results motivated us to evaluate the reactions of Cys thiyl radicals with larger, sterically more demanding amino acids such as Val. To this end, we synthesized the disulfide-containing peptides $(LG\mathbf{V}C\mathbf{V}GL)_2$, in which the Val residues displayed the natural C- and N-isotope distribution (i.e., 98.9% ^{12}C and 99.6% ^{15}N) or were uniformly ^{13}C-labeled (97-99%) and ^{15}N-labeled (97-99%) at either the i+1 or the i-1 position. Complementary experiments were performed with Cys thiyl radicals generated from the Cys-containing model peptide LGVCVGL. Our results will demonstrate that Cys thiyl radicals react with the Val residues, but also enter a pathway which yields a new reaction product, tentatively identified as isothiazole-3(2H)-one. The formation of this product is likely the result of steric constraints, which disfavor *inter*molecular reactions of thiyl radicals, since previous studies with $(LGACAGL)_2$ and $(GGCGGL)_2$ showed no significant yields of such product. These reactions are highly relevant

for degradation pathways of protein therapeutics, where disulfide bonds are subject to photodegradation.

2.2 Experimental methods

2.2.1 Materials. Ammonium bicarbonate (NH_4HCO_3), 2,2'-azobis-2-methyl-propanimidamide, dihydrochloride (AAPH), N-ethylmaleimide (NEM), dimethyl sulfoxide, β-mercaptoethanol (BME), thioanisole, 1,2 ethanedithiole (EDT), and anisole were supplied by Sigma-Aldrich (St. Louis, MO) at the highest commercially available purity. Methanol, dichloromethane, acetonitrile, and trifluoroacetic acid were supplied by Fisher Scientific (Pittsburg, PA). Deuterium oxide (D_2O, 99.9%) and stable isotope-labeled L-Valine-N-Fmoc (Valine U-$^{13}C_5$, 97-99%, ^{15}N, 97-99%) were purchased from Cambridge Isotope Laboratories (Andover, MA, USA). The U-$^{13}C_5$ notation indicates that all five carbon atoms of L-Val in the isotope-labeled L-Valine-N-Fmoc are ^{13}C-labeled, and the ^{15}N notion indicates ^{15}N-labeling of the amide bond (Chart 1). Fmoc-L-Ala, Fmoc-L-Val, Fmoc-L-Gly, Fmoc-L-Cys-trt, and Fmoc-L-Leu were supplied by Novabiochem (Darmstadt, Germany), and Fmoc-L-Leu-PEG-PS was supplied by Applied Biosystems (Foster City, CA). O-(7-Azabenzotriazole-1-yl)-N, N,N'N'-tetramethyluronium hexafluorophosphate (HATU) was supplied by GenScript Corporation (Piscataway, NJ).

2.2.2 Peptide Synthesis. The model peptide $(LGVCVGL)_2$ (**1a**), and its stable isotope-labeled derivatives $(LGV[U\text{-}^{13}C_5, {}^{15}N]CVGL)_2$ (**1b**) , and $(LGVCV[U\text{-}^{13}C_5, {}^{15}N]GL)_2$ (**1c**) (Chart 2.1) were synthesized from their respective linear Cys-containing peptides (of the general structure **1d**). The linear peptides were synthesized using solid phase Fmoc-chemistry on a Pioneer™ Peptide Synthesis System. Following the synthesis, the crude material was washed

Chart 2.1. Model peptides used in this study. Peptides 1b and 1c contain ^{13}C and ^{15}N labeled amino acids (indicated in bold font).

Peptide 1a

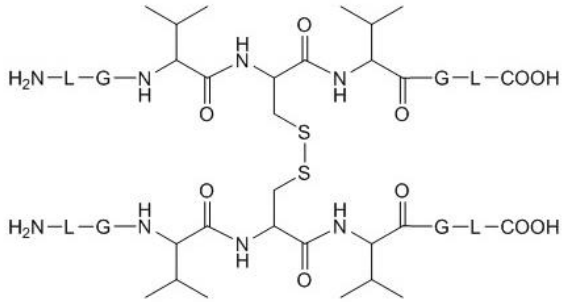

Peptide 1c

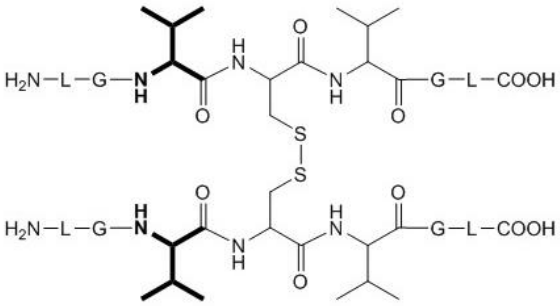

Peptide 1b

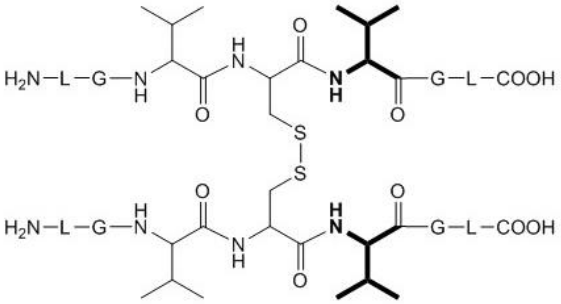

Peptide 1d

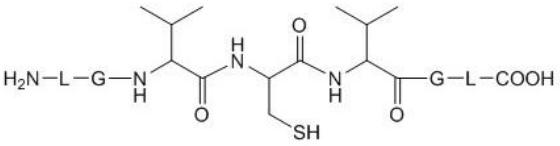

with methanol and dichloromethane. The thiol was deprotected and the peptide was cleaved from the resin using reagent R (TFA, thioanisole, EDT, and anisole at a ratio of 90%:5%:3%:2% (v:v:v)) as described in detail elsewhere.[45] Peptides **1d** were purified from the crude mixture by HPLC using a YMC-Pack ODS-A semipreparative C18 column with dimensions of 250 x 20 mm ID containing 5 µm particles (YMC America, Inc. Allentown, PA), with a 5 ml min^{-1} flow rate. Mobile phases consisted of water, acetonitrile, and trifluoroacetic acid at a ratio of 90%:10%:0.1% (v:v:v) for solvent A and a ratio of 10%:90%:0.1% (v:v:v) for solvent B. A linear gradient was developed from 10% to 90% B within 30 min. Following lyophilization, the purified thiol peptides were reconstituted for oxidation to 1 mg/mL in a solution of 50 mM ammonium bicarbonate buffer containing 20% dimethyl sulfoxide at pH 7.8. The oxidation reaction was allowed to proceed at room temperature, open to air, for four hours to form peptides

1a, **1b**, and **1c**.[46] The disulfide peptides were then purified using the semipreparative C18 column and lyophilized prior to experimentation.

2.2.3 UV Irradiation of Model Peptides. Peptides **1a**, **1b**, and **1c** (Chart 2.1) were dissolved in water at pH 4.0 or 7.0 to a concentration of either 100 nM or 100 μM. The solutions were Ar-saturated through head-space equilibration with Ar for thirty minutes in quartz tubes capped with rubber stoppers. The solutions were then irradiated at $\lambda = 254$ nm (flux of 2.96×10^{-4} einstein.min^{-1}, measured by actinometry) for up to ten minutes in a Rayonet photoreactor equipped with 4 lamps (Southern New England, Branford, CT, RMA-500) at room temperature. Directly after photolysis, samples were either derivatized with N-ethylmaleimide (NEM) or beta-mercaptoethanol (BME) or frozen at -20 °C until mass spectrometry analysis. Free thiols were derivatized with 1.8 mM NEM for one hour at 37˚C and one hour at room temperature in 50 mM ammonium bicarbonate buffer, pH 7.8. The free amines were also derivatized with NEM at this pH because amine derivatization is favorable at pH > 7.0.[47] To separate samples, α,β-unsaturated carbonyl products were reacted with 10 mM BME for two hours at room temperature in 50 mM ammonium bicarbonate buffer, pH 7.8.[48,49]

2.2.4 AAPH Reaction with Peptide 1d. Cys thiyl radicals were generated via reaction of peptide **1d** with carbon-centered radicals generated from the thermal decomposition of AAPH.[50] Peptide **1d** (Chart 2.1) was dissolved in 50 mM sodium phosphate buffer at a range of pH values from 6.0-10.0 at a concentration of 100 μM.[51] Peptide solutions were placed in glass tubes, capped with rubber stoppers, and saturated with Ar for 30 minutes. Similarly, a solution of 10 mM AAPH in pH 7.0, 50 mM sodium phosphate buffer was placed on ice and also saturated with Ar in a glass tube with a rubber stopper for 30 minutes. Following saturation, a final

concentration of 1 mM AAPH was added to the peptide samples under the Ar environment and incubated for 1 hour at 37 °C, generating $4.9x10^{-6}$ M AAPH-derived radicals.

2.2.5 LTQ-FT Mass Spectrometry Analysis. For higher sensitivity of product characterization, the peptides were analyzed on a linear trap quadrupole-Fourier transform (LTQ-FT) ion cyclotron resonance mass spectrometer (Thermo-Finnigan, Bremen, Germany) combined with an NanoAcquity UPLC System (Waters Corp., Milford, MA, USA). The instrument was operated in a data-dependent acquisition mode with all lenses optimized on the MH+ ion from leucine enkephalin. The ESI source was operated with a spray voltage of 2.8 kV, a tube lens offset of 96 V and a capillary temperature of 200 °C. The peptides were eluted from a reverse phase non-porous Imtakt Presto FF-C18 column with dimensions of 15 cm x 0.5 mm ID, containing 2 µm particles (Imtakt Corp., Philadelphia, PA, USA), at a flow rate of 5 µL min^{-1}. The mobile phases consisted of H_2O, acetonitrile, and formic acid at a ratio of 99.9%:0%:0.1% (v:v:v) for solvent A and a ratio of 0%:99.9%:0.1% (v:v:v) for solvent B. A linear gradient was developed from 3% to 40% B within 50 minutes. The XCalibur software was used to acquire and analyze the data.

2.2.6 Q-tof Mass Spectrometry Analysis. Peptides and photoproducts were analyzed on a Micromass Q-Tof Premier mass spectrometer (Micromass Ltd., Manchester, U.K.) combined with an Acquity UPLC System (Waters Corp., Milford, MA, USA). The instrument was operated in the MS^E mode with all lenses optimized on the MH+ ion from sodium iodide. The ESI source was operated with a spray voltage of 2.5 kV, a tube lens offset of 75 V and a capillary temperature of 250 °C. The peptides were eluted from a Grace reverse phase capillary C18 column with dimensions of 25 cm x 0.5 mm containing 5 µm particles (Fisher Scientific, Pittsburg, PA), at a flow rate of 20 µL min^{-1}. The mobile phases consisted of H_2O, acetonitrile,

and formic acid at a ratio of 99.9%:0%:0.1% (v:v:v) for solvent A and a ratio of 0%:99.9%:0.1% (v:v:v) for solvent B. A linear gradient was developed from 15% to 50% B in 43 minutes. MassLynx software was used to acquire and analyze the data.

2.2.7 ^{1}H-NMR. ^{1}H-NMR spectra were recorded on a Bruker Avance 400 MHz NMR instrument, equipped with a X-channel observe quadrupole nuclei probe. Peptide **1d** was dissolved to a concentration of 50 µM in 50 mM sodium phosphate buffer at pH 9.0,[51] and 10 mM AAPH was dissolved in 50 mM sodium phosphate buffer at pH 7.0 and placed on ice. Both solutions were placed in glass tubes, capped with rubber stoppers, and saturated with Ar for 30 minutes. Following saturation, a final concentration of 1 mM AAPH was added to the sample under Ar and incubated for 1 hour at 37 °C. The sample was left at room temperature for 2 days before being concentrated to dryness in a CentriVap concentrator and re-diluted with D_2O at pD 3.0. Then, 600 µL each of the sample and two controls (unreacted peptide **1d** and AAPH in the absence of peptide **1d,** respectively) were placed in NMR tubes (Wilmad LabGlass, Vineland, NJ) for NMR analysis. ^{1}H-NMR spectra were generated using 1024 scans and a pulse width of 14.25 seconds. Chemical shifts were predicted in ChemBioDraw Ultra 13.0 (Perkin Elmer, Waltham, MA) and an online NMR predictor program developed at the Ecole Polytechnique Fédérale de Lausanne (EPFL).[52] NMR data were analyzed using MestReNova version 9.0 (Mestrelab Research, Santiago de Compostela, Spain).

2.2.8 ^{1}H-^{1}H TOCSY (Total COrrelation SpectroscopY) NMR. ^{1}H-^{1}H TOCSY NMR spectra were recorded on a Bruker Avance 800 MHz NMR instrument, equipped with a TCI cryoprobe. Peptide **1a** was dissolved to a concentration of 100 µM and Ar-saturated through head-space equilibration with Ar for thirty minutes in quartz tubes capped with rubber stoppers. The solution was then irradiated at λ = 254 nm and frozen at -20 °C until further analysis. Then,

600 µL of irradiated peptide **1a** and control (non-irradiated) peptide **1a** were placed in NMR tubes (Wilmad LabGlass, Vineland, NJ) for NMR analysis. ^{1}H-^{1}H TOCSY NMR spectra were generated with a mixing time of 80 msec. Chemical shifts were predicted in ChemBioDraw Ultra 13.0 (Perkin Elmer, Waltham, MA). NMR data were analyzed using MestReNova version 9.0 (Mestrelab Research, Santiago de Compostela, Spain).

2.2.9 ^{1}H-^{13}C HSQC (Heteronuclear Single Quantum Coherence) NMR. ^{1}H-^{13}C HSQC NMR spectra were recorded on a Bruker Avance 800 MHz NMR instrument, equipped with a TCI cryoprobe. Peptides **1b and 1c** were dissolved to a concentration of 100 µM and Ar-saturated through head-space equilibration with Ar for thirty minutes in quartz tubes capped with rubber stoppers. The solutions were then irradiated at λ = 254 nm and frozen at -20 °C until further analysis. Then, 600 µL of irradiated peptide **1b, 1c** and control (non-irradiated) peptide **1a** and **1b** were placed in NMR tubes (Wilmad LabGlass, Vineland, NJ) and ^{1}H-^{13}C HSQC NMR spectra was acquired. Chemical shifts were predicted in ChemBioDraw Ultra 13.0 (Perkin Elmer, Waltham, MA). NMR data were analyzed using MestReNova version 9.0 (Mestrelab Research, Santiago de Compostela, Spain).

2.2.10 Ozonolysis Reaction with Peptide 1a Photoproducts. Peptide **1a** was dissolved in water at pH 7.0 to a concentration of 100 µM, Ar-saturated, and irradiated at λ = 254 nm for ten minutes. Directly after photolysis, samples were frozen at -20 °C until ozonolysis. Ozone (O_3) was generated using an ozonolysis apparatus (Ozotech, Inc., Yreka, CA). The O_3 was then bubbled directly into the samples for 30 seconds at room temperature or bubbled into water for 2 minutes, and then the O_3-containing water was added to the samples. Directly after the ozonolysis reactions were completed, 0.1 M sodium borohydride was added to the samples and

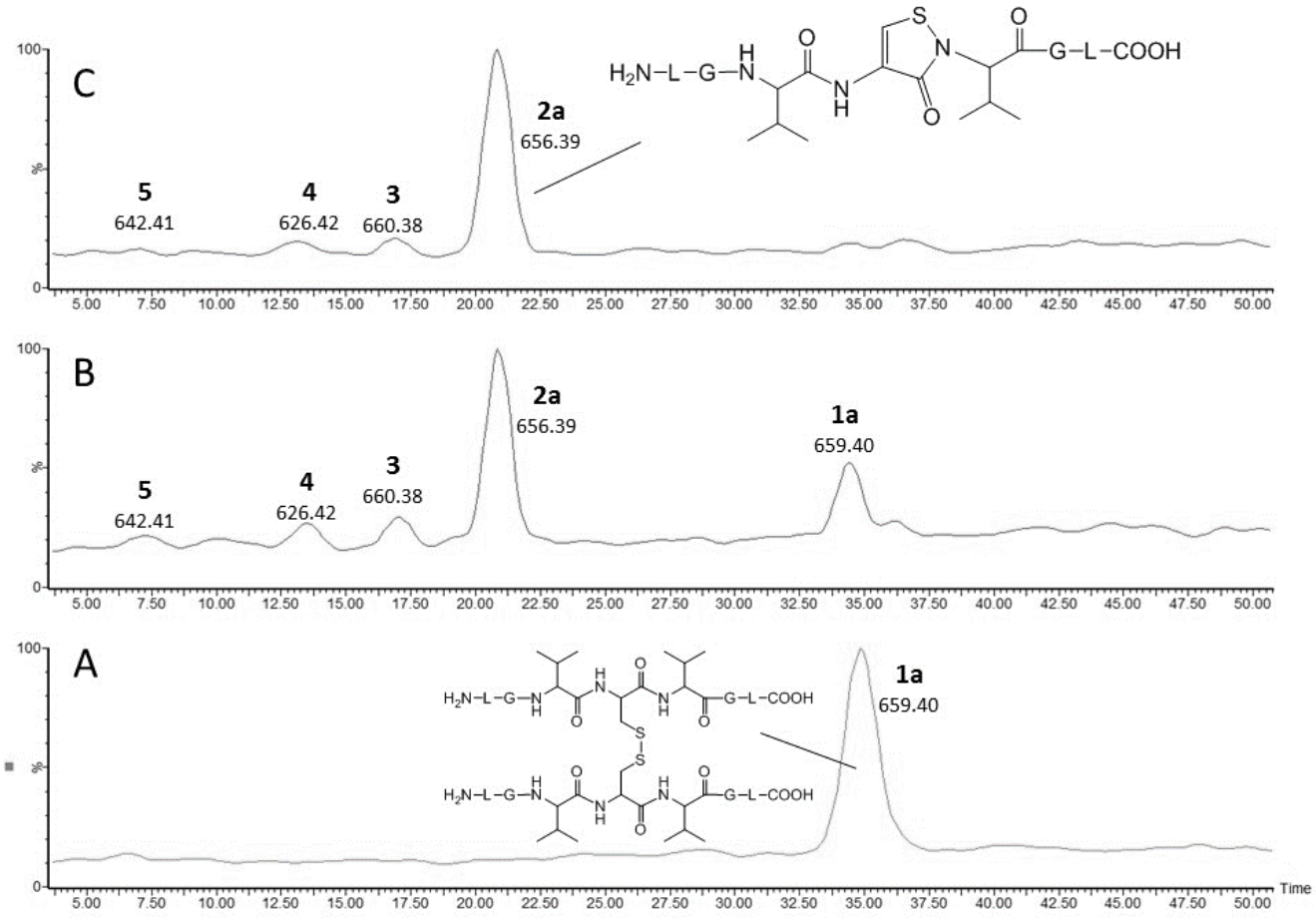

Figure 2.1 LC-MS analysis of the photoproducts generated by UV-irradiation at λ = 254 nm of peptide **1a** (100 nM) in Ar-saturated H_2O, pH 7.0: (A) no irradiation (control); (B) 30 seconds of irradiation; (C) 1 minute of irradiation.

reacted at room temperature for 30 minutes. The samples were then frozen at -20 °C until MS analysis.

2.3. Results

2.3.1 Photo-irradiation of 100 nM Peptide 1a at pH 7.0. Peptide **1a** (Chart 2.1) was dissolved in water to a concentration of 100 nM at pH 7.0. Solutions of 100 uL were exposed to light at λ = 254 nm at room temperature for up to 10 minutes in quartz tubes following Ar - saturation. The resultant photoproducts of peptide **1a** were then analyzed by LC-MS using the Q-tof Premier (Figure 2.1) and MS/MS using the LTQ-FT instrument. No traces of products were observed in non-irradiated control samples (Figure 2.1A). However, after 1 minute of irradiation

Product	Proposed Structure	MS/MS
2a	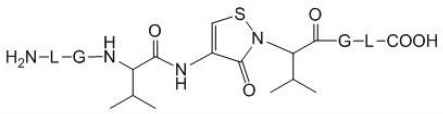	Fig. 2.2
2b	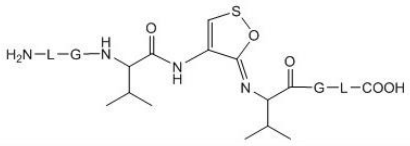	NA
3	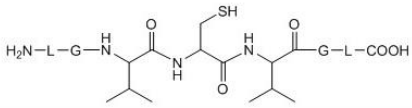	Fig. 2.3
4	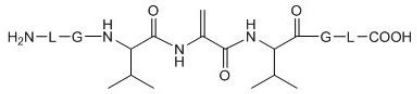	Fig. 2.4
5	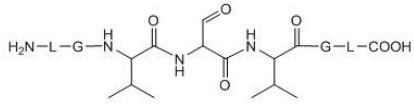	Fig. 2.5

Table 2.1. Peptide **1a** photoproducts observed after photolysis at λ = 254 nm.

(Figure 2.1C), peptide **1a** was completely degraded to one major photoproduct and three minor photoproducts. A tentative structure of product **2a** (m/z 656.4) is displayed in the chromatogram in Figure 2.1C and in Table 2.1. Table 2.1 also shows an alternative structure for product **2a,** the isobaric structure **2b** (m/z 656.4), and the structures for the minor photoproducts formed: **3** (m/z 660.4), **4** (m/z 626.4), and **5** (m/z 642.4). Mass spectrometry, NMR analysis and chemical derivatization were used to assign structures to the photoproducts, as will be described in the following sections.

i. Product 2a (m/z 656.4). After just 30 seconds of UV irradiation (Figure 2.1B), 60% of peptide **1a** were converted into product **2a**. Following one minute of irradiation (Figure 2.1C), 90% of peptide **1a** were converted to product **2a**, which was still the major photoproduct after 10 minutes of irradiation, albeit at a 35% yield because of the increase in yields of the other photoproducts (LC-chromatogram and table of photoproducts presented in Appendix A, Figure A.1 and Table A.1). Product **2a** was quantified via peak area of the chromatographic peak relative to the peak area of peptide **1a** (assuming similar response factors). The m/z value of product **2a** reveals a loss of 4 Da compared with peptide **1d**, i.e. the reduced, Cys-containing half of the original disulfide-containing peptide **1a**. By MS/MS analysis, the loss of 4 Da is localized to the Cys residue of the peptide, highlighted by the b3 and b4 ions in the fragmentation scheme

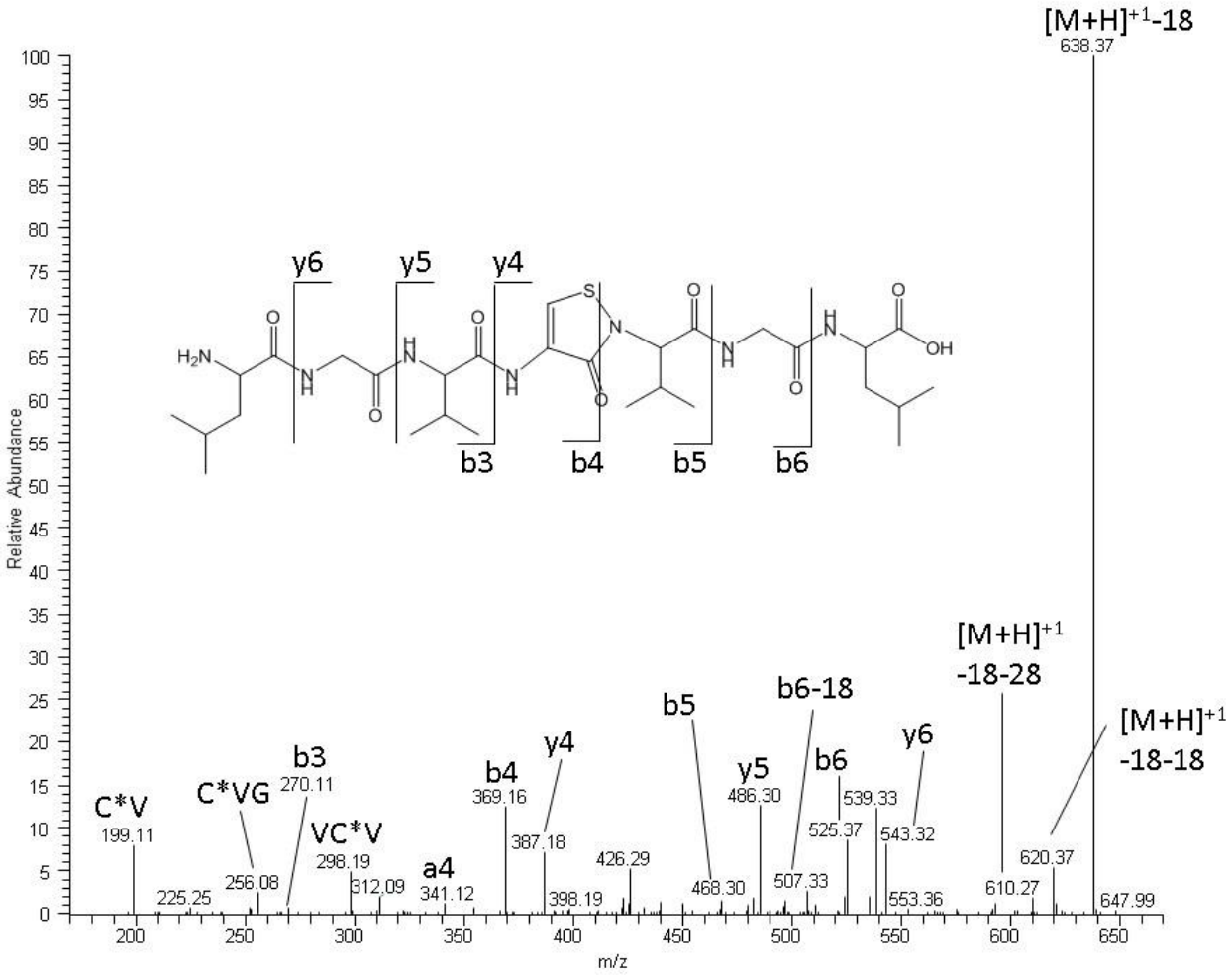

Figure 2.2. MS/MS spectrum of product **2a** after UV irradiation at λ = 254 nm of peptide **1a** at pH 7.0 (100 nM) in an Ar-saturated H_2O. C* corresponds to the modified Cys sulfenamide structure.

displayed in Figure 2.2. On the other hand, the y4, y5, and y6 ions clearly show that the N-terminal LGV moiety of the peptide is unaltered. Likewise, the b5 and b6 ions reveal that the C-terminal GL moiety is unaltered. Lower molecular weight ions (i.e. b1, b2, y1, and y2) are frequently not observed in the LTQ-MS data because of the m/z cutoff between 170-200 Da. At this point, we tentatively assign to product **2a** the structure of an isothiazol-3(2H)-one, which contains an S-N bond in combination with a double bond between the $^{\alpha}C$-$^{\beta}C$ bond of the original Cys residue. However, based on the mass spectrometry data alone we cannot exclude the possibility of an S-O bond such as shown in product **2b**. A clear distinction between both structures was subsequently achieved by ^{1}H-NMR experiments, as described in section 2.3.8 (see

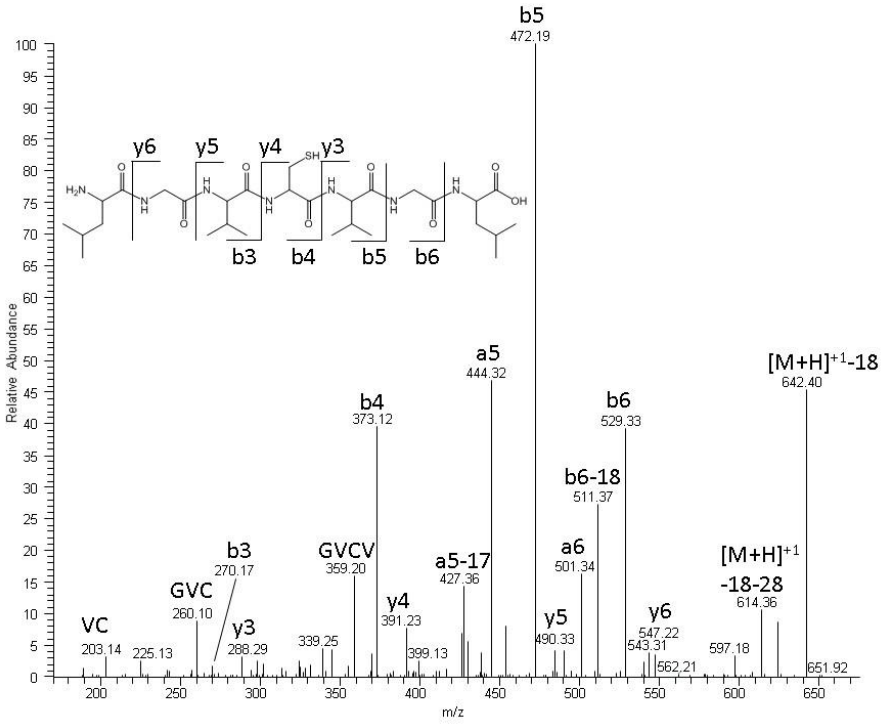

Figure 2.3. MS/MS spectrum of product **3** after UV irradiation at λ = 254 nm of peptide **1a** at pH 7.0 (100 nM) in an Ar-saturated H_2O.

below). The highest intensity fragment observed during MS/MS analysis of product **2a** is that of $[M+H]^{+1}$-18, i.e. of the molecular ion, which has lost one water molecule. Instead, the intensities of the remainder ions is between 5-15% compared to that of $[M+H]^{+1}$-18. Notably, the MS/MS lack any ions which display a loss of 34 Da, i.e. of H_2S, consistent with the lack of a free thiol. Importantly, the sulfenamide structure is consistent with the formation of the b4 ion, as it has been shown that the S-N bond in cyclic sulfenamides can be cleaved via gas phase fragmentation.[53] In the literature, the ESI fragmentation of a cyclic sulfenamide, sulfinamide, and sulfonamide formed between neighboring Lys and Cys residues in the peptide PFKCG reported the b and y ions consistent with a loss of 2 Da on the Cys residue (combined with oxidation in the case of sulfinamide and sulfonamide) through the cleavage of the S-N bond.

*ii. Product **3** (m/z 660.4).* The disproportionation of thiyl radicals leads to thiol and thioaldehyde, as documented for the photo-irradiation of $(GGCGGL)_2$[28] and $(LGACAGL)_2$.[40] Product **3** is structurally identical to peptide **1d** and accounts for 7% of the total products after 30 seconds of photo-irradiation (Figure 2.1B). The MS/MS spectrum (Figure 2.3) clearly shows all

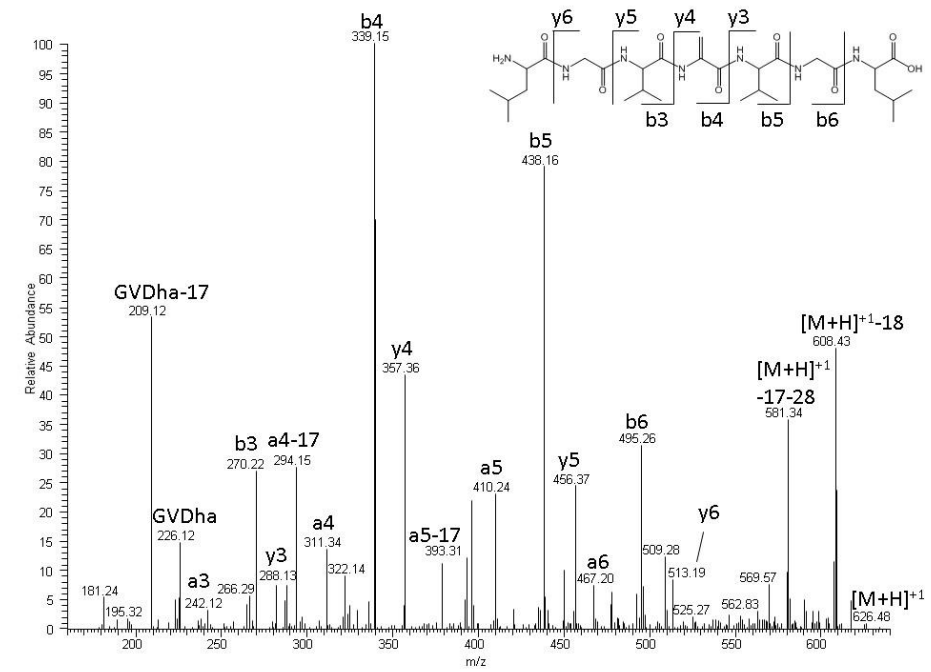

Figure 2.4. MS/MS spectrum of product **4** after UV irradiation at λ = 254 nm of peptide **1a** at pH 7.0 (100 nM) in an Ar-saturated H_2O.

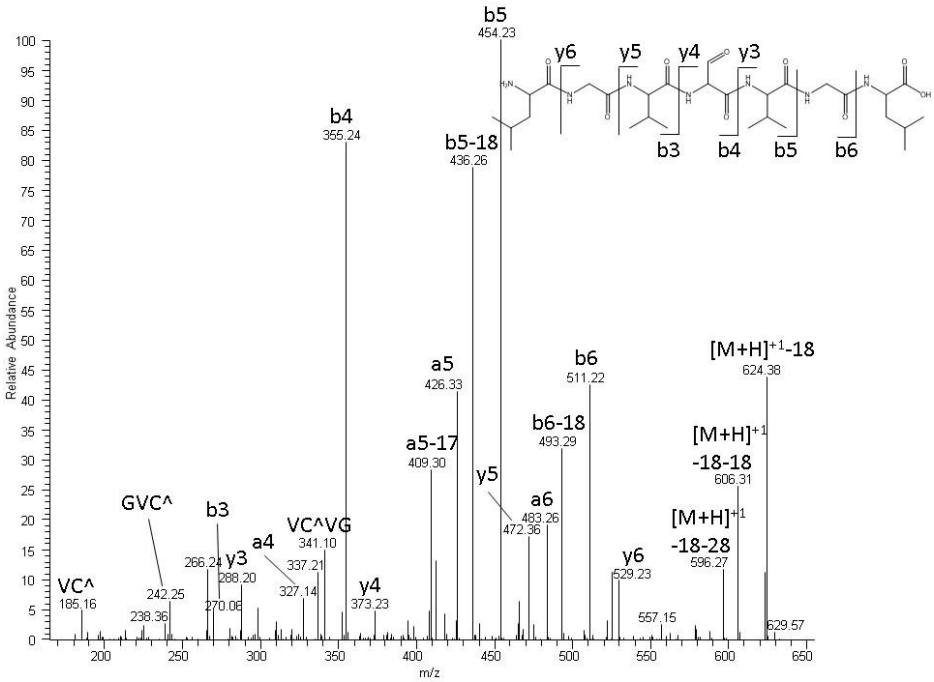

Figure 2.5. MS/MS spectrum of product **5** after UV irradiation at λ = 254 nm of peptide **1a** at pH 7.0 (100 nM) in an Ar-saturated H_2O. C^ corresponds to the modified Cys aldehyde structure.

the y and b ions which are consistent with the reduction of the disulfide to the thiol. Specifically, b3, b4, y3, and y4 confirm the presence of reduced Cys. The relative intensities of the fragment ions of this product are much more evenly distributed among all the product ions. The b5 ion is the most intense ion, but the ion generated from the loss of water by dehydration of the C-terminal, the b4, a5, and b6 ions are also intense.

*iii. Product **4** (m/z 626.4).* Product **4** contains a dehydroalanine (Dha) residue in place of the

Product	Proposed Structure	MS/MS
2a+NEM	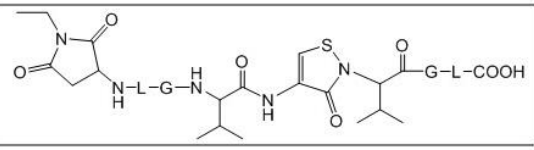	Fig. 2.6
3+NEM	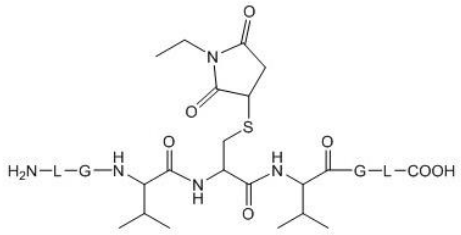	Fig. 2.7
4+NEM	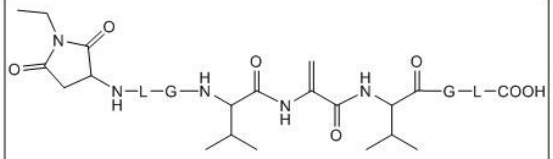	Fig. 2.8
5+NEM	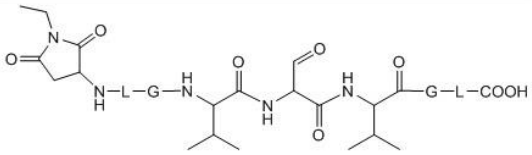	Fig. 2.9

Table 2.2. Peptide **1a** photoproducts derivatized with NEM.

original Cys residue. This product also accounts for 7% of the total products formed after 30 seconds of irradiation (Figure 2.1B). The formation of Dha had been earlier characterized for the photo-irradiation of $(LGACAGL)_2$.[40] The MS/MS spectrum (Figure 2.4) of this product reveals is consistent with Dha formation, where the b3, b4, b5 and y3, y4, and y5 ions localize the Dha residue to the original position of Cys.

*iv. Product **5** (m/z 642.4).* Figure 2.1B shows trace amounts of product **5** after 1 minute of photo-irradiation. The MS/MS spectrum (Figure 2.5) is consistent with the formation of an aldehyde at the original Cys residue, generated through hydrolysis of a thioaldehyde, the other disproportionation product of Cys thiyl radicals.[28] This product is formed through the oxidation of the thioaldehyde, the other disproportionation product besides the thiol.

2.3.2 Derivatization of Photoproducts with N-ethylmaleimide (NEM). Further product identification following 10 minutes of irradiation of 100 nM peptide **1a** at pH 7.0 was achieved by derivatization with NEM. For this, an aliquot of the sample was removed and a final concentration of 1.8 mM NEM was added. The pH was then adjusted to pH 7.8 with 50 mM ammonium bicarbonate buffer, amenable for both derivatization of free thiols and amines.[47] MS

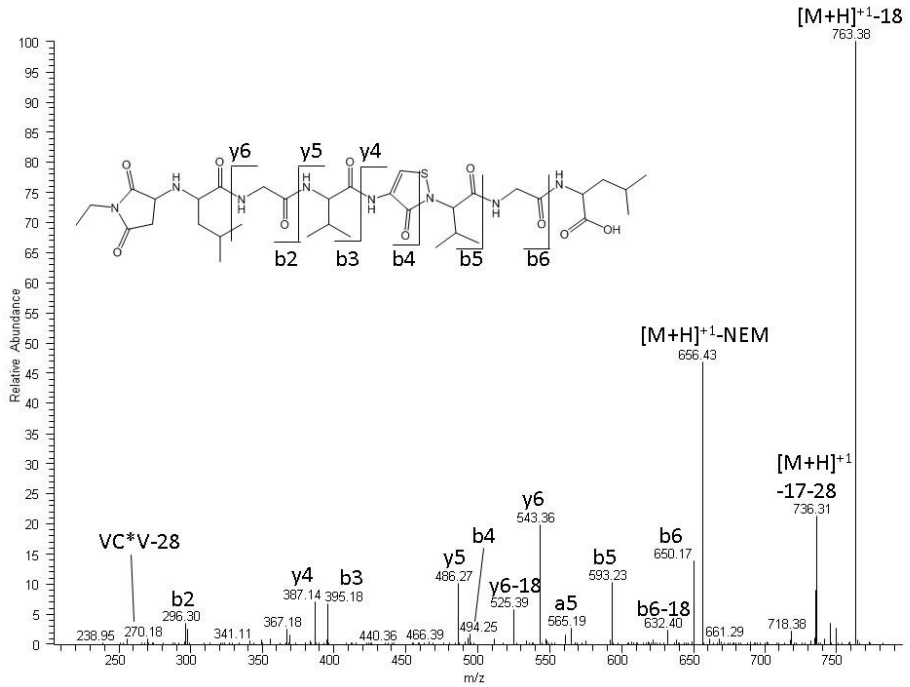

Figure 2.6. MS/MS spectrum of product **2a** derivatized with NEM. C* corresponds to the modified Cys sulfenamide structure.

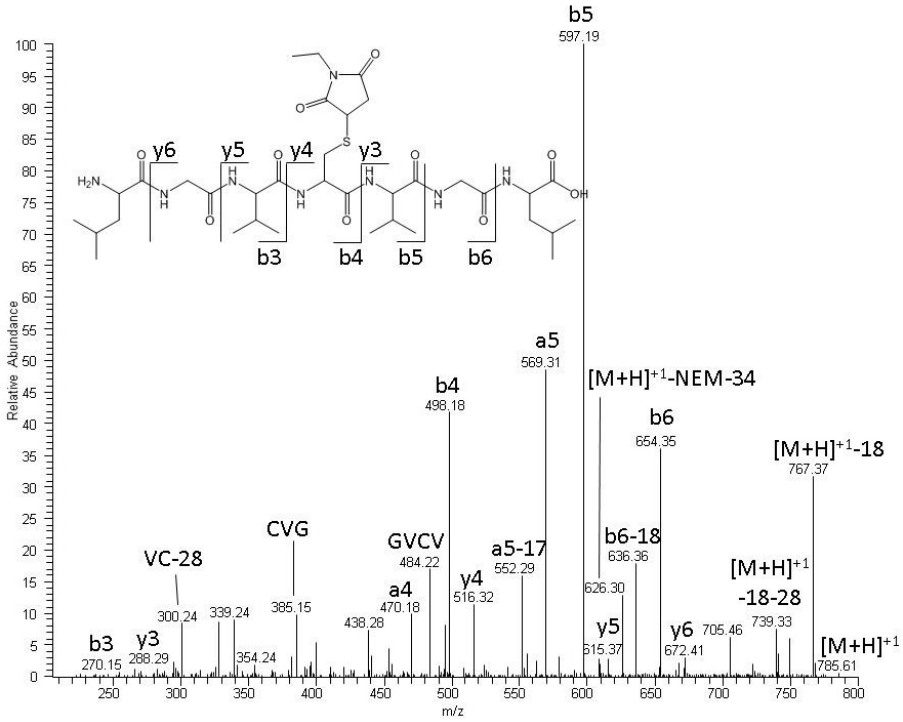

Figure 2.7. MS/MS spectrum of product **3** derivatized with NEM.

analysis was performed on the LTQ-FT instrument. Table 2.2 shows the products detected after NEM derivatization. Products **2a+NEM** (m/z 781.4), **4+NEM** (m/z 751.4), and **5+NEM** (m/z 767.4) had NEM added to the N-terminal amine while product **3+NEM** (m/z 785.4) had NEM added to the thiol.

*i. Product **2a+NEM** (m/z 781.4).* Table 2.2 shows the structure of product **2a+NEM**. Characterization by MS/MS analysis confirms the addition of NEM to the N-terminal amino group (Figure

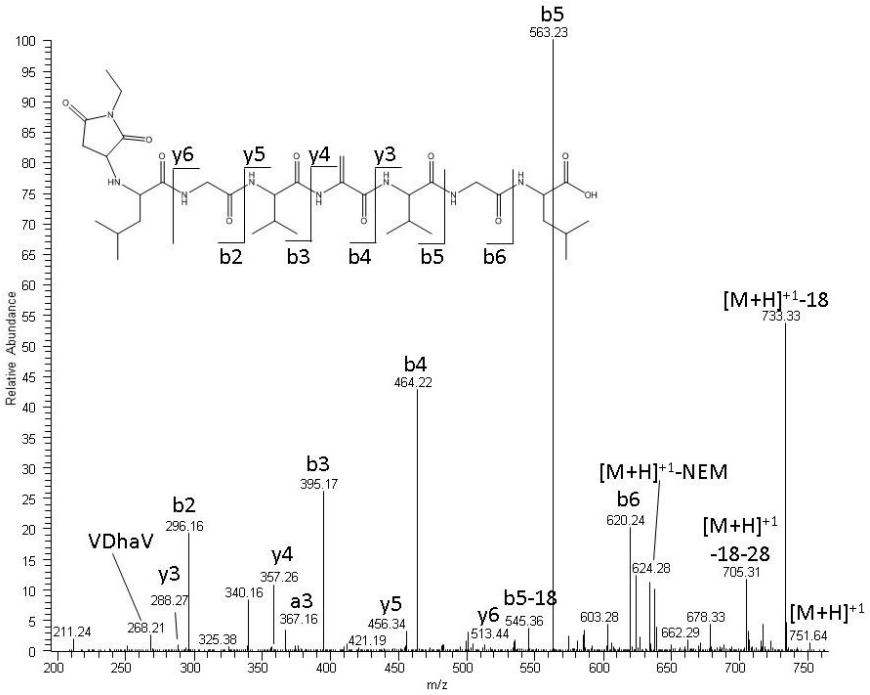

Figure 2.8. MS/MS spectrum of product **4** derivatized with NEM.

2.6). Neither of the y ions shows NEM addition while the b2 ion and subsequent b ions display the expected addition of 125 Da consistent with NEM addition to the N-terminal amino group. The ion intensities in this MS/MS spectrum are comparable to those of the non-derivatized product **2a** (Figure 2), except for the 125 Da mass change of the b-ions.

*ii. Product **3+NEM** (m/z 785.4).* As anticipated, product **3** is derivatized by NEM on the Cys moiety (Table 2.2). The ions b3, b4, y3, and y4 in the MS/MS spectrum localize the NEM addition to the Cys residue (Figure 2.7).

*iii. Product **4+NEM** (m/z 751.4).* The only nucleophile in product **4** amenable for reaction with NEM is the N-terminal amino group, and the MS/MS spectrum confirms the addition of NEM to the amino group in product **4+NEM** (Figure 2.8); the b2 ion of product **4+NEM** shows an increase by 125 Da compared to product **4**, and the remainder of the b ions support this derivatization. In contrast, the y-ion series does not display any increase by 125 Da.

*iv. Product **5+NEM** (m/z 767.4).*The MS/MS spectrum of product **5+NEM** indicates the addition of NEM to the N-terminal amine (Figure 2.9).

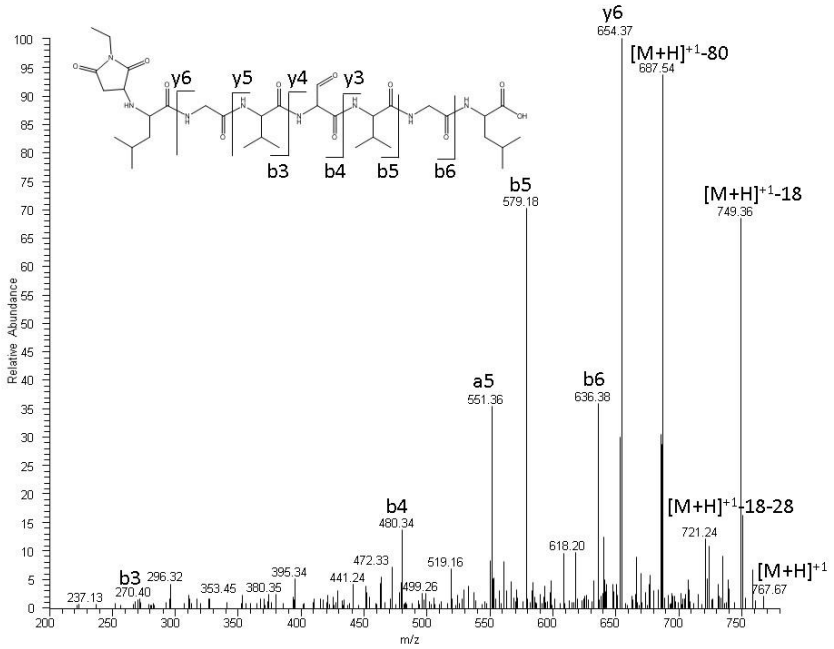

Figure 2.9. MS/MS spectrum of product **5** derivatized with NEM.

Product	Proposed Structure	MS/MS
2a+BME	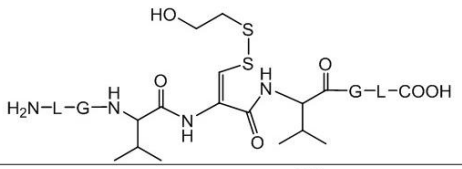	Fig. 2.10
2a+2BME	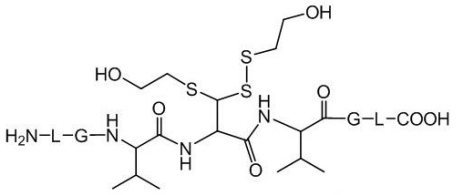	Fig. 2.12
4+BME	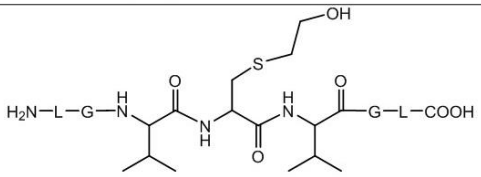	Fig. 2.12

Table 2.3. Peptide **1a** photoproducts derivatized with BME.

2.3.3 Derivatization of Photoproducts from 100nM Peptide 1a at pH 7.0 with β-mercaptoethanol (BME).

To localize α,β-unsaturated carbonyls, such as dehydroalanine, and the proposed S-N bond, a final concentration of 10 mM BME was added following 10 minutes photo-irradiation of 100nM peptide **1a**, pH 7.0. The pH was adjusted to pH 7.8 with 50 mM ammonium bicarbonate buffer, to shift the equilibrium toward the nucleophilic thiolate species. LC-MS/MS analysis was performed on the LTQ-FT instrument. Table 2.3 displays the products that formed after reaction with BME and the structures assigned to these products: product **2a+BME** (734.4), product **2a+2BME** (m/z 812.4), and product **4+BME** (m/z 704.4). Scheme 2.2 shows how product **2a** can be derivatized twice with BME: once through the cleavage of the S-N bond, and once to the double bond.

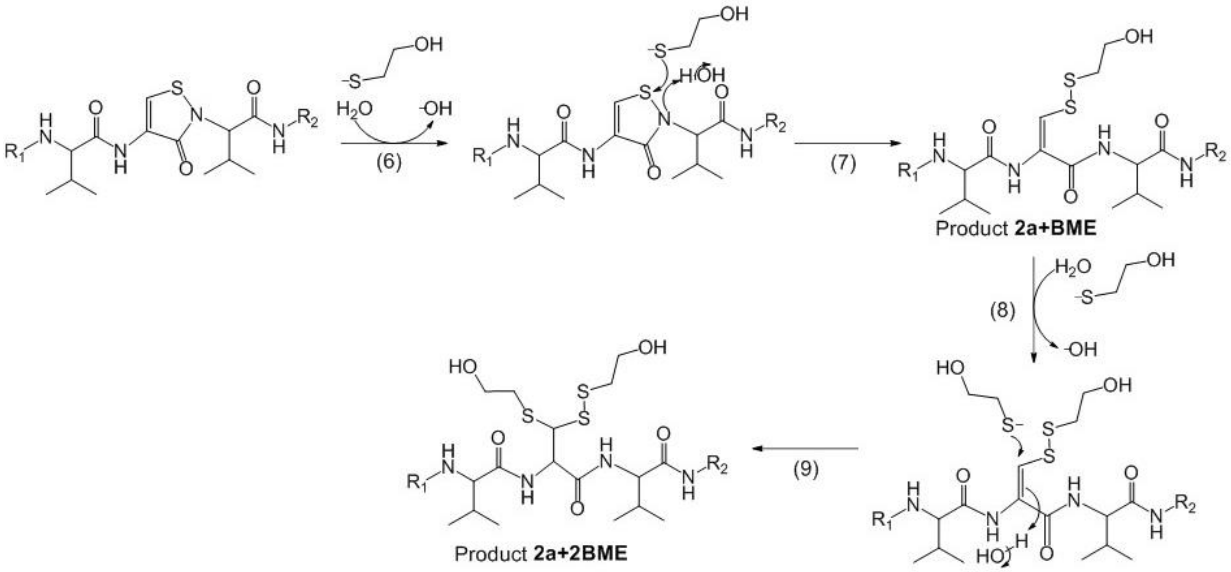

Scheme 2.2. Reaction of product **2a** with BME.

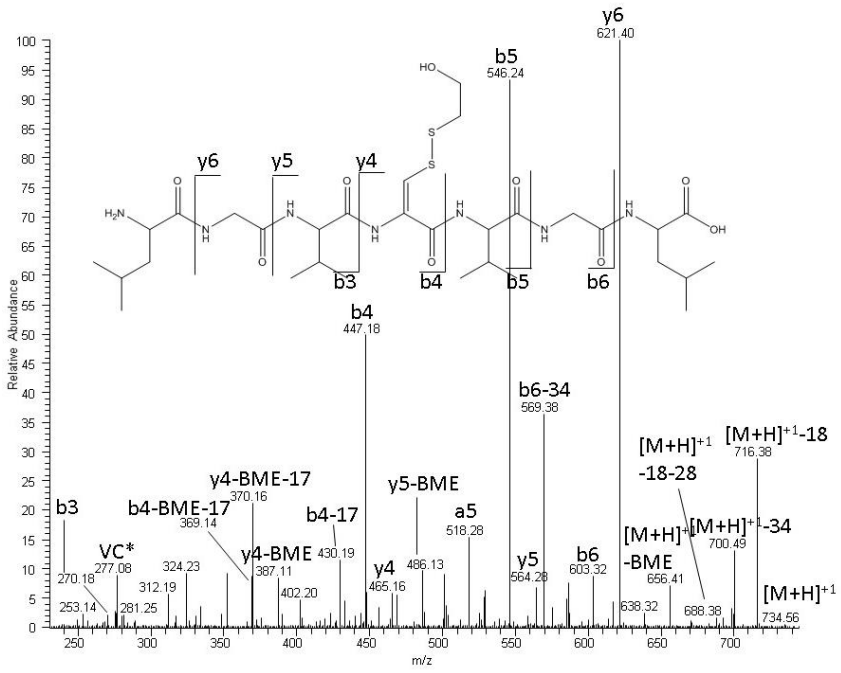

Figure 2.10. MS/MS spectrum of product **2a** mono-derivatized with BME.

*i. Product **2a+BME** (m/z 734.4).* MS analysis revealed a product from the addition of a single BME molecule to product **2a**.[54,55] Figure 2.10 shows the MS/MS spectrum, where the b3, b4 and y4 fragment ions indicate single BME derivatization on the Cys group. The b4, b5, and b6 fragments reveal that the C-terminal sequence VGL is unmodified, and the y4, y5, and y6 fragments reveal that the N-terminal sequence LGV is unmodified. The intensities of the fragment ions is different following BME addition to **2a** as compared to the precursor product **2a** (Figure 2.2). The most abundant ions are now the b5 and b6 ions. Interestingly, the b4 ion, which

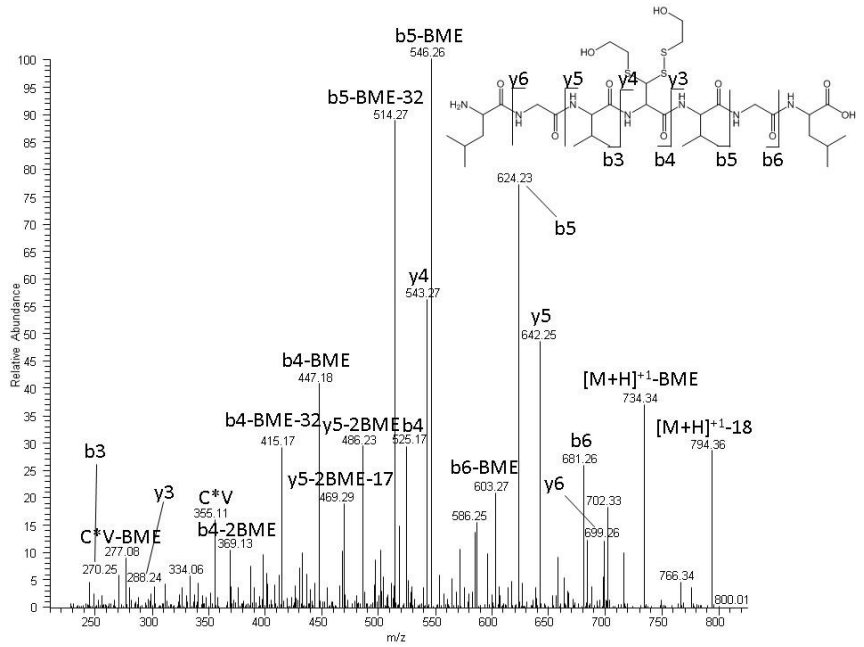

Figure 2.11. MS/MS spectrum of product **2a** di-derivatized with BME.

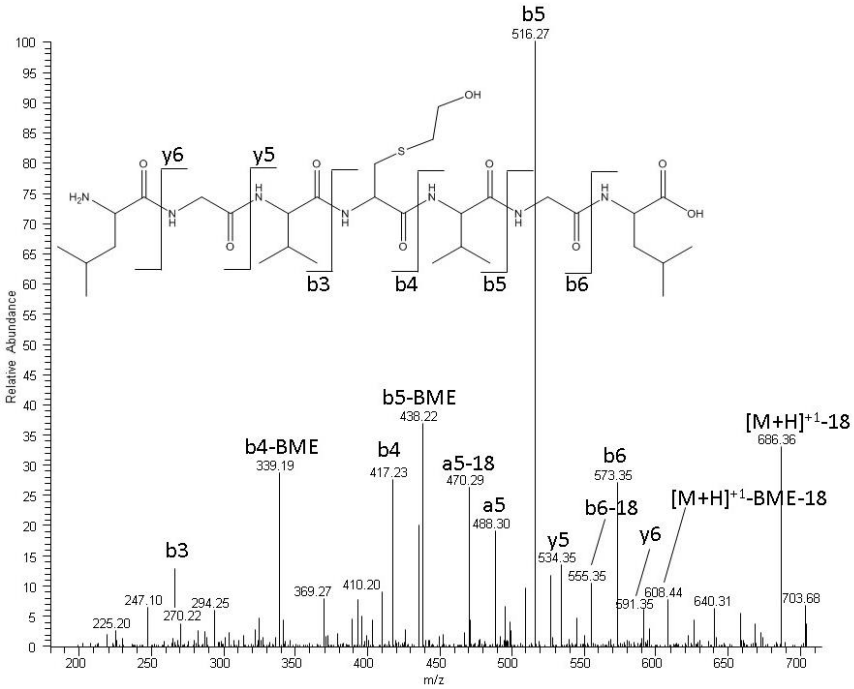

Figure 2.12. MS/MS of product **4** derivatized with BME.

must cleave the heterocyclic cross-link to undergo gas-phase fragmentation in product **2a**, is now much more intense after BME addition, which leads to chemical cleavage of the S-N bond prior to MS analysis (Scheme 2.2, reaction 6 and 7). Therefore, intensity of the b4 ion in Figure 2.2 is only about 15%, whereas the intensity of the b4 ion in Figure 2.10 is ca. 50%. Additionally, in the MS/MS spectrum of **2a+BME** we observe ions corresponding to the loss of BME, a common fragmentation product.

*ii. Product **2a+2BME** (m/z 812.4).* In addition to mono-derivatization, we observe a product revealing the addition of two molecules BME to product **2a**. The MS/MS spectrum of **2a+2BME** (Figure 2.11) reveals that these two BME molecules are added to the original Cys

residue. Specifically, the b3, b4, y3, and y4 ions localize the addition of 156 Da to the original Cys residue, consistent with Scheme 2.2. Many of the large fragments in the MS/MS spectrum show a loss of 1 or 2 BME molecules from the parent ion during gas phase ionization.

*iii. Product **4+BME** (m/z 704.4).* The MS/MS spectrum of product **4+BME**, and especially the b3, b4, y3 and y4 ions, is consistent with a Michael addition of BME to Dha produced from Cys (Figure 2.12).

2.3.4 Isothiazole-3(2H)-one Formation in Peptides 1a, 1b, and 1c at pH 7.0. We synthesized stable isotope-labeled peptides **1b** and **1c** in order to unambiguously locate the cyclic sulfenamide by means of isotopic substitution of the mass spectrometric fragment ions. Peptides **1a**, **1b** or **1c** were dissolved in water to a concentration of 100 µM at pH 7.0. Solutions of 100 uL were then exposed to light at λ = 254 nm for ten minutes in quartz tubes at room temperature after Ar-saturation. The resultant photoproducts from all three peptides were then analyzed by LC-MS on the Qtof Premier instrument. Figure 2.13 shows representative chromatograms recorded for the control (Figure 2.13A) and photo-irradiated peptide **1a** after ten minutes (Figure 2.13B). The sulfenamide product **2a** is the main product also under these experimental conditions; however, a number of additional products are generated as

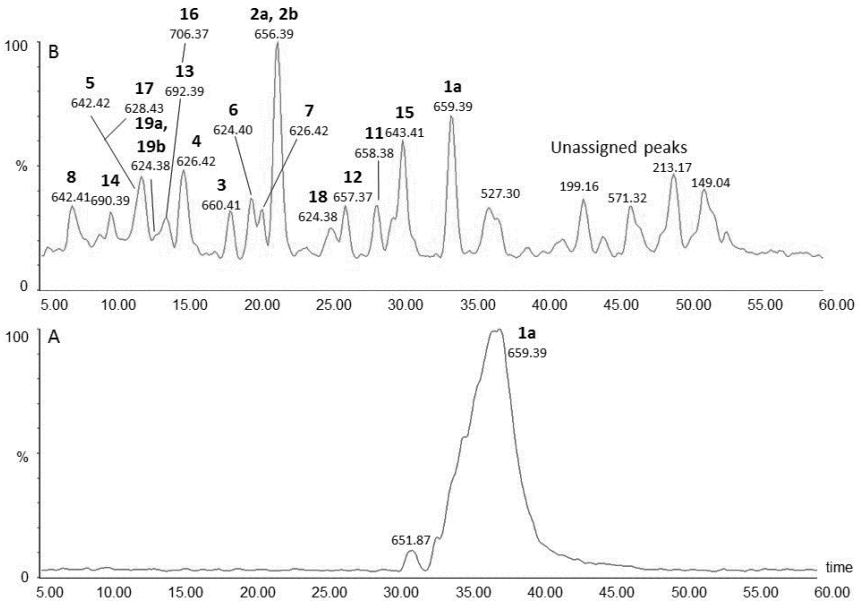

Figure 2.13. LC-MS analysis of the photoproducts generated by UV-irradiation at λ = 254 nm of peptide **1a** (100 µM) in Ar-saturated H_2O at pH 7.0 in the (A) control and (B) the sample after 10 minutes of irradiation.

Product	Proposed Structure	MS/MS
9	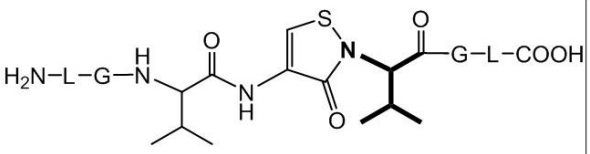	Fig. 2.14
10	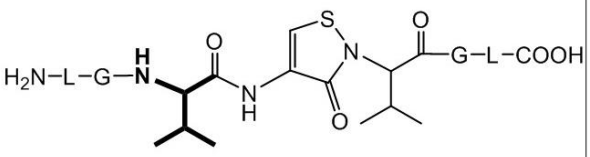	Fig. 2.15

Table 2.4. Peptide **1b** and **1c** sulfenamide photoproducts observed after 10 minutes of photolysis at λ = 254 nm. The ^{13}C and ^{15}N labeled amino acids are indicated in bold font.

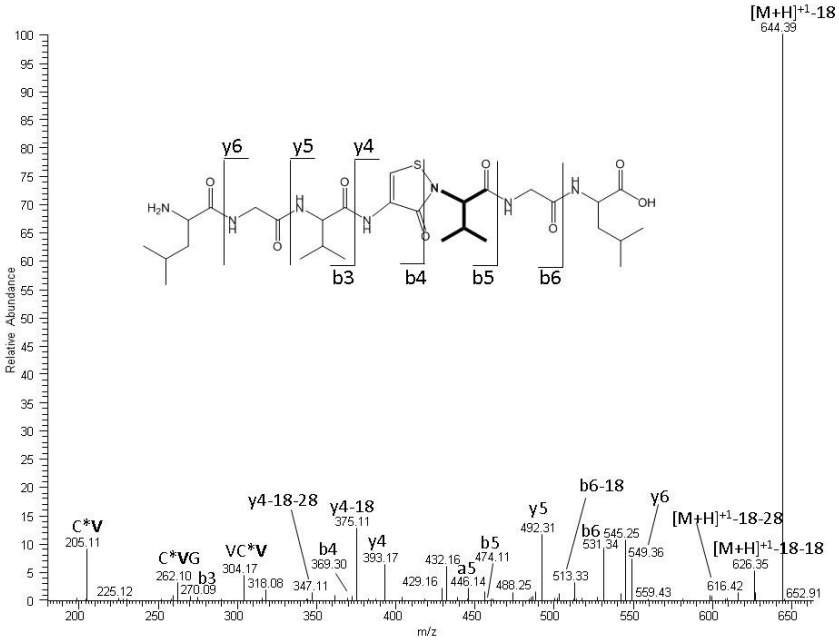

Figure 2.14. MS/MS spectrum of product **9** after UV irradiation at 254 nm. The ^{13}C and ^{15}N labeled amino acids are indicated in bold font, and the C* corresponds to the modified Cys sulfenamide structure.

well. These products, together with their MS and MS/MS data and tentative structural assignments are detailed in described in Section 2.3.9 (below). Our current focus is on product **2a**, which displays m/z 656.4 when generated from peptide **1a**, and as expected, m/z 662.4 for products **9** and **10** (Table 2.4), when generated from peptides **1b** and **1c**, respectively, due to the presence of ^{13}C and ^{15}N in one of the two Val residues. All the resultant photoproducts from peptide **1d** were analyzed on the LTQ-FT instrument in the M/MS and MS^3 modes. However, product **9** and **10** were purified by HPLC, and the purified products were analyzed on the LTQ-FT instrument in the MS/MS and MS^3 modes. The MS/MS data of product **2a** will not be described in detail here, as the MS/MS spectrum and results were described in Section 2.3.1.

*i. Product **9** (m/z 662.4).* Following the irradiation of peptide **1b**, product **9** was generated as a major photoproduct (Table 2.4). The m/z value of product **9** (m/z 666.4; Figure 2.14) shows a loss of 4 Da compared to the reduced Cys-containing derivative of peptide **1b**. As expected, product **9** eluted chromatographically exactly where product **2a** eluted. The MS/MS fragmentation of product **9** shows the same fragment ions as product **2a**, except for a mass shift of 6 Da for fragments containing the stable isotope-labeled C-terminal Val residue. For instance, while the b3 and b4 ions display m/z 270.1 and m/z 369.3, identical to the MS/MS data of product **2a** (Figure 2.2), the higher b ions and the y3 ions and higher show an increase of 6 Da compared to that of product **2a**. Product **9** shows a fragmentation profile comparable to product **2a**: the y4, y5, and y6 ions clearly show that the N-terminal LGV sequence of the peptide is unaltered and the b5 and b 6 ions show that the C-terminal GL sequence is unaltered. Importantly, there is a loss of 4 Da from the original Cys residue of the peptide, highlighted by the b3 and b4 ions.

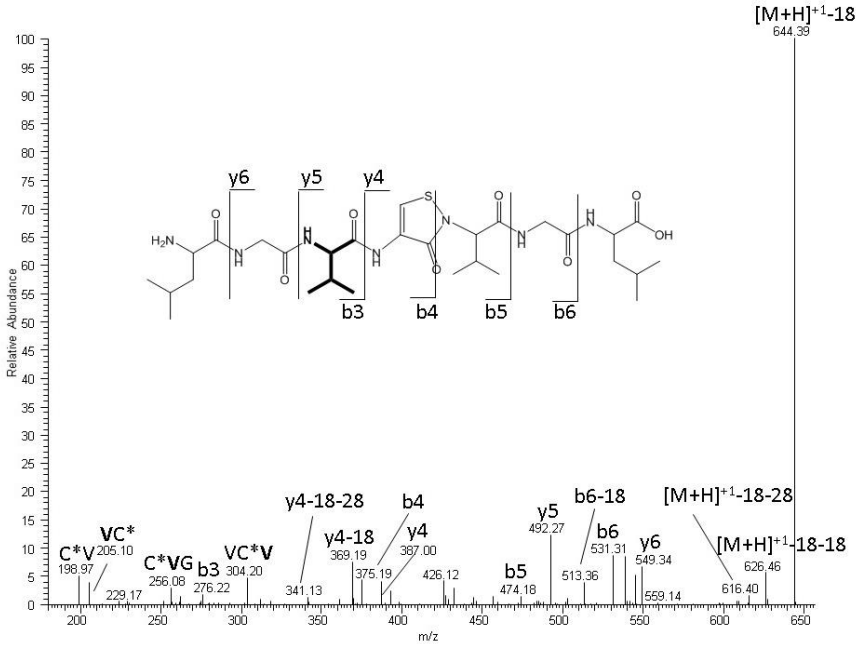

Figure 2.15. MS/MS spectrum of product **10** after UV irradiation at 254 nm. The ^{13}C and ^{15}N labeled amino acids are indicated in bold font, and the C* corresponds to the modified Cys sulfenamide structure.

*ii. Product **10** (m/z 662.4).* Photo-irradiation of Peptide **1c** generated product **10** (Table 2.4) as a major photoproduct. Product **10** (m/z 662.4; Figure 2.15) shows a loss of 4 Da compared to the reduced Cys-containing form of peptide **1c**. Product **10** co-eluted with

products **2a** and **9**. However, the MS/MS spectra of products **9** and **10** differ. The MS/MS spectrum of product **10** displays a y4 ion (m/z 387.0), similar to that of product **2a**, but a y5 ion (m/z 492.3) which is 6 Da heavier as compared to the y5 ion of product **2a**. The b ions show an increase in 6 Da compared to product **2a**. These data are, again, consistent with a modification of the Cys residue and a cyclic sulfenamide, highlighted by the b3 and b4 ions. The y4, y5, and y6 ions show that the N-terminal LGV sequence of the peptide is unaltered and the b5 and b6 ions show that the C-terminal GL sequence is unaltered.

2.3.5 MS^3 Fragmentation of Products 2a, 9, and 10. To further characterize the structures of products **2a**, **9**, and **10**, MS^3 experiments were performed on the respective b3, b4 and VC*V (where C* indicated the modified Cys sulfenamide structure) fragment ions extracted from the MS/MS data in Figures 2.2, 2.14, and 2.15, respectively. Other than isotopic mass differences between the fragments, the fragmentation profiles look generally similar, as expected for three identical products which only differ in the isotopic distributions on one of the Val residues. The MS^3 data, especially those for MS^3 of the internal fragment VC*V, support the structures of products **2a**, **9** and **10** and illustrate that only the Cys and the Val residue C-terminal to Cys are involved in sulfenamide formation. In addition, the distribution of isotopes in the MS^3 fragment ions allows us to assign fragmentation pathways (see Discussion).

*i. b3 fragment ions (m/z 270.2, 270.2, and 276.2 for products **2a, 9**, and **10**, respectively).* Figure 2.16 displays the MS^3 spectrum of the b3 ion from products **2a** (m/z 270.3), **9** (m/z 270.3), and **10** (m/z 276.3). In product **10** the isotopically labeled Val residue is located N-terminal to Cys, rendering the m/z value of the b3 ion 6 Da higher compared to the b3 ions from products **2a** and **9**. Figure 2.16A shows the MS^3 fragmentation of the b3 ion from product **2a** (m/z 270.3). All the ions seen in these spectra are common neutral losses indicative of a linear

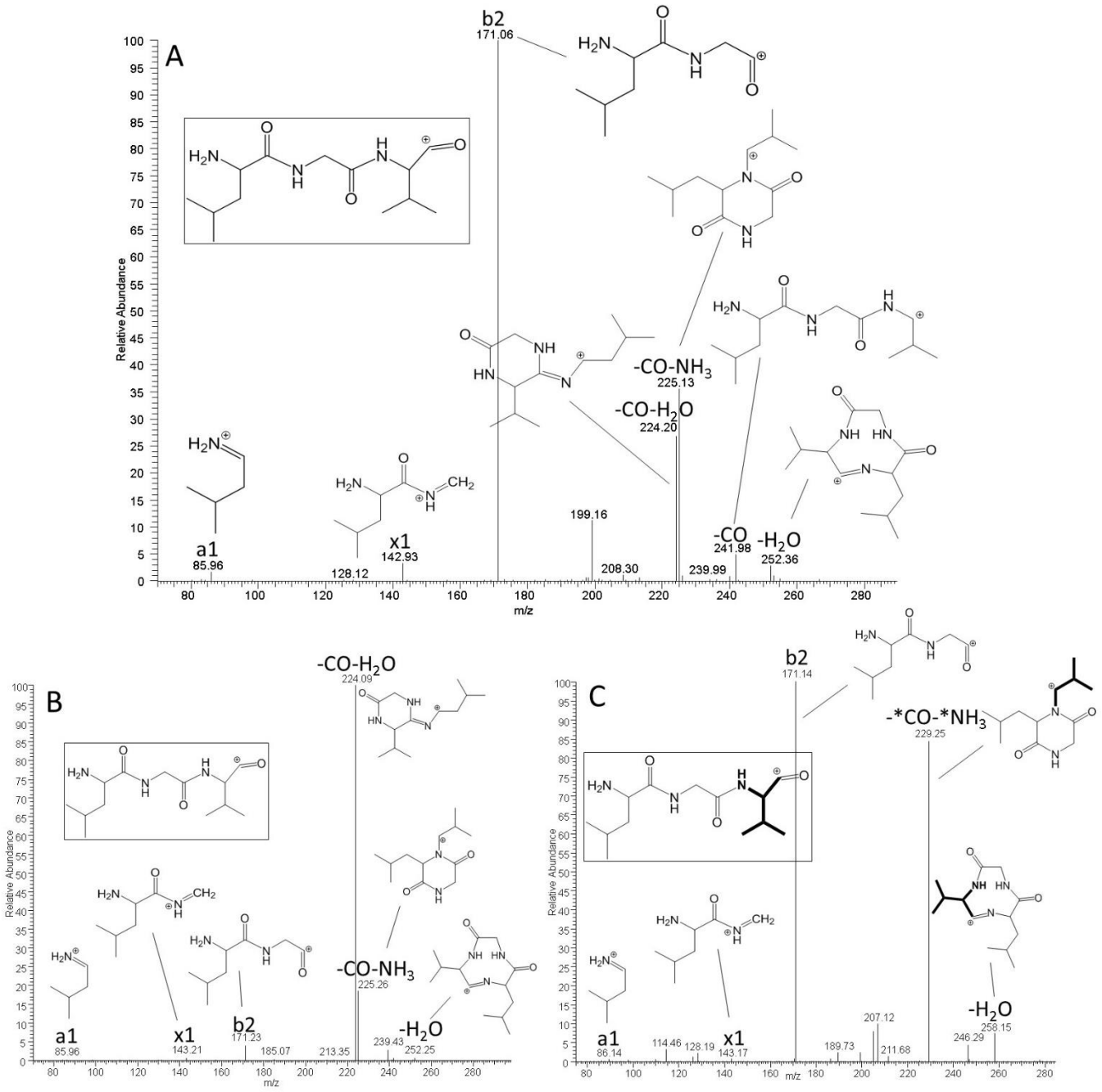

Figure 2.16. MS^3 fragmentation of the b3 ion from the MS/MS spectra of (A) product **2a**; (B) product **9**; (C) product **10**. The ^{13}C and ^{15}N labeled amino acids are indicated in bold font and with *C/N.

peptide with no modifications or internal cyclization. The ion with the highest intensity is the b2 ion (m/z 171.06) (a mechanistic scheme for the fragmentation pathways will be provided in the Discussion). The b2 ion is written in a linear fashion, although we acknowledge it could be cyclic with the N-terminal, but it has been displayed in this way for clarity. There are also moderately intense peaks for neutral losses of water (m/z 252.36), and CO (m/z 241.98) from b3,

and combined losses of CO and either water (m/z 224.20) or ammonia (m/z 225.1) from b3, respectively. The a1 ion (m/z 85.96) and x1 ion (m/z 142.93) are also identifiable peaks in the spectrum. The m/z 199.16 ion could not be identified, although it could be interesting as product **10** has a peak with m/z 207.12 (Figure 2.16C). Figure 2.16B shows the MS^3 spectrum of the b3 ion from product **9** (m/z 270.3). This spectrum is slightly different than the other two, unexpected since we assume this fragment is structurally identical to the b3 ion of **2a** and **10**. The difference could be related to lower ionization energy in the FT-MS in this single experiment. The ion of highest intensity is the fragment ion generated by a combined loss of CO and water from b3 in of highest intensity (m/z 224.1). Other observed ions are the b2 ion (m/z 171.1), and ions derived from the neutral loss of water (m/z 252.4), the combined loss of CO and ammonia (m/z 225.3) from b3, the a1 ion (m/z 85.9), and the x1 ion (m/z 143.2). Figure 6C shows the MS^3 spectrum of the b3 ion from product **10** (m/z 276.3). The major ions in this spectrum are the b2 ion (m/z 171.1), and the ion derived from the combined loss of CO and ammonia (m/z 229.3). We also observe ions derived from the neutral loss of water from b3 (m/z 258.2), the a1 ion (m/z 86.1), and the x1 ion (m/z 143.2).

*ii. b4 fragment ions (m/z 369.2, 369.2, and 375.2 for products **2a, 9**, and **10,** respectively).* Figure 2.17 displays the MS^3 spectra of the b4 ions from products **2a** (m/z 369.2), **9** (m/z 369.2), and **10** (m/z 375.3). This fragment, shown in the insert in Figure 2.17A, is derived from the cyclic sulfenamide through cleavage of the amide bond and the heterocyclic S-N bond. It is important to note that b4 is isobaric to y4-H_2O in product **2a**. However, based on the isotopic substitution in b4 from products **9** and **10**, m/z 369.2 and m/z 375.2 cannot be assigned to y4-H_2O. The most intense MS^3 fragment ions derived from the b4 ions of all three peptides are

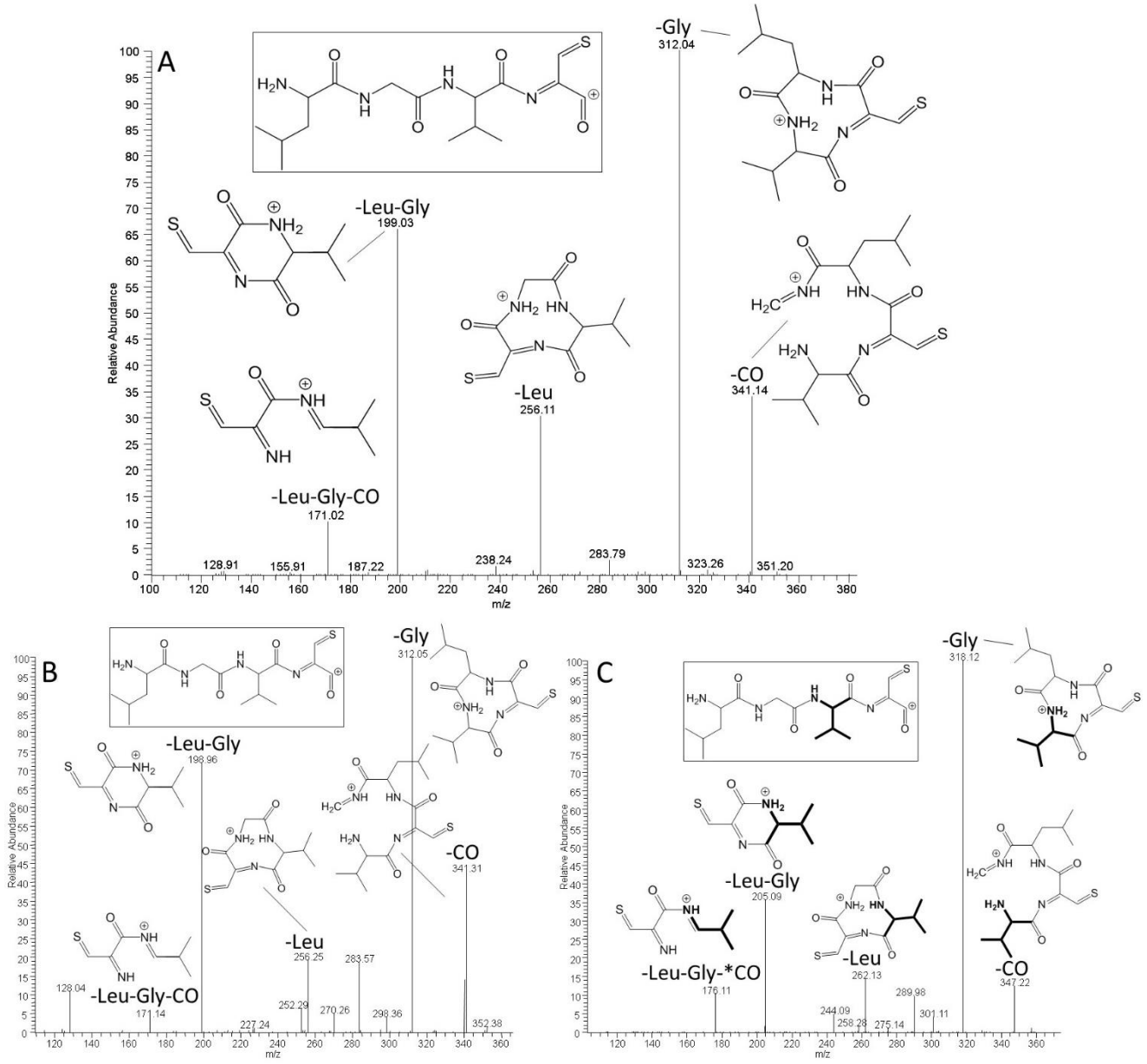

Figure 2.17. MS^3 fragmentation of the b4 ion from the MS/MS spectra of (A) product **2a**; (B) product **9**; (C) product **10**. The ^{13}C and ^{15}N labeled amino acids are indicated in bold font and with *C/N.

the ions characterized by a loss of 57 Da, i.e., m/z 312.0, 312.1, and 318.1 for products **2a**, **9**, and **10**, respectively (Figures 2.17A, 2.17B, and 2.17C). The loss of 57 Da may reflect either a direct loss of Gly or a sequential loss of CO (28 Da) and CH_2=NH (29Da) (a mechanistic scheme for the fragmentation pathways will be provided in the Discussion). Other intense fragment ions are generated through the loss of Leu and Leu-Gly, i.e. ions with m/z 256.1 and m/z 199.0 for product **2a**, m/z 256.2 and m/z 199.0 for product **9**, and m/z 262.1 and m/z 205.1 for product **10**,

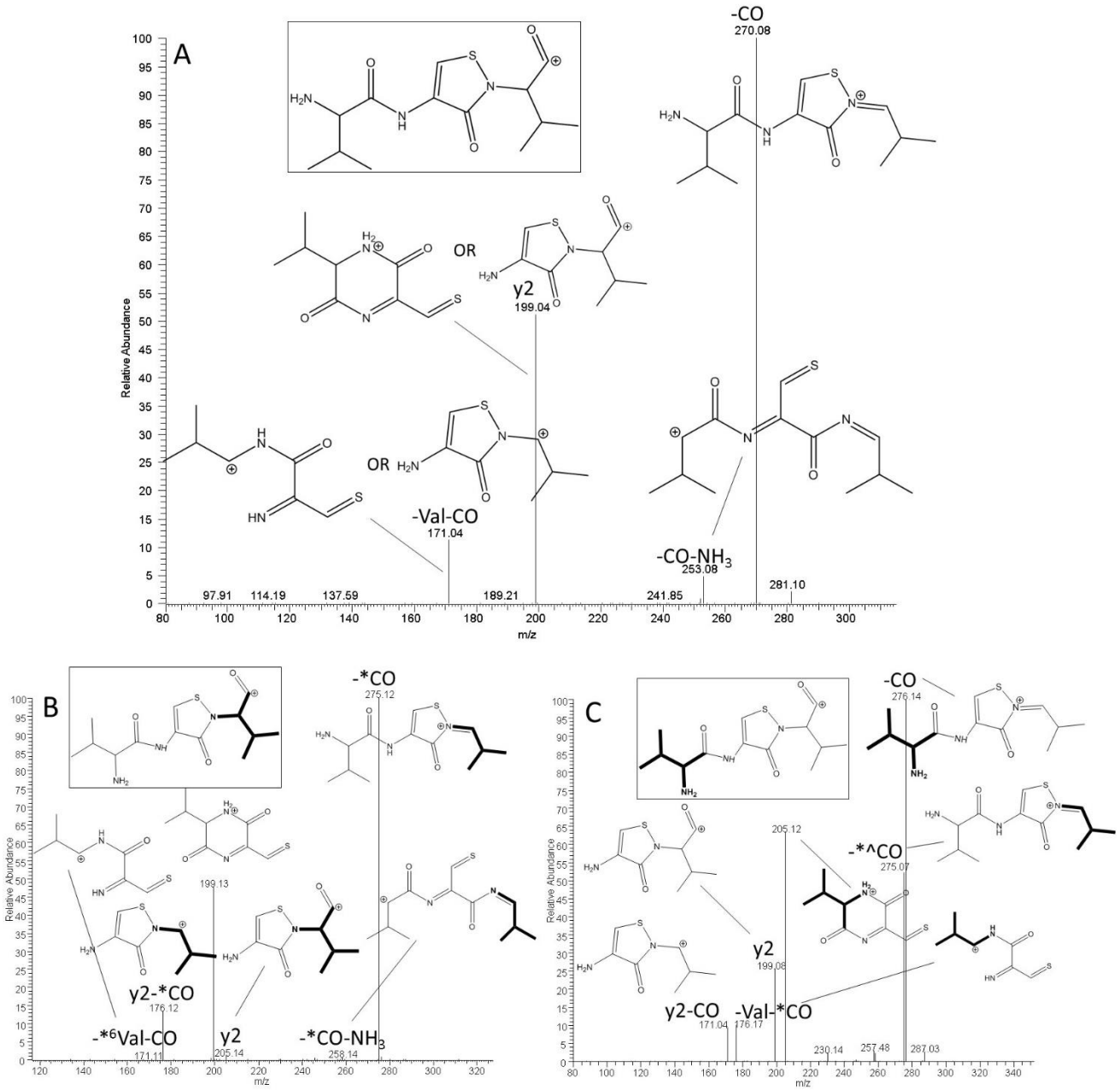

Figure 2.18. MS^3 fragmentation of the VC*V internal fragment ion from the MS/MS spectra of (A) product **2a**; (B) product **9**; (C) product **10**. The ^{13}C and ^{15}N labeled amino acids are indicated in bold font and with *C/N, and *^CO indicates the possibility of a product **9** peak in Figure 2.18C.

respectively. Additionally, a neutral loss of CO following the loss of Leu-Gly is observed for products **2a**, **9**, and **10**, i.e. ions with m/z 171.1, 171.1, and 176.1, respectively. A direct neutral loss CO generated ions with m/z 341.1, m/z 341.3, and m/z 347.2 for products **2a**, **9**, and **10**, respectively.

*iii.VC*V fragment ions (m/z 298.2, 304.2, and 304.2 for products **2a, 9,** and **10**, respectively).* More evidence for the cyclic sulfenamide structure is derived from the MS^3 spectra

of the internal VC*V fragment of products **2a** (m/z 298.2), **9** (m/z 304.2), and **10** (m/z 304.2) (Figure 2.18), where C* corresponds to the modified Cys sulfenamide structure. Product **9** and **10** contained the isotopically labeled Val residues C- and N-terminal of the original Cys residue. The main fragment ions of VC*V were derived through the loss of CO, i.e. ions with m/z 270.1, m/z 275.1, and m/z 276.1 for products **2a**, **9**, and **10**, respectively. The resulting fragment ions were further amenable to loss to ammonia, generating ions with m/z 253.1, m/z 258.1, and m/z 258.1 for products **2a**, **9**, and **10**, respectively. Fragmentation of VC*V from product **2a** leads to ions with m/z 171.0 and m/z 199.0, which could each correspond to two different structures (displayed in Figure 2.18A). This became apparent through comparison with the fragmentation of VC*V from products **9** and **10**, which yielded ions with m/z 171.2 and m/z 176.1, and with m/z 199.1 and m/z 205.1, respectively. For VC*V from product **9**, m/z 199.1 corresponds to the loss of CO and 2-methylpropan-1-imine (Figure 2.18B), whereas for VC*V from product **10**, m/z 199.1 corresponds to the y2 ion (Figure 2.18C). Vice versa, m/z 205.1 corresponds to the loss of CO and 2-methylpropan-1-imine from VC*V of product **10**, whereas the y2 ion from VC*V of product **9** corresponds to m/z 199.1. Furthermore, m/z 171.1 and m/z 176.1 correspond to the losses of CO from m/z 199.1 and m/z 205.1 for VC*V from both products **9** and **10**.

2.3.6 Reaction of Cys-Containing Peptide 1d with Carbon-Centered Radicals

derived from AAPH. Peptide **1d** was dissolved to a concentration of 50 µM in 50 mM sodium phosphate at pH 6.0, 7.0, 8.0, 9.0, and 10.0. 400 µL of these solutions were saturated with Ar for 30 minutes in glass tubes closed with rubber stoppers. Similarly, a solution of 10 mM AAPH was saturated with Ar on ice in a glass tube closed with a rubber stopper. Following saturation with

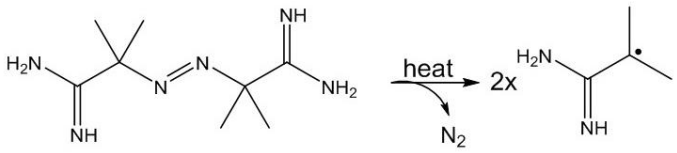

Scheme 2.3. Thermal AAPH decomposition reaction.

Ar, a final concentration of 1 mM AAPH was added to the solution containing peptide **1d** and the reaction mixture incubated for 1 hour at 37 °C under the Ar. Under these conditions, the thermal decomposition of AAPH over 1 hour yielded a total of $4.9x10^{-6}$ M carbon-centered radicals.[50] Scheme 2.3 shows how C-centered radicals are formed by the thermal decomposition of AAPH, following release of N_2(g) from the molecule. After the reaction was completed, the samples were frozen at -20 °C until MS analysis. The reaction products were placed in a 4 °C

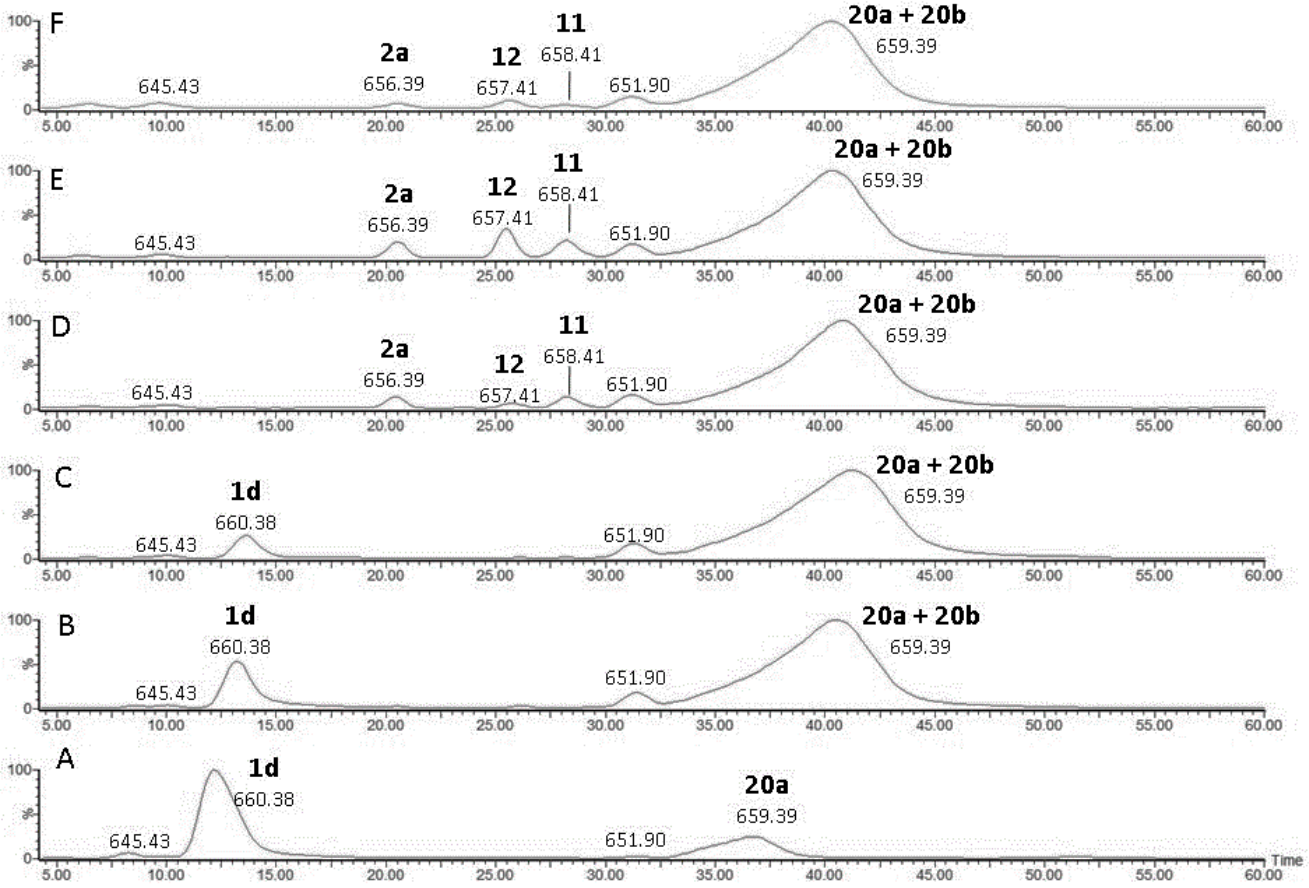

Figure 2.19. LC-MS of the products generated from reaction of peptide **1d** with the C-centered radicals derived by thermal decomposition of AAPH for 1 hour at 37 °C at different pH values: (A) Control peptide **1d**; (B) pH 6.0; (C) pH 7.0; (D) pH 8.0; (E) pH 9.0; (F) pH 10.0.

Product	Proposed Structure	MS/MS
20a	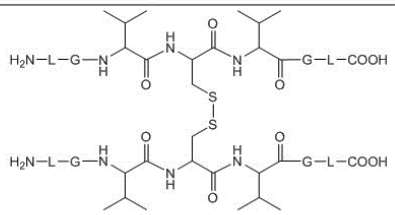	Fig. 2.20
20b	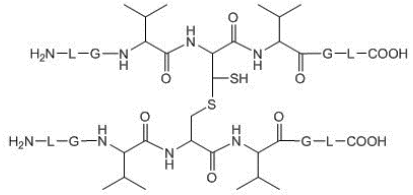	NA
11	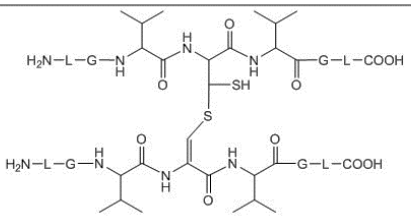	Fig. 2.21
12	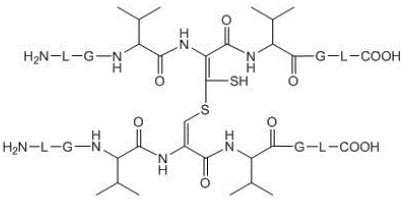	Fig. 2.22

Table 2.5. Products generated after the reaction of peptide **1d** with C-centered radicals derived from AAPH.

autosampler and analyzed by HPLC-MS and MS/MS using the Q-tof Premier instrument (Figure 2.19). Table 2.5 summarizes the products generated from the reaction of peptide **1d** with the C-centered radicals derived from AAPH. However, for clarity, the MS/MS fragmentation data presented below was generated on the LTQ-FT instrument from the irradiation of 100 µM peptide **1a** (Figure 2.13), since the products generated during the reaction of peptide **1d** with AAPH were structurally identical to those generated photolytically. This was done because the MS/MS fragmentation on the LTQ-FT is superior to that of the Q-tof Premier instrument. The major reaction products formed at all pH values were the disulfide of peptide **1d**, product **20a** (identical to peptide **1a**) and an isobaric species, product **20b** (Figure 2.19) The characterization of product **20b** is described below. Interestingly, the broad peak containing products **20a** and **20b** after the exposure of peptide **1d** to AAPH is shifted towards longer retention times as compared to the peak eluting at ca. 37 minutes in Figure 2.19A, representing the disulfide present in small amounts in the control sample (this was repeatedly observed in three independent experiments). Product **2a** was formed in low yields at pH 8.0-10.0, along with two additional disulfide-containing products, products **11** and **12** (Figure 2.19D-F).

*i. Product **2a** (m/z 656.4).* Following a 1 hour reaction with AAPH-derived radicals at pH 8.0, 9.0, and 10.0 (Figure 2.19D-F), product **2a** appeared in yields of approximately 3% relative to all products. The MS/MS spectrum for product **2a** was identical to the MS/MS spectrum generated by photo-irradiation of peptide **1a** (Figure 2.2).

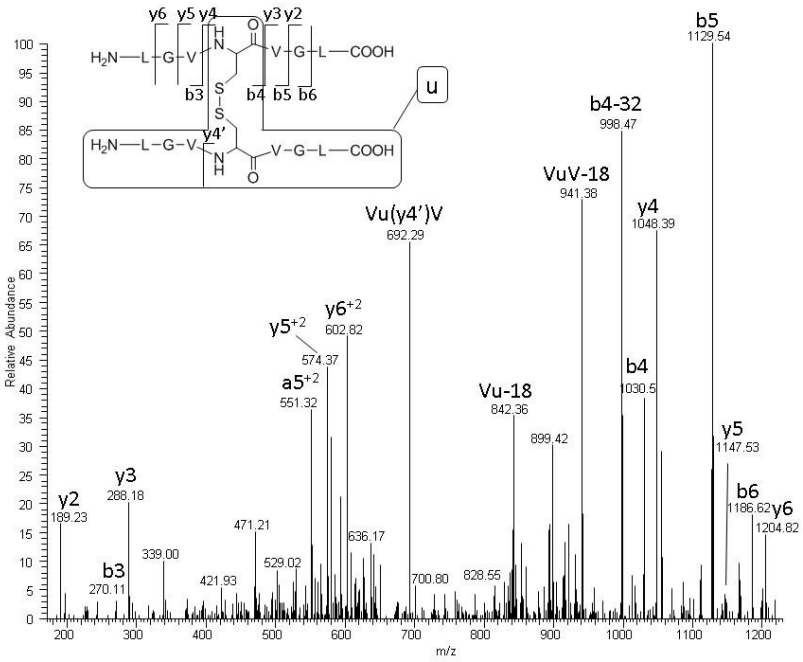

Figure 2.20. MS/MS spectrum of product **20a/20b** after the reaction of peptide **1d** with C-centered radicals derived from AAPH. In the figure 'u' is the structure highlighted in the box.

*ii. Products **20a** and **20b** (m/z 659.4^{+2}/1317.8^{+1}).* At all pH values, products **20a** and **20b** were the major reaction products detected after the reaction of AAPH-derived radicals with peptide **1d** (Figure 2.19A-F). Products **20a** and **20b** were the only products observed at pH 6.0 and 7.0. The wide peak shape of products **20a** and **20b** at all pH values is consistent with the coelution of isobaric reaction products (see below). The MS/MS spectra of all the scans over the large peak containing products **20a** and **20b** were similar (Figure 2.20), suggesting that products **20a** and **20b** represent products with a disulfide bond and an isobaric cross-link, respectively. Importantly, the MS/MS fragmentation does not distinguish between the disulfide and the isobaric cross-link, but does indicate that the Cys residue is involved in the cross-link (i.e. the b3, b4, y3, and y4 ions). A suitable cross-link isobaric with the disulfide bond would be a dithiohemiacetal (such as shown in structure **20b** in Table 2.5), which we have detected as a reaction product of various photolytically generated peptide thiyl

radicals.[29] In order to distinguish structures **20a** and **20b**, we performed derivatization with NEM, as described in section 2.3.7 below.

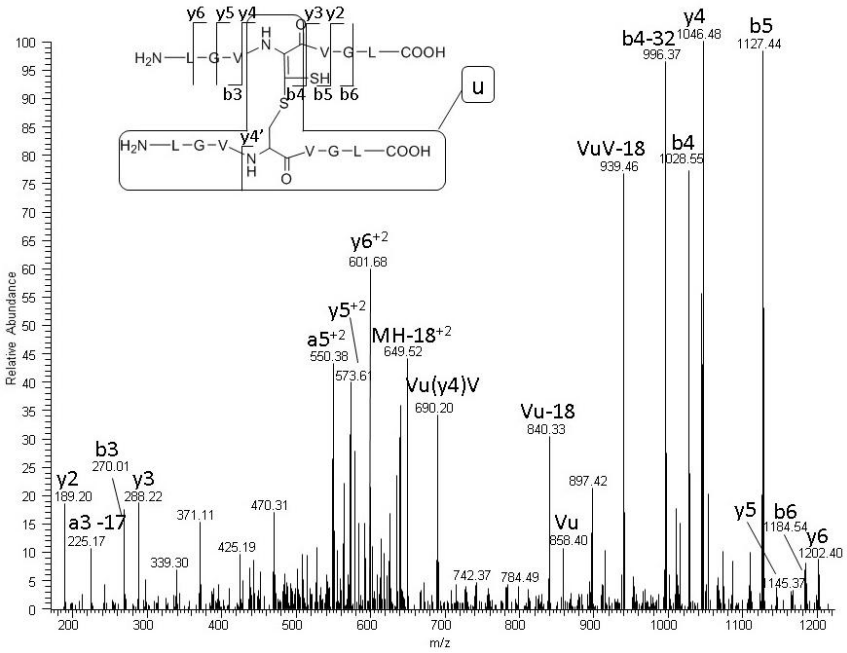

Figure 2.21. MS/MS spectrum of product **11** after the reaction of peptide **1d** with C-centered radicals derived from AAPH. In the figure 'u' is the structure highlighted in the box.

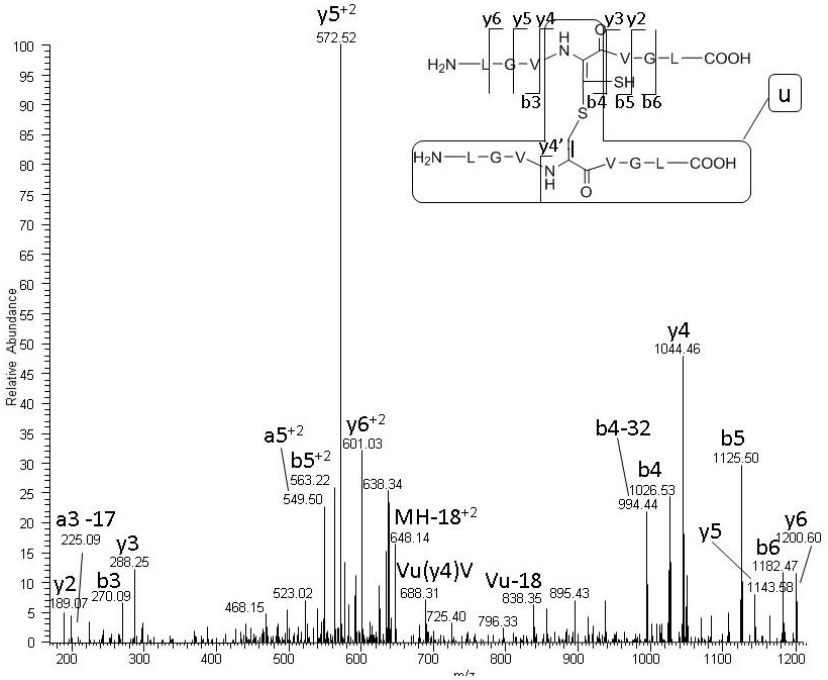

Figure 2.22. MS/MS spectrum of product **12** after the reaction of peptide **1d** with C-centered radicals derived from AAPH. In the figure 'u' is the structure highlighted in the box.

*iii. Product **11** (m/z 658.4^{+2}/1315.8^{+1}).* Product **11** was formed at pH 8.0-10.0 (Figure 2.19D-F). The m/z value suggests that product **11** is a derivative of products **20a** and **20b** generated by the loss 2 Da, consistent with one double bond in the structure. However the MS/MS data presented in Figure 2.21 cannot provide a clear assignment from which precursor product **11** is derived, although the structure presented is derived from product **20b**. The b3, b4, y3, and y4 MS/MS fragmentation ions do however confirm the location of the double bond to

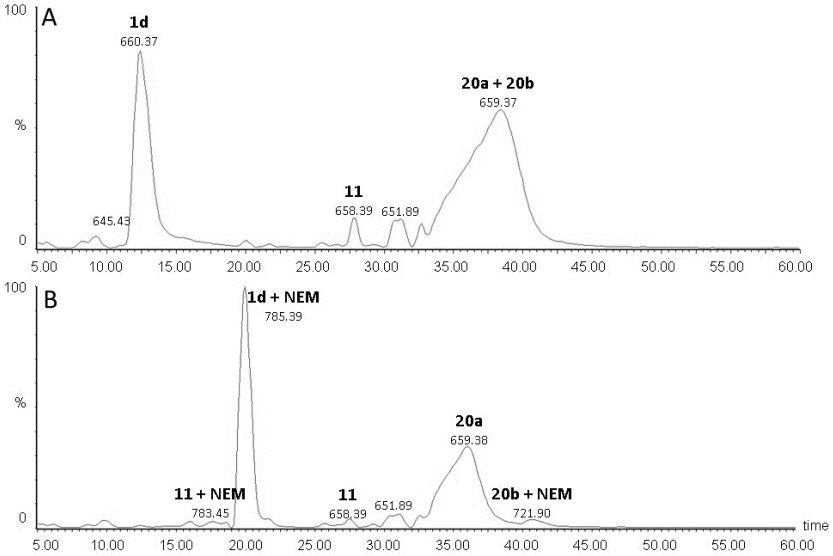

Figure 2.23. LC-MS of the products generated from reaction of peptide **1d** with the C-centered radicals derived by thermal decomposition of AAPH for 1 hour at 37 °C at (A) pH 7.0 and (B) pH 7.0 followed by NEM derivatization.

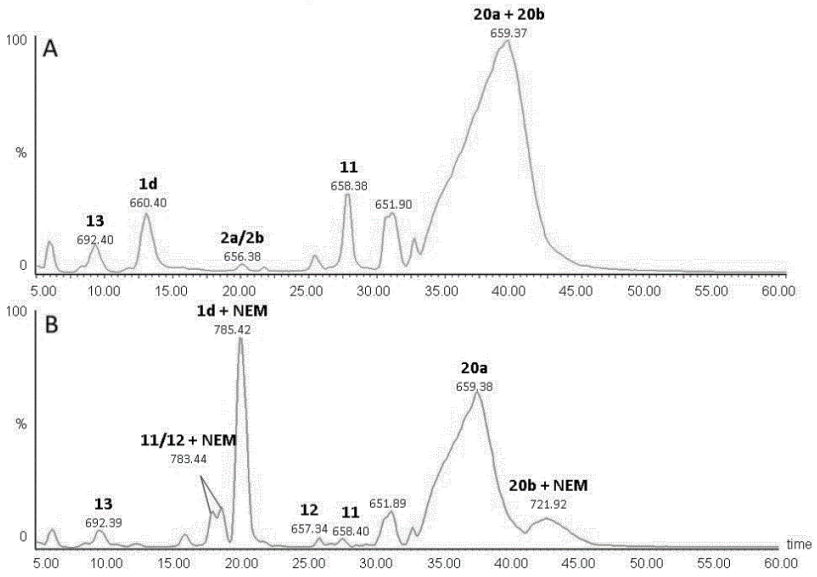

Figure 2.24. LC-MS of the products generated from reaction of peptide **1d** with the C-centered radicals derived by thermal decomposition of AAPH for 1 hour at 37 °C at (A) pH 8.0 and (B) pH 8.0 followed by NEM derivatization.

a Cys residue, i.e. between $^{\alpha}$C and $^{\beta}$C.

*iv. Product **12** (m/z $657.4^{+2}/1313.8^{+1}$).* Product **12** was formed at pH 8.0-10.0 (Figure 2.19D-F). The m/z value is consistent with a derivative of products **20a** and **20b** generated by the loss of 4 Da, consistent with two double bonds in the structure. However, like for product **11**, the MS/MS data do not indicate whether the peptide contains a disulfide or an isobaric cross-link such as a dithiohemiacetal (Figure 2.22). The MS/MS does localize the double bonds to the original Cys residues, most likely one double bond each to one Cys resdue (cf., the b3, b4, y3, and y4 ions). The double bonds are located between the $^{\alpha}$C and the $^{\beta}$C atoms.

2.3.7 Derivatization of AAPH generated Products with NEM. NEM derivatization was employed to distinguish between the isobaric products

Product	Proposed Structure	MS/MS
Peptide 1d +NEM	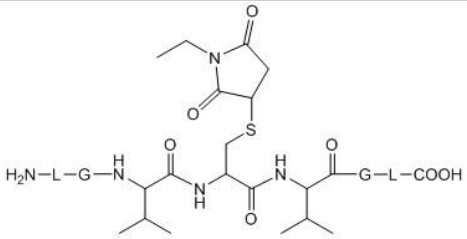	Fig. 2.7
20b+NEM, (A)	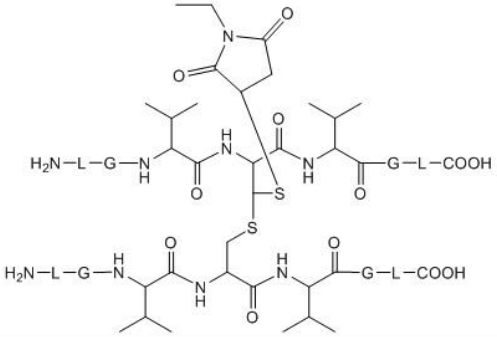	Fig. 2.25
20b+NEM, (B)	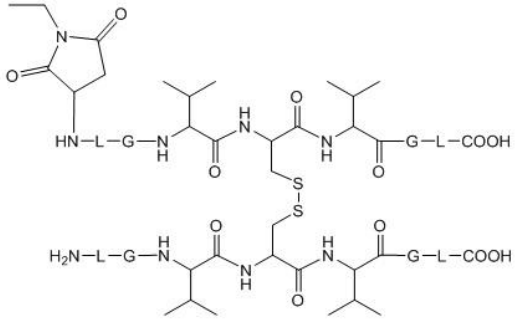	Fig. 2.25
11,12 +NEM	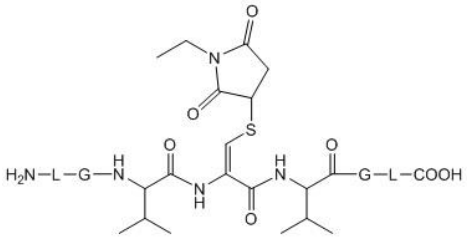	Fig. 2.26

Table 2.6. NEM-derivatized products generated after the reaction of peptide **1d** with C-centered radicals derived from AAPH.

20a and **20b**, and to assign the structures of products **11** and **12**. We chose to derivatize the products formed at pH 7.0 and pH 8.0 and compare the results because at pH 7.0, products **11** and **12** were not generated, but the starting material, peptide **1d**, remained, whereas at pH 8.0, no starting material remained, but products **11** and **12** were present (Figure 2.19). Following the incubation of peptide **1d** with AAPH at pH 7.0 and pH 8.0, aliquots were removed and a final concentration of 1.8 mM NEM was added to the samples. The samples were incubated at room temperature for one hour, and frozen at -20°C until MS analysis. The resultant reaction products were then analyzed by HPLC-MS/MS using the Q-tof Premier instrument (Figure 2.23 for pH 7.0 and Figure 2.24 for pH 8.0). However, again for clarity, the MS/MS fragmentation data presented below was generated on the LTQ-FT instrument from the

irradiation of 100 µM peptide **1a** (Figure 2.13), since the products generated during the AAPH-induced oxidation of peptide **1d** were structurally identical to those generated photolytically. Table 2.6 shows the products generated from the AAPH reaction after NEM derivatization of the free thiols: peptide **1d+NEM** (m/z 785.4), and product **20b+NEM** (m/z 721.9^{+2}), **11+NEM** (m/z 783.3), and **12+NEM** (m/z 783.4).

*i. Peptide **1d+NEM** (m/z 785.4^{+1}).* Before NEM derivatization, peptide **1d** elutes at 12.5 minutes (Figure 2.23A and 2.24A for pH 7.0, and 8.0, respectively), but NEM derivatization abolishes this peak. A new peak elutes at 20 minutes with a combined mass of peptide **1d** and 125 Da (m/z 785.4), corresponding to NEM derivatization (Figure 2.23A and 2.24A for pH 7.0, and 8.0, respectively). The MS/MS fragmentation of this product was identical to the MS/MS fragmentation of Product **3** after NEM derivatization of the photochemical products from peptide **1a** (see above; Figure 2.7). Interestingly, the peak area of the derivatized peptide **1d** is larger than the peak area of the peptide **1d** (47% vs. 29% for pH 7.0 and 19% vs. 4% for pH 8.0). The reason behind this discrepancy in peak area is described below.

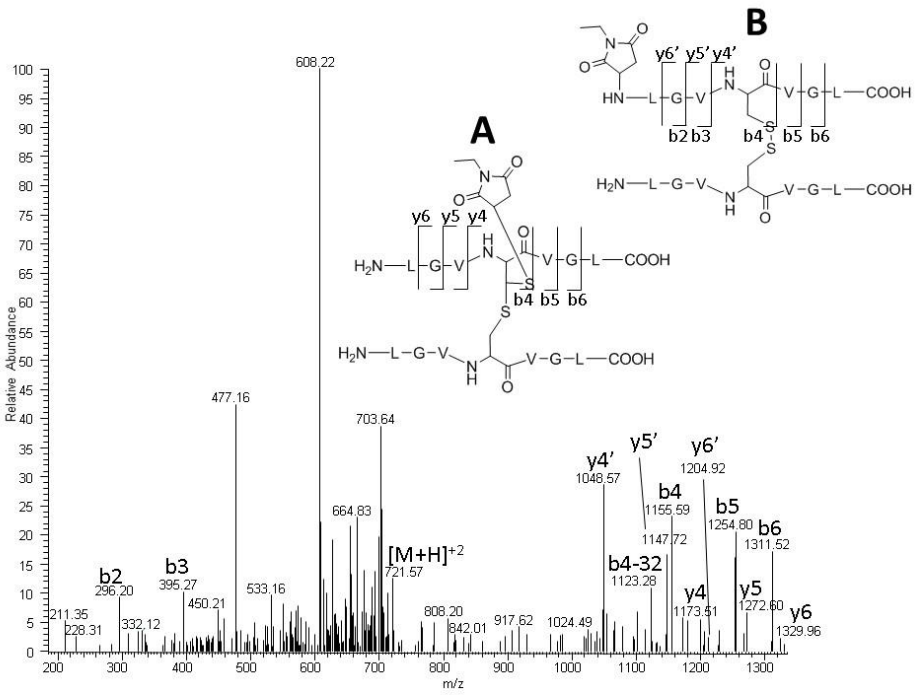

Figure 2.25. MS/MS spectrum of products **20a** and **20b** after NEM derivatization.

*ii. Products **20a and 20b+NEM** (m/z 721.9^{+2}/1442.8^{+1}).* NEM derivatization

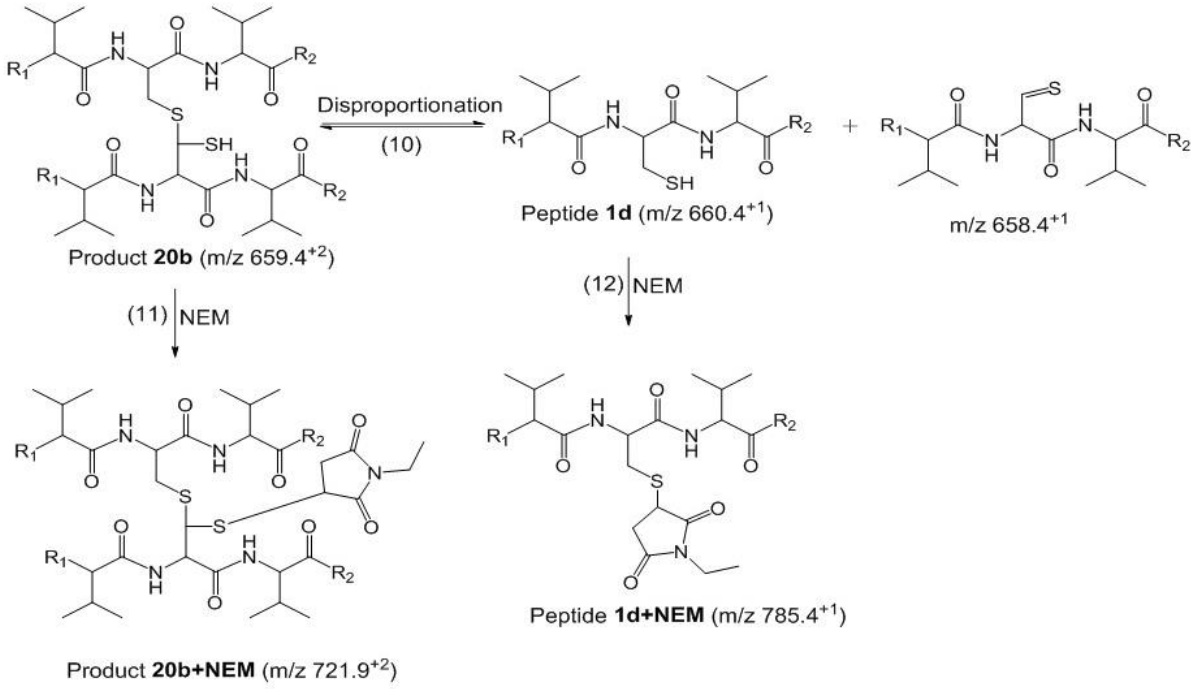

Scheme 2.4. NEM derivatization products of product **20b**.

transforms the large, wide peak eluting at ca. 40 minutes (Figure 2.23A and Figure 2.24A, for pH 7.0 and 8.0, respectively) into two distinct peaks eluting at 37 and 43 minutes, respectively (Figure 2.23B and Figure 2.24B, for pH 7.0 and 8.0, respectively). The MS/MS of m/z 721.9^{+2} is shown in Figure 2.25. Again, there are co-eluting products in the peak: product **20a** with NEM derivatization on the N-terminal amine (structure B), and product **20b** with NEM derivatization on the Cys thiol (structure A). The b2 and b3 ions are only observed for structure B, and the y ion fragmentation intensity is much higher for structure B than structure A. However, product **20b** is in equilibrium with its disproportionation products (Scheme 2.4), reforming the thiol, structurally identical to peptide **1d**, (m/z 660.4) and the thioaldehyde (658.4) (reaction 10). Consequently, product **20b** has two NEM-derivatization products: m/z 721.9^{+2} (reaction 11) and m/z 785.4 (reaction 12). The second product (m/z 785.4) accounts for the discrepancy between the peak areas of peptide **1d** before NEM derivatization (m/z 660.4) and after NEM derivatization (m/z 785.4) (Figures 2.23 and 2.24). The extra peak area after NEM derivatization

actually corresponds to the disproportionation product of product **20b**. To calculate the % yield of product **20b**, the peak area of m/z 721.9^{+2} (Figures 2.23B and 2.24B, for pH 7.0 and 8.0, respectively) was added to the difference in peak area between m/z 660.4 (Figures 2.23A and 2.24B, for pH 7.0 and 8.0, respectively) and m/z 785.4 (Figures 2.23B and 2.24B, for pH 7.0 and 8.0, respectively). Therefore, product **20b** accounts for ca. 23% of the products generated after the reaction of peptide **1d** with the C-centered radicals derived from AAPH at both pH 7.0 and pH 8.0. Product **20a** accounts for ca. 50% and 64% of the products generated at pH 7.0 and 8.0, respectively. Additionally, at 34 minutes, the front of the product **20a** peak shows a slight shoulder, evidence for another product that could not be assigned because the MS/MS was consistent with product **20a**. This could point to other isobaric products such as one or more peptides containing D-amino acids. Previously, D-amino acids have been observed during the photolysis of disulfide-containing model peptides[42] and monoclonal antibodies,[44] and thiyl radical reactions have been proposed to initiate these isomerization reactions.

*iii. Products **11 and 12+NEM** (m/z 783.4^{+1}).* At pH 8.0, products **11** and **12** are generated from the C-centered radicals derived from AAPH. However, when NEM is added to the solution, product **11** disappears and the signal of product **12** is greatly reduced. No products corresponding to the NEM addition of the original products were observed, but two new peaks with m/z values of 783.4^{+1} were detected. These products are most likely due to the disproportionation reactions of products **11** and **12** via the same mechanism as shown in Scheme 2.4 for product **20b**, except that the starting materials (products **11** and **12**) now contain double bonds on the original Cys residues. Therefore so the final products are 2 Da lower in mass than observed for product **20a**. Although two peaks were observed, the MS/MS spectra of both were identical; therefore, only

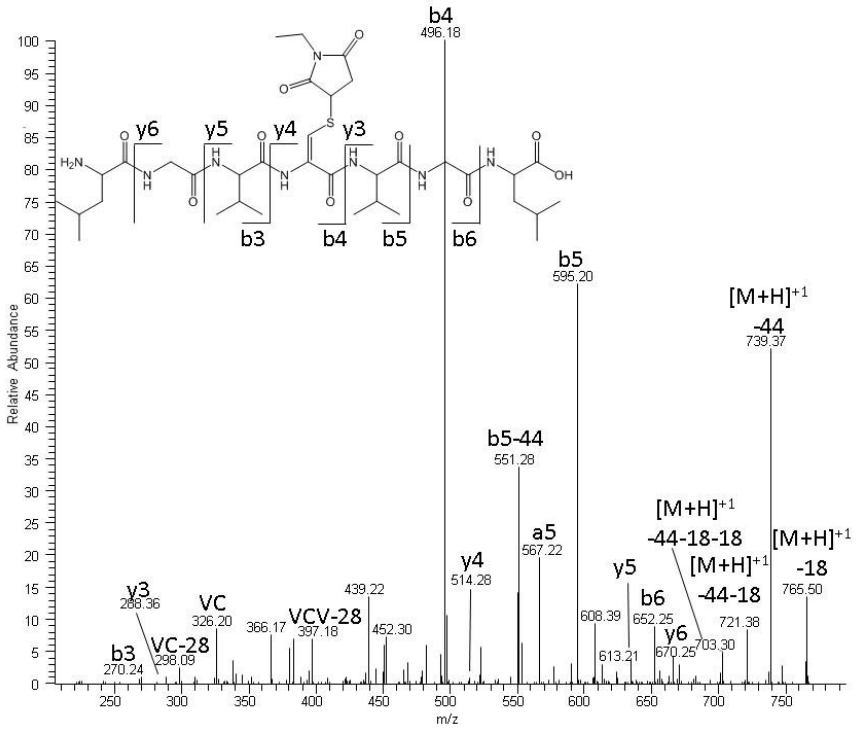

Figure 2.26. MS/MS spectrum of products **11** and **12** after NEM derivatization.

one representative spectrum is shown in Figure 2.26. The b3, b4, y3, and y4 localize the NEM addition and the loss of 2 Da from the native peptide **1d** to the Cys residue.

2.3.8 ^{1}H-NMR of Product 2a. Product **2a** was generated through the reaction of 50 µM Peptide **1d** with AAPH. Peptide **1d** was dissolved in 50 mM sodium phosphate buffer prepared at pH 9. 10 mM AAPH was dissolved in 50 mM sodium phosphate buffer prepared at pH 7.0, and placed on ice. Both solutions were placed in glass tubes, capped with rubber stoppers, and saturated with Ar for 30 minutes. Following saturation, a final concentration of 1 mM AAPH was added to the peptide solution under Ar and the solution incubated for 1 hour at 37 °C. The sample was dried down in a CentriVap concentrator and reconstituted in D_2O at pD 3.0. The samples were left at room temperature for two days before NMR analysis, which was advantageous as the yield of product **2a** increased by 10 times compared to products **11** and **12**, unlike the results shown in Figure 2.19E. (This was confirmed by MS following the ^{1}H-NMR acquisition.) ^{1}H-NMR data were collected after 1024 scans and a pulse width of 14.25 seconds. ^{1}H-NMR spectra of the unreacted control peptide **1d** (1 mM) and of pure AAPH (1 mM) were obtained after 32 scans and a pulse width of 14.25 seconds. The region of

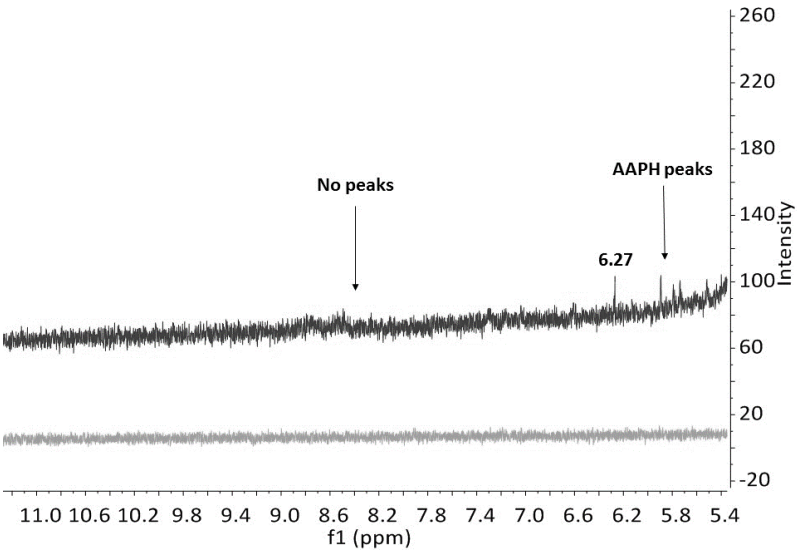

Figure 2.27. ^{1}H NMR of the control peptide **1d** (bottom, light gray) and the AAPH sample containing product **2a** (top, dark gray).

interest for product **2a** is between 5 and 10 ppm where the proton of the $^{\beta}$C-H bond from the double bond at $^{\alpha}$C-$^{\beta}$C of the original Cys residue is predicted to show a signal around 6.25-6.91 ppm (ChemDraw and NMR predictor,[52] respectively). The control peptide **1a** and AAPH display no signals in this region (the $^{\beta}$C-H proton of the Cys residue in **1d** is predicted by application of ChemDraw to show a signal at 2.9/3.2 ppm). The solution pD was maintained at pD 3.0 in order to distinguish between sulfenamide **2a** and the S-O-bonded product **2b**. At pD 3.0, the imine in structure **2b** is expected to be protonated,[56] which results in a downfield shift of the vinylic proton from 7.4 ppm to 8.4 ppm (calculated by NMR predictor).

In Figure 2.27, the NMR spectrum between 5.4 ppm and 11.0 ppm is depicted. Peptide **1d** (bottom panel, light gray) shows no signals in this region. In contrast, AAPH oxidation of **1d** leads to a signal at 6.27 ppm consistent with the formation of product **2a** (top, dark gray), and AAPH peaks at 5.8 ppm confirmed by NMR on pure AAPH. This new peak corresponds to the predicted peak shifts of the proton attached to the $^{\beta}$C-H that is involved in the double bond between the $^{\alpha}$C-$^{\beta}$C of the Cys residue that is part of the heterocyclic sulfenamide Product **2a**.

2.3.9 Photo-irradiation of 100 µM Peptide 1a at pH 7.0. In section 2.3.7, the photo-irradiation of peptides **1a**, **1b**, and **1c** at a concentration of 100 µM at pH 7.0 with $\lambda = 254$ nm was described with the intent to characterize the sulfenamide structures **2a, 9**, and **10**. The

Product	Proposed Structure	Product	Proposed Structure
6	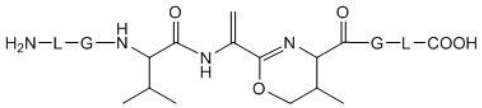	16	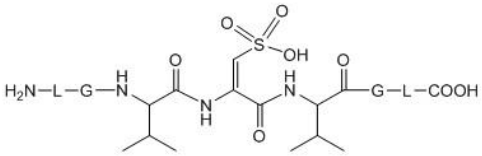
7	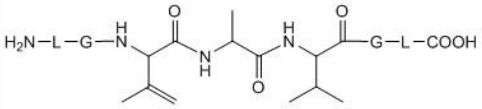	17	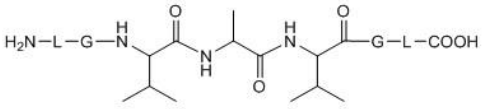
8	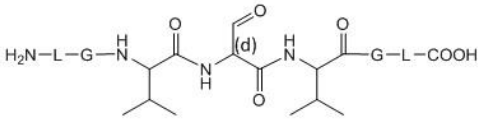	18	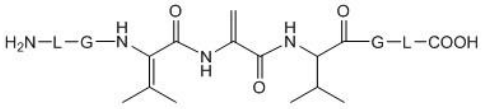
13	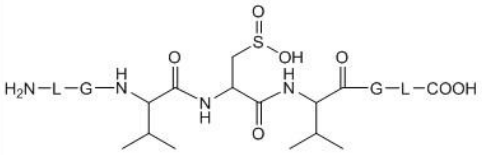	19a	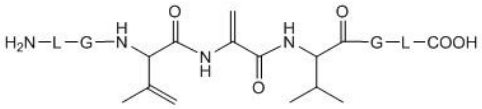
14	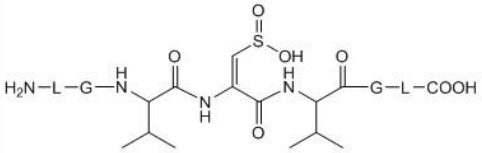	19b	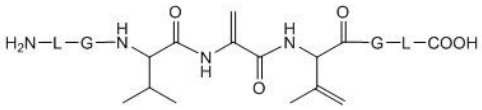
15	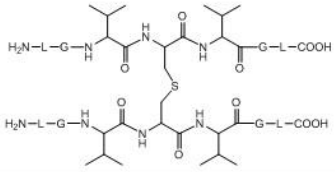		

Table 2.7. Peptide **1a** photoproducts observed after photolysis at λ = 254 nm (100 µm).

photoproducts generated by the irradiation of 100 µM peptide **1a** under Ar-saturated conditions were analyzed by LC-MS on the Qtof Premier and MS/MS using the LTQ-FT. A representative chromatogram was shown after the photo-irradiation of peptide **1a** after ten minutes (Figure 2.13B), however the other interesting photoproducts of peptide **1a** were also characterized by MS, and will be detailed in this section and Appendix A. It should be noted that the control sample in Figure 2.13A contained no trace of photoproducts, however, the LC-MS shows a wide

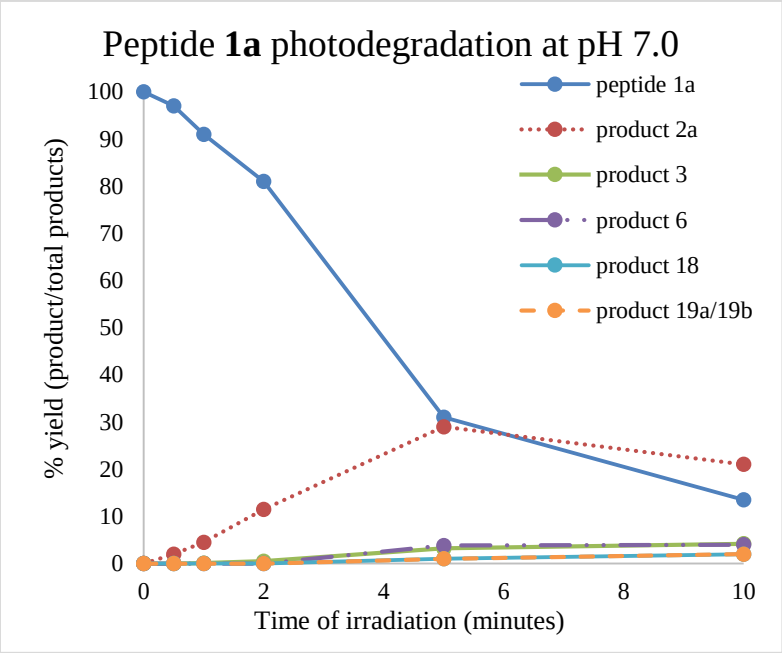

Figure 2.28. Kinetics of formation for products **1a**, **2a**, **3**, **6**, **18**, and **19a/19b** after UV irradiation at λ = 254 nm of peptide **1a** at pH 7.0 (100 μM) in an Ar-saturated H_2O.

peak, not unlike that observed in Figure 2.19 during the AAPH reaction with Peptide **1d**. Therefore, the control may have contained not only the disulfide peptide **1a**, but a dithiohemiacetal product (**20b**) as well, but this was not tested at that time. The tentative structures of the resultant photoproducts that have not yet been discussed are shown in Table 2.7, and the kinetics of peptide **1a** degradation were followed for the photoproducts of interest in Figure 2.28. There were four major types of photoproducts generated in this experiment: disproportionation products (products **3** (m/z 660.41), **5** (m/z 642.41) and **8** (m/z 642.42)), oxidation products (products **13** (m/z 692.42), **14** (m/z 690.39), and **16** (m/z 706.37)), disulfide derivatives (products **11** (m/z 658.38^{+2}), **12** (m/z 657.37^{+2}), and **15** (m/z 643.41^{+2})), and products generated through H-atom transfer reactions (products **2a** and **2b** (m/z 656.39), **4** (m/z 626.42), **6** (m/z 624.40), **7** (m/z 626.42), **17** (m/z 628.43), **18** (m/z 624.38), and **19a** and **19b** (m/z 624.38)). In the following, we will focus predominantly on the characterization of products generated via H-atom transfer reactions, specifically products which were not previously observed for other, sterically less restricted, model peptides. Hence, we focus specifically on the isobaric products with m/z 624.4. The MS/MS spectra of the other products are presented in Appendix A, Figures A.2-A.7.

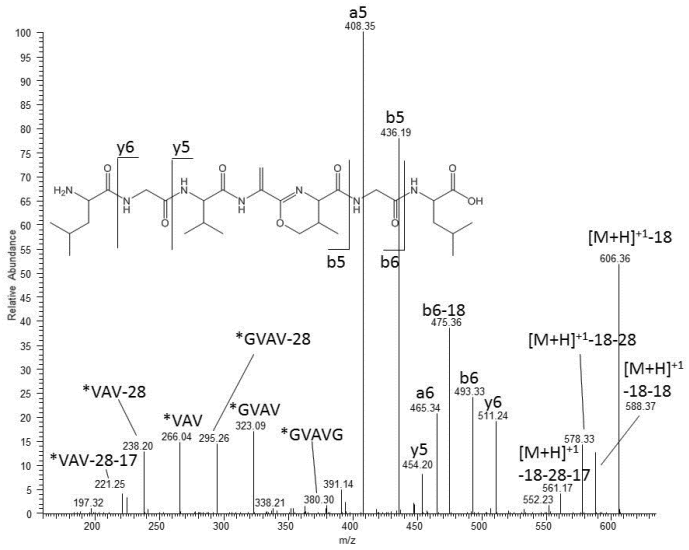

Figure 2.29. MS/MS spectrum of product **6** after UV irradiation at λ = 254 nm of peptide **1a** at pH 7.0 (100 μM), and tentative assignment of a product structure.

The time course of photodegradation of peptide **1a** at pH 7.0 is shown in Figure 2.28. The disulfide shows a biphasic decomposition with a faster rate within the first 5 minutes, followed by a slower rate for the following 5 minutes. However, it is possible that the disulfide is completely consumed after 5 minutes, and the remaining peak is a dithiohemiacetal, similar to product **20b**. The major product generated by the irradiation of 100 μM peptide **1a** was the sulfenamide product **2a** that is described above (Figure 2.28) However, the yield was only 4.5% after 1 minute of irradiation, not 90% as compared to the irradiation of 100 nM peptide **1a**, and only increased to 29% at 5 minutes before starting to degrade. It should be mentioned that the yield of the thiol, product **3**, was only 4% in this experiment after 10 minutes of irradiation at pH 7.0, but yields were much larger in experiments at pH 4.0 (data shown in Section 2.3.14), so the data was included in Figure 2.28 for comparison. The generation of products **6**, **18**, **19a** and **19b** after 5 minutes of irradiation was interesting because of their isobaric m/z values, m/z624.4, so we attempted to characterize these structures by MS and NMR analysis.

*i. Product **6** (624.38).* A trace of product **6** was observed after the irradiation of 100 nM peptide **1a**, but during the irradiation of 100 μM peptide **1a**, product **6** was observed at a 4% yield after 10 minutes of irradiation (Figure 2.28). This product elutes at 18 minutes (Figure

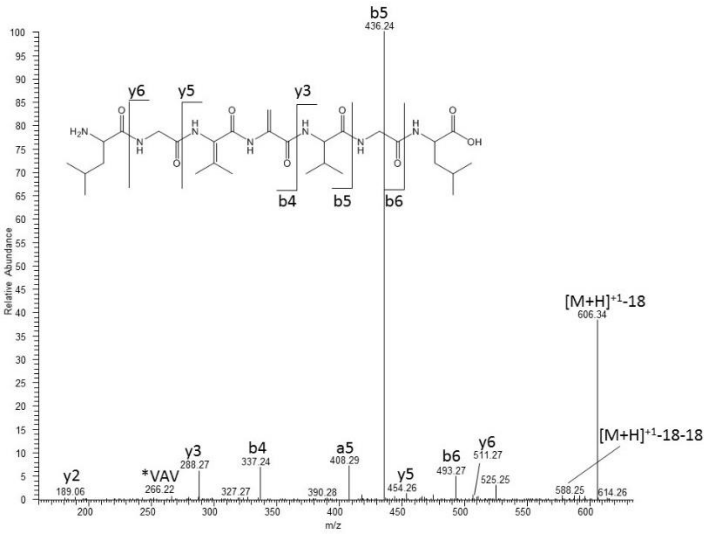

Figure 2.30. MS/MS spectrum of product **18** after UV irradiation at λ = 254 nm of peptide **1a** at pH 7.0 (100 μM), and tentative assignment of a product structure.

2.13B), and the m/z value is consistent with the conversion of Cys to Dha and a loss of 2 Da from the peptide (photochemical Cys to Ala conversions have been detected earlier with other model peptides).[40] The MS/MS data show an interesting fragmentation pattern: no fragment ions could easily be assigned to either Dha, or the loss of 2 Da elsewhere on the peptide (Figure 2.29). However, the m/z values of the b5 and y5 fragments (compared to the thiol, product **3**) clearly indicate the Cys to Ala conversion and the loss of 4 Da is confined to the interior residues, and that the N-terminal LG and C-terminal GL sequences are unmodified. The signals with the highest intensity are the a5 and b5 ions, but below 400 Da, the only signals observed correspond to internal *VAV fragmentation, where the *VAV indicates a modification of the original amino acids. One possible rationale for this fragmentation pattern would be a cross-link between the C-terminal Val and the carbonyl group of the new Dha residue as indicated in the tentative structure given in Figure 2.29. Further NMR analysis will be presented below to support the structure presented in Figure 2.29.

*ii. Product **18** (624.38).* Product **18**, with a m/z value of 624.38, is isobaric to product **6**, corresponding to the Cys to Dha transformation with an additional loss of 2 Da. This product appears after 5 minutes of irradiation and elutes ca. 5 minutes later than product **6**. In the MS/MS spectrum the b5 fragment is the ion of highest intensity (Figure 2.30), whereas the remainder of the ions show intensities of 10% or less compared to that of the b5 ion. One exception is the ion

generated by the loss of water from the molecular ion ($[M+H]^{+1}$-18; 40% relative intensity). A tentative structure of product **18** is shown in Figure 2.30, which contains Dha and a double bond between the $^{\alpha}$C and $^{\beta}$C position of the N-terminal Val (dehydrovaline, Dhv). However, we cannot detect b3 or y4 ions to confirm this structure. We only detect the b4, y3, and y5 ions localizing the loss of a total of 4 Da between the N-terminal Val and Ala residues. This could easily be a cross-link, but more experiments must be run to elucidate this structure.

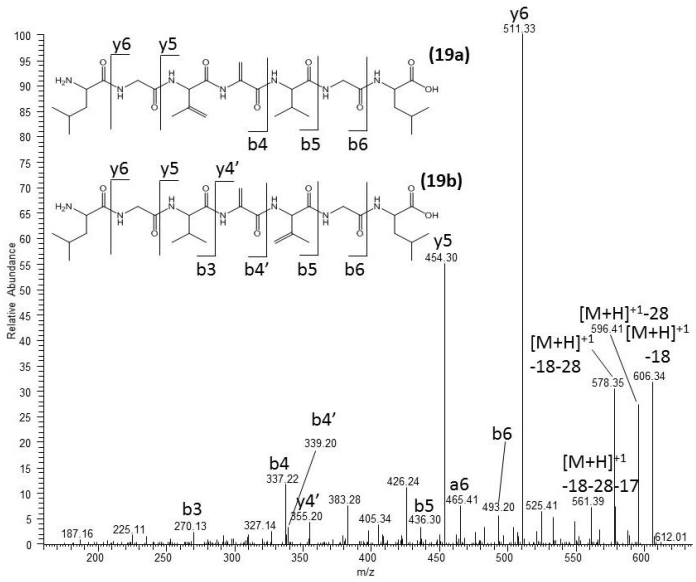

Figure 2.31. MS/MS spectrum of product **19a/19b** after UV irradiation at λ = 254 nm of peptide **1a** at pH 7.0 (100 μM), and tentative assignment of a product structures.

*iii. Products **19a and 19b** (m/z 624.38).* A third set of isobaric products to product **6** and **18** elutes at 12 minutes after 5 minutes of irradiation (Figure 2.13B), and again, the m/z value of 624.38 corresponds to the conversion of Cys to Dha and Val to Dhv. In the MS/MS spectrum (Figure 2.31) of products **19a** and **19b** we detect a b4 ion corresponding to Dha and N-terminal Dhv residues (product 19a), and b4 and y4 ions corresponding to Dha and C-terminal Dhv (notated b4' and y4') (product **19b**). The structures presented in Figure 2.31 show the double bond on the Dhv residues between the $^{\beta}$C and $^{\gamma}$C position, and not the $^{\alpha}$C and $^{\beta}$C position; however, like in product **7**, we cannot make this distinction purely from this MS/MS analysis, but BME derivatization results (shown below) support such a structure.

2.3.10 Derivatization of Products 6, 18, 19a, and 19b with β-mercaptoethanol (BME). To determine whether the double bonds in the isobaric products **6**, **18**, **19a** and **19b** are

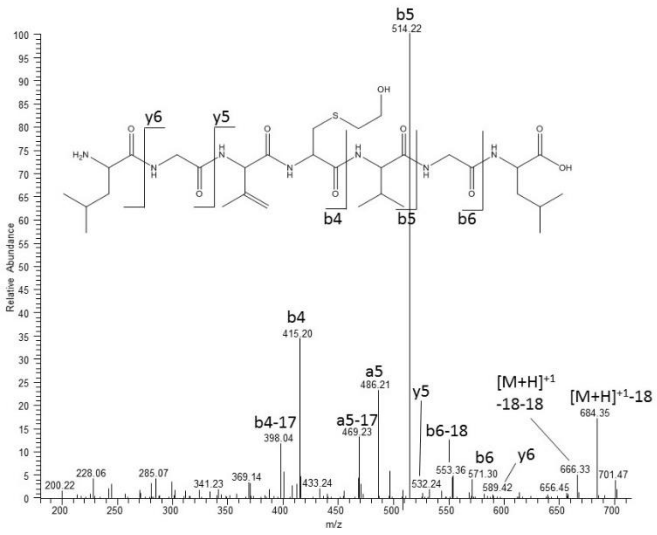

Figure 2.32. MS/MS spectrum of product **19a** after BME derivatization, and tentative assignment of a product structure.

located between the $^{\beta}$C and $^{\gamma}$C or the $^{\alpha}$C and $^{\beta}$C position, the photoproducts generated from the 100 µM peptide **1a** were derivatized with a final concentration of 10 mM BME. The distinction of the double bond location was possible because BME only adds to α,β-unsaturated carbonyls[48,49] (i.e., only if the double bond is located between the $^{\alpha}$C-$^{\beta}$C bond). The pH was adjusted to pH 7.8 with 50 mM ammonium bicarbonate buffer, and the reaction proceeded at room temperature for two hours. MS analysis was performed on the LTQ-FT instrument. Since a thorough analysis of the BME-derivatized photoproducts was described in Section 2.3.3, only BME addition to products **6**, **18**, **19a**, and **19b** were searched for in the new mass spectrometry. Interestingly, BME added only to product **19a**, resulting in product **19a+BME** with an m/z value of 702.39 (Figure 2.32). No products resulting from the addition of two equivalents of BME were observed, as was expected with product **18**. The MS/MS spectrum of the BME-derivatized product, **19a+BME**, is not entirely conclusive. The b4 and y5 ions localize the BME addition to either the Ala (as drawn) or the N-terminal Dhv, if the double bond were located between the $^{\alpha}$C and $^{\beta}$C position of Val (as is the case for product **18**). Since the reaction mixture contained the four isobaric products, it is unclear which product(s) reacted with BME, but it is fair to assume that based on these results, the double bond in at least some of the isobaric products with m/z 624.4 is located between the $^{\beta}$C and $^{\gamma}$C position. Another reason for the lack of BME addition could be related to incorrect structural assignment of the products. Cross-links in the structures,

and not Dha and Dhv, could explain the lack of BME addition. However, due to the lack of supporting data, other structures are just speculative and therefore, not presented.

2.3.11 ^{1}H-^{1}H TOCSY NMR (TOtal Correlated SpectroscopY) of irradiated peptide 1a. To identify the structures of the isobaric products, specifically product **6**, peptide **1a** was dissolved in water at pH 7.0 to a concentration of 100 µM, saturated with Ar, and irradiated at λ = 254 nm for 10 minutes. The resultant photoproducts were then purified by HPLC on a reverse phase C18 column, but sufficient yields of the purified products could not be collected for NMR analysis. To this end, we analyzed the entire photo-irradiated sample before (control) after irradiation at λ = 254 nm for 10 minutes. The samples were dried down in a CentriVap concentrator and diluted with D_2O prior to NMR analysis. ^{1}H-^{1}H TOCSY NMR spectra were recorded on a Bruker Avance 800 MHz NMR instrument, equipped with a TCI cryoprobe, and chemical shifts were predicted in ChemBioDraw Ultra 13.0 (Perkin Elmer, Waltham, MA). NMR data were analyzed using MestReNova version 9.0 (Mestrelab Research, Santiago de Compostela, Spain). ^{1}H-^{1}H TOCSY experiments help elucidate coupling networks for protons directly coupled together (i.e. mutual J-coupling) and protons connected by a chain of couplings, such as amino acids (i.e. same spin system, but not mutual J-coupling. Through these interactions, the same amino acid in different locations of a peptide (such as the Leu, Gly, and Val residues) can be distinguished, since each amino acid has a separate spin system in the peptides. The spectra show diagonal and cross-peaks, where the cross-peaks indicate coupling between protons.

Figure 2.33 shows the ^{1}H-^{1}H TOCSY NMR spectraof the control (purple) overlayed on the photo-irradiated samples (black), and the corresponding amino acids characterized by the crosspeaks. The crosspeaks in the spectra overlayed nicely, except that the Cys peaks (3.0, 2.9

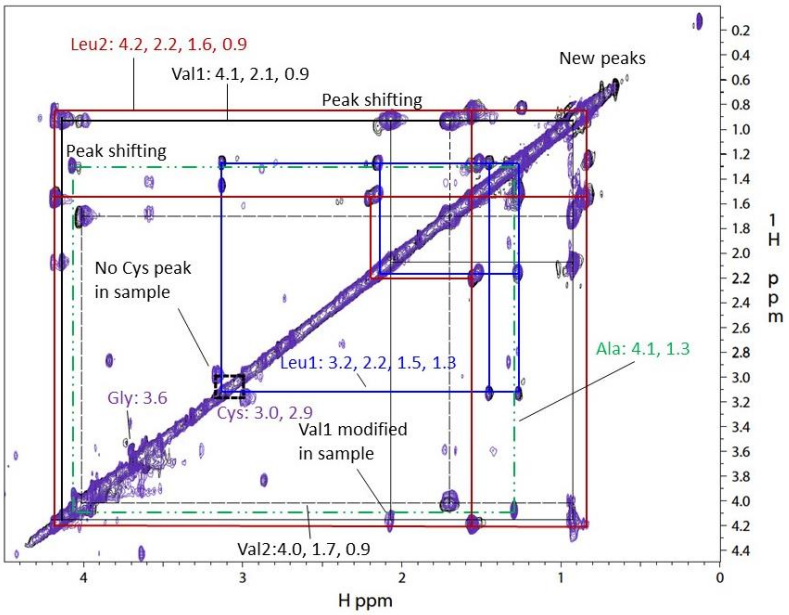

Figure 2.33. ^{1}H-^{1}H TOCSY NMR spectrum of the control non-irradiated (purple) and irradiated (black) peptide **1a** samples after photolysis at λ = 254 nm for 10 minutes.

ppm) were missing in the irradiated samples. This was expected as the mass spectrometry analysis revealed that the Cys residues were modified in many of the photoproducts, e.g. to Ala and Dha. Several peaks shifted in the regions around 0.8 and 1 ppm, and 1.2 and 4 ppm. Another noticeable difference was the absence of a Val peak (2.1, 4.0 ppm), notated 'Val 1' in the spectra since there are two Val residues in peptide **1a**, an indication that one of the Val residues was modified after irradiation. Nevertheless, a new peak could not be assigned to a modified Val residue, so the structure for product **6** is still tentative.

2.2.12 ^{1}H-^{13}C HSQC NMR (Heteronuclear Single Quantum Coherence) of irradiated peptide 1a.

We continued to probe the structure of product **6** by NMR spectroscopy of the stable isotope-labeled peptides **1b** and **1c**, since the ^{1}H-^{1}H TOCSY NMR analysis of the photoproducts from non-isotopically labeled peptide **1a** was encouraging, yet non-conclusive. Peptides **1b** and **1c** were dissolved at pH 7.0 to a concentration of 100 µM, Ar-saturated, and irradiated at λ = 254 nm for 10 minutes. The resultant photoproducts were then purified by HPLC on a reverse phase C18 column, but again, sufficient yields of purified material could not be collected for NMR analysis. As for the other NMR experiments, we analyzed the entire 100 µM sample before (control) and after photo-irradiation at λ = 254 nm for 10 minutes. The

samples were dried down in the CentriVap concentrator and diluted with D_2O prior to NMR analysis. ^{1}H-^{13}C HSQC NMR spectra were recorded on a Bruker Avance 800 MHz NMR instrument, equipped with a TCI cryoprobe and the chemical shifts were predicted in ChemBioDraw Ultra 13.0 (Perkin Elmer, Waltham, MA). NMR data were analyzed using MestReNova version 9.0 (Mestrelab Research, Santiago de Compostela, Spain). ^{1}H-^{13}C HSQC NMR experiments help elucidate coupling networks for protons directly coupled to ^{13}C. Since only the Val residues were ^{13}C-labeled, only the Val residues will be observed by ^{1}H-^{13}C HSQC NMR analysis, rendering the analysis much simpler than for the whole peptide. The chemical shifts of modified Val with double bonds were markedly different, as predicted by ChemDraw. The ^{13}C chemical shift predictions for the $^{\alpha}C$, $^{\beta}C$, and $^{\gamma}C$ positions of the unmodified Val residues were 61.7, 31.1, and 18.5 ppm, respectively. The ^{13}C chemical shift predictions for the $^{\alpha}C$, $^{\beta}C$, and $^{\gamma}C$ positions of the Val with a double bond between the $^{\alpha}C$ and the $^{\beta}C$ position were 149.5, 120.3, and 21.6 ppm, respectively. The ^{13}C chemical shift predictions for the $^{\alpha}C$, $^{\beta}C$, and $^{\gamma}C$ positions of the Val with a double bond between the $^{\beta}C$ and the $^{\gamma}C$ position were 68.8, 136.6, 19.8 and 118.6 ppm, respectively. If the $^{\gamma}C$ atom of a Val residue is cross-linked to the Ala carbonyl group, the ^{13}C chemical shift predictions for the $^{\alpha}C$, $^{\beta}C$, and $^{\gamma}C$ positions of the modified Val residue were 56.4, 34.1, 11.4 and 69.1ppm, respectively. When the control peptide **1b** was analyzed by NMR, the chemical shifts of $^{\alpha}C$, $^{\beta}C$, and $^{\gamma}C$ carbons recorded were very similar to the predicted values (59.3, 30.0, and 18.0 ppm, respectively) (data not shown because the peaks were also observed in the irradiated sample, see below).

Figure 2.34 shows the ^{1}H-^{13}C HSQC NMR spectrum of a solution of peptide **1b** after photolysis. The peaks of the control sample (59.42, 30.20, and 17.88 ppm for the $^{\alpha}C$, $^{\beta}C$, and $^{\gamma}C$ position, respectively) are still observed indicating that only part of peptide **1d** was converted to

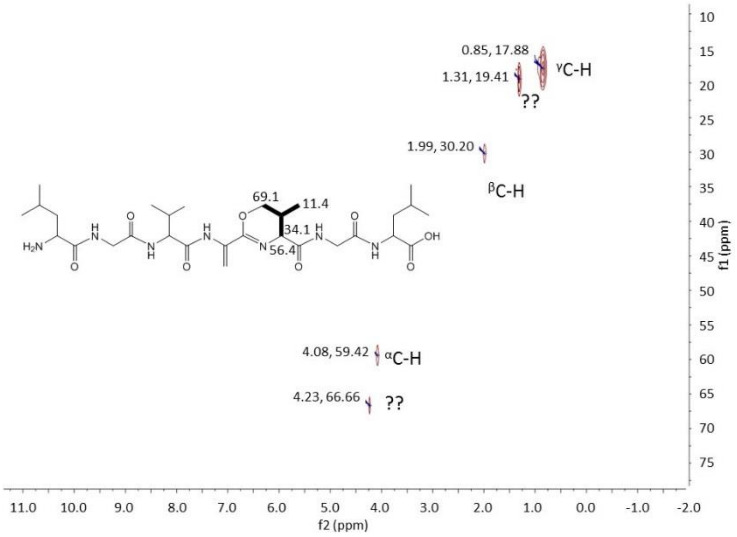

Figure 2.34. ^{1}H-^{12}C HSQC NMR spectrum of peptide **1b** after photolysis at λ = 254 nm for 10 minutes.

products. However, two additional ^{13}C signals were observed at 66.66 and 19.41 ppm. Clearly, these additional peaks do not correspond to a double bond on the Val residue located either between the $^{\alpha}$C and $^{\beta}$C or the $^{\beta}$C and $^{\gamma}$C position. However, the peaks are fairly consistent with the proposed cross-link between the Val $^{\gamma}$C and the Ala carbonyl group proposed for product **6**. The proposed structure of product **6** is displayed Figure 2.34 together with the predicted chemical shifts for the individual ^{13}C atoms. Here the $^{\beta}$C signal remains largely unchanged, but new signals appear for the $^{\alpha}$C-H and $^{\gamma}$C-H positions. Although the peak predictions do not completely agree with our experimental data, this modified Val structure is our best estimate as to the structure of product **6**. NMR experiments with the photo-irradiated peptide **1c** were not successful (too low yields of individual products).

2.3.13 Ozonolysis of Photoproducts Generated during Photo-irradiation of 100 µM Peptide 1a at pH 7.0. In an attempt to further characterize the location of the double bonds in products **6**, **18**, **19a**, and **19b**, the photoproducts generated during the 10 minute photo-irradiation of peptide **1a** at λ = 254 nm at pH 7.0 were treated with ozone (O_3) following irradiation. The O_3 was generated with an Ozotech ozonolysis apparatus and bubbled directly into the control and irradiated samples for 30 seconds at room temperature (in glass tubes) or bubbled into water for 2 minutes, and then the O_3-containing water was added to the samples. Reduction of the resultant

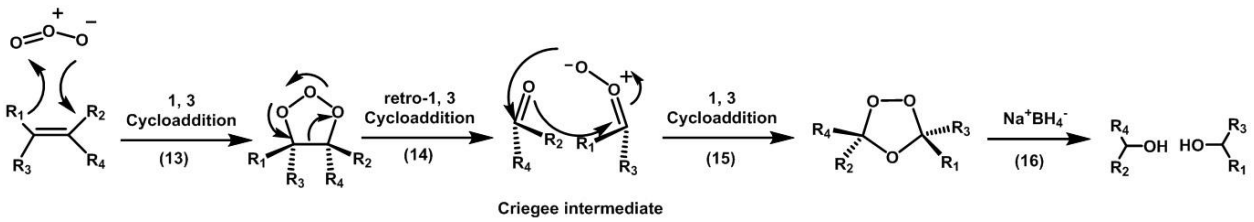

Scheme 2.5. Reaction scheme of the ozonolysis reaction.

Criegee intermediate (Scheme 2.5, reaction 15) was accomplished with sodium borohydride. The samples were then frozen at -20 °C until MS analysis. Scheme 2.5 shows how ozone reacts with double bonds, and how it is reduced with sodium borohydride to yield hyoxyl adducts.

Interestingly, no hydroxyl products were observed in the photo-irradiated samples, although we hypothesized that ozonolysis of products **6**, **18**, **19a**, and **19b** may generate such products. There was also no trace of backbone fragmentation products, commonly observed when hydroxyl groups are present on the $^{\alpha}$C of a peptide.[57] We know from our BME experiments that there is at least a trace of Dha in one of the products. The absence of expected ozonolysis products could again indicate our initial structural assignments of products **6**, **18**, **19a**, and **19b** were incorrect, or the bulkiness of the Val residues hinders the 1, 3-cycloaddition of O_3, and therefore the ozonolysis products cannot be formed.

2.3.14 Photo-irradiation of 100 µM Peptide 1a at pH 4.0. Peptide **1a** was dissolved in water at pH 4.0 to a concentration of 100 µM. Solutions were saturated with Ar and irradiated at λ = 254 nm. The photoproducts generated were analyzed by LC-MS on the Qtof Premier and MS/MS using the LTQ-FT instrument. A representative chromatogram for control and photo-irradiated peptide 1a at pH 4.0 is shown in Figure 2.35, and the kinetics of photoproduct formation are shown in Figure 2.36. It should be noted that the control sample in Figure 2.35A shows no traces of photoproducts; however, the chromatogram shows a wide peak for peptide 1a. Therefore, the control may have contained not only the disulfide peptide **1a**, but additionally a

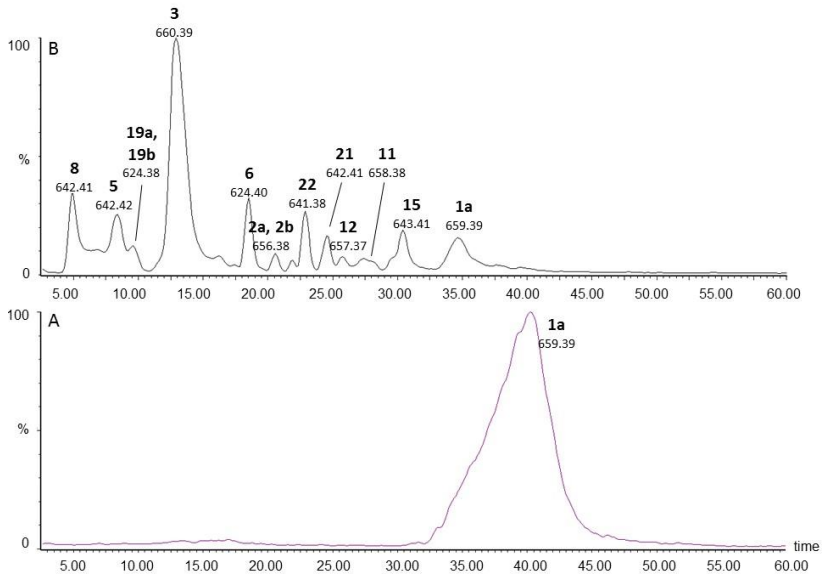

Figure 2.35. LC-MS analysis of the photoproducts generated by UV-irradiation at λ = 254 nm of peptide **1a** (100 μM) in Ar-saturated H_2O at pH 4.0 in the (A) control and (B) the sample after 10 minutes of irradiation.

Product	Proposed Structure	MS/MS
21	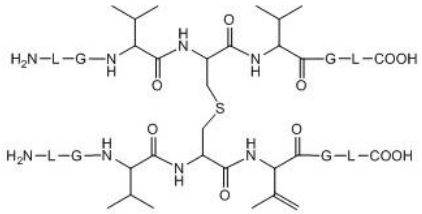	A.8
22	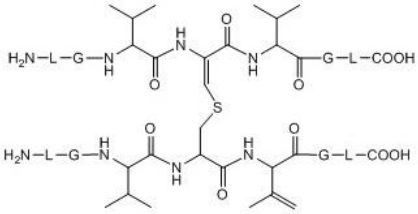	A.9

Table 2.8. Peptide **1a** photoproducts observed after photolysis at λ = 254 nm at pH 4.0 (100 μm).

dithiohemiacetal product (**20b**), but this was not tested at the time. In addition to the photoproducts discussed in the previous sections, the tentative structures of the resultant photoproducts, generated at pH 4.0, that have not yet been discussed are shown in Table 2.8. There were four major types of photoproducts generated in this experiment: disproportionation products (product **3** (m/z 660.41), **5** (m/z 642.41) and **8** (m/z 642.42)), disulfide derivatives (product **11** (m/z 658.38^{+2}), **12** (m/z 657.37^{+2}), **15** (m/z 43.41^{+2}), **21** (m/z 642.41^{+2}), and **22** (m/z 641.42^{+2})), and products generated through H-atom transfer reactions (m/z products **2a** and **2b** (m/z 656.39), **6** (m/z 624.40), **19a** and **19b** (m/z 624.38)).

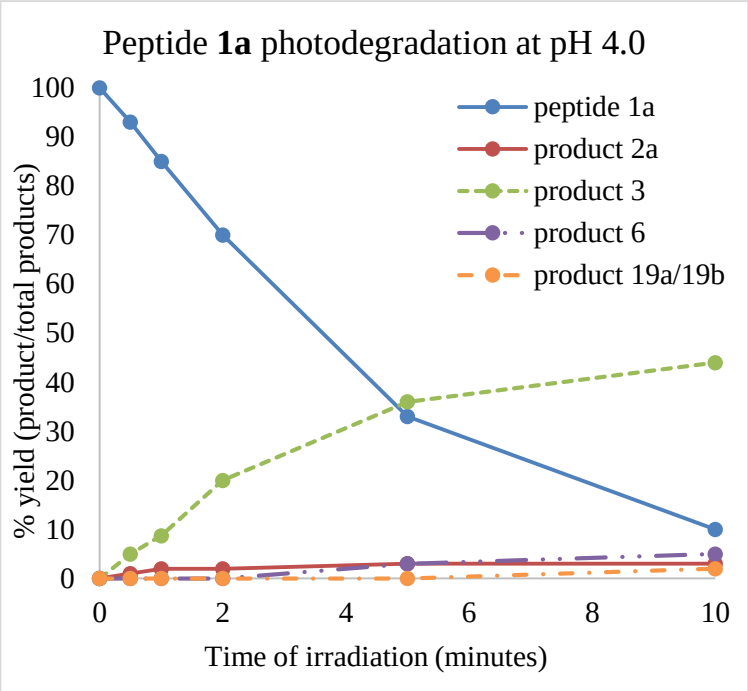

Figure 2.36. Kinetics of formation for products **1a**, **2a**, **3**, **6** and **19a/19b** after UV irradiation at λ = 254 nm of Peptide **1a** at pH 4.0 (100 µM) in an Ar-saturated H_2O.

The time course of photodegradation of peptide **1a** at pH 4.0 is shown in Figure 2.36. Like in the experiments at pH 7.0, the disulfide decomposition shows biphasic kinetics. The major product generated by the irradiation of 100 µM peptide **1a** at pH 4.0 was product **3**. The yield of product **3** was much higher at pH 4.0 as compared to pH 7.0, reaching 45% after 10 minutes of irradiation. Two new disulfide derivative products were observed during the irradiation, thioether products **21** and **22**, with m/z 642.41^{+2} and m/z 641.38^{+2}, respectively. Another interesting observation during the irradiation at this low pH was the absence of the isobaric product **18,** whereas products **6, 19a** and **19b** were formed in similar yields. The MS/MS data between the irradiation at pH 4.0 was consistent with the MS/MS data presented at pH 7.0.

2.4 Discussion

The photolysis of low concentrations of peptide **1a**, $(LGVCVGL)_2$, at λ = 254 nm under Ar predominantly generates the isothiazole-3(2H)-one **2a**. This product contains an S-N bond between the sulfur of the original Cys residue and the nitrogen of its C-terminal peptide bond. During just one minute of irradiation, peptide **1a** was converted ca. 90% into product **2a**. This product was characterized by MS, chemical derivatization with N-ethylmaleimide (NEM) and

beta-mercaptoethanol (BME), and ^{1}H-NMR. The analogous product was also formed in the isotopically-labeled peptides **1b** and **1c**, i.e., products **9** and **10**, respectively. In addition, product **2a** is generated via AAPH-dependent oxidation of peptide **1d** at pH 8.0-10.0, although in much lower yield.

The chemical derivatization reactions of NEM and BME with product **2a** were imperative in characterizing the S-N bond. NEM reacts with free thiols and amines,[47] whereas BME reacts with α, β-unsaturated carbonyl groups[48,49] and cleaves the S-N bond.[58] The MS/MS fragmentation patterns between underivatized product **2a** (Figure 2.2), and N-terminal NEM-derivatized product **2a** (Figure 2.6) were very similar in the sense that in both MS/MS spectra the loss of water from the parent ion was the most intense fragment ion and the intensity of all the b and y ions were ca. 15% normalized to the parent ion which lost water, indicating that NEM did not react with the modified Cys residue. Furthermore, C*V, VC*V, and C*VG internal fragments (where C* represents the modified Cys residue) also fell in this range of relative abundance, suggesting that the original Cys and the C-terminal Val residue were cross-linked in another way than solely the amide bond. This is suggested by the relatively high intensity of these internal fragment ions compared to the standard b and y ions. When product **2a** was derivatized with BME, two products were formed: a mono-derivatization and di-derivatization product. The mono-derivatized product **2a+BME** contained a single BME adduct on the original Cys residue (Figure 2.10). During fragmentation, no longer was the b4 ion of low intensity (15%), but now it was of ca. 50% signal intensity relative to the hightest intensity ion, the y6 ion. This large change in b4 ion intensity is most likely due to the cleavage of the S-N bond, forming a new disulfide between the isothiazole-3(2H)-one sulfur and the BME thiol. This should allow for an easier formation of the b4 ion since energy does not have to be expended for cleavage of

the S-N bond in the gas-phase. Similarly, with sulfenamide pro-drugs, the mechanism of drug release involves cleaving the S-N bond through hydrolysis or the formation of a disulfide by addition of a nucleophilic thiol.[59,58] The MS/MS analysis of the double BME derivatization product **2a+2BME** (Figure 2.11), reveals that two BME molecules are attached to the original Cys residue, consistent with the additional derivatization of the double bond between the $^{\alpha}$C and $^{\beta}$C positions of the modified Cys residue.

^{1}H-NMR analysis provided complementary support for the formation of the isothiazole-3(2H)-one structure in product **2a**. The experimental chemical shift, 6.27 ppm, matched the predicted chemical shift of the $^{\beta}$C-H group involved in the double bond between the $^{\alpha}$C and the $^{\beta}$C position of the original Cys residue in product **2a**, and not the predicted chemical shift for product **2b**. Unfortunately, since this NMR sample did not contain pure product **2a**, we cannot say that this peak was only due to product **2a**, just an indication since small amounts of product **11** and **12** were also present. Additionally, NMR predictors do not generally take into account the conformation of the peptide, which plays an important role in distinguishing product **2a** from product **2b**. Ideally, pure products **2a**, **9**, and **10** should be collected for ^{1}H-NMR and ^{13}C-NMR, and a standard peptide with a known isothiazole-3(2H)-one structure should be synthesized and analyzed to be entirely confident in our structural assignment of product **2a**.

Sulfenamide formation has been reported in oxidative environments, through reduction of sulfinic acid, or transformation of a thiol into a reactive sulfur halide followed by reaction with an amine.[60] Interestingly, a cyclic sulfenamide was formed in the peptide PFKCG under oxidative conditions only if a nearby Lys was available for cross-linking, and not if the Lys was replaced by Val.[53] After oxidation of PFLCG, only *inter*molecular cross-links were observed. Since the peptide we used to generate the *intra*molecular sulfenamide (isothiazole-3(2H)-one) did contain Val

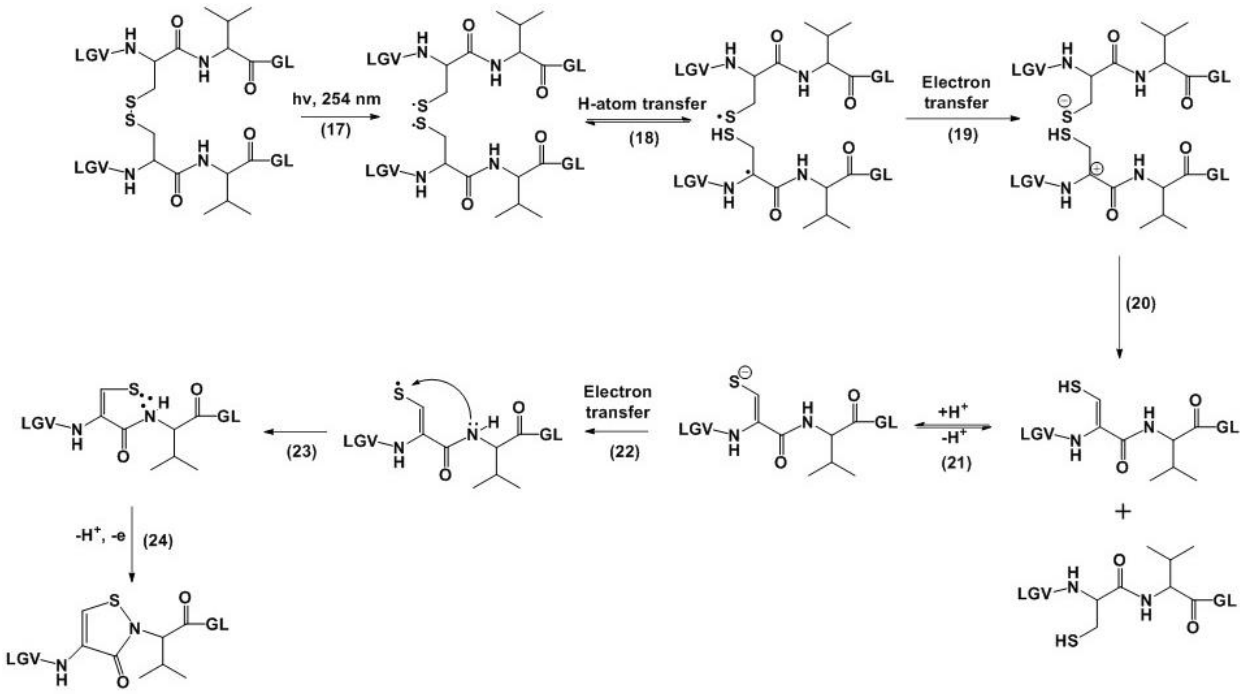

Scheme 2.6. Proposed reaction scheme for the formation of products **2a, 9,** and **10**.

residues, the sulfenamide products generated by these two different methods (oxidation and photolysis) are likely formed by very different mechanisms. The formation of the isothiazole-3(2H)-one **2a** is likely the result of steric constraints, which disfavor *inter*molecular reactions of thiyl radicals, since previous studies with model peptides $(LGACAGL)_2$ and $(GGCGGL)_2$ showed no significant yields of any heterocyclic product. The only differences between these model peptides are the amino acid residues in the i+1 and i-1 position to the Cys disulfide. The bulky lateral isopropyl groups of Val provide much greater steric hindrance in peptides compared to the Ala methyl group and the proton on Gly. Photolysis of a model peptide with Leu at the i+1 and i-1 positions will be important to test the steric constraints when a tert-butyl group is near the disulfide bond.

In scheme 2.6, we propose a mechanism for the formation of the isothiazole-3(2H)-one products **2a, 9** and **10**. During the irradiation, the disulfide bonds in peptides **1a, 1b** and **1c** are homolytically cleaved, each yielding a pair of thiyl radicals (reaction 17). Within the solvent

cage, a thiyl radical can undergo intramolecular H-atom transfer with the $^{\alpha}$C-H bond (reaction 18). Next, electron transfer between the newly generated C-centered radical and a thiyl radical create a $^{\alpha}$C carbocation and a thiolate (reaction 19). Subsequently, the thiolate can abstract the $^{\beta}$C-H proton from the carbocation to neutralize the charges, yielding a thiol and vinyl thiol (reaction 20). From here, we hypothesize that at pH 7.0 or above (where our reactions take place), the thiol is in equilibration with the thiolate anion (reaction 21). Light-induced electron ejection from a vinyl thiolate under continuous photo-irradiation with UV light forms a vinyl thiyl radical (reaction 22).[61] Subsequently, the amide nitrogen reacts with this S-centered radical to create a 2 center, 3 electron bond[62,63] (reaction 23), which is then oxidized to form the S-N cross-link in product **2a**, **9**, and **10** (reaction 24). The same reaction scheme, presented in Scheme 2.6, is consistent with the formation of product **2a** during the reaction of peptide **1d** with AAPH, except that the vinyl thiyl radical will be generated through reaction of vinyl thiol with AAPH-derived carbon-centered radicals.

Very unique to product **2a** is the double bond between the $^{\alpha}$C and the $^{\beta}$C position. This is indicative of a radical mechanism including thiyl H-atom and electron transfer from the $^{\alpha}$C-H. In Scheme 2.6, we presented a vinyl Cys as the intermediate step before the sulfenamide formation, but we hardly see a trace of the vinyl thiol product during irradiation. We propose that this is a very short-lived intermediate that is quickly transformed into the isothiazole-3(2H)-one product **2a**. Product **2a** is relatively stable, surviving irradiation for up to ten minutes under harsh conditions that completely cleave the original disulfide bond within a minute.

Peptide **1a** and the ^{13}C and ^{15}N isotopically-labeled peptides, **1b** and **1c**, were used to support the structure of the isothiazole-3(2H)-one by MS^3 characterization (Figures 2.16-2.18).

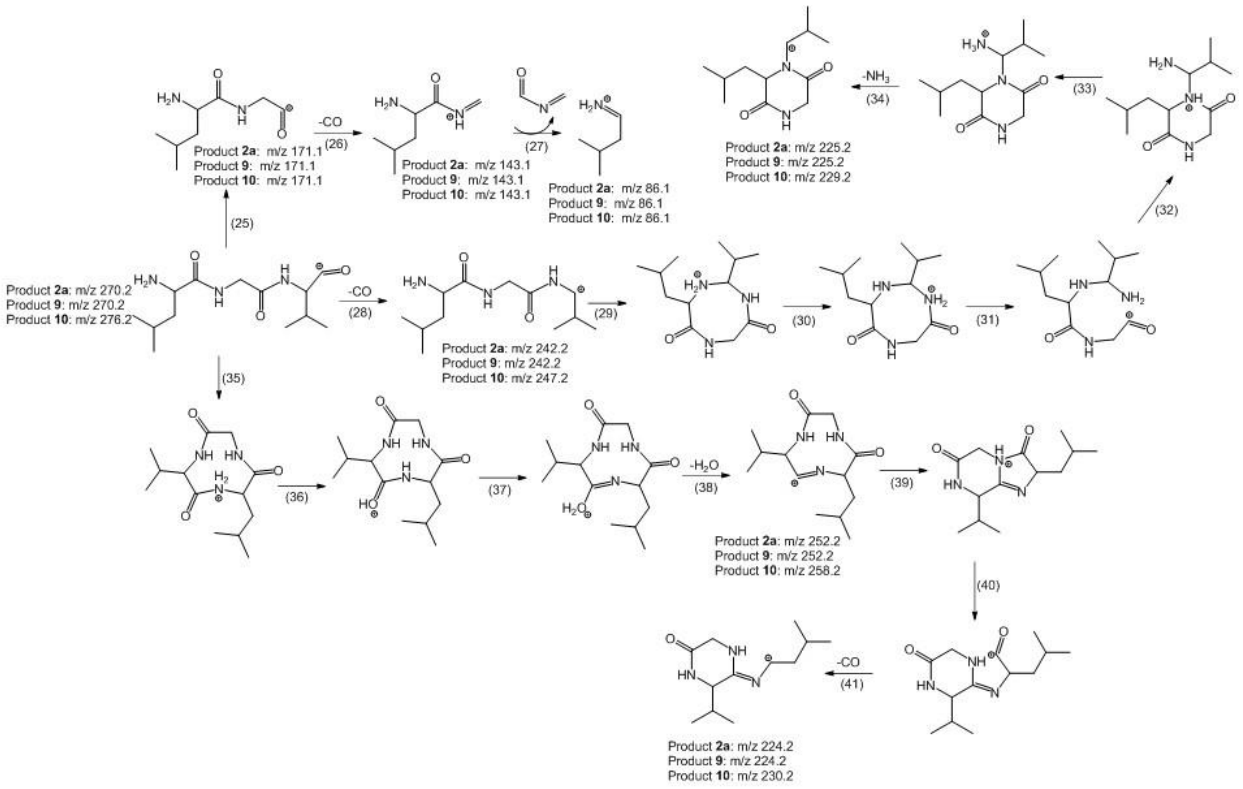

Scheme 2.7. Proposed reaction scheme for the MS^3 fragmentation of the b3 ion of product **2a** (m/z 270.2), **9** (m/z 270.2), and **10** (m/z 276.2).

The different isotopic distributions between the peptides has allowed us to assign fragmentation pathways, which will be discussed below (Schemes 2.7-2.9). We acknowledge that the structures assigned to the fragment ions presented in Figures 2.16-2.18 and Schemes 2.7-2.9 are tentative.

*i. MS^3 fragmentation mechanisms for the b3 ions (m/z 270.2, 270.2, and 276.2 for products **2a**, **9**, and **10**, respectively).* The b3 fragment ions of products **2a**, **9**, and **10** did not include the sulfenamide S-N bond, only the LGV sequence on the N-terminal side of the peptide (Figure 2.16). The m/z values of products **2a** and **9** were identical, whereas product **10** contained the isotopically-labeled N-terminal Val group, so some fragment ions were 6 Da higher than those of the other two products. Scheme 2.7 shows a proposed mechanism for the generation and reactions of fragment ions of b3. There seems to be three initial pathways stemming from the fragmentation of the initial b3 ion: peptide bond cleavage (reaction 25), neutral loss (reaction 28), and internal cyclization (reaction 36). The ion with the highest intensity in products **2a** and

10 is the b2 ion, generated by cleavage of the Val residue, m/z 171.1 (reaction 25). This ion was present in the MS/MS of product **9**, but not as the ion with the highest intensity. Although this could indicate that product **9** has a different structure than the other two products, the MS/MS of this product exactly matched those of products **2a** and **10**, and the MS^3 of the b4 ion and of the VC*V internal fragment ion also matched closely. Therefore, the difference was not examined further. Following the b2 ion fragmentation, loss of the carbonyl (reaction 26) and glycyl-like (reaction 27) groups were observed, generating ions with m/z 143.1 and m/z 86.1, respectively. The second major pathway began with the loss of the carbonyl group (reaction 28), followed by internal cyclization (reaction 29) and loss of the ammonia group (reactions 30-34). The third pathway started with internal cyclization (reaction 35), and along the way, loss of water (reaction 38) and a carbonyl group (reaction 41) were observed.

*ii. MS^3 fragmentation mechanisms for the b4 ions (m/z 369.2, 369.2, and 375.2 for products **2a**, **9**, and **10**, respectively).* Scheme 2.8 shows the proposed mechanisms of ion formation from the fragmentation of the b4 ion. This b4 fragmentation cleaves the sulfenamide bond as well as the peptide bond between the Cys and C-terminal Val residue. The b4 ion is larger in size than the b3 ion, so more of the major fragments include the loss of amino acids, not neutral fragments. Initially, cyclization between the N-terminal amine and the C-terminal carbonyl cation forms a large 12-membered ring (reaction 42). Then, the mobile proton moves to a different amide nitrogen (reaction 43), leading to the favorable amide bond cleavage (reaction 44), carbonyl loss (m/z 341.14, 341.2, and 347.2 for product **2a**, **9**, and **10** respectively) (reaction 45), and finally methanimine loss (m/z 312.2, 312.2, and 318.2 for product **2a**, **9**, and **10**, respectively) (reaction 46). When the mobile proton moves to a different amide nitrogen after the first cyclization (reaction 47), ring opening between the Leu and Gly (reaction 48) allows Leu

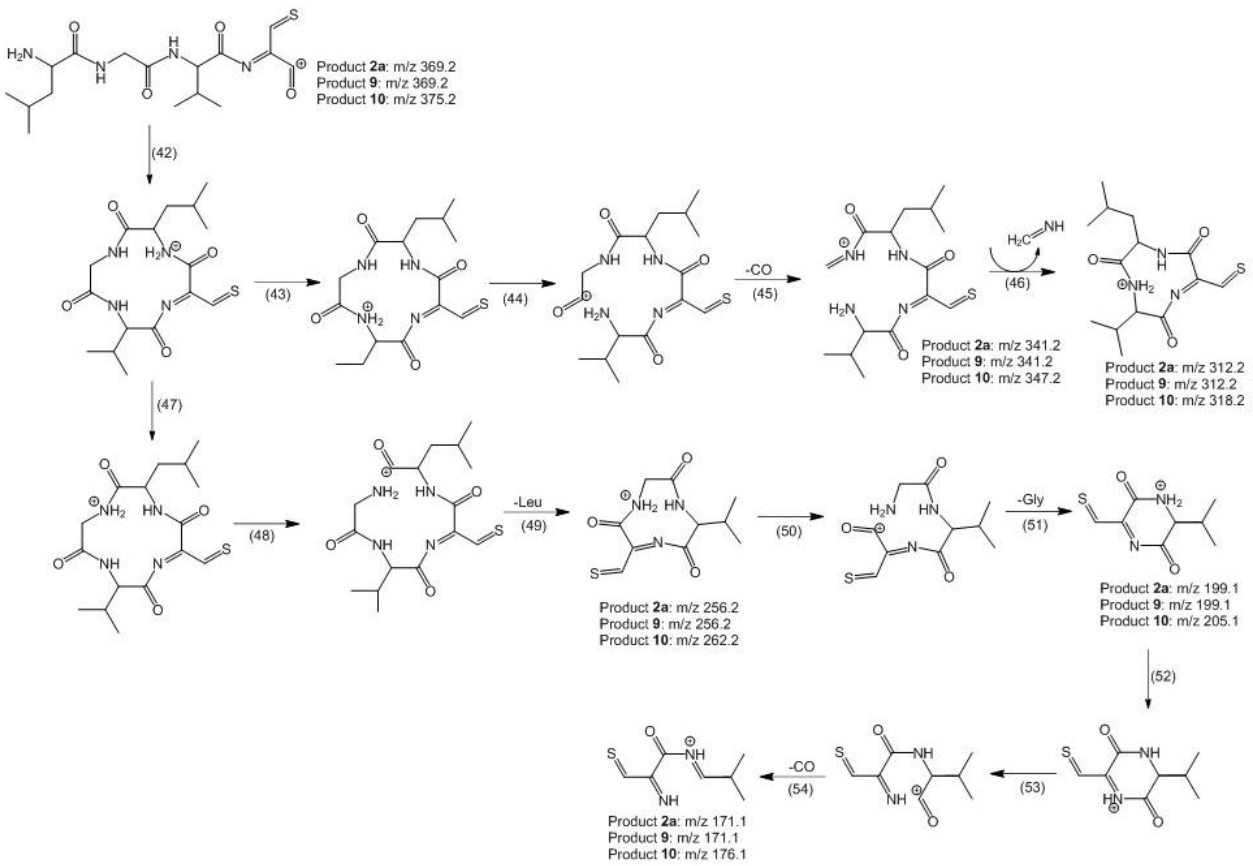

Scheme 2.8. Proposed reaction scheme for the MS^3 fragmentation of the b4 ion of product **2a** (m/z 369.2), **9** (m/z 369.2), and **10** (m/z 375.2).

fragmentation (reaction 49), followed by Gly fragmentation in reaction 51. From here, the mobile proton can move to protonate the Cys amide nitrogen (reaction 52) and open the cycle (reaction 53), creating the carbonyl cation on the Val group. This is then quickly cleaved, creating the fragment ions with m/z 171.1, 171.1, and 176.1 for product **2a**, **9**, and **10**, respectively (reaction 54). It should be noted that for product **10**, the carbonyl was ^{13}C-labeled, so a loss of 29 Da was observed, not of 28 Da. Interestingly, a fragment ion with m/z 171.1 was previously seen during b3 ion fragmentation, but now instead of being a major peak, it is minor. There is also no hint of a carbonyl loss from the ion with m/z 171.1 here in the b4 fragmentation that we, instead, observed in the b3 ion fragmentation (i.e. m/z 143.1). This suggests the structure from the ion with m/z 171.1 in the b4 fragmentation is very different from the b3 fragment ion with m/z 171.1 and does not contain a C-terminal carbonyl group.

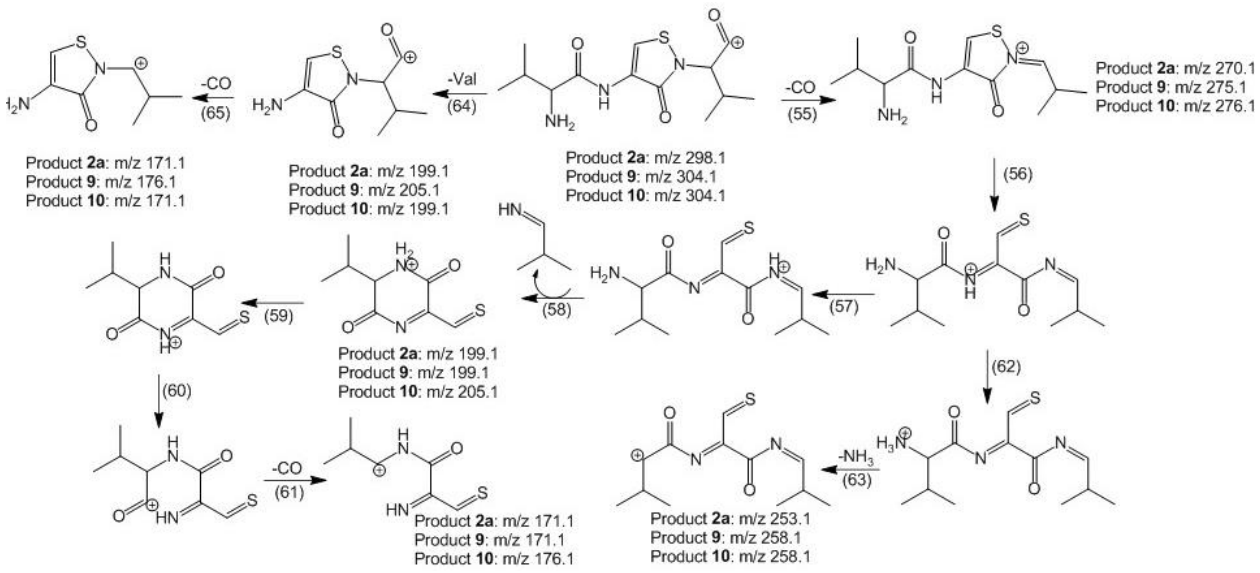

Scheme 2.9. Proposed reaction scheme for the MS^3 fragmentation of the b4 ion of product **2a** (m/z 298.1), **9** (m/z 304.1), and **10** (m/z 304.1).

*iii. MS^3 fragmentation mechanisms for the VC*V internal fragment ions (m/z 298.2, 304.2, and 304.2 for products **2a**, **9**, and **10**, respectively).* The pathway of formation to the MS^3 ions from the internal fragment ion VC*V is shown in Scheme 2.9. This fragment ion still contains the intact isothiazole-3(2H)-one, and both product **9** and **10** contain isotopically labeled Val residues, albeit on the C-and N-terminal Val, respectively. The largest fragment ion observed in Figure 2.18 corresponds to the loss of the C-terminal carbonyl group (reaction 55). Next along this pathway, the heterocycle is opened and the mobile proton moves to the Cys amide nitrogen (reaction 56). Here, the mobile proton can move to the N-terminus and ammonia is cleaved (reactions 62 and 63), or it can move to the Val amide nitrogen (reaction 57), whereby internal cyclization from the N-terminal amine to the Cys carbonyl group cleaves off the C-terminal Val group (reaction 58). The remaining product **10** fragment ion contains the N-terminal isotopically labeled Val residue (m/z 205.1), whereas product **2a** and **9** do not contain an isotopically N-terminal Val residue (m/z 199.1). Movement of the mobile proton to the Cys amide (reaction 59) and ring opening (reaction 60) allows the Val carbonyl group to be cleaved (m/z 171.1, 171.1, and 176.1 for products **2a**, **9**, and **10**, respectively (reaction 61). Interestingly, another

fragmentation pathway yields ions with the exact same m/z values, but the isotopically labeled C-terminal Val residue is retained instead of the N-terminal Val (reactions 64 and 65). The y2 fragment ion generates ions with m/z 199.1 in products **2a** and **10**, and m/z 205.1 in product **9** (reaction 64). The carbonyl group is easily cleaved from the y2 fragment yielding ions with m/z 171.1, 176.1, and 171.1 for products **2a**, **9**, and **10**, respectively (reaction 65). Interestingly, this y2 fragmentation pathway does not seem to be as favorable as the former pathway because the intensities of these ions seem to be lower in product **9** and **10**. Since product **2a** does not contain any isotopic labels, the m/z values for the different fragment ions are the same. It should also be noted that product **10** yields an ion with m/z 275.1, corresponding to a carbonyl loss from product **9**.

Although the major objective in this chapter was the elucidation of the isothiazole-3(2H)-one structure, we were also interested in the four minor isobaric photoproducts generated after the photolysis of peptide **1a** at 100 μM concentration (products **6, 18**, **19a**, and **19b**). Although they were formed in low yields, they were most likely products of H-atom transfer reactions. These products all were consistent with the transformation of Cys to Dha and an additional loss of 2 Da from the product peptide. Their MS/MS spectra were all very different, and likely characteristic for their structures, but presently we could not elucidate their structures in all detail except that for product **6**, although BME addition and NMR spectra were recorded. These photoproducts need to be collected individually so that specific derivatization chemistry can be performed separately to allow for more accurate analysis.

The formation of the isothiazole-3(2H)-one products from peptide **1a** was proposed to occur *intra*molecularly, however, *inter*molecular dithiohemiacetal products were also observed during the photolysis of peptide **1a** and the reaction of peptide **1d** with C-centered radicals

derived from AAPH. In fact, the dithiohemiacetal product **20b** was a major product, accounting for ca. 23% of the reaction products after the AAPH reaction at pH 7.0 and pH 8.0, whereas the disulfide, product **20a**, accounted for 50 and 64%, respectively. The dithiohemiacetal products have been reported previously as photolysis products from several peptides and proteins,[29,30,64] but not after the reaction of thiols with AAPH.

2.5 Conclusion

This report provides the first evidence for a heterocyclic peptide product generated via light stress. The potential for light to form an isothiazole-3(2H)-one structure with such efficiency is of interest to the pharmaceutical industry as disulfide bonds are present in many protein therapeutics. The peptide studied, $(LGVCVGL)_2$, was unique due to the Val residues at the i+1 and i-1 positions relative to the reactive disulfide bond, sterically straining this peptide. Previous peptides containing Ala or Gly next to the disulfide bond showed no trace of such structures after photolysis, highlighting the importance of conformation for protein and peptide stability. This product is of further interest to protein stability because dehydroamino acids and intermolecular heterocycles could lead to aggregation or immunogenic products.

2.6. References

1. Wang, W.; Singh, S.; Zeng, D. L.; King, K.; Nema, S., Antibody structure, instability, and formulation. *J Pharm Sci* **2007,** *96* (1), 1-26.
2. Reichert, J. M.; Valge-Archer, V. E., Development trends for monoclonal antibody cancer therapeutics. *Nat Rev Drug Discov* **2007,** *6* (5), 349-56.
3. Filipe, V.; Jiskoot, W.; Basmeleh, A. H.; Halim, A.; Schellekens, H.; Brinks, V., Immunogenicity of different stressed IgG monoclonal antibody formulations in immune tolerant transgenic mice. *mAbs* **2012,** *4* (6), 740-52.
4. Wei, Z.; Feng, J.; Lin, H. Y.; Mullapudi, S.; Bishop, E.; Tous, G. I.; Casas-Finet, J.; Hakki, F.; Strouse, R.; Schenerman, M. A., Identification of a single tryptophan residue as critical for binding activity in a humanized monoclonal antibody against respiratory syncytial virus. *Analytical chemistry* **2007,** *79* (7), 2797-805.
5. Torosantucci, R.; Schöneich, C.; Jiskoot, W., Oxidation of therapeutic proteins and peptides: structural and biological consequences. *Pharmaceutical research* **2014,** *31* (3), 541-53.
6. Jiskoot, W.; Randolph, T. W.; Volkin, D. B.; Middaugh, C. R.; Schöneich, C.; Winter, G.; Friess, W.; Crommelin, D. J.; Carpenter, J. F., Protein instability and immunogenicity: roadblocks to clinical application of injectable protein delivery systems for sustained release. *J Pharm Sci* **2012,** *101* (3), 946-54.
7. Li, S.; Schöneich, C.; Borchardt, R. T., Chemical instability of protein pharmaceuticals: Mechanisms of oxidation and strategies for stabilization. *Biotechnol Bioeng* **1995,** *48* (5), 490-500.

8. Cornes, P., The economic pressures for biosimilar drug use in cancer medicine. *Target Oncol* **2012,** *7 Suppl 1*, S57-67.

9. Kerwin, B. A.; Remmele, R. L., Jr., Protect from light: photodegradation and protein biologics. *J Pharm Sci* **2007,** *96* (6), 1468-79.

10. Mallaney, M.; Wang, S. H.; Sreedhara, A., Effect of ambient light on monoclonal antibody product quality during small-scale mammalian cell culture process in clear glass bioreactors. *Biotechnol Prog* **2014,** *30* (3), 562-70.

11. Creed, D., The photophysics and photochemistry of the near-UV absorbing amino-acids .I. Tryptophan and its simple derivatives. *Photochem Photobiol* **1984,** *39* (4), 537-562.

12. Bent, D. V.; Hayon, E., Excited state chemistry of aromatic amino acids and related peptides. III. Tryptophan. *J Am Chem Soc* **1975,** *97* (10), 2612-9.

13. Creed, D., The photophysics and photochemistry of the near-UV absorbing amino-acids .II. Tyrosine and its simple derivatives. *Photochem Photobiol* **1984,** *39* (4), 563-575.

14. Bent, D. V.; Hayon, E., Excited-state chemistry of aromatic amino-acids and related peptides .I. Tyrosine. *J Am Chem Soc* **1975,** *97* (10), 2599-2606.

15. Bent, D. V.; Hayon, E., Excited-state chemistry of aromatic amino-acids and related peptides .II. Phenylalanine. *J Am Chem Soc* **1975,** *97* (10), 2606-2612.

16. Finley, E. L.; Dillon, J.; Crouch, R. K.; Schey, K. L., Identification of tryptophan oxidation products in bovine alpha-crystallin. *Protein Sci* **1998,** *7* (11), 2391-7.

17. Parker, N. R.; Jamie, J. F.; Davies, M. J.; Truscott, R. J., Protein-bound kynurenine is a photosensitizer of oxidative damage. *Free Radic Biol Med* **2004,** *37* (9), 1479-89.

18. Grossweiner, L. I., Photochemistry of proteins: a review. *Curr Eye Res* **1984,** *3* (1), 137-44.

19. Laustriat, G.; Hasselmann, C., Photochemistry of proteins. *Photochem Photobiol* **1975,** *22* (6), 295-8.

20. Dremina, E. S.; Sharov, V. S.; Davies, M. J.; Schöneich, C., Oxidation and inactivation of SERCA by selective reaction of cysteine residues with amino acid peroxides. *Chem Res Toxicol* **2007,** *20* (10), 1462-9.

21. Gracanin, M.; Hawkins, C. L.; Pattison, D. I.; Davies, M. J., Singlet-oxygen-mediated amino acid and protein oxidation: formation of tryptophan peroxides and decomposition products. *Free Radic Biol Med* **2009,** *47* (1), 92-102.

22. Vanhooren, A.; Devreese, B.; Vanhee, K.; Van Beeumen, J.; Hanssens, I., Photoexcitation of tryptophan groups induces reduction of two disulfide bonds in goat alpha-lactalbumin. *Biochemistry* **2002,** *41* (36), 11035-43.

23. Miller, B. L.; Hageman, M. J.; Thamann, T. J.; Barron, L. B.; Schöneich, C., Solid-state photodegradation of bovine somatotropin (bovine growth hormone): evidence for tryptophan-mediated photooxidation of disulfide bonds. *J Pharm Sci* **2003,** *92* (8), 1698-709.

24. Prompers, J. J.; Hilbers, C. W.; Pepermans, H. A., Tryptophan mediated photoreduction of disulfide bond causes unusual fluorescence behaviour of Fusarium solani pisi cutinase. *FEBS Lett* **1999,** *456* (3), 409-16.

25. The photophysics and photochemistry of the near-UV absorbing amino-acids .III. Cystine and its simple derivatives. *Photochem Photobiol* **1984,** *39* (4), 577-583.

26. Everett, S. A. S., Christian; Stewart, John H.; Asmus, Klaus Dieter, Perthiyl radicals, trisulfide radical ions, and sulfate formation: a combined photolysis and radiolysis study

on redox processes with organic di- and trisulfides. *Journal of Physical Chemistry* **1992,** *96* (1), 306-14.

27. Bonifacic, M.; Asmus, K., Adduct formation and absolute rate constants in the displacement reaction of thiyl radicals with disulfides. *The Journal of Physical Chemistry* **1984,** *88* (25), 6286-6290.

28. Mozziconacci, O.; Sharov, V.; Williams, T. D.; Kerwin, B. A.; Schöneich, C., Peptide cysteine thiyl radicals abstract hydrogen atoms from surrounding amino acids: the photolysis of a cystine containing model peptide. *J Phys Chem B* **2008,** *112* (30), 9250-7.

29. Mozziconacci, O.; Kerwin, B. A.; Schöneich, C., Photolysis of an intrachain peptide disulfide bond: primary and secondary processes, formation of H2S, and hydrogen transfer reactions. *J Phys Chem B* **2010,** *114* (10), 3668-88.

30. Mozziconacci, O.; Kerwin, B. A.; Schöneich, C., Exposure of a monoclonal antibody, IgG1, to UV-light leads to protein dithiohemiacetal and thioether cross-links: a role for thiyl radicals? *Chem Res Toxicol* **2010,** *23* (8), 1310-2.

31. Tamba, M.; Simone, G.; Quintiliani, M., Interactions of thiyl free radicals with oxygen: a pulse radiolysis study. *Int J Radiat Biol Relat Stud Phys Chem Med* **1986,** *50* (4), 595-600.

32. Wardman, P.; von Sonntag, C., Kinetic factors that control the fate of thiyl radicals in cells. *Methods Enzymol* **1995,** *251*, 31-45.

33. Schöneich, C., Kinetics of thiol reactions. *Methods Enzymol* **1995,** *251*, 45-55.

34. Claiborne, A.; Yeh, J. I.; Mallett, T. C.; Luba, J.; Crane, E. J., 3rd; Charrier, V.; Parsonage, D., Protein-sulfenic acids: diverse roles for an unlikely player in enzyme catalysis and redox regulation. *Biochemistry* **1999,** *38* (47), 15407-16.

35. Turell, L.; Botti, H.; Carballal, S.; Ferrer-Sueta, G.; Souza, J. M.; Duran, R.; Freeman, B. A.; Radi, R.; Alvarez, B., Reactivity of sulfenic acid in human serum albumin. *Biochemistry* **2008,** *47* (1), 358-67.

36. Wedemeyer, W. J.; Welker, E.; Narayan, M.; Scheraga, H. A., Disulfide bonds and protein folding. *Biochemistry* **2000,** *39* (23), 7032.

37. Kosen, P., Disulfide bonds in proteins. *Stability of protein pharmaceuticals. A. Chemical and physical pathways of protein degradation. Plenum Press, New York* **1992**, 31-67.

38. Patchornik, A.; Sokolovsky, M., Chemical interactions between lysine and dehydroalanine in modified bovine pancreatic ribonuclease. *J Am Chem Soc* **1964,** *86* (9), 1860-1861.

39. Mozziconacci, O.; Williams, T. D.; Schöneich, C., Intramolecular hydrogen transfer reactions of thiyl radicals from glutathione: Formation of carbon-centered radical at Glu, Cys, and Gly. *Chem Res Toxicol* **2012**.

40. Mozziconacci, O.; Kerwin, B. A.; Schöneich, C., Reversible hydrogen transfer reactions of cysteine thiyl radicals in peptides: the conversion of cysteine into dehydroalanine and alanine, and of alanine into dehydroalanine. *J Phys Chem B* **2011,** *115* (42), 12287-305.

41. Davies, M. J.; Truscott, R. J., Photo-oxidation of proteins and its role in cataractogenesis. *J Photochem Photobiol B* **2001,** *63* (1-3), 114-25.

42. Mozziconacci, O.; Kerwin, B. A.; Schöneich, C., Reversible hydrogen transfer between cysteine thiyl radical and glycine and alanine in model peptides: covalent H/D exchange, radical-radical reactions, and L- to D-Ala conversion. *J Phys Chem B* **2010,** *114* (19), 6751-62.

43. Pattison, D. I.; Rahmanto, A. S.; Davies, M. J., Photo-oxidation of proteins. *Photochem Photobiol Sci* **2012,** *11* (1), 38-53.

44. Mozziconacci, O.; Schöneich, C., Sequence-specific formation of d-amino acids in a monoclonal antibody during light exposure. *Mol Pharm* **2014,** *11* (11), 4291-7.

45. Biosystems, A. *Cleavage, Deprotection, and Isolation of Peptides after Fmoc Synthesis*; May 1998, 1998.

46. Annis, I.; Hargittai, B.; Barany, G., Disulfide bond formation in peptides. *Methods Enzymol* **1997,** *289*, 198-221.

47. Brewer, C. F.; Riehm, J. P., Evidence for possible nonspecific reactions between N-ethylmaleimide and proteins. *Anal Biochem* **1967,** *18* (2), 248-&.

48. Zhu, Y.; van der Donk, W. A., Convergent synthesis of peptide conjugates using dehydroalanines for chemoselective ligations. *Org Lett* **2001,** *3* (8), 1189-92.

49. Snow, J. T.; Finley, J. W.; Friedman, M., Relative reactivities of sulfhydryl groups with N-acetyl dehydroalanine and N-acetyl dehydroalanine methyl ester. *Int J Pept Protein Res* **1976,** *8* (1), 57-64.

50. Niki, E., Free radical initiators as source of water- or lipid-soluble peroxyl radicals. *Methods Enzymol* **1990,** *186*, 100-8.

51. Steinmann, D.; Ji, J. A.; Wang, Y. J.; Schöneich, C., Oxidation of human growth hormone by oxygen-centered radicals: formation of Leu-101 hydroperoxide and Tyr-103 oxidation products. *Mol Pharm* **2012,** *9* (4), 803-14.

52. Banfi, D.; Patiny, L., www. nmrdb. org: Resurrecting and Processing NMR Spectra On-line. *CHIMIA International Journal for Chemistry* **2008,** *62* (4), 280-281.

53. Fu, X. Y.; Mueller, D. M.; Heinecke, J. W., Generation of intramolecular and intermolecular sulfenamides, sulfinamides, and Sulfonamides by hypochlorous acid: A potential pathway for oxidative cross-linking of low-density lipoprotein by myeloperoxidase. *Biochemistry* **2002,** *41* (4), 1293-1301.

54. Hemenway, J. N.; Nti-Addae, K.; Guarino, V. R.; Stella, V. J., Preparation, characterization and in vivo conversion of new water-soluble sulfenamide prodrugs of carbamazepine. *Bioorg Med Chem Lett* **2007,** *17* (23), 6629-32.

55. Nti-Addae, K. W.; Laurence, J. S.; Skinner, A. L.; Stella, V. J., Reversion of sulfenamide prodrugs in the presence of free thiol-containing proteins. *J Pharm Sci* **2011,** *100* (7), 3023-7.

56. Sakmar, T. P.; Franke, R. R.; Khorana, H. G., The role of the retinylidene Schiff base counterion in rhodopsin in determining wavelength absorbance and Schiff base pKa. *Proceedings of the National Academy of Sciences* **1991,** *88* (8), 3079-3083.

57. Davies, M. J., The oxidative environment and protein damage. *Biochim Biophys Acta* **2005,** *1703* (2), 93-109.

58. Nti-Addae, K. W.; Stella, V. J., In vitro conversion of model sulfenamide prodrugs in the presence of small molecule thiols. *J Pharm Sci* **2011,** *100* (3), 1001-8.

59. Guarino, V. R.; Karunaratne, V.; Stella, V. J., Sulfenamides as prodrugs of NH-acidic compounds: a new prodrug option for the amide bond. *Bioorg Med Chem Lett* **2007,** *17* (17), 4910-3.

60. Craine, L.; Raban, M., The Chemistry of Sulfenamides. *Chem Rev* **1989,** *89* (4), 689-712.

61. Kerwin, B. A.; Remmele, R. L., Jr., Protect from light: photodegradation and protein biologics. *Journal of pharmaceutical sciences* **2007,** *96* (6), 1468-79.

62. Asmus, K. D., Stabilization of oxidized sulfur centers in organic sulfides. Radical cations and odd-electron sulfur-sulfur bonds. *Accounts of chemical research* **1979,** *12* (12), 436-442.

63. Musker, W. K.; Hirschon, A. S.; Doi, J. T., A nitrogen-sulfur bonded cation radical [R3N-SR2]+.cntdot.and a dication [R3N-SR2]2+ from 5-methyl-1-thia-5-azacyclooctane. *Journal of the American Chemical Society* **1978,** *100* (24), 7754-7756.

64. Mozziconacci, O.; Haywood, J.; Gorman, E. M.; Munson, E.; Schöneich, C., Photolysis of recombinant human insulin in the solid state: formation of a dithiohemiacetal product at the C-terminal disulfide bond. *Pharm Res* **2012,** *29* (1), 121-33.

2.7 Appendix A

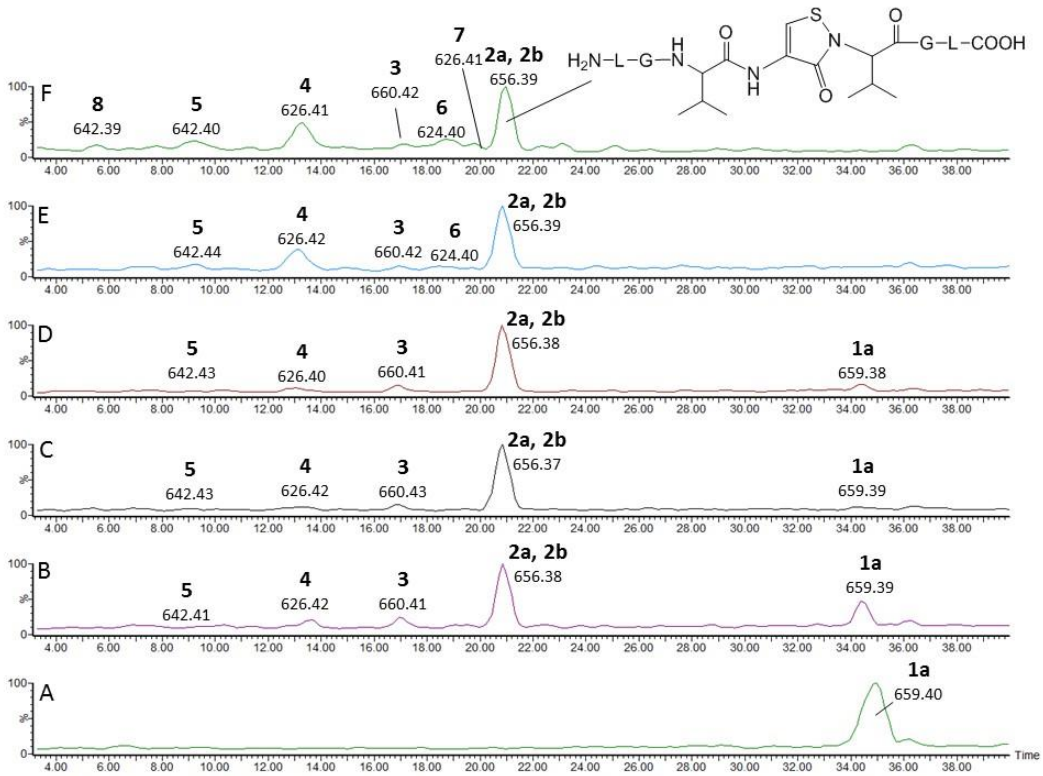

Figure A.1. LC-MS analysis of the photoproducts generated by UV-irradiation at λ = 254 nm of Peptide **1a** (100 nM) in Ar-saturated H_2O, pH 7.0: (A) no irradiation (control); (B) 30 seconds of irradiation; (C) 1 minute of irradiation; (D) 2 minutes of irradiation; (E) 5 minutes of irradiation; (F) 10 minutes of irradiation.

Product	Proposed Structure	MS/MS
6	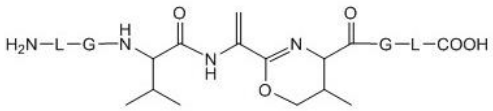	Fig. 2.29
7	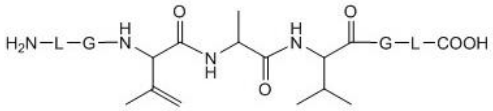	Fig. A.2
8	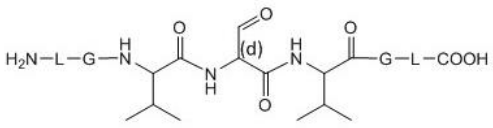	(similar to Fig. 2.5)

Table A.2. Peptide **1a** photoproducts observed after photolysis at λ = 254 nm.

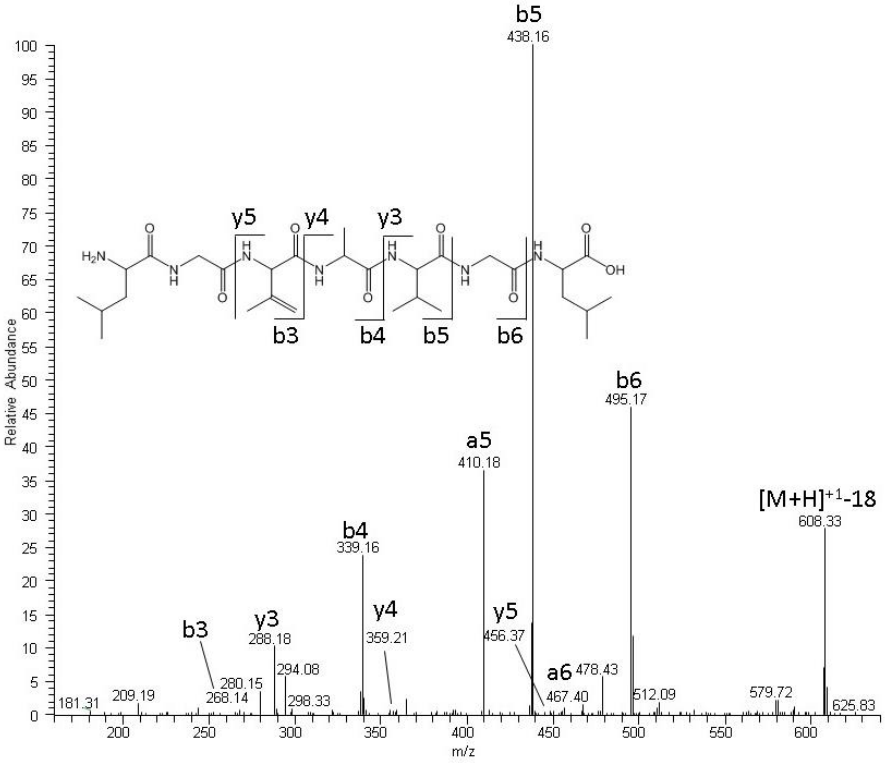

Figure A.2. MS/MS spectrum of product **7** after UV irradiation at λ = 254 nm of Peptide 1a at pH 7.0 (100 μM) in an Ar-saturated H_2O.

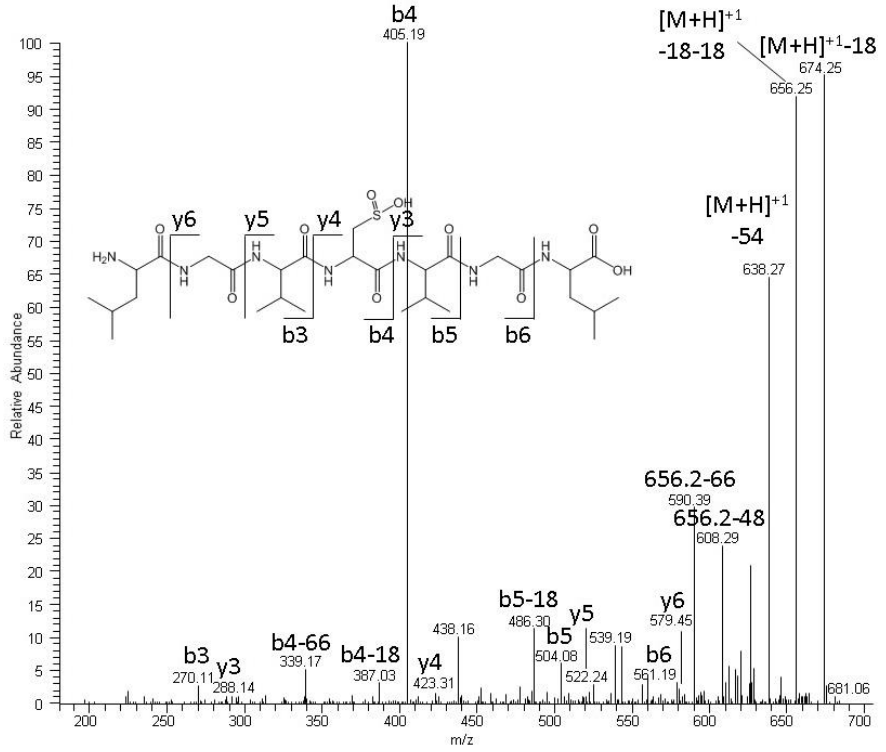

Figure A.3. MS/MS spectrum of product **13** after UV irradiation at λ = 254 nm of Peptide 1a at pH 7.0 (100 μM) in an Ar-saturated H_2O.

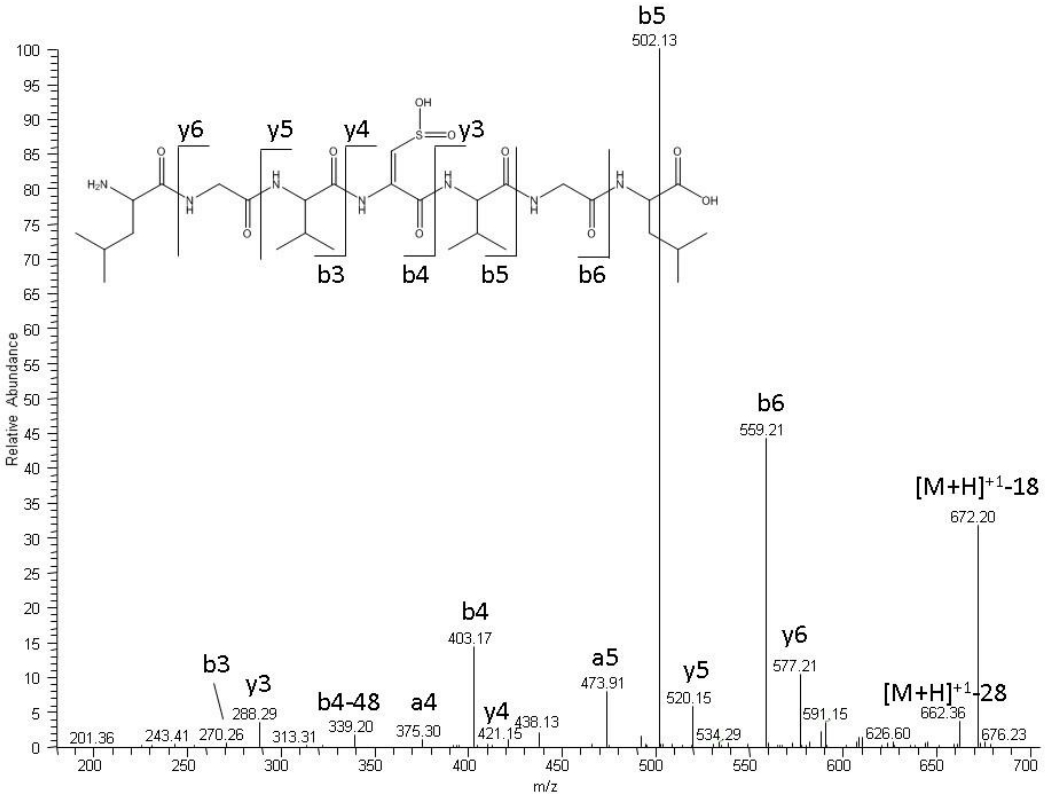

Figure A.4. MS/MS spectrum of product **14** after UV irradiation at λ = 254 nm of Peptide 1a at pH 7.0 (100 μM) in an Ar-saturated H_2O.

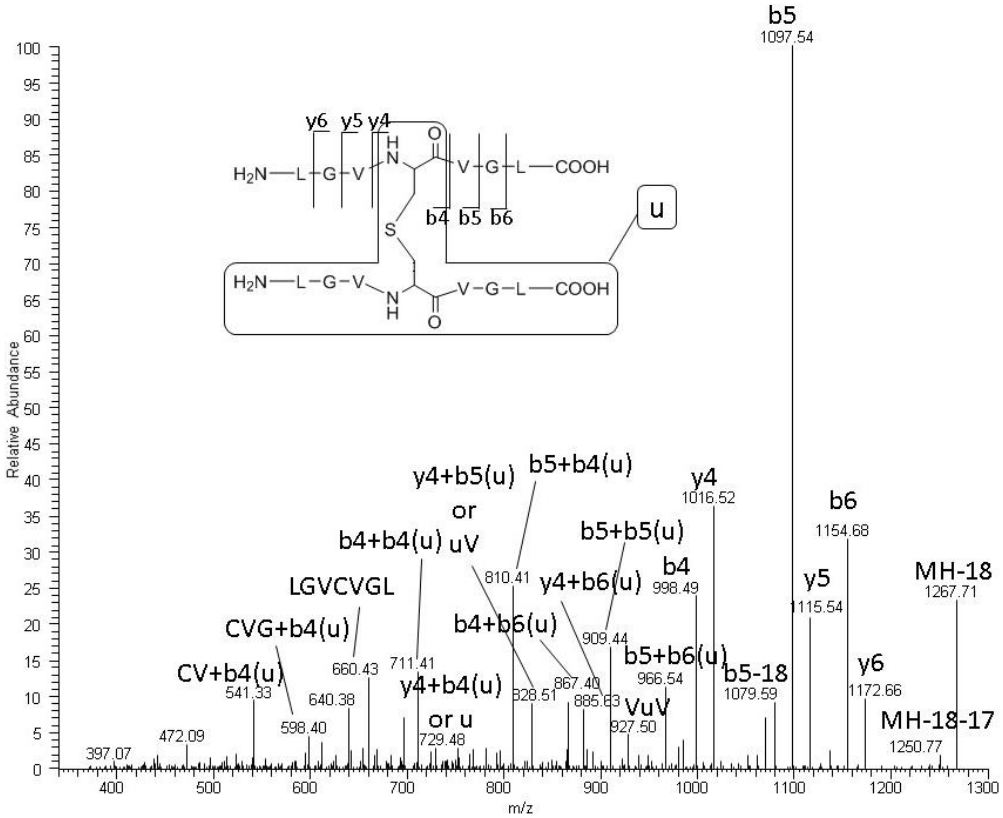

Figure A.5. MS/MS spectrum of product **15** after UV irradiation at λ = 254 nm of Peptide 1a at pH 7.0 (100 μM) in an Ar-saturated H_2O.

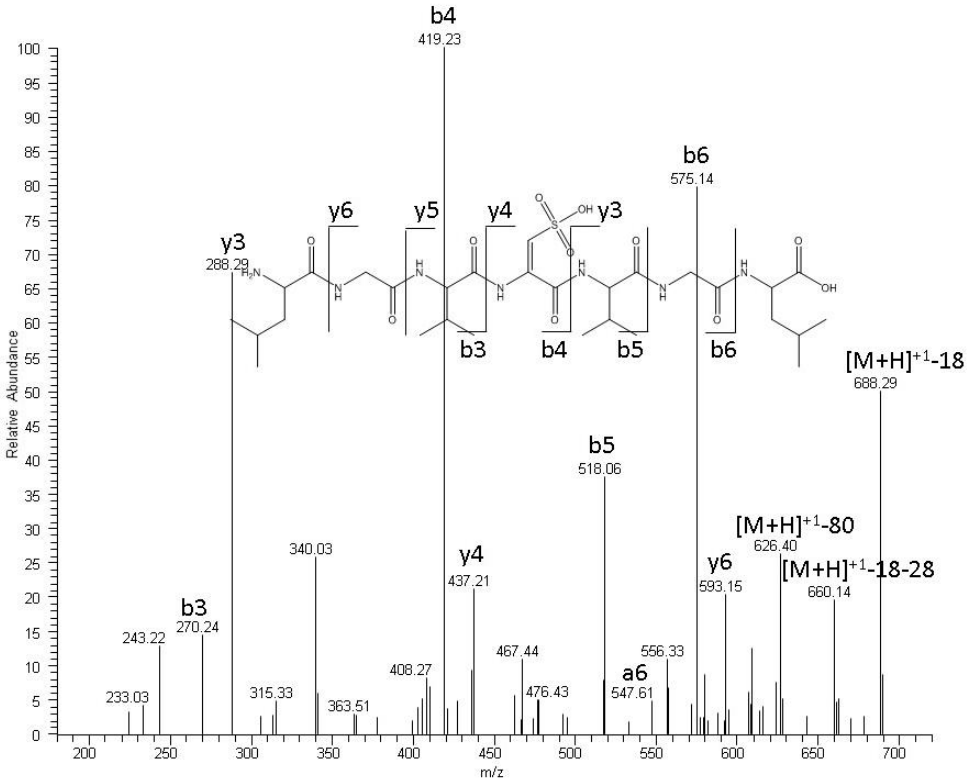

Figure A.6. MS/MS spectrum of product **16** after UV irradiation at λ = 254 nm of Peptide 1a at pH 7.0 (100 μM) in an Ar-saturated H_2O.

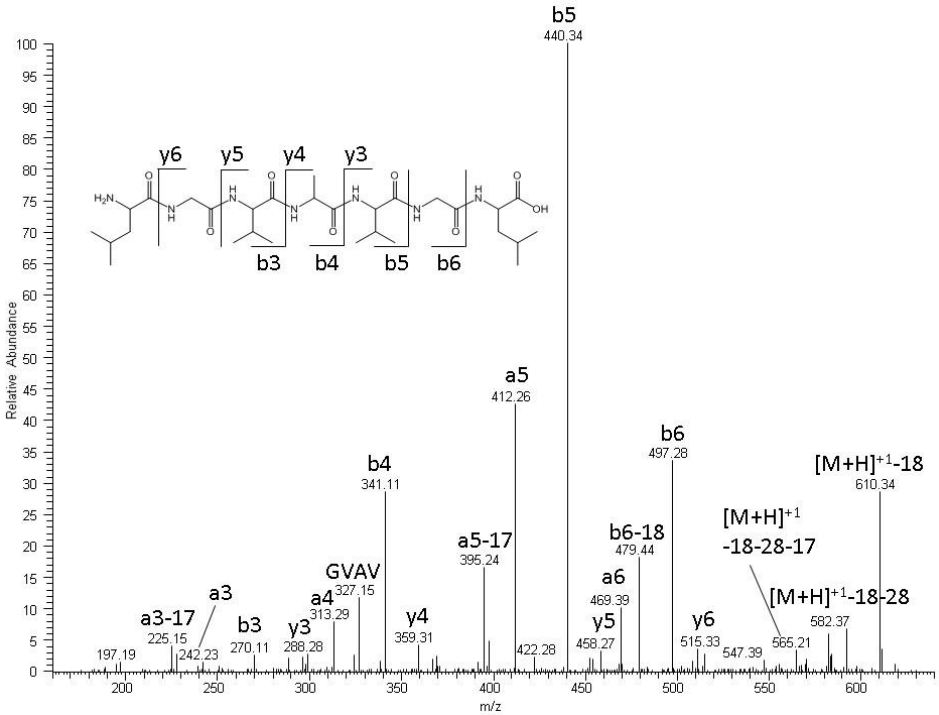

Figure A.7. MS/MS spectrum of product **17** after UV irradiation at λ = 254 nm of Peptide 1a at pH 7.0 (100 μM) in an Ar-saturated H_2O.

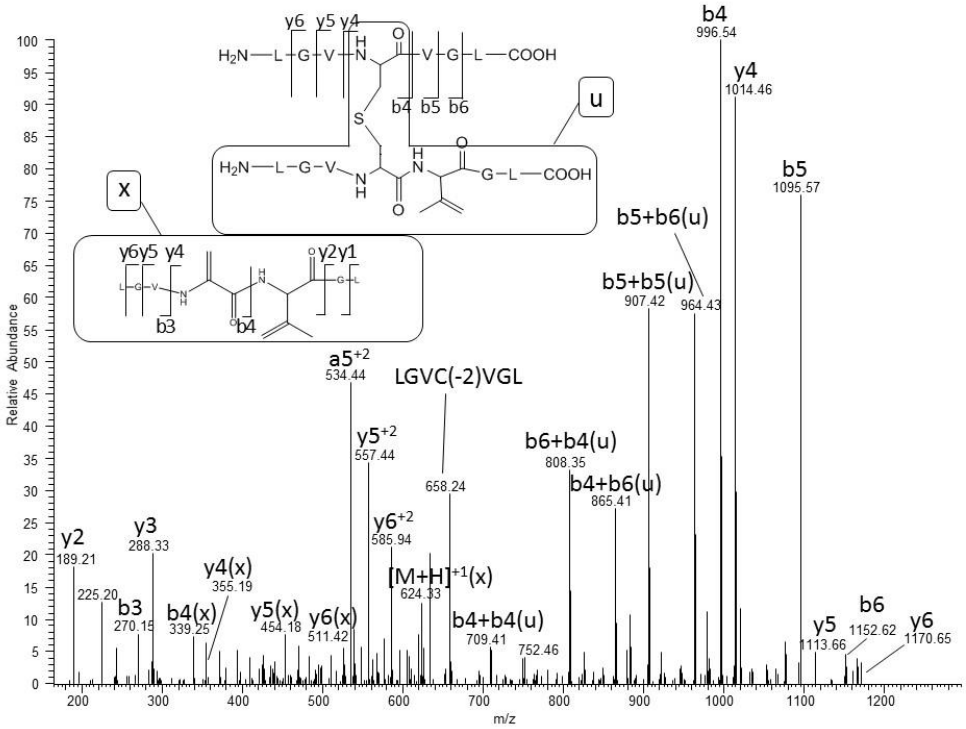

Figure A.8. MS/MS spectrum of product **21** after UV irradiation at λ = 254 nm of Peptide 1a at pH 4.0 (100 µM) in an Ar-saturated H_2O.

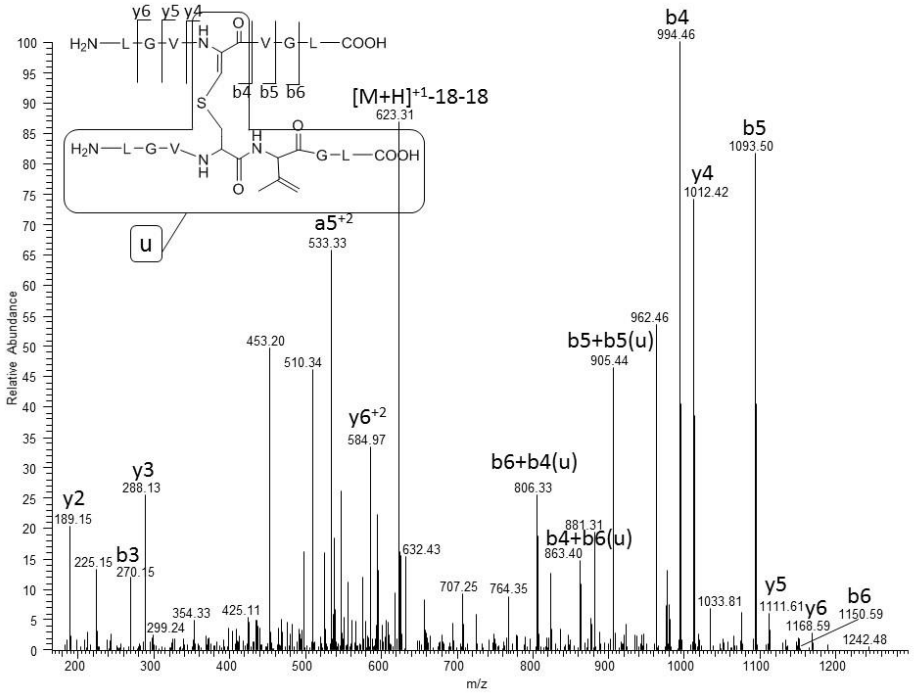

Figure A.9. MS/MS spectrum of product **22** after UV irradiation at λ = 254 nm of Peptide 1a at pH 4.0 (100 µM) in an Ar-saturated H_2O.

Chapter 3. Light-induced conversion of Trp to Gly and Gly hydroperoxide

3.1.1 Parts of this section have been published in a peer-reviewed journal.[1]

3.1 Introduction

Due to its indole side chain, tryptophan (Trp) is the strongest UV-absorbing amino acid and a major target for photochemical degradation.[2] For example, Trp can be oxidized to N-formyl kynurenine (NFK) and kynurenine and sensitize the reduction of peptide and/or disulfide bonds, forming thiyl radicals and thiolate.[3,4] The latter process requires photo-induced electron- or H-atom transfer between Trp and the disulfide bond. Modification of Trp residues in proteins has resulted in conformational changes and loss of biologic activity, and presents a major concern for the production and formulation of biopharmaceuticals.[5,6,7] Moreover, kynurenines are efficient photosensitizers, inferring that Trp oxidation can lead to additional photosensitivity of a protein formulation.[8]

Gas-phase mass spectrometry studies have indicated the possibility for $^{\alpha}C$-$^{\beta}C$ side chain fragmentation reactions of Trp-derived radical cations.[9,10,11] A side chain fragmentation was also reported as key to the enzyme-catalyzed conversion of Trp to 3-methyl-2-indolic acid, but the mechanism has not been characterized in detail.[12] Considering the potential of protein Trp residues for photoionization[2], a $^{\alpha}C$-$^{\beta}C$ side chain cleavage of Trp may also be expected during photodegradation of protein pharmaceuticals. Here, we show that the exposure of IgG1 to light indeed results in the fragmentation of Trp, resulting in the formation of Gly and/or Gly hydroperoxide. Additionally, photoirradiation of a synthetic model peptide containing Trp and a disulfide bond shows the Trp to Gly hydroperoxide modification. As a consequence, light exposure not only modifies the original amino acid (Trp) but also leads to the generation of a reactive hydroperoxide. Amino acid hydroperoxides have been shown to exhibit higher reactivity towards some oxidation targets as compared to hydrogen peroxide, implying that products such

as Gly hydroperoxide may induce further protein oxidation (and/or fragmentation) upon storage.[13,14]

3.2 Experimental methods

3.2.1 Materials. Ammonium bicarbonate (NH_4HCO_3), N-ethylmaleimide (NEM), dimethyl sulfoxide, sodium borohydride, L-glutathione oxidized (GSSG), β-mercaptoethanol (BME), thioanisole, 1,2 ethanedithiole (EDT), and anisole were supplied by Sigma-Aldrich (St. Louis, MO) at the highest commercially available purity. Methanol, ethanol, dichloromethane, acetonitrile, and trifluoroacetic acid were supplied by Fisher Scientific (Pittsburg, PA). Sequencing grade Trypsin and Glu-C were purchased from Promega (Madison, WI). Deuterium oxide (D_2O, 99.9%) was purchased from Cambridge Isotope Laboratories (Andover, MA, USA). Fmoc-L-Gly, Fmoc-L-Cys-trt, and Fmoc-L-Leu, and Fmoc-L-Trp-Boc were supplied by Novabiochem (Darmstadt, Germany), and Fmoc-L-Leu-PEG-PS was supplied by Applied Biosystems (Foster City, CA). O-(7-Azabenzotriazole-1-yl)-N, N,N'N'-tetramethyluronium hexafluorophosphate (HATU) was supplied by GenScript Corporation (Piscataway, NJ). The peptide GGCGGL-GGCWGL was supplied by American Peptide Company (Sunnyvale, CA), and the IgG1 was provided by Amgen Inc.

3.2.2 Peptide Synthesis. The model peptide $(LGGCWGL)_2$ was synthesized from its linear Cys-containing peptide LGGCWGL using solid phase Fmoc-chemistry on a Pioneer™ Peptide Synthesis System. Following the synthesis, the crude material was washed with methanol and dichloromethane. The thiol was deprotected and the peptide was cleaved from the resin using reagent R (TFA, thioanisole, EDT, and anisole at a ratio of 90%:5%:3%:2% (v:v:v)) as described in detail elsewhere.[15] LGGCWGL was purified from the crude mixture by HPLC using a YMC-Pack ODS-A semipreparative C18 column with dimensions of 250 x 20 mm ID

containing 5 μm particles (YMC America, Inc. Allentown, PA), with a 5 ml min^{-1} flow rate. Mobile phases consisted of water, acetonitrile, and trifluoroacetic acid at a ratio of 90%:10%:0.1% (v:v:v) for solvent A and a ratio of 10%:90%:0.1% (v:v:v) for solvent B. A linear gradient was developed from 10% to 90% B within 30 min. Following lyophilization, the purified LGGCWGL peptide was reconstituted to 1 mg/mL in a solution of 50 mM ammonium bicarbonate buffer containing 20% dimethyl sulfoxide at pH 7.8 for oxidation to the disulfide. The oxidation reaction was allowed to proceed at room temperature, open to air, for four hours to form $(LGGCWGL)_2$. The peptide was then purified using the semipreparative C18 column and lyophilized prior to experimentation.

3.2.3 UV Irradiation of IgG1. IgG1 was dialyzed against water prior to use, and then aliquots of 500 μL IgG1 were diluted with water to a concentration of 2.3 mg/ml. The final pH of the non-buffered solution was 5.6. The model peptides were dissolved in water at pH 4.0 to a concentration of 100 μM. The solutions were saturated through head-space equilibration with oxygen, argon, or air for one hour in a quartz or Pyrex tube capped with a rubber stopper. Next, the solutions were irradiated at $\lambda = 254$ or $\lambda_{max} = 305$ nm for up to 30 minutes in a Rayonet system (Southern New England, Branford, CT, RMA-500). (Actinometry gave a flux of photons at $\lambda = 254$ nm of 2.96×10^{-4} einstein.min^{-1}. In Watt per cm^2, the flux at λ=254 nm and λ=305 nm is ~15 W cm^{-2}). Photo-irradiations at $\lambda_{max} = 305$ nm involved four phosphor-coated low pressure mercury lamps (RPR-3000Å) which emit predominantly between $\lambda = 285$-315 nm ($\lambda_{max} = 305$ nm) and where wavelengths below 295 nm were filtered out by the use of Pyrex glass vials.

3.2.4 UV Irradiation of Model Peptides. The GGCGGL-GGCWGL and $(LGGCWGL)_2$ model peptides were dissolved in water or deuterium oxide at pH 4.0 to a concentration of 100 μM. 1 mM N-acetyl-L-tryptophanamide and 1 mM oxidized L-glutathione were added together

and dissolved in water to pH 7.0. The peptide solutions were saturated through head-space equilibration with oxygen or argon for thirty minutes in a quartz or Pyrex tube capped with a rubber stopper. Next, the solutions were irradiated at $\lambda = 254$ or $\lambda_{max} = 305$ nm for up to 30 minutes in a Rayonet system (Southern New England, Branford, CT, RMA-500). (Actinometry gave a flux of photons at $\lambda = 254$ nm of 2.96×10^{-4} einstein.min^{-1}. In Watt per cm^2, the flux at λ=254 nm and λ=305 nm is ~15 W cm^{-2}). Photo-irradiations at $\lambda_{max} = 305$ nm involved four phosphor-coated low pressure mercury lamps (RPR-3000Å) which emit predominantly between $\lambda = 285$-315 nm ($\lambda_{max} = 305$ nm) and where wavelengths below 295 nm were filtered out by the use of Pyrex glass vials.

3.2.5 IgG1 Enzymatic Digest. Directly after photolysis, IgG1 was denatured by increasing the temperature to 75˚C at a rate of 1.4˚C/minute. Following denaturation, the disulfide bonds in IgG1 were reduced with 0.6 mM dithiothreitol (DTT) for 30 minutes at 45˚C. Free thiols and amino groups were derivatized with 1.8 mM N-ethylmaleimide (NEM) for one hour at 37˚C and one hour at room temperature. The protein was purified by precipitation in cold ethanol and centrifugation for 30 minutes at 5,500 RPM at 4˚C. The pellet was reconstituted in ammonium bicarbonate buffer (50 mM, pH 7.8) prior to digestion. Following the addition of 20 µg of trypsin (ratio trypsin:protein = 1:65), the samples were incubated for 2 hours at 45˚C. Then, 10 µg of Glu-C (ratio Glu-C:protein = 1:130) were added together with an additional 20 µg of trypsin and the samples were incubated for an additional 5 hours at 37 ˚C, and subsequently stored at -20˚C until MS analysis.

3.2.6 IgG1 Reduction of Hydroperoxides. Aliquots of IgG1 after light exposure and digestion were reduced with 2 mM sodium borohydride ($NaBH_4$) at room temperature for 1 hour. Following the reaction, the samples were stored at 20 ˚C until MS analysis.

3.2.7 Measurement of Alkyl Peroxides in the GGCGGL-GGCWGL Peptide by the FOX2 Assay. The alkyl peroxides generated during UV light exposure of the Trp-L peptide were measured with the FOX2 assay, as described previously.[16,17] Prior to measuring the alkyl peroxides, catalase was added to the samples to react with all the hydrogen peroxide. A solution of catalase was prepared at 1200 U/mL at pH 7.0 in 20 mM phosphate buffer, and added to the irradiated samples and non-irradiated controls in a 1:5 ratio of catalase to sample. The reaction proceeded at room temperature for one hour. Next, 100 µL of 0.2 M perchloric acid, 1.25 mM xylenol orange (XO), 0.5 mM iron (II) sulfate was pre-incubated at 4 ˚C for 15 minutes prior to the addition of 600 µL of 6M guanidine hydrochloride and 100 µL of sample. The samples were capped tight in quartz cuvettes with screw caps and the absorbance was measured at 560 nm for 30 minutes, or until the absorbance reached a plateau. After the absorbance was recorded, the extinction coefficient for the Fe (III)-XO complex was determined by adding 12.5 µM iron (III) sulfate to the sample and recording this value after 15 minutes of reaction.

3.2.8 LTQ-FT Mass Spectrometry Analysis. The peptides generated from the IgG1 digest treated and non-treated with $NaBH_4$ were analyzed by liquid chromatography-mass spectrometry (LC-MS) employing a Fourier-transform ion cyclotron resonance mass spectrometer (FT-ICR, Thermo-Finnigan, Bremen, Germany) combined with an Acquity chromatographer (Waters Corp., Milford, MA). The analytes were eluted from a reverse-phase C18 column (5 cm, 320 µm ID, CVC Microtech, Fontana, CA) at a flow rate of 20 µL/min. Mobile phases consisted of H_2O/acetonitrile (ACN)/formic acid (FA) at a ratio of 99%:1%:0.1% (v:v:v) for solvent A and a ratio of 1%:99%:0.1% (v:v:v) for solvent B. The column was equilibrated with 1% B for 2 min. Between 2-30 min, the eluent composition was linearly increased to 50% B. Collision-induced dissociation (CID) data for MS/MS analysis were

obtained after an attenuation of the parent ion by 35%. The MassMatrix software program was used for peptide mapping[18] with the IgG1 sequence provided by Amgen.

3.2.9 Synapt G2 Mass Spectrometry Analysis. The model peptides and photoproducts were analyzed on a Synapt G2 mass spectrometer (Micromass Ltd., Manchester, U.K.) combined with an Acquity UPLC System (Waters Corp., Milford, MA, USA). The instrument was operated in the data dependent acquisition (DDA) mode with all lenses optimized on the MH+ ion from sodium iodide. The ESI source was operated with a spray voltage of 2.5 kV, a tube lens offset of 75 V and a capillary temperature of 250 °C. The peptides were eluted from a Grace reverse phase capillary C18 column with dimensions of 25 cm x 0.5 mm containing 5 µm particles (Fisher Scientific, Pittsburg, PA), at a flow rate of 20 µL min^{-1}. The mobile phases consisted of H_2O, acetonitrile, and formic acid at a ratio of 99.9%:0%:0.1% (v:v:v) for solvent A and a ratio of 0%:99.9%:0.1% (v:v:v) for solvent B. A linear gradient was developed from 15% to 50% B in 43 minutes. MassLynx software was used to acquire and analyze the data.

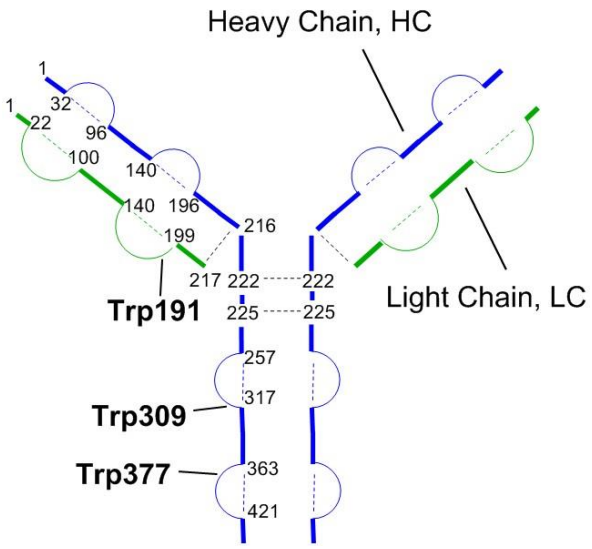

Chart 3.1. IgG1 structure, where Trp[191, LC], and Trp[309, HC] are transformed into Gly and Gly hydroperoxide, and Trp[377, HC] is transformed into Gly.

3.3 Results

3.3.1 UV Irradiation of IgG1. During the exposure of IgG1 to light in an oxygen-saturated solution photolyzed at λ = 254 nm, fragmentation of Trp[191, LC] resulted in the formation of Gly and Gly hydroperoxide (Chart 3.1). Furthermore, fragmentation of Trp[309, HC] and Trp[377, HC] resulted in the formation of Gly[309, HC] hydroperoxide and Gly[377, HC], respectively. Chart 3.1 shows where the original Trp residues are

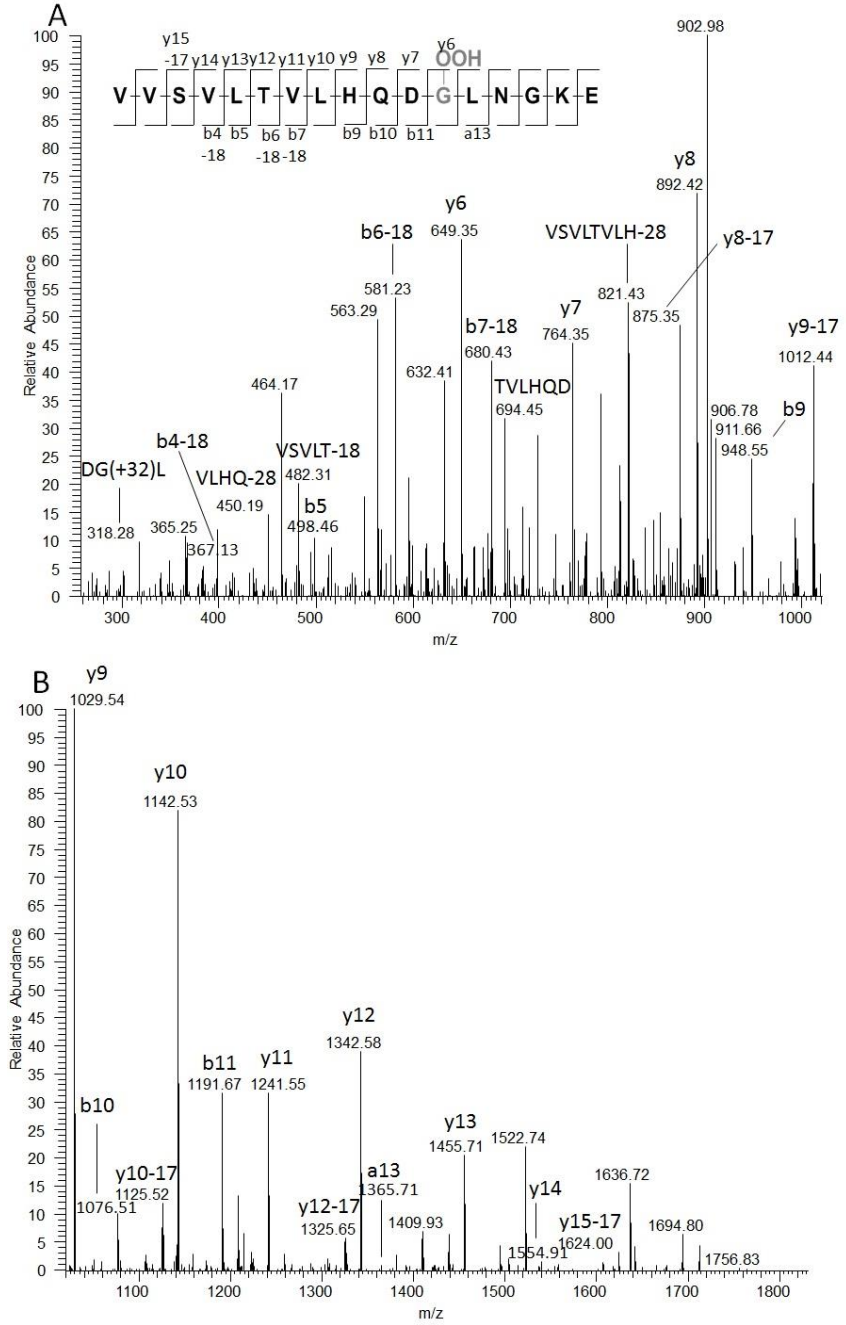

Figure 3.1. MS/MS spectra of the peptide sequence [178-192, LC] in IgG1 where Trp[191, LC] is transformed into Gly[191, LC] hydroperoxide during λ = 254 nm irradiation. (Top spectrum: m/z 300-730, bottom spectrum: m/z 730-1600)

located on the IgG1 molecule. The original Trp[191, LC] is located on the light chain (LC) sequence near intra- and interchain disulfide bonds and close to the hinge region of IgG1. The original Trp[309, HC] and Trp[377, HC] residues are located on the heavy chain (HC) sequence near intrachain disulfide bonds. The interchain disulfide bonds located near residue 191 have been reported to undergo photochemical cleavage, ultimately forming covalent crosslinks such as dithiohemiacetals and cyclic-thioethers.[19]

The MS/MS spectrum of the tryptic peptide sequence [178-192, LC] containing the Gly[191, LC] hydroperoxide is shown in Figure 3.1. In the ion series, the annotations -17 and -18 refer to the loss of ammonia and water, respectively. The y2 and b13 ions, as well as the putative

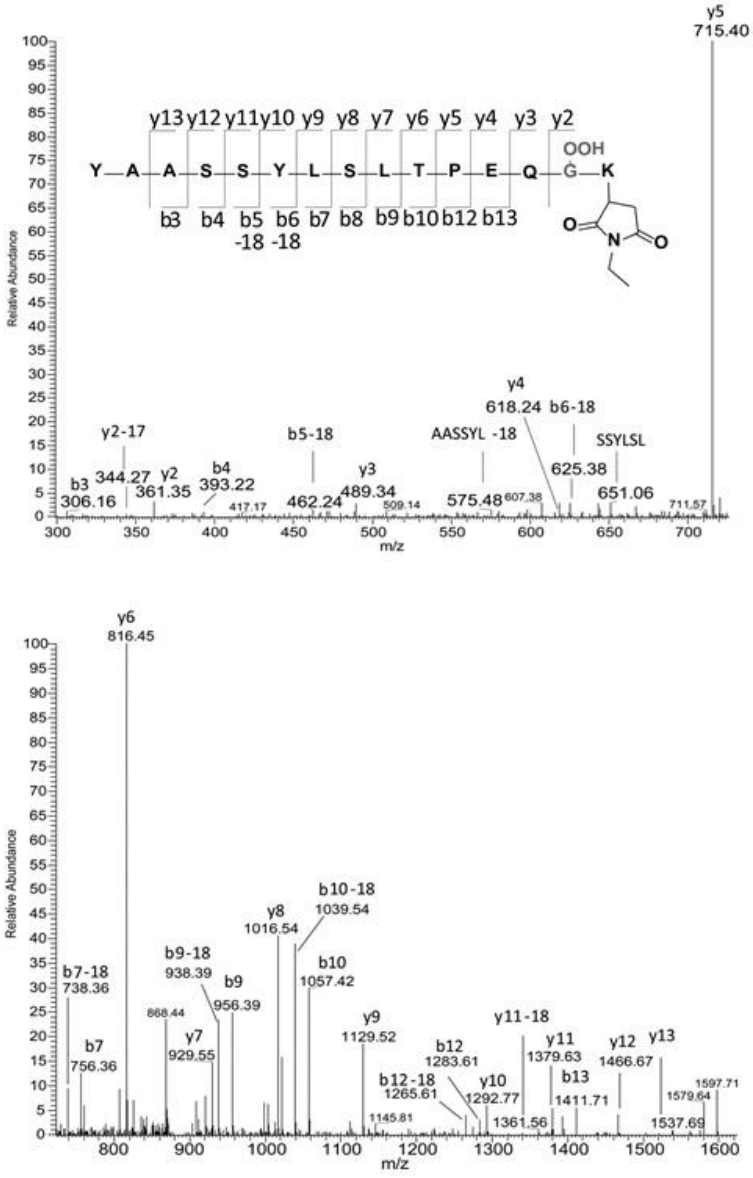

Figure 3.2. MS/MS spectra of the peptide sequence [298-314, HC] of IgG1 where Trp[309, HC] is transformed into Gly[309, HC] hydroperoxide during λ = 254 nm irradiation. (A) m/z 260-1020, bottom spectrum: m/z 1025-1820).

loss of 34 Da from the b14 ion provide evidence for the replacement of the original Trp side-chain by a hydroperoxide. Interestingly, there is evidence for derivatization of the C-terminal Lys residue by NEM. In order for trypsin to effectively cleave the C-terminal lysine, the lysine amino group must be protonated;[20] while such protonation is still possible after NEM-derivatization, we believe that Lys derivatization likely occurred after digestion with some NEM left after protein precipitation. The NEM derivatization of the Lys side chain has been reported before.[21]

The MS/MS spectrum of the peptide sequence [276-388, HC] containing the Gly[377, HC] product is shown in Figure B.1. Here, the y11, b3, and y12-17 ions provide evidence for the replacement of the original Trp side-chain by Gly.

	Product		
Trp residue	**Air**	**O_2**	**Ar**
191, LC	-	Gly-OOH	Gly
309, HC	Gly-OOH	Gly-OOH	-
377, HC	-	Gly	-

Table 3.1. IgG1 photoproducts formed during irradiation at λ = 254 nm under air, O2, and Ar.

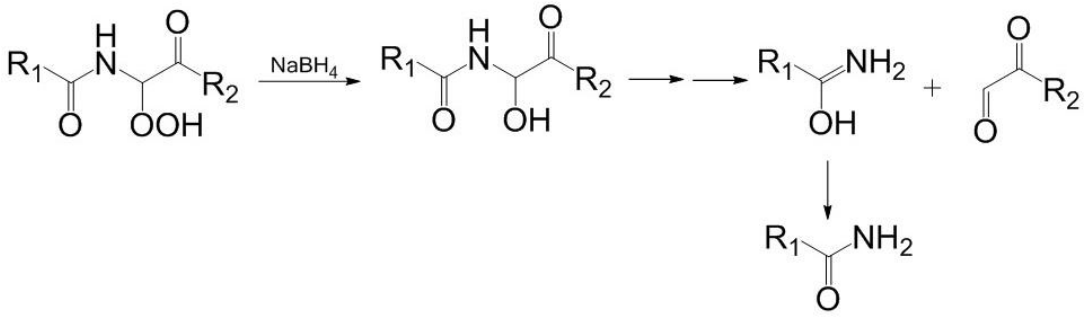

Scheme 3.1. Proposed reaction scheme of the fragmentation of the peptide after transformation of Trp into Gly-OOH.

The MS/MS spectrum of the tryptic peptide sequence [298-314, LC] containing the Gly[309, HC] hydroperoxide is shown in Figure 3.2. Here, the y6, b11, and a13 ions provide evidence for the replacement of the original Trp side-chain by Gly hydroperoxide. In addition to this product formation in an oxygen-saturated system photolyzed at λ = 254 nm, Gly[309, HC] hydroperoxide was also detected in an air-saturated solution (ca. 20% lower yield compared to the oxygen-saturated solution) (Table 3.1). Importantly, Gly[309, HC] hydroperoxide formed upon photolysis of IgG1 with light of λmax = 305 nm in Pyrex vials (Figure B.2).

To confirm the hydroperoxide modification on the Gly residues, we added a reducing agent to the irradiated sample, sodium borohydride, $NaBH_4$. Scheme 3.1 shows the expected Gly hydroperoxide products following the reduction: a hydroxide, and the amidated n-1 residue to the Gly hydroxide following the cleavage of the Gly hydroxide at the N-$^{\alpha}$C bond of the residue. Experimentally, we observed both the hydroxide (Figure B.3) and cleavage product in the Gly

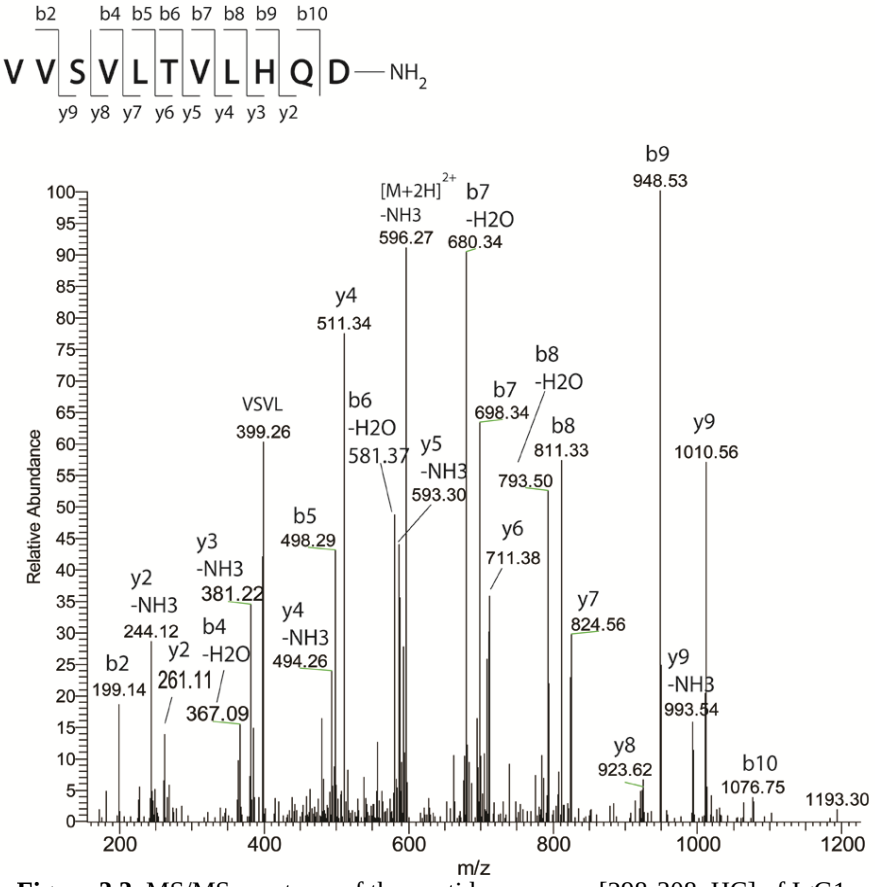

Figure 3.3. MS/MS spectrum of the peptide sequence [298-308, HC] of IgG1 where the n-1 amino acid (Asp) is amidated after Gly[309, HC] hydroperoxide was reduced with $NaBH_4$ reduction.

[309, HC] hydroperoxide (Figure 3.3). Figure 3.3 shows the MS/MS spectrum of this cleavage product, showing all the b and y ions consistent with the new product. This cleavage product and the Gly[309, HC] hydroxide were not observed in the control (non-irradiated) sample.

It is important to note that hydroperoxide groups were detected even after 30 minute DTT reduction prior to tryptic digestion. However, when IgG1 was digested overnight, the yield of the Gly hydroperoxides was significantly reduced, likely due to a prolonged exposure to residual DTT. No Gly hydroperoxides were observed after sodium borohydride reduction, consistent with a reaction of $NaBH_4$ with the hydroperoxides.

In an Ar-saturated solution, the photolysis of IgG1 at $\lambda = 254$ nm generated Gly[191, LC], but no hydroperoxides were detected. In addition to the formation of Gly and Gly hydroperoxides, we detected the formation of NFK and hydroxytryptophan, together with the respective unmodified peptides containing the native Trp residues. The non-irradiated controls showed no Trp to Gly or Gly hydroperoxide fragmentation products.

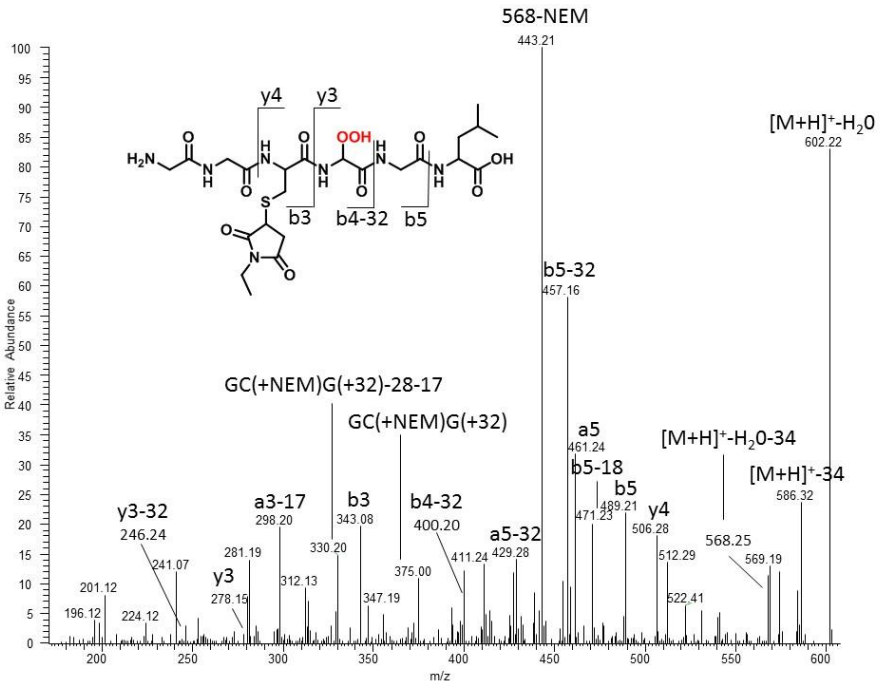

Figure 3.4. MS/MS spectrum of the model peptide GGCGGL-GGCWGL containing the Trp to Gly hydroperoxide modification during λ = 254 nm irradiation.

3.3.2 UV Irradiation of GGCGGL-GGCWGL.

To independently confirm the light-induced Trp fragmentation, a model Trp-containing peptide connected by a disulfide bond was synthesized, GGCGGL-GGCWGL. This peptide was subjected to the same photolytic conditions as IgG1 (λ = 254 nm in an oxygen-saturated system), and we observed the transformation of the disulfide bond into a thiol (and derivatized with NEM) as well as the conversion of the Trp residue into Gly hydroperoxide (Figure 3.4). During MS/MS analysis, y3 and b5 fragments were detected, localizing the Gly-OOH product to the original Trp residue. Additionally, a b4-32 Da ion was observed, potentially indicating the loss of O_2 from the hydroperoxide group on the original Trp residue. We also observed a loss of 34 Da (H_2O_2) from ions in this spectrum, a more common fragmentation.[22] The b3 and y4 ions highlight the Cys derivatized with NEM.

To quantitate the peptide-bound hydroperoxide (ROOH) for our model peptide, we added catalase to the irradiated solution to remove H_2O_2 and analyzed ROOH with the FOX2 assay, as described previously. The ratio of peak areas (hydroperoxide/native Trp-containing peptide) from the LC-MS and a direct comparison of the ratios of MS signal intensities for the hydroperoxide

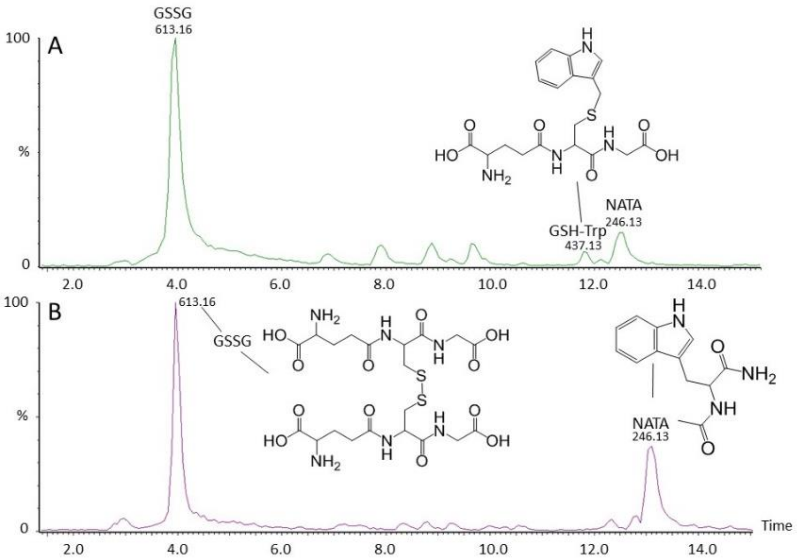

Figure 3.5. LC-MS of irradiated N-acetyl-L-tryptophanamide with oxidized glutathione (GSSG): (A) under O_2 and (B) under Ar.

product versus the native peptide gave an upper limit of 3-6% of transformation of the native peptide into the hydroperoxide product (λ = 254 nm), consistent with the analysis by the FOX2 assay which gave 6.0 ± 0.5 μM ROOH/ 100 μM irradiated peptide. An estimate for the Gly and Gly hydroperoxide-containing peptides formed during photo-irradiation of the antibody (λ = 254 nm) yielded an upper limit of 10 and 40-100%, respectively, relative to unmodified peptides based on MS signal intensity. Confirmation of the Gly hydroperoxide yield in IgG1 by the FOX2 assay is presently not possible because radical chain reactions and singlet oxygen chemistry may lead to additional hydroperoxides.

3.3.3 UV Irradiation of N-acetyl-L-tryptophanamide (NATA) with Oxidized L-glutathione (GSSG). To observe the intermolecular reaction between the cleaved Trp side chain cleavage and an external nucleophile, a solution of 1 mM N-acetyl-L-tryptophanamide (NATA) was purged with O_2 or Ar and irradiated at 254 nm in the presence of 1 mM oxidized L-glutathione (GSSG) at pH 7.5 for 20 minutes. The resultant photoproducts were analyzed by LC-MS on the Q-tof Premier. Figures 3.5A and 3.5B show the LC-MS of the photoproducts formed in O_2 and Ar. In both chromatograms, GSSG elutes at 4 minutes and NATA elutes at ca. 13 minutes. Only in the chromatogram of the O_2-purged sample does a peak appear at ca. 12 minutes with a m/z value of 437.1. This m/z corresponds to the reduction of the disulfide bond in

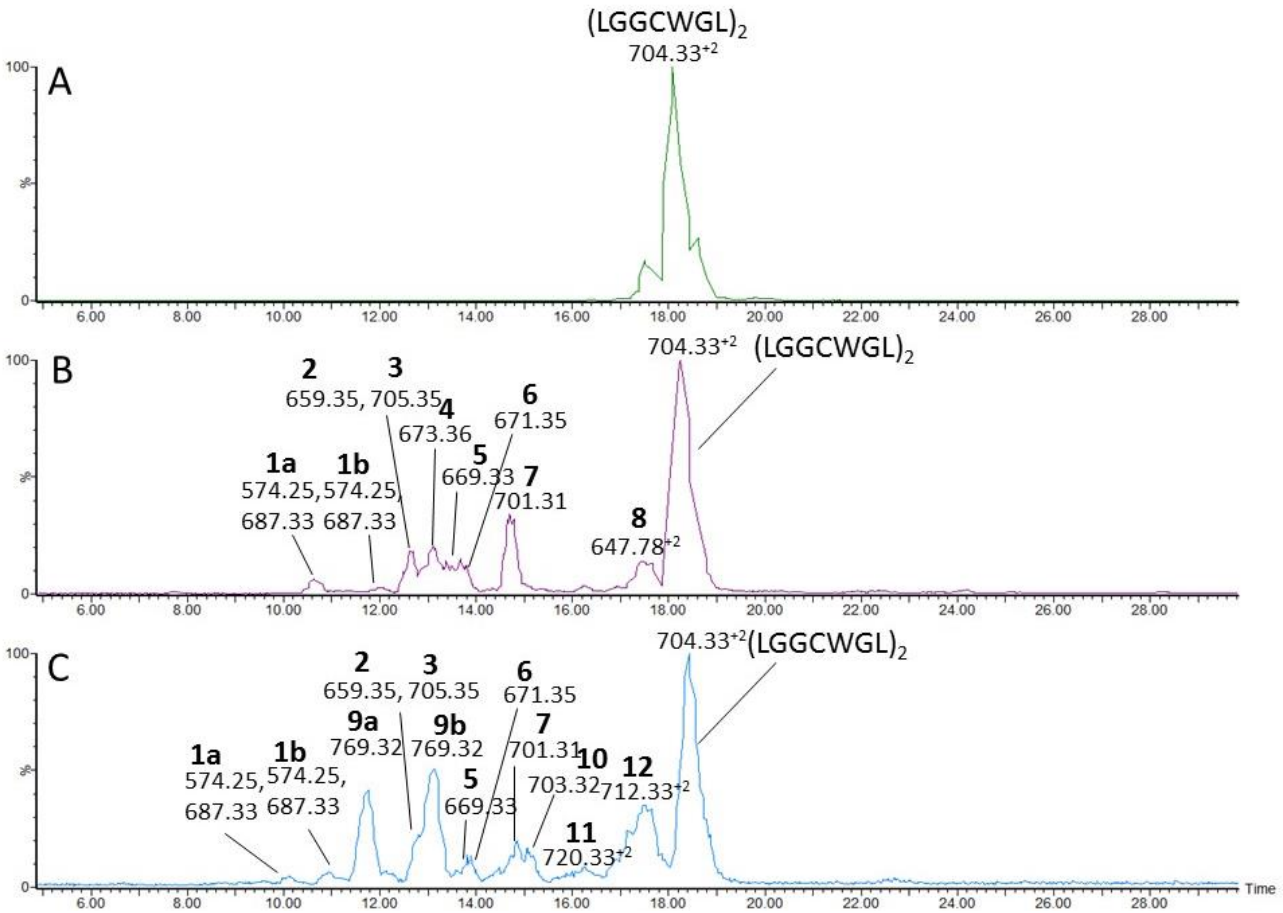

Figure 3.6. LC-MS of the $(LGGCWGL)_2$ peptide (A) control (non-irradiated); (B) irradiated at $\lambda = 254$ nm under Ar for 5 minutes; (C) irradiated at $\lambda = 254$ nm under O_2 for 5 minutes.

GSSG to GSH and the addition of the Trp side chain (with the structures drawn in the figure). This hinted toward the cleavage of the Trp side chain from NATA and the trapping by the nucleophile GSSG, however, no MS/MS analysis was performed to confirm the structure. The m/z of the transformation of NATA to N-acetyl-L-glycinamide or N-acetyl-L-glycinamide hydroperoxide was not detected.

3.3.4 UV irradiation of $(LGGCWGL)_2$. To confirm to Trp to Gly hydroperoxide with another model peptide, $(LGGCWGL)_2$ was synthesized. This model peptide differed from the first one described, GGCGGL-GGCGWL, because Trp was synthesized in both chains, not just one. Therefore, if the Trp to Gly or Gly hydroperoxide is detected, there will be no ambiguity as to where the Gly came from. The $(LGGCWGL)_2$ peptide was saturated separately in Ar or O_2

and irradiated at pH 4.0 for up to 15 minutes, and analyzed by LC-MS on the Synapt G2 instrument.

Figure 3.6 shows representative chromatograms for the $(LGGCWGL)_2$ peptide irradiated under Ar and O_2 for 5 minutes at $\lambda = 254$ nm. The LC-MS of the control peptide (Figure 3.6A) shows the peptide eluting at ca. 18 minutes, and small shoulder peaks on the front and tail of the peak, however, the side products did not affect the photoproducts generated. Figure 3.6B shows the LC-MS of the $(LGGCWGL)_2$ peptide irradiated under Ar, with several new peaks appearing between 10 and 18 minutes of elution. Although the peaks are not fully chromatographically separated, the m/z values distinguish 9 major products: product **1a** (m/z 574.25), **1b** (m/z 574.25), **2** (m/z 659.35), **4** (m/z 673.36), **5** (m/z 669.33), **6** (m/z 671.36), **7** (m/z 701.31), and **8** (m/z 647.78^{+2}). The LC-MS of the $(LGGCWGL)_2$ peptide irradiated under O_2 (Figure 3.6C) shows many of the same peaks observed during the irradiation under Ar, but the major peaks in the chromatogram corresponded to products not observed in the Ar-saturated samples: product **9a** (m/z 769.32), **9b** (m/z 769.32), **10** (703.32), **11** (720.33^{+2}), and **12** (m/z 712.33^{+2}). The aim of this research described in this chapter was not to characterize all the photoproducts in each spectrum, as was the case for the work in Chapter 2. We were specifically looking for the Trp to Gly and/or Gly hydroperoxide product, and any novel photoproducts not observed previously. Additionally, since the peaks were not well separated, the MS/MS of some of the products included fragment ions from other peptides. To this end, we will only discuss product **1b**, **2**, and **7** in the text here. Table 3.2 displays the proposed structures for these products. However, the proposed structures for the rest of the products, most of which are Cys H-atom transfer products described in Chapter 2, are displayed in Table A.1. Their respective MS/MS spectrums are shown in Figure A4-11.

Product	Proposed Structure	MS/MS
1b	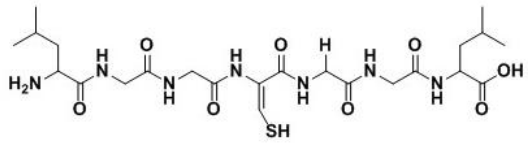	Fig. 3.7
2	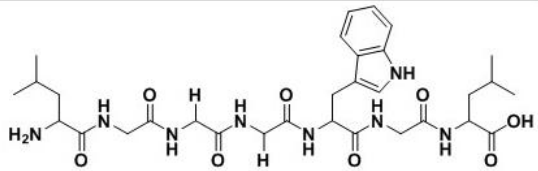	Fig. 3.8
7	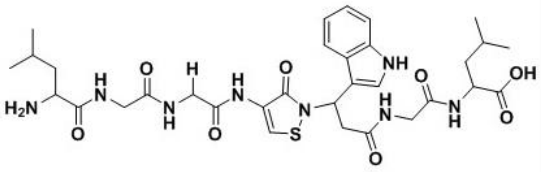	Fig. 3.9

Table 3.2. $(LGGCWGL)_2$ photoproducts observed after photolysis at λ = 254 nm.

*i. Product **1b** (m/z 574.25).* Product **1b** was observed in both the Ar-saturated and O_2-saturated samples during the irradiation of peptide $(LGGCWGL)_2$ at λ = 254 nm, eluting at 12 and 11 minutes, respectively. The difference in retention times could be related to the additional products observed in the O_2-saturated samples coating the column, changing the retention times of the photoproducts. Interestingly, the m/z value of product **1b**, m/z 574.25, corresponded to the loss of the Trp side chain and the additional loss of 2 Da from the peptide. The MS/MS fragmentation ions in Figure 3.7 localize the loss of 2 Da to the Cys residue and the cleavage of the Trp side chain to Gly, however they are not traditional y and b ions. Most of the ions in the MS/MS spectrum contained neutral losses. When the Cys was involved in the fragment ion (i.e. b4 and y4 ions and greater), neutral losses of 34 Da were frequently detected from the ions, consistent with fragmentation of the Cys, releasing H_2S from the residue. The largest ion in the spectrum is the loss of 34 Da from the $[M+H]^{+1}$ ion. The Trp to Gly hydroperoxide product was not observed in the O_2-saturated sample.

*ii. Product **2** (m/z 659.35).* Product **2** was observed in both the Ar-saturated and O_2-saturated samples during the irradiation of peptide $(LGGCWGL)_2$ at λ = 254 nm, co-eluting with product **3** at 12.5 minutes. The MS data indicate that the structure of product **2** is consistent with

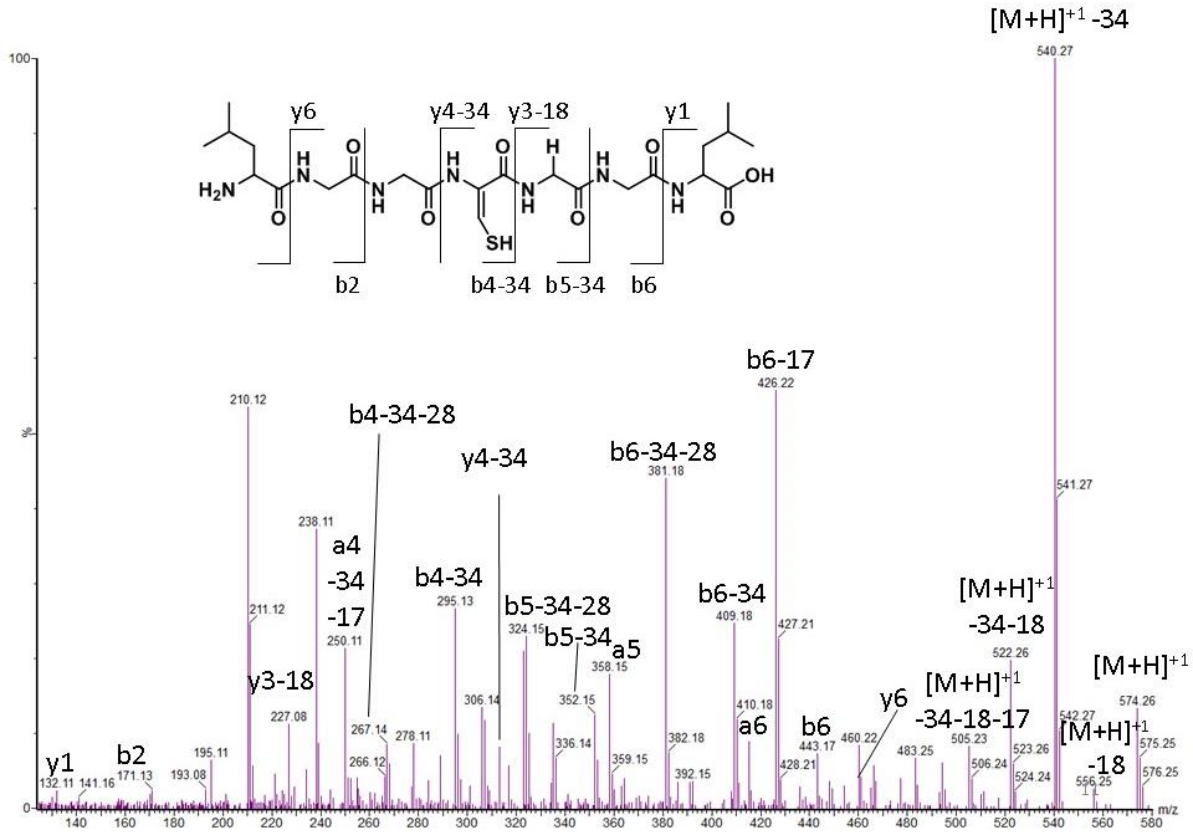

Figure 3.7. MS/MS spectrum of product **1b** generated during the irradiation of $(LGGCWGL)_2$.

the transformation of Cys into Gly. The MS/MS fragmentation b5 and y3 ions clearly show that the Trp is unmodified in the peptide, and the b3 and b4 ions are consistent with the transformation of Cys to Gly (Figure 3.8). The Trp to Gly transformation has not been observed before in our model peptide work.

*iii. Product **7** (m/z 659.35).* Product **7** elutes at 14.8 minutes in the LC-MS (Figure 3.5), and is the largest photoproduct observed in the Ar-saturated irradiation of the $(LGGCWGL)_2$ peptide. Product **7** has a m/z value of 4 Da less than the reduced form of $(LGGCWGL)_2$. When the MS/MS spectrum was analyzed, the fragmentation ions were consistent with the loss of 4 Da on the Cys residue, specifically the b3, b4, y3, and y4 ions (Figure 3.9). A similar product with a loss of 4 Da on the Cys residue, the isothiazol-3(2H)-one product, was thoroughly characterized in Chapter 2 following the irradiation of the $(LGVCVGL)_2$ peptide.

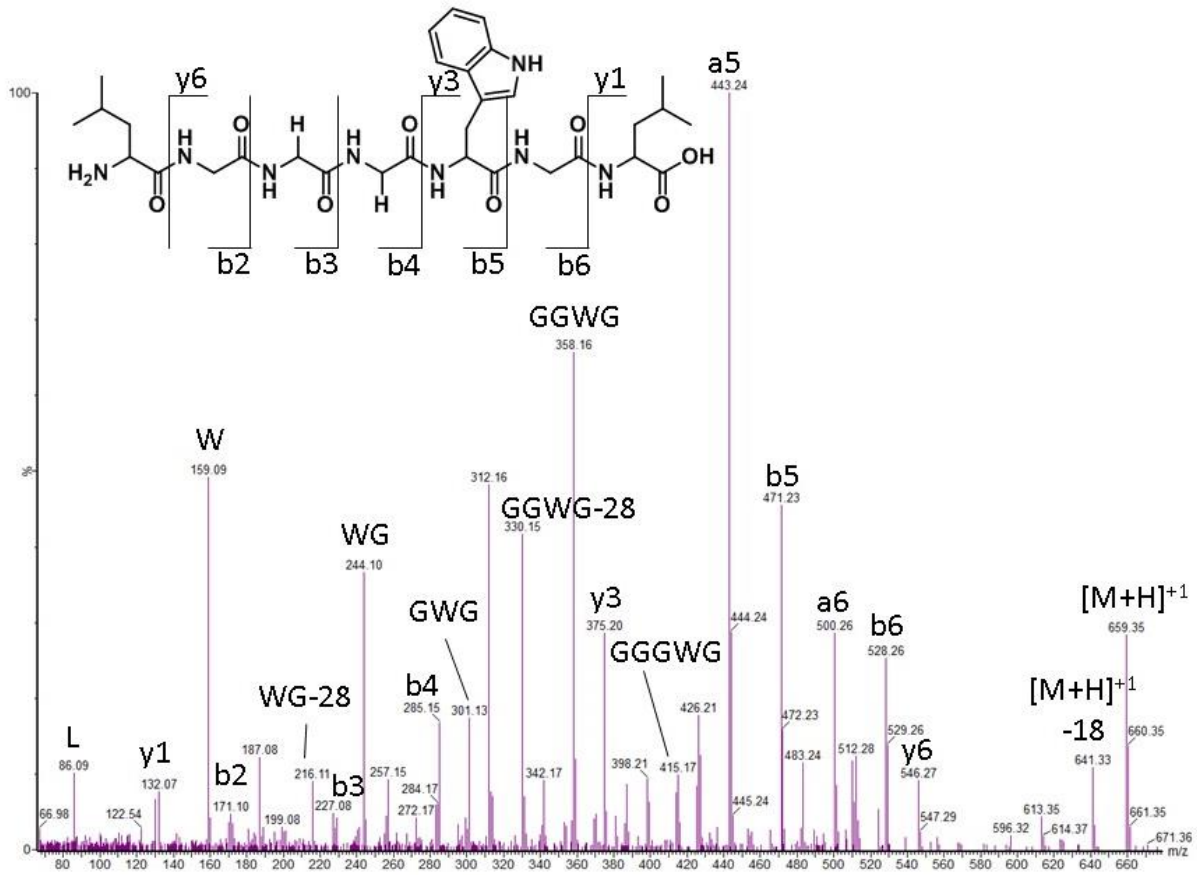

Figure 3.8. MS/MS spectrum of product **2** generated during the irradiation of $(LGGCWGL)_2$.

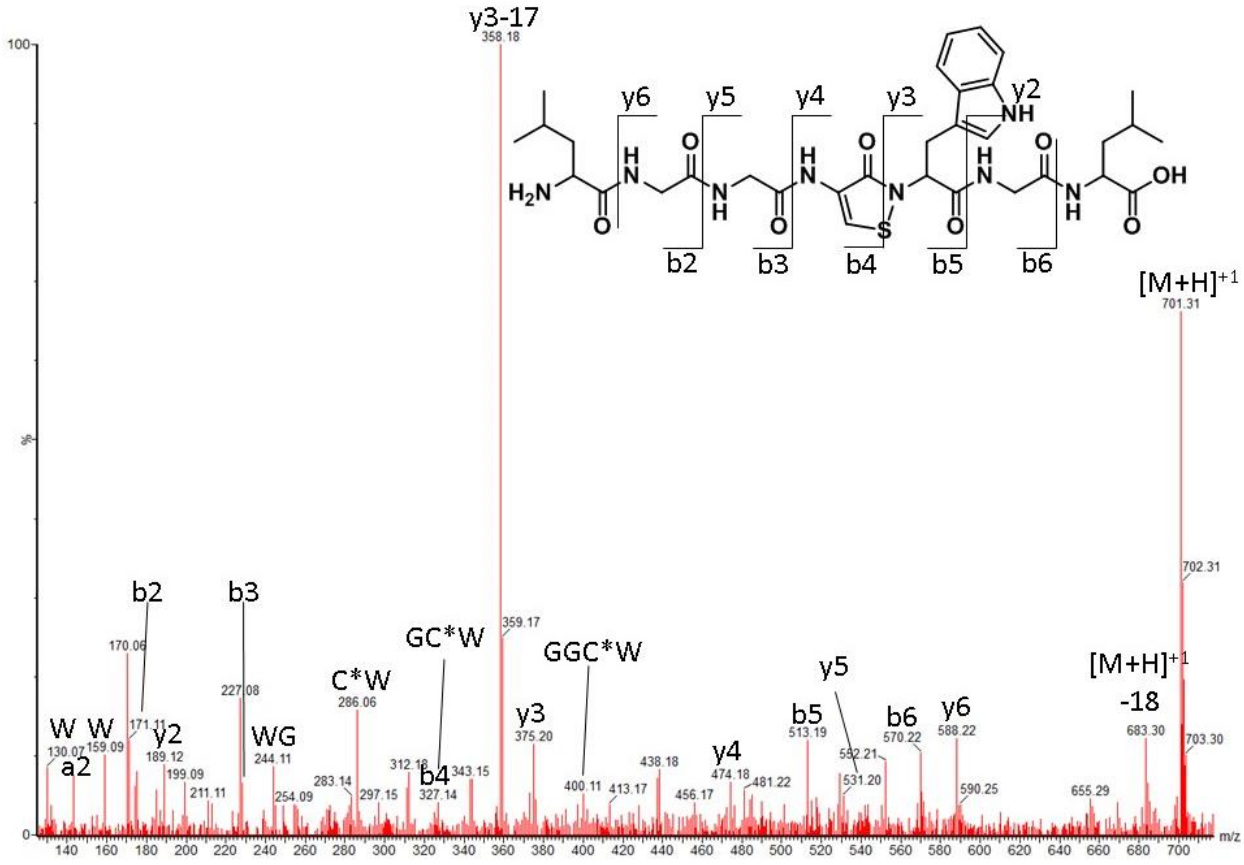

Figure 3.9. MS/MS spectrum of product **7** generated during the irradiation of $(LGGCWGL)_2$.

3.4 Discussion

During O_2-saturated conditions, the irradiation of IgG1, GGCGGL-GGCWGL, NATA, and $(LGGCWGL)_2$ resulted in the cleavage of the Trp side chain. Both Gly and Gly hydroperoxide were detected in place of Trp in the different model systems. Previous studies have documented the $^{\alpha}C$-$^{\beta}C$ bond cleavage of amino acid radical cations in the gas phase[9,10,11,23,24] and in solution.[25] In the gas phase, one proposed $^{\alpha}C$-$^{\beta}C$ bond cleavage mechanism of Trp involves electron transfer from the excited state Trp to the amino group, followed by the loss of an H-atom and $^{\alpha}C$-$^{\beta}C$ carbon-cleavage.[23]

The formation of the photoproducts in IgG1 likely results from a multi-step reaction: the photo-transformation of the disulfide bond to thiol as well as the transformation of Trp to Gly hydroperoxide in our model peptide suggest that the photochemistry of the disulfide bond and of the Trp residue need to be understood together to explain the formation of the different photoproducts in IgG1. The thiol results either from the one-electron reduction of the disulfide bond following photoionization of the Trp residue, or the homolytic cleavage of the disulfide bond, followed by disproportionation of the thiyl radical pair.[19,26] In IgG1, the former is likely the case. We propose that, in solution, the photolytic cleavage of Trp proceeds through an intermediary radical cation ($TrpNH^{+\bullet}$) and leads to a C-centered radical (Scheme 3.1). In the case of Trp[191, LC] and Trp[309, HC], the C-centered radical likely adds O_2 followed by reaction with an H-donor to form the hydroperoxyl group. Instead, Trp[377, HC] was transformed into non-oxidized Gly[377, HC]. This Trp residue is located in the same environment as Trp[309, HC], so O_2 should have been available for oxidation, but the C-centered radical intermediate likely reacted faster with an H-atom donor, such as a thiol, than with O_2. The effect of oxygen on product formation can be rationalized in multiple ways. Certainly, oxygen is important for the

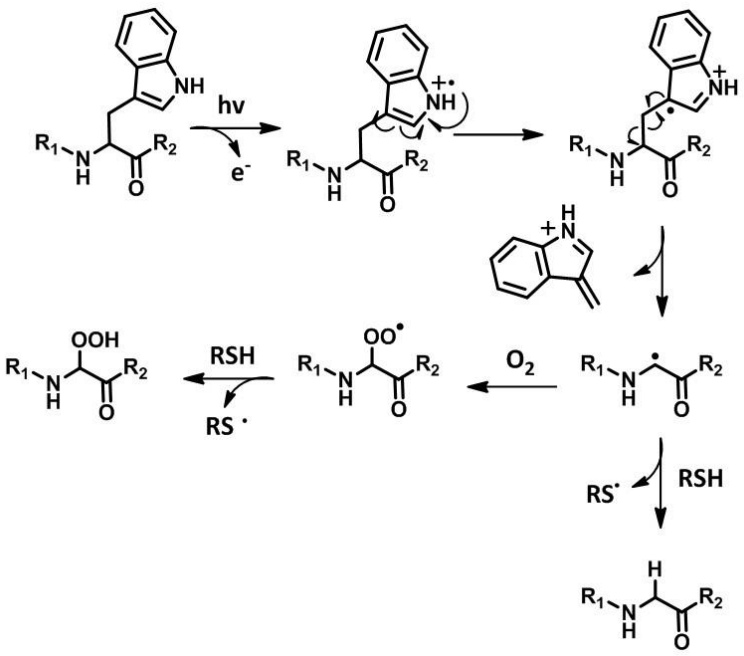

Scheme 3.2. Proposed reaction scheme demonstrating the photolytic cleavage of the Trp side chain and oxidation of the protein backbone.

formation of the Gly hydroperoxide. However, oxygen may also function as an acceptor of the electrons photoejected from Trp, limiting a potential back reaction to restore the reactants. The final product yield may also be affected by intramolecular electron transfer reactions between tryptophan radical cations and electron donors such as tyrosine.

Interestingly, when the Trp side chain was cleaved in N-acetyl-L-tryptophanamide (NATA) in the presence of a nucleophile, oxidized glutathione, the side chain was trapped by the glutathione. This reaction product is important because in a protein, if the Trp side chain is cleaved, there are many available nucleophiles that could trap the Trp side chain. This could greatly affect the protein if the conformation was modified, especially if it the trapping amino acid was located in a region involved in binding or recognition.

The irradiation of $(LGGCWGL)_2$ did not yield a Gly hydroperoxide when the Trp side chain was cleaved in O_2, as expected from the results with the model peptide GGCGGL-GGCWGL. However, a product with Trp to Gly combined with Cys thioaldehyde was observed, product **1b**. The MS/MS fragmentation of this product (Figure 3.7) was not as straight-forward as the MS/MS fragmentation of the Gly hydroperoxide product in GGCGGL-GGCWGL (Figure 3.4). The MS/MS data for product **1b** contained many neutral losses and water (-18), ammonia (-

17), and H_2S (-34). Although these neutral losses are easily explained, their ion intensity compared to the native ions (i.e. b4, b5) is very high. This could be due to the conformation of the peptide, allowing these neutral losses so easily, or the structure assigned to product **1b** could be misguided. The structure could actually correspond to a peptide modification somewhere else on the molecule, freeing up an amine or thiol for more facile cleavage. What is most interesting about the irradiation of this peptide is product **7**, where we hypothesize another isothiazol-3(2H)-one product could be formed, just as with the $(LGVCVGL)_2$ peptide from Chapter 2. In Chapter 2, we proposed that the steric hindrance of the Val residues to the i+1 and i-1 residue of the Cys were the reason for this product formation, since no such product was observed in peptides with Gly or Ala in these positions. The Trp reside in the $(LGGCWGL)_2$ peptide studied in this chapter does have a Trp residue next to the Cys, and this could have the same effect as the Val residues had on the steric conformation of the molecule. Whereas the isothiazol-3(2H)-one product in Chapter 2 was the main product generated in 90% yields, with the Trp-and disulfide containing peptide it is not. This is likely because the Trp absorbs most of the light energy, not the disulfide bond. It would be interesting to modify the irradiation conditions with the Trp and disulfide containing peptide to see if higher yields of this product could form.

3.5 Conclusion

The amino acid hydroperoxide represents not only a significant chemical alteration, but could serve as origin for further protein oxidation. For example, amino acid hydroperoxides have been shown to inactivate proteins via oxidation of Cys residues.[13] Our work also demonstrates that light exposure, and subsequent radical formation produces Gly hydroperoxides at λ_{max} = 305 nm, i.e. wavelengths not filtered out by glass. The conversion of Trp to Gly and Gly hydroperoxide converts an aromatic amino acid into a small, highly flexible aliphatic amino acid

(or its hydroperoxide derivative). These alterations may in part rationalize the loss of conformational integrity observed during photo-irradiation of the antibody, quantified through biophysical measurements.[27] Further mechanistic experiments with (LG**GCW**GL)$_2$ and (LG**CGW**GL)$_2$ are needed to characterize the influence of peptide/protein sequence and structure on the fragmentation of Trp to Gly and Gly hydroperoxide.

3.6 References

1. Haywood, J.; Mozziconacci, O.; Allegre, K. M.; Kerwin, B. A.; Schöneich, C., Light-induced conversion of Trp to Gly and Gly hydroperoxide in IgG1. *Mol Pharm* **2013,** *10* (3), 1146-50.
2. Creed, D., The photophysics and photochemistry of the near-UV absorbing amino-acids .I. Tryptophan and its simple derivatives. *Photochem Photobiol* **1984,** *39* (4), 537-562.
3. Vanhooren, A.; Devreese, B.; Vanhee, K.; Van Beeumen, J.; Hanssens, I., Photoexcitation of tryptophan groups induces reduction of two disulfide bonds in goat alpha-lactalbumin. *Biochemistry* **2002,** *41* (36), 11035-43.
4. Pattison, D. I.; Rahmanto, A. S.; Davies, M. J., Photo-oxidation of proteins. *Photochem Photobiol Sci* **2012,** *11* (1), 38-53.
5. Russell, J.; Katzhendler, J.; Kowalski, K.; Schneider, A. B.; Sherwood, L. M., The single tryptophan residue of human placental lactogen. Effects of modification and cleavage on biologic activity and protein conformation. *J Biol Chem* **1981,** *256* (1), 304-7.
6. Wei, Z.; Feng, J.; Lin, H. Y.; Mullapudi, S.; Bishop, E.; Tous, G. I.; Casas-Finet, J.; Hakki, F.; Strouse, R.; Schenerman, M. A., Identification of a single tryptophan residue as critical for binding activity in a humanized monoclonal antibody against respiratory syncytial virus. *Anal Chem* **2007,** *79* (7), 2797-805.
7. Kerwin, B. A.; Remmele, R. L., Jr., Protect from light: photodegradation and protein biologics. *J Pharm Sci* **2007,** *96* (6), 1468-79.
8. Parker, N. R.; Jamie, J. F.; Davies, M. J.; Truscott, R. J., Protein-bound kynurenine is a photosensitizer of oxidative damage. *Free Radic Biol Med* **2004,** *37* (9), 1479-89.

9. Kang, H.; Dedonder-Lardeux, C.; Jouvet, C.; Martrenchard, S.; Gregoire, G.; Desfrancois, C.; Schermann, J. P.; Barat, M.; Fayeton, J. A., Photo-induced dissociation of protonated tryptophan TrpH(+): A direct dissociation channel in the excited states controls the hydrogen atom loss. *Phys Chem Chem Phys* **2004,** *6* (10), 2628-2632.

10. Bagheri-Majdi, E.; Ke, Y. Y.; Orlova, G.; Chu, I. K.; Hopkinson, A. C.; Siu, K. W. M., Copper-mediated peptide radical ions in the gas phase. *Journal of Physical Chemistry B* **2004,** *108* (30), 11170-11181.

11. Tabarin, T.; Antoine, R.; Broyer, M.; Dugourd, P., Specific photodissociation of peptides with multi-stage mass spectrometry. *Rapid Commun Mass Sp* **2005,** *19* (20), 2883-2892.

12. Zhang, Q.; Li, Y.; Chen, D.; Yu, Y.; Duan, L.; Shen, B.; Liu, W., Radical-mediated enzymatic carbon chain fragmentation-recombination. *Nat Chem Biol* **2011,** *7* (3), 154-60.

13. Dremina, E. S.; Sharov, V. S.; Davies, M. J.; Schöneich, C., Oxidation and inactivation of SERCA by selective reaction of cysteine residues with amino acid peroxides. *Chem Res Toxicol* **2007,** *20* (10), 1462-9.

14. Davies, M. J.; Fu, S.; Dean, R. T., Protein hydroperoxides can give rise to reactive free radicals. *Biochem J* **1995,** *305 (Pt 2)*, 643-9.

15. Biosystems, A. *Cleavage, Deprotection, and Isolation of Peptides after Fmoc Synthesis*; May 1998, **1998**.

16. Gay, C. A.; Gebicki, J. M., Measurement of protein and lipid hydroperoxides in biological systems by the ferric-xylenol orange method. *Anal Biochem* **2003,** *315* (1), 29-35.

17. Wasylaschuk, W. R.; Harmon, P. A.; Wagner, G.; Harman, A. B.; Templeton, A. C.; Xu, H.; Reed, R. A., Evaluation of hydroperoxides in common pharmaceutical excipients. *J Pharm Sci* **2007,** *96* (1), 106-16.

18. Xu, H.; Freitas, M. A., MassMatrix: a database search program for rapid characterization of proteins and peptides from tandem mass spectrometry data. *Proteomics* **2009,** *9* (6), 1548-55.

19. Mozziconacci, O.; Kerwin, B. A.; Schöneich, C., Exposure of a monoclonal antibody, IgG1, to UV-light leads to protein dithiohemiacetal and thioether cross-links: a role for thiyl radicals? *Chem Res Toxicol* **2010,** *23* (8), 1310-2.

20. Olsen, J. V.; Ong, S. E.; Mann, M., Trypsin cleaves exclusively C-terminal to arginine and lysine residues. *Mol Cell Proteomics* **2004,** *3* (6), 608-14.

21. Huang, Y. C.; Haselbeck, R. J.; McAlister-Henn, L.; Colman, R. F., N-ethylmaleimide profiling of yeast NADP-dependent isocitrate dehydrogenase. *Arch Biochem Biophys* **1995,** *316* (1), 485-92.

22. Morgan, P. E.; Pattison, D. I.; Davies, M. J., Quantification of hydroxyl radical-derived oxidation products in peptides containing glycine, alanine, valine, and proline. *Free Radic Biol Med* **2012,** *52* (2), 328-39.

23. Lucas, B.; Barat, M.; Fayeton, J. A.; Perot, M.; Jouvet, C.; Gregoire, G.; Brondsted Nielsen, S., Mechanisms of photoinduced Cα-Cβ bond breakage in protonated aromatic amino acids. *J Chem Phys* **2008,** *128* (16), 164302.

24. Li, X.; Lin, C.; Han, L.; Costello, C. E.; O'Connor, P. B., Charge remote fragmentation in electron capture and electron transfer dissociation. *J Am Soc Mass Spectrom* **2010,** *21* (4), 646-56.

25. Bent, D. V.; Hayon, E., Excited-state chemistry of aromatic amino-acids and related peptides .II. Phenylalanine. *J Am Chem Soc* **1975,** *97* (10), 2606-2612.

26. Mozziconacci, O.; Sharov, V.; Williams, T. D.; Kerwin, B. A.; Schöneich, C., Peptide cysteine thiyl radicals abstract hydrogen atoms from surrounding amino acids: the photolysis of a cystine containing model peptide. *J Phys Chem B* **2008,** *112* (30), 9250-7.

27. Mason, B. D.; Schöneich, C.; Kerwin, B. A., Effect of pH and light on aggregation and conformation of an IgG1 mAb. *Mol Pharm* **2012,** *9* (4), 774-90.

3.7 Appendix B

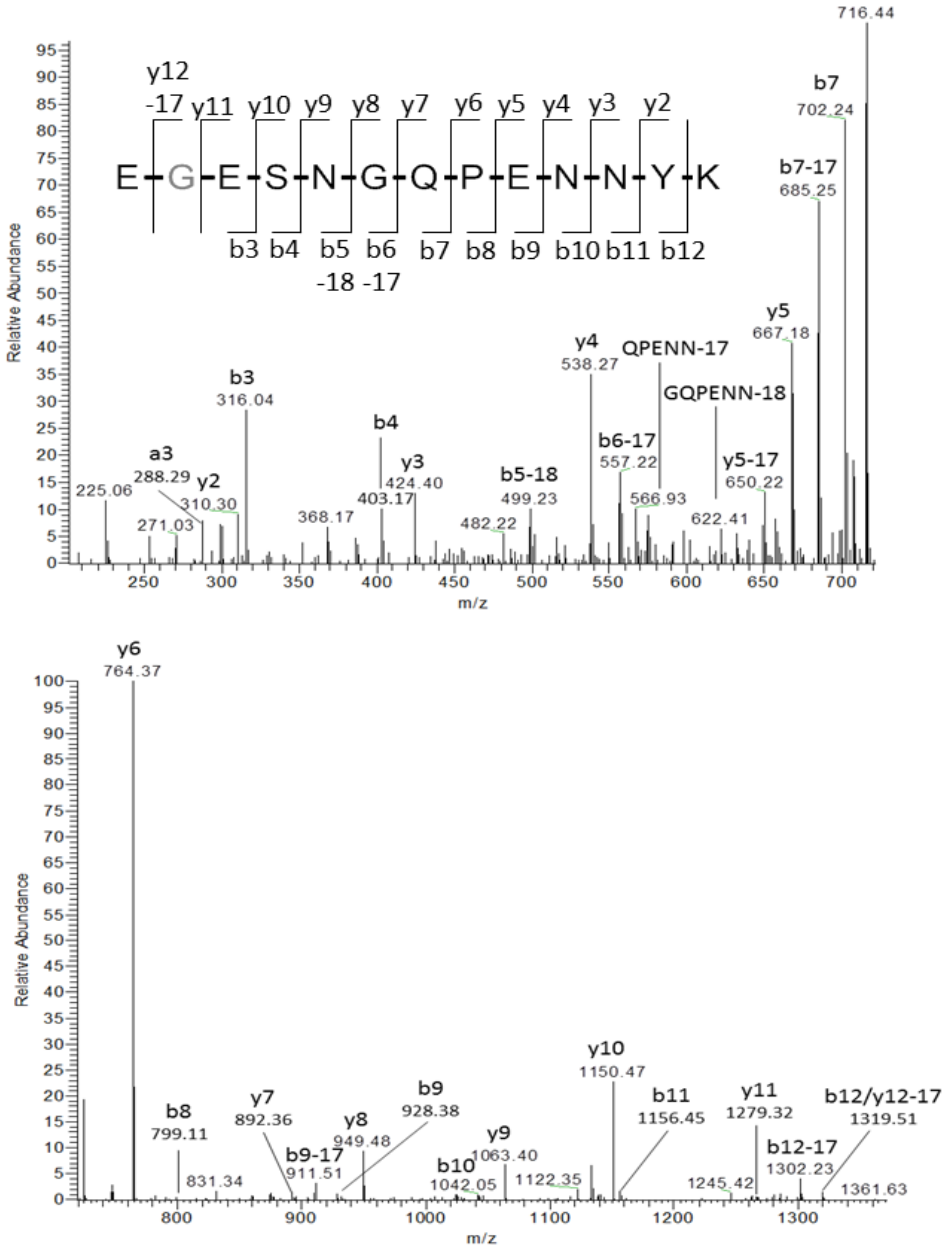

Figure B.1. MS/MS spectra of the peptide sequence [376-388, HC] of IgG1 where Trp[377, HC] is transformed into Gly[377, HC] during 254 nm irradiation. (Top spectrum: m/z 200-750, bottom spectrum: m/z 750-1400).

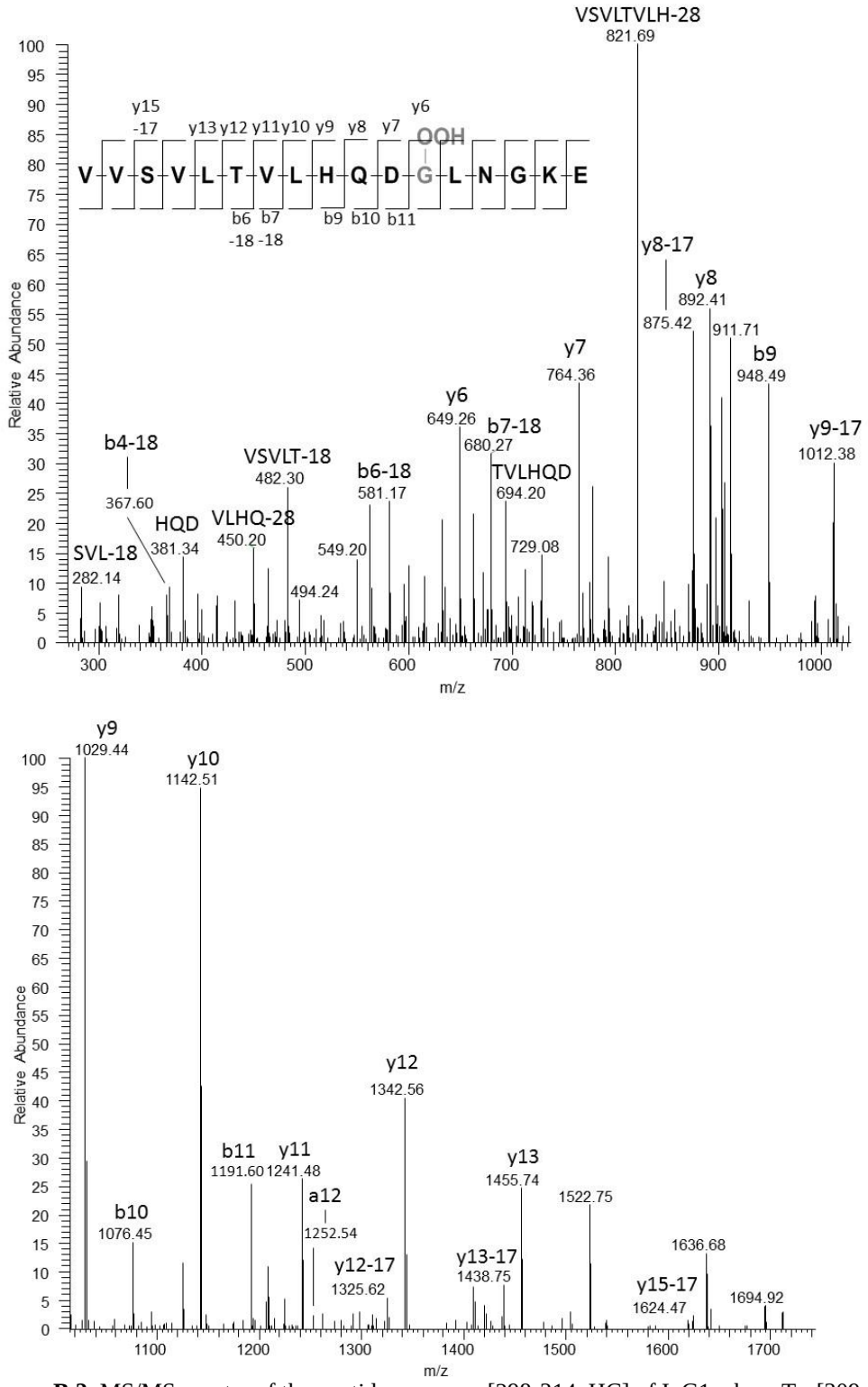

Figure B.2. MS/MS spectra of the peptide sequence [298-314, HC] of IgG1 where Trp[309, HC] is transformed into Gly[309, HC] hydroperoxide during 305 nm irradiation. (Top spectrum: m/z 260-1020, bottom spectrum: m/z 1025-1740).

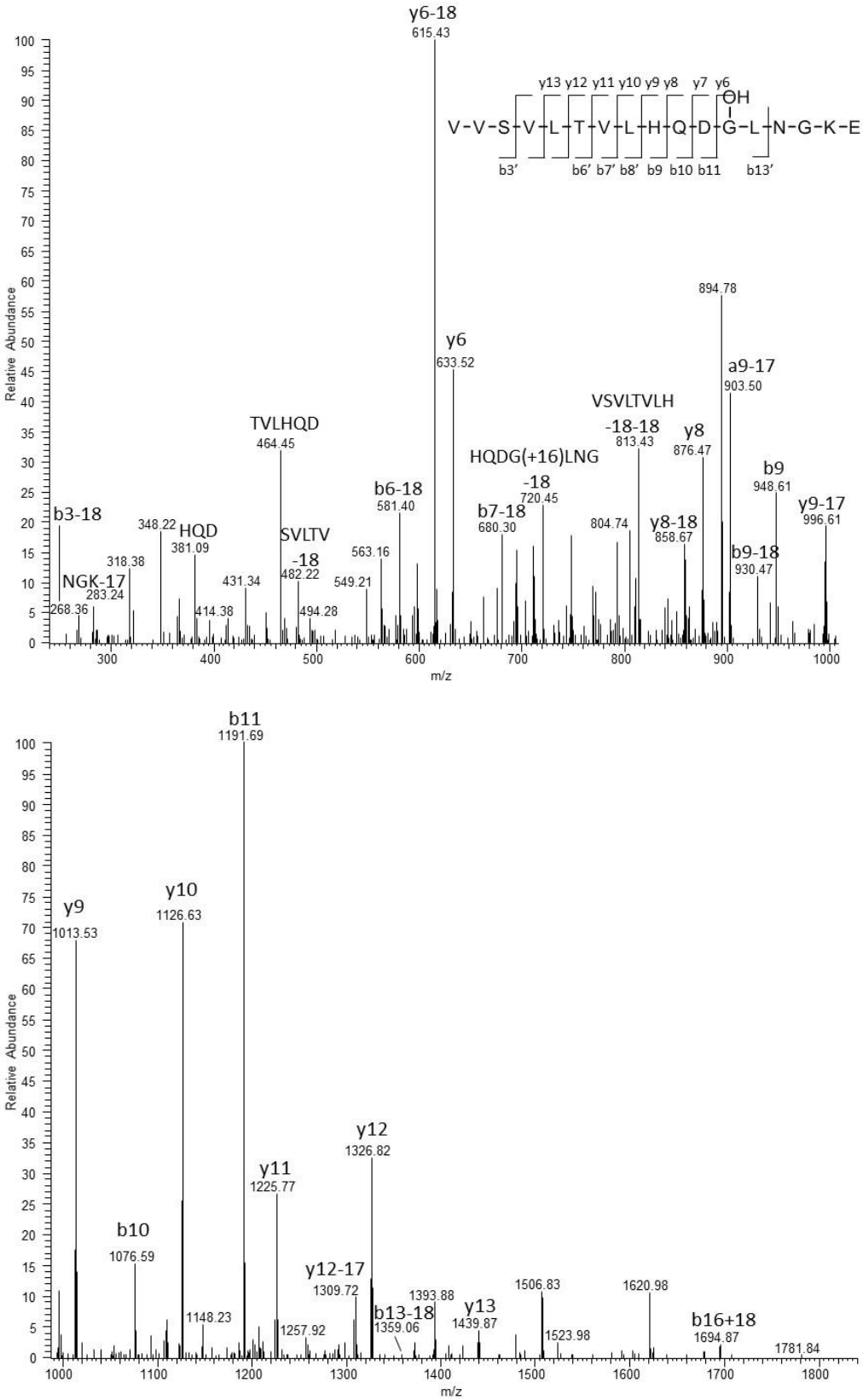

Figure B.3. MS/MS spectra of the peptide sequence [298-314, HC] of IgG1 where Trp[309, HC] is transformed into Gly[309, HC] hydroxide after $NaBH_4$ reduction. (Top spectrum: m/z 260-1020, bottom spectrum: m/z 1025-1820).

Product	Proposed Structure	MS/MS	Product	Proposed Structure	MS/MS
1a	-	-	9a	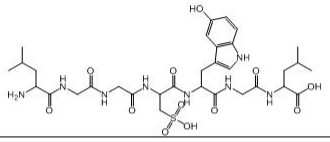	Fig. B.8
3	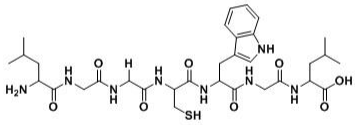	Fig. B.4	9b	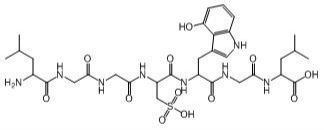	-
4	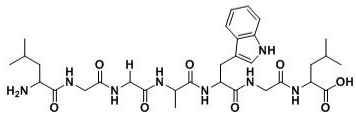	Fig. B.5	10	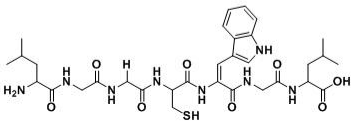	Fig. B.9
5	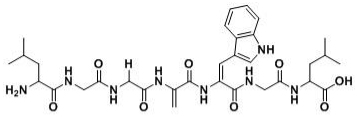	Fig. B.6	11	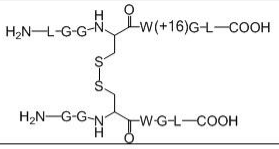	-
6	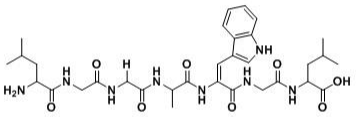	Fig. B.7	12	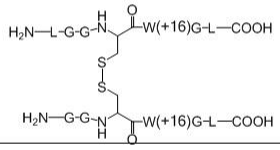	-
8	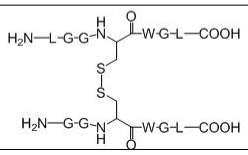	-			

Table B.1. $(LGGCWGL)_2$ photoproducts observed after photolysis at $\lambda = 254$ nm not described in Section 3.3.4.

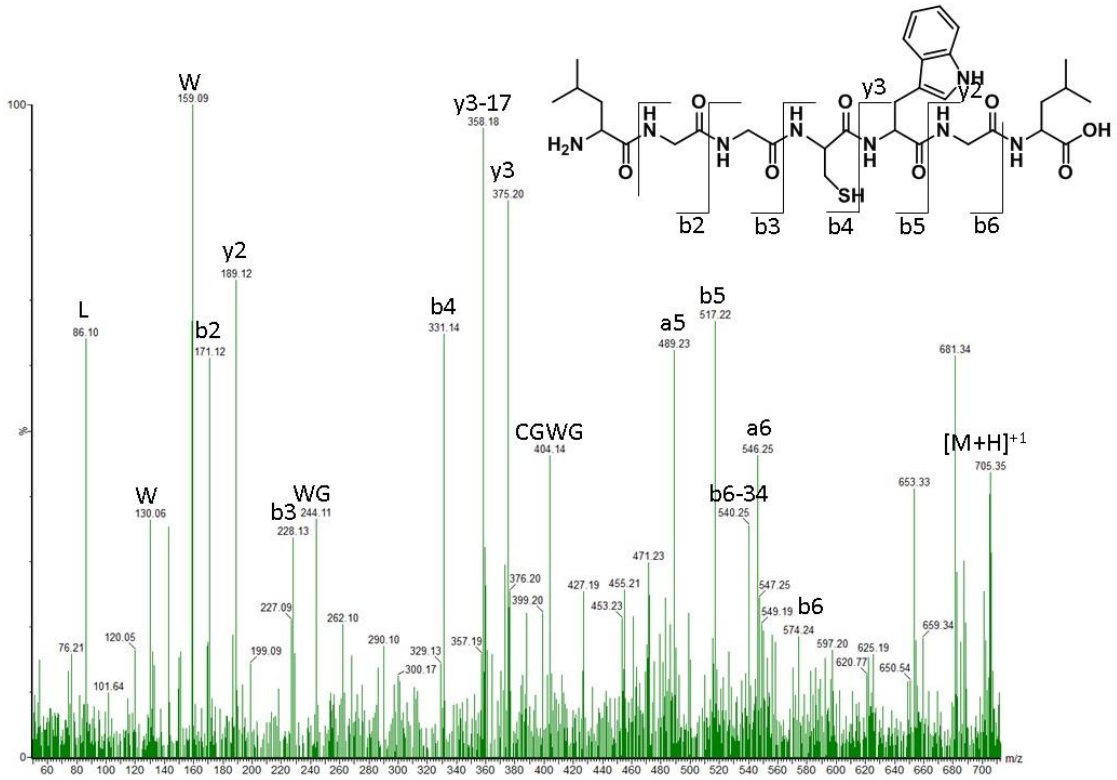

Figure B.4. MS/MS spectra of product **3**, generated during the photolysis of $(LGGCWGL)_2$ at λ = 254 nm.

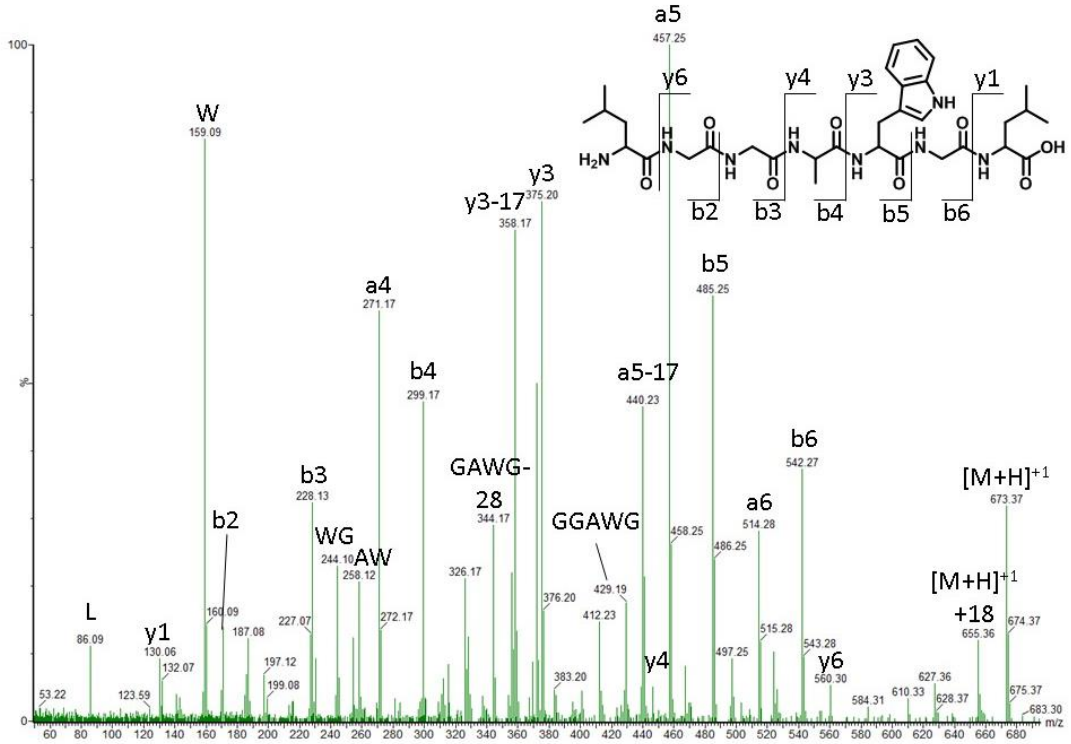

Figure B.5. MS/MS spectra of product **4**, generated during the photolysis of $(LGGCWGL)_2$ at λ = 254 nm.

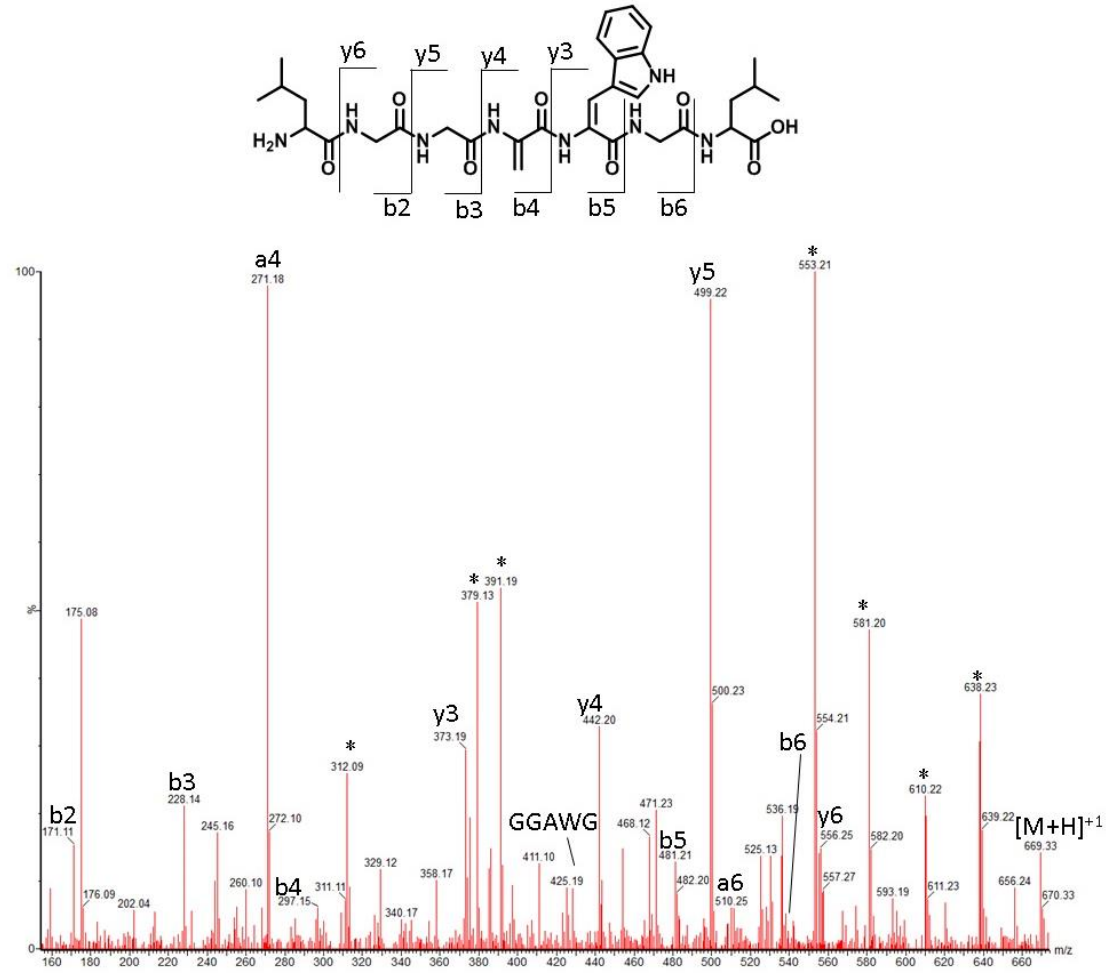

Figure B.6. MS/MS spectra of product **5**, generated during the photolysis of $(LGGCWGL)_2$ at λ = 254 nm. *Represents fragment ions of oxidized Trp residue (not from product **5**).

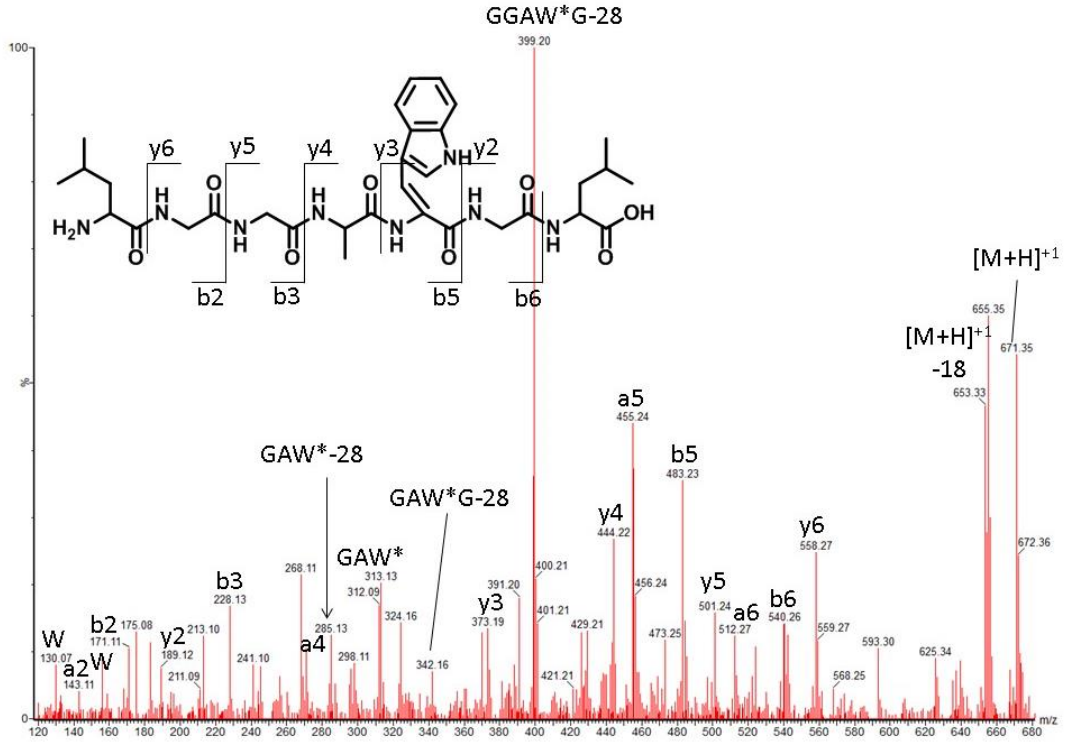

Figure B.7. MS/MS spectra of product **6**, generated during the photolysis of $(LGGCWGL)_2$ at λ = 254 nm. *Represents modified Trp.

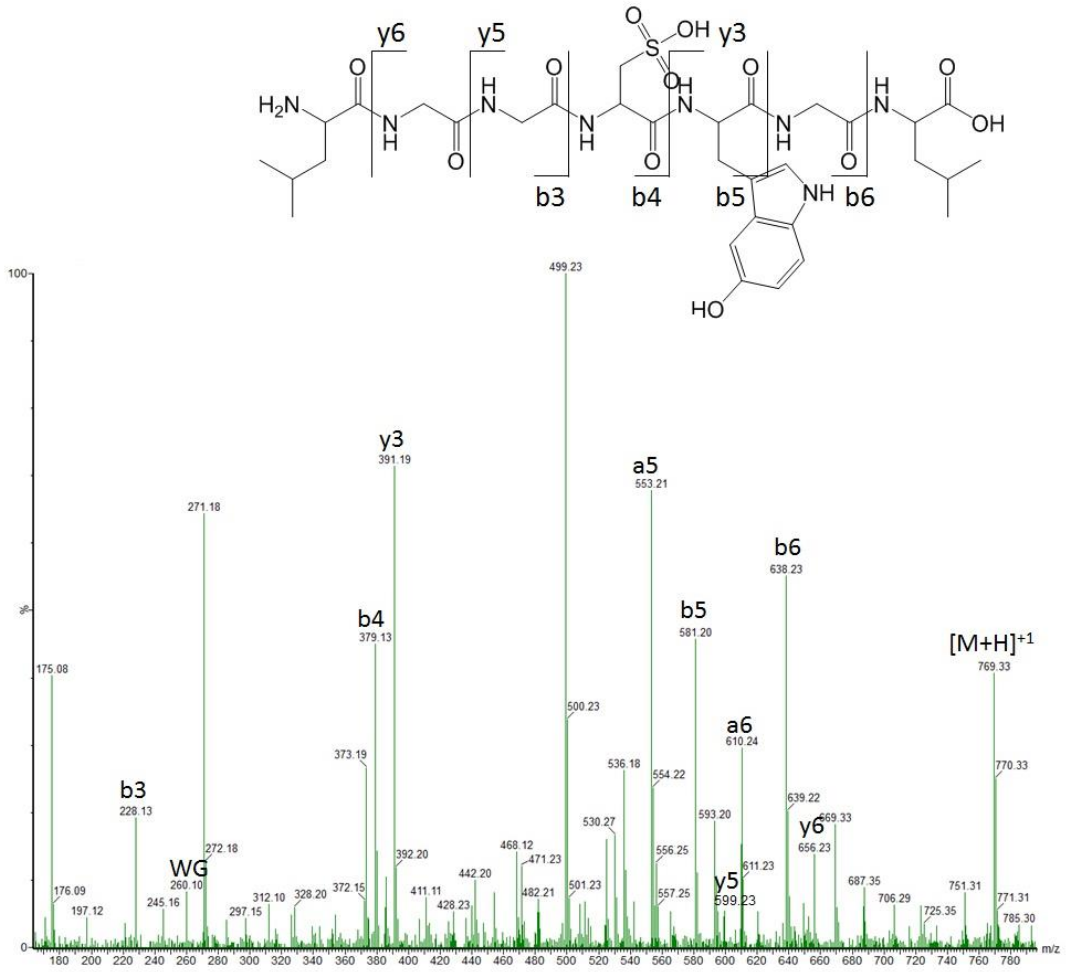

Figure B.8. MS/MS spectra of product **9a/9b**, generated during the photolysis of $(LGGCWGL)_2$ at $\lambda = 254$ nm.

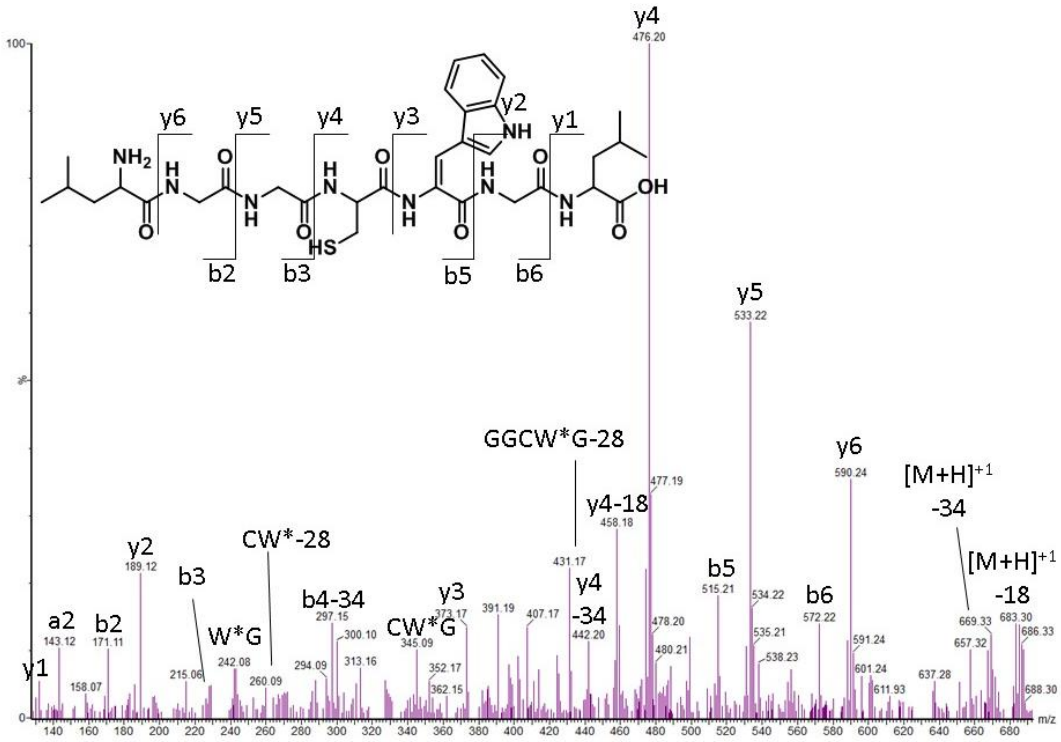

Figure B.9. MS/MS spectra of product **10**, generated during the photolysis of $(LGGCWGL)_2$ at $\lambda = 254$ nm. *Represents modified Trp.

Chapter 4. Photo-oxidation of model peptides: Formation of triply oxidized His and Trp side chain cleavage products

4.1 Introduction

A great amount of work has been published on protein oxidation and its effect on protein stability, especially since all amino acids have the potential to oxidize.[1,2,3] Oxidation is often initiated by light exposure or reactive oxygen species generated by metal-catalyzed oxidation (MCO).[4,5] In therapeutic proteins such as monoclonal antibodies (mAbs), the most common oxidation products are detected on the Trp and Met residues, although His, Cys, Tyr, and Phe are also targets for oxidation.[6,7,8,9] The oxidation of these residues has been reported to effect the efficacy and stability of the entire protein, thereby reducing shelf-life and drug safety. For instance, Trp oxidation in the complementarity-determining region (CDR) was reported to significantly reduce antigen binding and biological activity in an IgG1 monoclonal antibody following UV light exposure.[7] Methionine oxidation in the neonatal Fc (fragment crystallizable) receptor (FcRn) region shortened serum half-life[10] and reduced binding affinity to the FcRn receptors.[11] Oxidation of His, Met, and Trp in IgG2 was observed after MCO with Cu(II) and ascorbate, leading to changes in both the secondary and tertiary structure.[12] His oxidation has also been reported in human growth hormone by both light[13] and MCO (with Cu(II) and ascorbate) in regions located in the metal binding site.[14,15]

Recently, novel protein modifications have been observed for His and Trp residues. Doubly oxidized His[289, HC] (i.e. hydroxylated imidazolone) was reported in the Fc region of IgG1 using mass spectrometry (MS) analysis.[16] This oxidation was only detected after light stress (2000 lux hours of visible light at 25 °C with 65% relative humidity (RH) for 25 days), not thermal stress conditions (40 °C with 75% relative humidity (RH) for 3 months); therefore, it was proposed that the oxidation was initiated by singlet oxygen.[5] In separate IgG1 molecules, the same His residue was triply and doubly oxidized after exposing IgG1 to ICH light stress

conditions (1.2 million lux hours of visible light and 200 Watt hours/m^2 of UV light during 24 hours, unpublished data). Singlet oxygen was also proposed to initiate a His-His crosslink in photo-oxidized IgG1, detected through ^{18}O-labeling and MS analysis using the XChem-Finder crosslinking software program.[17] The crosslink was observed between two separate His[220, HC] amino acids, with the crosslink proposed between one His imidazole N-1 atom and a separate imidazole C-4 atom. Furthermore, light exposure of IgG1 in the presence of oxygen converted the Trp to Gly and Gly hydroperoxide (Chapter 3).[18] A similar Trp side chain cleavage was observed when the synthetic analogue of the peptide hormone somatostatin, octreotide, was photo-irradiated.[19] One of the major differences between somatostatin and octreotide is the amino acid configuration of the Trp residue: L-Trp in somatostatin and D-Trp in octreotide. Due to the D-Trp configuration in octreotide, the distance between the carbonyl group of the D-Trp and the disulfide bond in the peptide is only 4.5 Å, whereas in somatostatin, the distance between the carbonyl of the L-Trp and the disulfide bond is 7.8 Å. Following exposure of both peptides to UV and cool white light, somatostatin was relatively inert to photodegradation, while the D-Trp

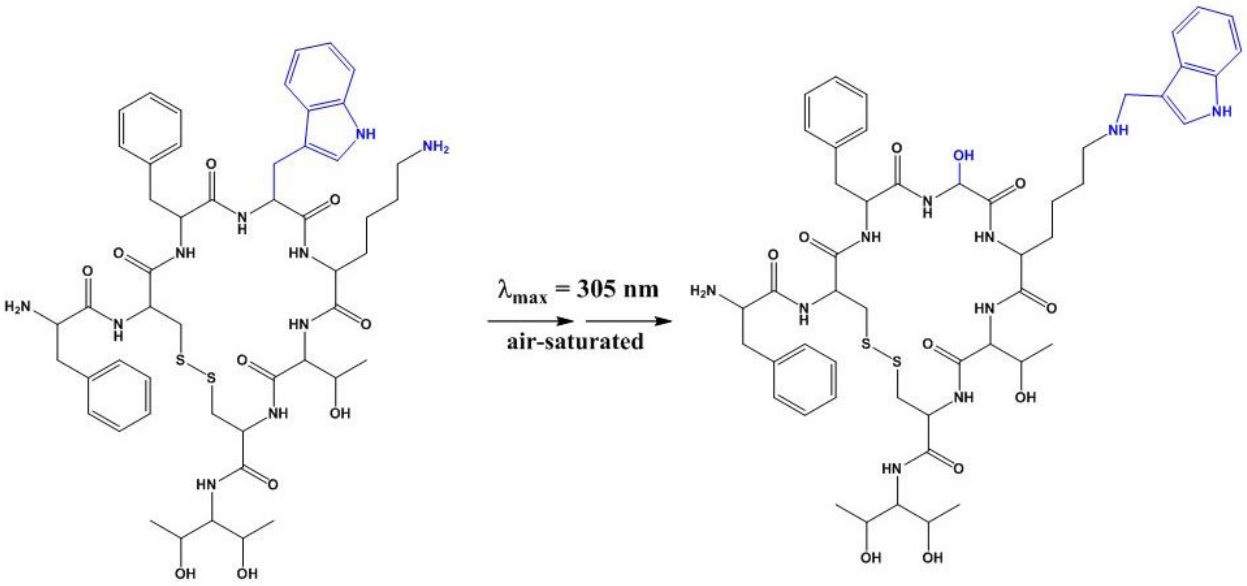

Scheme 4.1. Photodegradation of octreotide during exposure to UV light at λ_{max} = 305 nm.[19]

in octreotide was converted to a hydroxyl group, and the resultant Trp side chain (3-methyleneindolenine, i.e. 3-MEI) was abstracted by the nearby Lys in the peptide (Scheme 4.1). These novel photoproducts highlight the importance of continued research in protein stability, and particularly photostability.

To understand the His degradation pathway more fully and determine the role of Trp photosensitization, model peptides were synthesized for peptides where His oxidation has been observed, and for comparison, mutant peptides were synthesized in which Ala was substituted in place of Trp. Interestingly, after photo-irradiation of the peptides, MS analysis revealed a triply oxidized His residue on one of the Ala-containing peptides, but not the Trp-containing peptides. However, an isobaric product with the same m/z value to the native peptide was detected in a Trp-containing model peptide, and further experimentation determined that Trp was converted to Gly and the N-terminal Lys had abstracted the resultant Trp side chain (3-MEI). Moreover, when the Lys amine was methylated prior to irradiation to inhibit the reaction with 3-MEI, an isobaric product was detected again, albeit the Tyr residue was responsible for abstracting the 3-MEI group. Only when both the Tyr and Lys residues were acetylated to inhibit reactions with the photolytically generated 3-MEI group were no isobaric products observed. This could indicate that Trp radical cations do not cleave if there is not an acceptor for 3-MEI or they are re-attached to the Trp, re-forming the original Trp residue.

4.2 Experimental methods

4.2.1 Materials. Ammonium bicarbonate, dimethyl sulfoxide (DMSO), sodium borohydride ($NaBH_4$), sodium hydroxide, sodium phosphate monobasic, sodium phosphate dibasic, L-glutathione oxidized (GSSG), acetic anhydride, and trypsin (from porcine pancreas) were supplied by Sigma-Aldrich (St. Louis, MO) at the highest commercially available purity.

Sequencing grade Glu-C and trypsin were purchased from Promega (Madison, WI). N-succinimidyl acetate was supplied by TCI America (Portland, OR), and formaldehyde (37%) was supplied by Amersham Biosciences (Piscataway, NJ). The model peptides, Ac-KTVLHQDWLNGK-Am (H318W), Ac-KTVLHQDALNGK-Am (H318A), Ac-KNWYVDGVEVHNAK-Am (H293W), and Ac-KNAYVDGVEVHNAK-Am (H293A), were provided by a pharmaceutical company.

4.2.2 Methylation of the Lys Residues in H293W. Reductive methylation of the H293W Lys residues was accomplished with formaldehyde and $NaBH_4$.[20] Briefly, 1M $NaBH_4$ in 200 mM sodium borate buffer and 1M formaldehyde in 200 mM sodium borate buffer were freshly prepared and placed on ice for the duration of the reaction. The peptide was prepared at a concentration of 1 mg/mL in 200 mM sodium borate buffer at pH 8.5. To the solution, final concentrations of 30 mM formaldehyde and 6 mM $NaBH_4$ were added and the solution was stirred at 0 ˚C on ice. After 10 minutes of reaction, another 3 mM $NaBH_4$ was added and the solution stirred at 0 ˚C on ice for an additional 20 minutes. These steps were repeated three times, and a final addition of 6 mM $NaBH_4$ was added to the samples. To quench the reaction, a final concentration of 2.5 mM Gly containing 0.1% formic acid (v/v) was added to the solution. The buffer and residual reagents were removed from the methylated peptide with an HPLC purification step gradient method on a Shimadzu SCL-10A instrument. A C18 Grace Vydac 218TP guard column with dimensions of 7.5 x 4.6 mm ID, containing 5μm particles (Fisher Scientific, Pittsburg, PA) was used. The mobile phases consisted of H_2O and acetonitrile at a ratio of 95%:5% (v:v) for solvent A and a ratio of 5%:95% (v:v) for solvent B. At a flow rate of 1 ml/min, 100% solvent A was maintained for five minutes and then switched to 100% solvent B for peptide elution. The collected solution was lyophilized and reconstituted in water to a

concentration of 100 μM (as determined using the Beer-Lambert law after measuring the absorbance of the solution at 280 nm in a Cary 50 Bio UV-Visible spectrometer (Varian Inc., Palo Alto, CA) and assuming Trp and Tyr molar absorption coefficients of 5690 $M^{-1}cm^{-1}$ and 1280 $M^{-1}cm^{-1}$, respectively). The pH was adjusted to pH 4.5 with 0.1 M HCl. The methylation was confirmed by mass spectrometry using the Q-tof Premier mass spectrometer (See section 4.2.11).

4.2.3 Acetylation of the Lys and Tyr Residues in H293W. Acetylation of the Lys and Tyr residues was accomplished using N-succinimidyl acetate (NSA).[21] A stock solution of NSA was prepared at 500 mM in DMSO. 20 μL of the stock solution of NSA was mixed with 25 μL of 200 μM H293W peptide and 55 μL of 50 mM pH 9.0 phosphate buffer. The reaction mixture was incubated at room temperature for 15 minutes. The NSA and phosphate buffer were removed from the acetylated peptides with an HPLC purification step gradient method on a Shimadzu SCL-10A instrument. A C18 Grace Vydac 218TP guard column with dimensions of 7.5 x 4.6 mm ID, containing 5μm particles (Fisher Scientific, Pittsburg, PA) was used. The mobile phases consisted of H_2O and acetonitrile at a ratio of 95%:5% (v:v) for solvent A and a ratio of 5%:95% (v:v) for solvent B. At a flow rate of 1 ml min^{-1}, 100% solvent A was maintained for five minutes, then changed immediately to 100% solvent B for peptide elution. The collected solution was lyophilized and reconstituted in water to a concentration of ca. 100 μM. The acetylated peptides were separated using a YMC-Pack ODS-A C18 reverse phase column with dimensions of 250 x 4.6 mm ID containing 5μm particles (YMC America, Inc. Allentown, PA). The mobile phases consisted of H_2O, acetonitrile, and trifluoroacetic acid at a ratio of 95%:4.9%:0.1% (v:v:v) for solvent A and a ratio of 4.9%:95%:0.1% (v:v:v) for solvent B. A linear gradient was developed by increasing solvent B from 10% to 45% in 25 minutes with

a flow rate of 1ml/min. The collected solution was then lyophilized and reconstituted in water to a concentration of 100 μM (as determined using the Beer-Lambert law after measuring the absorbance of the solution at 280 nm in a Cary 50 Bio UV-Visible spectrometer (Varian Inc., Palo Alto, CA) and assuming Trp and Tyr molar absorption coefficients of 5690 $M^{-1}cm^{-1}$ and 1280 $M^{-1}cm^{-1}$, respectively). The pH was adjusted to pH 4.5 with 0.1 M HCl. The acetylation was confirmed by mass spectrometry using the Q-tof Premier mass spectrometer (See Section 4.2.11).

4.2.4 UV Irradiation of Model Peptides. Peptides were dissolved in water at pH 4.0 to a concentration of 100 μM. The solutions were O_2-saturated through head-space equilibration with O_2 for up to thirty minutes in quartz tubes capped with rubber stoppers. The samples were then exposed at room temperature to light for up to thirty minutes at $\lambda = 254$ nm in a Rayonet RPR-200 photoreactor equipped with four phosphor-coated low pressure mercury lamps, RPR-2537, and a RMA-500 Merry-Go-Round unit (Southern New England, Branford, CT, RMA-500). Actinometry measurements for the $\lambda = 254$ nm lamp gave a flux of 2.96×10^{-4} einstein/min and irradiance of ~15 W cm^{-2}. Directly after photolysis, samples were frozen at -20 °C until MS analysis.

4.2.5 UV Irradiation of H293W and Oxidized L-glutathione. A final concentration of 100 μM oxidized L-glutathione (GSSG) was added to 100 μL of 100 μM H293W at pH 7.0 in water. The solution was saturated through head-space equilibration with oxygen for thirty minutes and then irradiated at $\lambda = 254$ nm for twenty minutes, and frozen at -20 °C until MS analysis.

4.2.6 Glu-C Digestion of H293W and H293A. Following the irradiation of H293W and H293A, the peptides were digested with freshly prepared Glu-C in a 1:20 ratio of enzyme to

peptide in 50 mM ammonium bicarbonate buffer at pH 7.8. The samples were placed in a 37 °C incubator overnight and subsequently frozen at -20 °C until MS analysis.

4.2.7 Tryptic Digestion of H293W. Trypsin (from Promega and Sigma-Aldrich) was diluted to a concentration of 1 mg/mL with 1 mM HCl and 20 mM $CaCl_2$, aliquoted, and stored at -20 °C until needed. Then, the enzyme from each supplier was added separately to peptide samples separately in a 1:20 enzyme to peptide ratio, and the pH of the solution was adjusted with ammonium bicarbonate (50 mM, pH 7.8). The samples were placed in a 37 °C incubator for four hours, and frozen at -20 °C until MS analysis.

4.2.8 LTQ-FT Mass Spectrometry Analysis. The peptides were analyzed on a linear trap quadrupole-Fourier transform (LTQ-FT) ion cyclotron resonance mass spectrometer (Thermo-Finnigan, Bremen, Germany) equipped with a NanoAcquity UPLC System (Waters Corp., Milford, MA, USA). The instrument was operated in a data-dependent acquisition mode with all lenses optimized on the MH+ ion from leucine enkephalin. The ESI source was operated with a spray voltage of 2.8 kV, a tube lens offset of 96 V and a capillary temperature of 200 °C. The peptides were eluted from a reverse phase non-porous Imtakt Presto FF-C18 column with dimensions of 15 cm x 0.5 mm ID containing 2 µm particles (Imtakt Corp., Philadelphia, PA, USA), at a flow rate of 5 µL min^{-1}. The mobile phases consisted of H_2O, acetonitrile, and formic acid at a ratio of 99.9%:0%:0.1% (v:v:v) for solvent A and a ratio of 0%:99.9%:0.1% (v:v:v) for solvent B. A linear gradient was developed by increasing solvent B from 3% to 40% in 50 minutes. The XCalibur software was used to acquire and analyze the data.

4.2.9 Q-Tof Mass Spectrometry Analysis. The peptides were analyzed by a Micromass Q-Tof Premier mass spectrometer (Micromass Ltd., Manchester, U.K.) equipped with an Acquity UPLC System (Waters Corp., Milford, MA, USA). The instrument was operated in the

MS^E mode with all lenses optimized on the MH+ ion from sodium iodide. The ESI source was operated with a spray voltage of 2.5 kV, a tube lens offset of 75 V and a capillary temperature of 250 °C. The peptides were eluted from a Grace reverse phase capillary C18 column with dimensions of 25 cm x 0.5 mm containing 5 μm particles (Fisher Scientific, Pittsburg, PA), at a flow rate of 20 μL min^{-1}. The mobile phases consisted of H_2O, acetonitrile, and formic acid at a ratio of 99.9%:0%:0.1% (v:v:v) for solvent A and a ratio of 0%:99.9%:0.1% (v:v:v) for solvent B. A linear gradient was developed by increasing solvent B from 15% to 50% in 43 minutes. The MassLynx software was used to acquire and analyze the data.

4.3 Results

4.3.1 His and Trp Modifications observed in the Model Peptides. To elucidate the mechanism of triple His oxidation in IgG1, model peptides were synthesized to represent the tryptic peptides in IgG1 where His oxidation was observed. The peptides either contained Trp residues or for comparison, the Trp was replaced with Ala to examine the role of Trp photosensitization in His oxidation. The model peptides contained an N-acetyl Lys and a C-terminal Lys amide residue to aid in solubility. The following peptides were synthesized: Ac-KNWYVDGVEVHNAK-Am (H293W), Ac-KNAYVDGVEVHNAK-Am (H293A), Ac-KTVLHQDWLNGK-Am (H318W), and Ac-KTVLHQDALNGK-Am (H318A). The model peptides were photo-irradiated for 20 minutes in oxygen-saturated water, pH 4.0, with $\lambda = 254$ nm, and subsequently analyzed with the LTQ-FT MS instrument. The resultant photoproduct yields are summarized in Table 4.1. The yields were measured by LTQ-FT signal intensity and shown as the relative intensity of the products divided by the intensity of the native parent ion. LTQ-FT signal intensity is not the best way to quantify peptides because this quantitation assumes all peptides are ionized (and therefore detected) at a similar level, but this is not always

	Photoproduct yield (%) for each peptide			
His modifications	**H293A**	**H293W**	**H318A**	**H318W**
His to Asn	1.0	0.5	1.3	0.2
His to Asp	-	0.4	0.4	0.4
His + 16	-	-	1.2	0.1
His + 48	-	-	3.2	-
Trp modifications				
Trp side chain cleavage (product **1**)	-	18.5	-	-
Kynurenine (Ky)	-	7.3	-	11.6
Hydroxytryptophan	-	13.8	-	15.8, 13.6
N-formylkynurenine (NFK)	-	5.3	-	18.8
Trp to Asp	-	-	-	1.6

Table 4.1. The relative intensity (by MS signal intensity) of the degradation photoproducts observed after irradiation of 100 μM model peptides at λ = 254 nm in water at pH 4.0.

a reasonable assumption. However, because we wanted to distinguish the oxidation of His from that of Trp and Tyr in our peptides, we needed high-resolution MS/MS data, which the LTQ-FT MS does provide. The MS data revealed that His was not oxidized to a great extent in any of the photo-irradiated model peptides, as was expected due to the low yields of His oxidation observed in mAb A. The H293A peptide showed only transformation of His to Asn in a 1% yield, whereas the H318A peptide showed modifications of His to Asn and Asp, and mono and tri-oxidation of His at yields of 1.3%, 0.4%, 1.2%, and 3.2%, respectively. The conversion of His into Asp and Asn has been reported previously.[22] The MS/MS characterization of the triply oxidized His residue in the H318A peptide will be described below. It was interesting to detect triply oxidized His after irradiation for the mutant H318A peptide because this was not the peptide modeled after the triply oxidized His in mAb A. Following photo-oxidation of the Trp-containing peptide H318W, a small yield of the His to Asn (0.2%) and Asp (0.4%) products, and mono-oxidized His was observed (0.1%). The H293W peptide did not show much His oxidation,

except the conversion of His to Asn (0.5%) and Asp (0.4%). Besides His oxidation, the Ala-containing peptides, H293A and H318A, were not efficiently photo-oxidized and did not show other degradation products. However, there was significant Trp oxidation in the Trp-containing peptides, H293W and H318W. The H318W peptide was most susceptible to photo-oxidation. Kynurenine (Ky), N-formylkynurenine (NFK), and two hydroxytryptophan products were detected in high yields: 11.6%, 18.8%, 15.8% and 13.6%, respectively. The two hydroxytryptophan products eluted at different retention times, but since they were isobaric in mass, the location of the hydroxyl group on the Trp could not be determined. Another uncommon Trp degradation product was observed in a 1.6% yield after H318W irradiation, the conversion of Trp to Asp. To our knowledge, this degradation product has not been reported during the photodegradation of peptides before, but evidence for conversion of Trp to Asp has been documented for the oxidant ruthenium (VIII) oxide.[23] The MS/MS spectrum of this product, compared to the control peptide is presented in Appendix C, Figures C.1 and C.2, respectively. Following irradiation, the H293W peptide was oxidized to Ky, hydroxytryptophan, and NFK in yields of 7.3%, 13.8%, and 5.3%, respectively. The yields of these Trp oxidation products were an order of magnitude higher than the His oxidation products. Interestingly, the largest yielding degradation product was not a common Trp oxidation product, but a Trp side chain cleavage product (with a yield of 18.6%), notated from here on as product **1**. More detailed characterization of product **1** and of the underlying reactions will be presented in Section 4.3.2.

The extracted ion chromatograms (XIC) of the H318A peptide and of its triply oxidized His product are shown in Figure 4.1. The non-modified model peptide, with m/z 1364.76, elutes at 6 minutes in both the control (Figure 4.1A) and the photo-irradiated sample (Figure 4.1B). Photo-irradiation leads to a new product, eluting at 7.6 minutes, with m/z 1412.76, i.e. a product

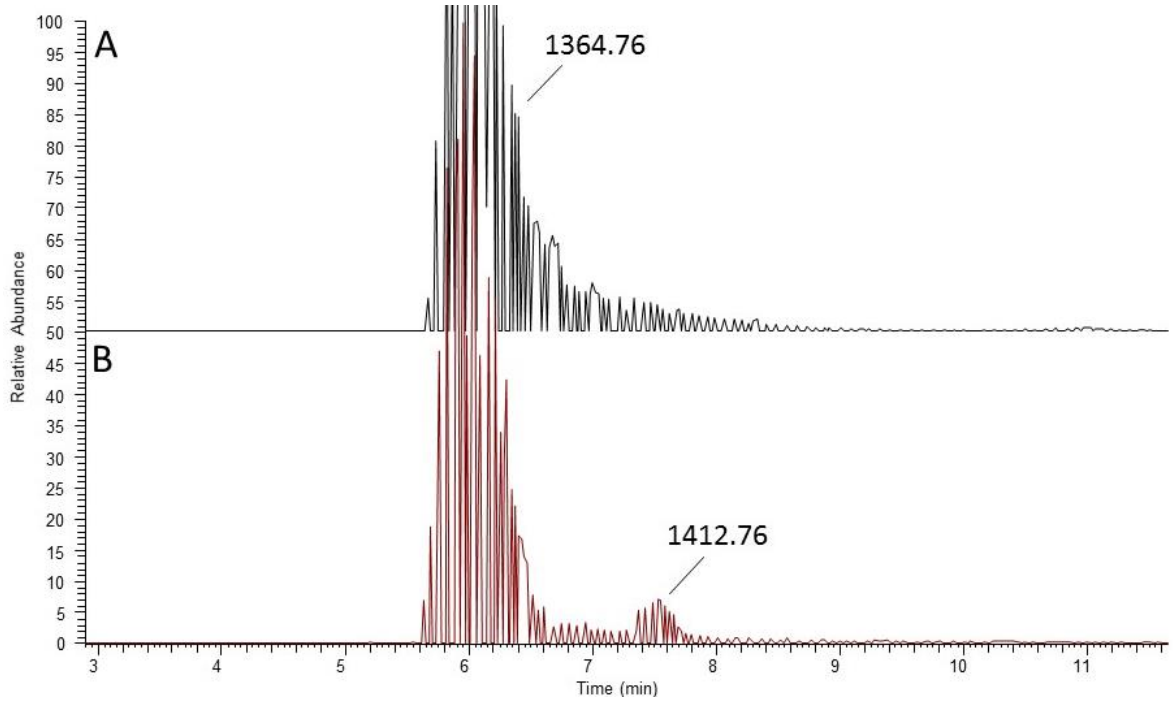

Figure 4.1. Extracted ion chromatograms (XIC) of the H318A model peptide in the (A) control and (B) irradiated sample (λ = 254 nm) in water at pH 4.0.

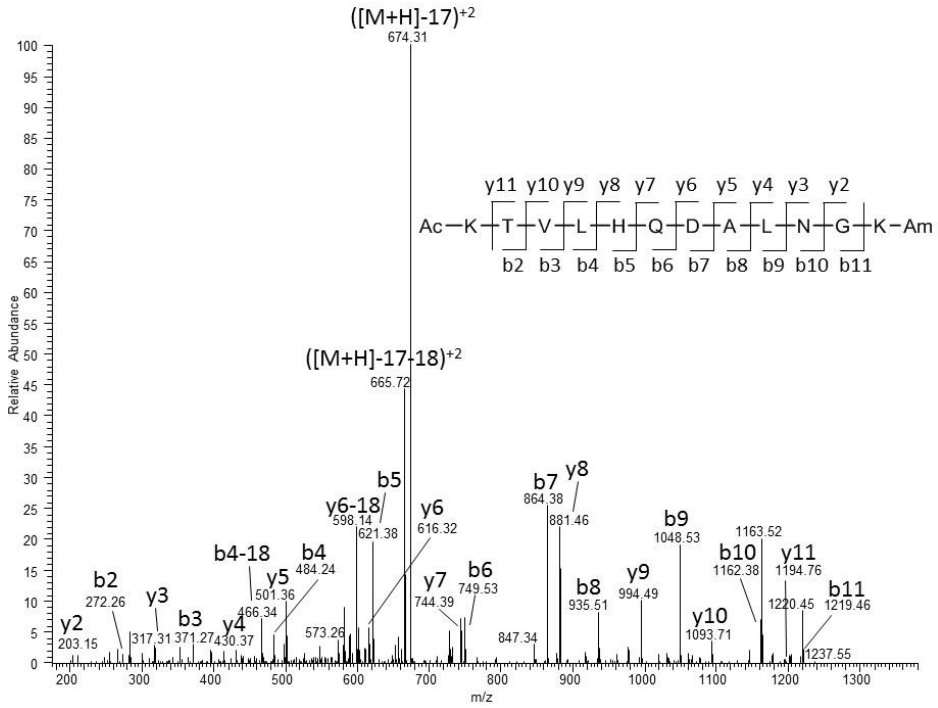

Figure 4.2. MS/MS spectrum of the control H318A model peptide.

48 Da heavier than the control peptide. The MS/MS spectrum of the control, non-modified H318A peptide is shown in Figure 4.2. The most intense fragment ion detected was the doubly charged $[M+2H]^{+2}$-17 ion, i.e. the molecular ion, which has lost one

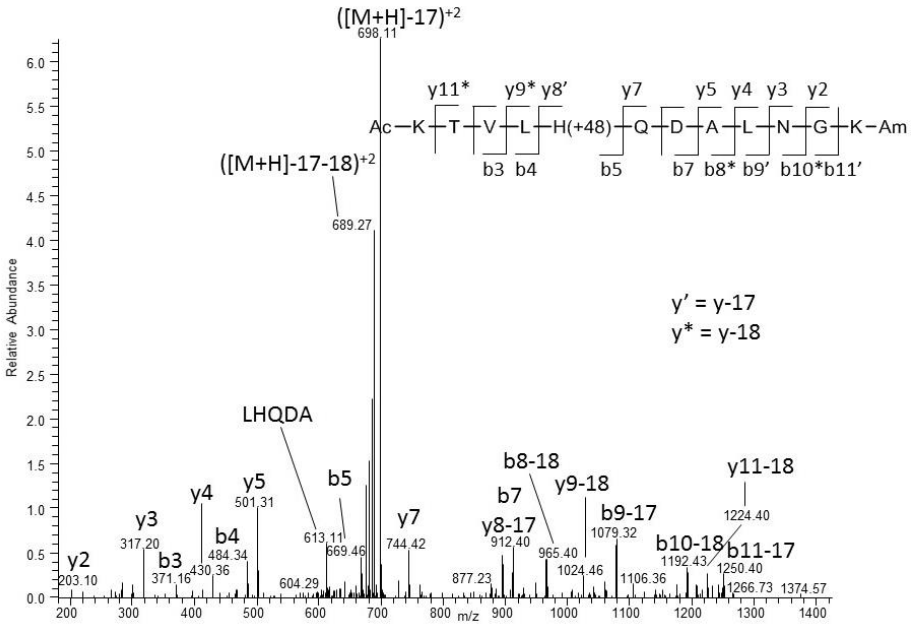

Figure 4.3. MS/MS spectrum of the triply oxidized H318A model peptide formed after irradiation of 100 μM H318A at λ = 254 nm in water at pH 4.0.

ammonia molecule. The b4, b5, y7, and y8 ions show no oxidation on the His residue. The MS/MS spectrum of the oxidized product (Figure 4.3) shows a similar high intensity fragment ion corresponding to the doubly charged $[M+2H]^{+2}$-17 ion. The b4 and y7 ions show no change in m/z values compared to the unmodified peptide, but the b5 and y8-17 ions, show an increase of 48 Da relative to the native, unmodified peptide, localizing the oxidation solely to the His residue. This spectrum was also shows that when the His is in the fragment ions (i.e. b5-b11 and y7-y11), neutral losses of water or ammonia were commonly observed.

4.3.2 Characterization of Product 1 Formation in H293W. Interestingly, by LC-MS analysis on the LTQ- FT instrument, the most prevalent product following photo-irradiation of H293W at λ = 254 nm was a product isobaric in mass to the native H293W peptide (product **1**). In the following, we will demonstrate that in product **1**, Trp is converted to Gly and the N-terminal Lys abstracts the resultant Trp side chain (3-methyleneindolenine, i.e. 3-MEI). The proposed structure is presented in Table 4.2.

Peptide	Product	Proposed product structure	MS/MS
H293W	Product **1**	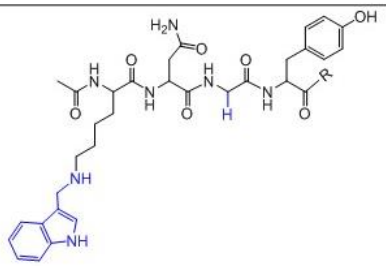	Figure 4.7

Table 4.2. Proposed structure of product **1**. R = VDGVE or VDGVEVHNAK-NH_2.

i. Glu-C Digestion of H293W and H293A. To first determine whether His or Trp was involved in product **1** formation, the two amino acids in peptide H293W were separated into two peptides after the photo-oxidation of H293W. The Glu-C enzyme is ideal for separating the His- and Trp-derived products after photo-irradiation because Glu-C cleaves preferentially C-terminal of Glu in ammonium bicarbonate buffer, i.e. C-terminal of the Glu residue located between Trp and His in H293W. Therefore, the H293W peptide (Ac-KNWYVDGVEVHNAK-NH_2; m/z 1699.8) was fragmented into two smaller peptides: Ac-KNWYVDGVE (m/z 1151.4) and VHNAK-NH_2 (m/z 567.4). Likewise, the H293A peptide (Ac-KNAYVDGVEVHNAK-NH_2; m/z 1584.8) was fragmented into two smaller peptides: Ac-KNAYVDGVE (m/z 1036.4) and VHNAK-NH_2 (m/z 567.4).

H293A and H293W were dissolved in water to a concentration of 100 μM at pH 4.0, saturated with O_2, and irradiated at $\lambda = 254$ nm for 20 minutes. The irradiated samples and control (non-irradiated) samples were adjusted to pH 7.8 with 50 mM ammonium bicarbonate buffer and digested with Glu-C overnight at 37 °C. The resultant products were then analyzed by LC-MS using the Q-tof Premier and MS/MS using the LTQ-FT instrument.

For clarity, Figure 4.4 shows the XIC of the control and photo-irradiated peptides H293W and H293A, displaying only the m/z values associated with the respective Ac-KNWYVDGVE sequences obtained by Glu-C digestion. The H293W control (Figure 4.4B) elutes at 9 minutes, and there is no other peak in the chromatogram; however, photo-irradiation

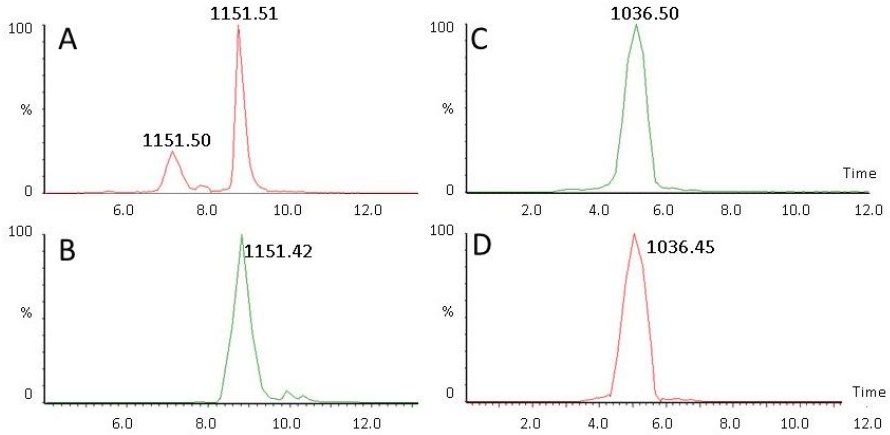

Figure 4.4. Extracted ion chromatograms (XIC) from model peptides before and after irradiation at λ = 254 nm in water at pH 4.0: (A) H293W after light exposure; (B) H293W control; (C) H293A after light exposure; (D) H293A control.

of H293W (Figure 4.4A) generates an additional peak eluting at 7 minutes (product **1**). MS analysis reveals that both peaks contain peptides with identical m/z values, i.e. the new peak eluting at 7 minutes appears to be an isobaric product. (Note: An isobaric product in mass spectrometry is defined as atomic or molecular species with the same nominal mass but different exact masses.[24,25]) Figures 4.4D and 4.4C show the XIC of control and photo-irradiated H293A, respectively. Both chromatograms contain only one peak that elutes at 5 minutes, with the expected m/z value for the Ac-KNWYVDGVE sequence. The VHNAK-NH_2 sequence of the digested H293W and H293A peptides eluted at ca. 3.8 minutes in the LC-MS (data not shown). A comparison between the Glu-C digested peptides H293W and H293A shows that the product **1** is derived from Trp. When Trp was replaced by Ala, no isobaric product was observed. The MS/MS analysis of the native Ac-KNWYVDGVE peptide eluting at 9 minutes and product **1** eluting at 7 minutes in Figure 4.4A are shown in Appendix C, Figures C.3 and C.4, respectively.

*ii. Kinetics of Product **1***

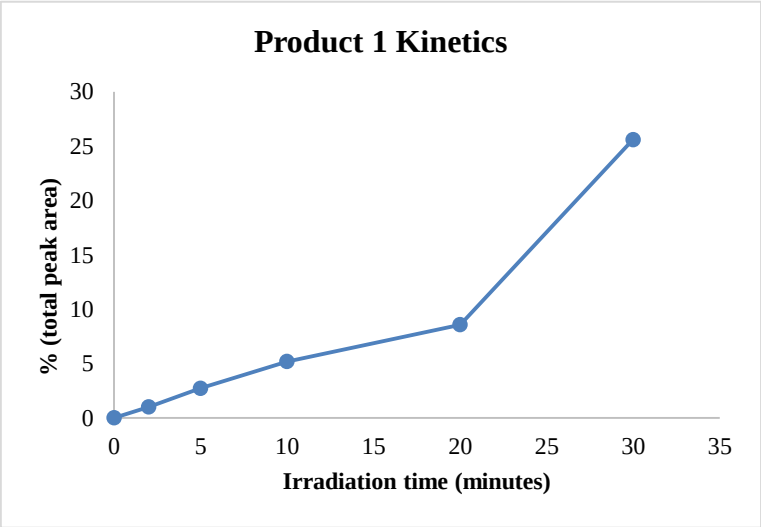

Figure 4.5. Kinetics of the product **1** formation after irradiation of H293W at λ = 254 nm in water at pH 4.0 for up to 30 minutes as measure by peak area in the total chromatogram.

Formation. After confirming that Trp was the amino acid involved in product **1** formation, experiments were then conducted without the use of Glu-C digestion. Although the Glu-C digest worked to separate the His and Trp into two peptides after photo-oxidation, it was an unnecessary, cost-prohibitive step in the analysis after the initial experiment to determine whether His or Trp was the amino acid involved in product **1** formation.

H293W was photo-irradiated at λ = 254 nm in water at pH 4.0 for up to 30 minutes after O_2-saturation. The samples were then analyzed by LC-MS/MS using the Q-tof Premier instrument. Figure 4.5 shows the kinetics of product **1** formation as the yield increases in a biphasic mode, a slower process between 0 and 20 minutes, and a faster process after 20 minutes, to a yield of about 25% within 30 minutes. For the rest of our experiments, we chose to photo-irradiate the peptide for 20 minutes, where about 10% of H293W were converted to product **1**. The MS/MS spectra obtained from the Q-tof Premier of the control H293W peptide and product **1** is presented in Figures 4.6 and 4.7, respectively. Both spectra were enlarged by 2-fold for clarity because the His and Lys immonium ions were of greater intensity than the other m/z ions. The spectra of the control peptide (Figure 4.6) shows all the fragment ions associated with unmodified amino acids, and specifically, all the fragments on the N-terminal portion of the

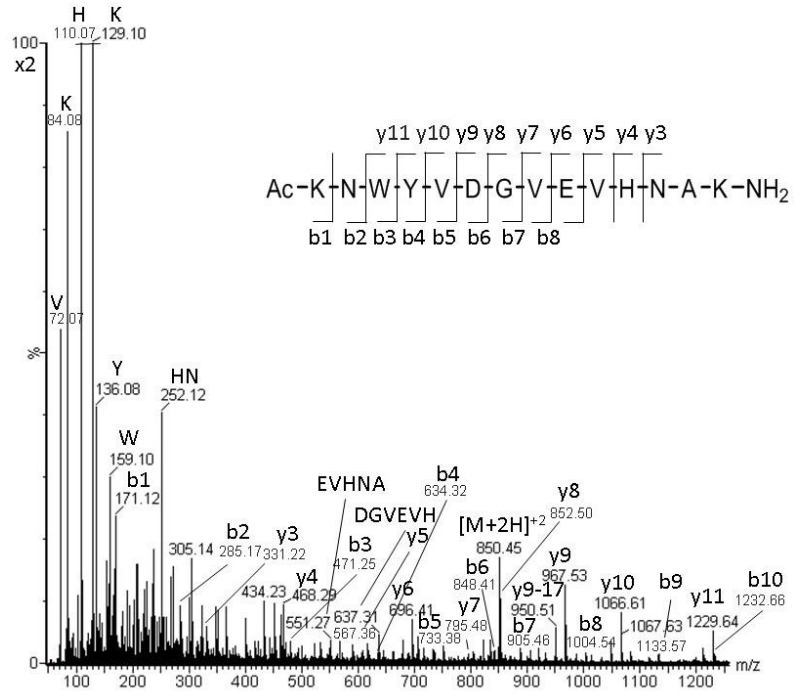

Figure 4.6. MS/MS spectrum of the control H293W peptide.

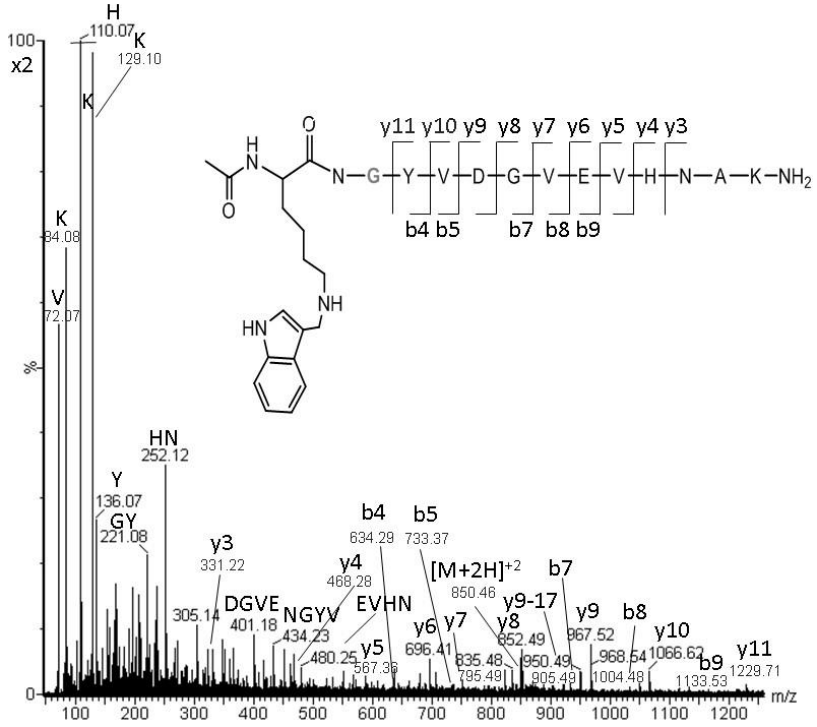

Figure 4.7. MS/MS spectrum of product **1** generated by the irradiation of 100 µM H293W at λ = 254 nm in water at pH 4.0.

peptide: b1, b2, b3, and b4. Importantly, the Trp immonium ion is observed with m/z 159.10. Figure 4.7 displays the MS/MS spectrum of product **1**, which looks very similar to the MS/MS spectrum of the control H293W peptide, except for the absence of the b1, b2, or b3 ions and the Trp immonium ion. Instead, internal fragment ions corresponding to GY and NGYV (m/z 434.23) were observed. Since there was initially no sequential GY in the peptide sequence, we can assume this fragmentation ion is indicative of the Trp side chain cleavage and conversion to a Gly residue, however the m/z 434.23, assigned to the NGYV sequence, is observed in the MS/MS spectrum of the control peptide,

so this ion could have a different structure. The MS/MS spectrum in Figure 4.7 is not clearly indicative of the Trp side chain cleavage since no b ions were observed supporting the movement of the Trp side chain, just the absence of b ions. However the differences between the MS/MS spectra in product **1** compared to the control H293W peptide were significant enough for us to form the hypothesis that the Trp side chain was cleaved, Gly formed in its place, and Lys trapped the resultant Trp side chain.

iii. Tryptic Digestion of H293W. To determine if the N-terminal Lys had indeed trapped the Trp side chain, we wanted to separate the N-terminal Lys from the rest of the peptide by tryptic digestion. If the Trp side chain is connected to the N-terminal Lys amine group, trypsin will most likely not recognize the amino acid as a substrate and no Lys cleavage will occur in product **1**. Conversely, if the N-terminal Lys does not contain the Trp side chain (like the control, non-irradiated), the Lys group in product **1** will be cleaved during the digestion. The tryptic digestion was accomplished with two different sources of trypsin: sequencing grade from Promega and non-sequencing grade from Sigma-Aldrich. The trypsin from Sigma-Aldrich also contained chymotryptic activity, therefore cleaving C-terminal of the Lys and Tyr, Trp, and His residues, adding complexity to the analysis.

Following the irradiation of the H293W peptide, the pH of the solution was adjusted to pH 7.8 with ammonium bicarbonate buffer. Trypsin (both types) was added to samples in a 1:20 enzyme to protein ratio and incubated at 37 °C for four hours. Figure 4.8 shows the LC-MS of the control (non-irradiated) H293W peptide (Figure 4.8A), the irradiated sample (Figure 4.8B), and the irradiated sample after digestion with the Promega trypsin (Figure 4.8C). Figure 4.8A only contains one peak with the doubly charged ion m/z 850.40^{+2} at 20 minutes associated with the control H293W peptide. In Figure 4.8B, the native peptide elutes around 21.5 minutes,

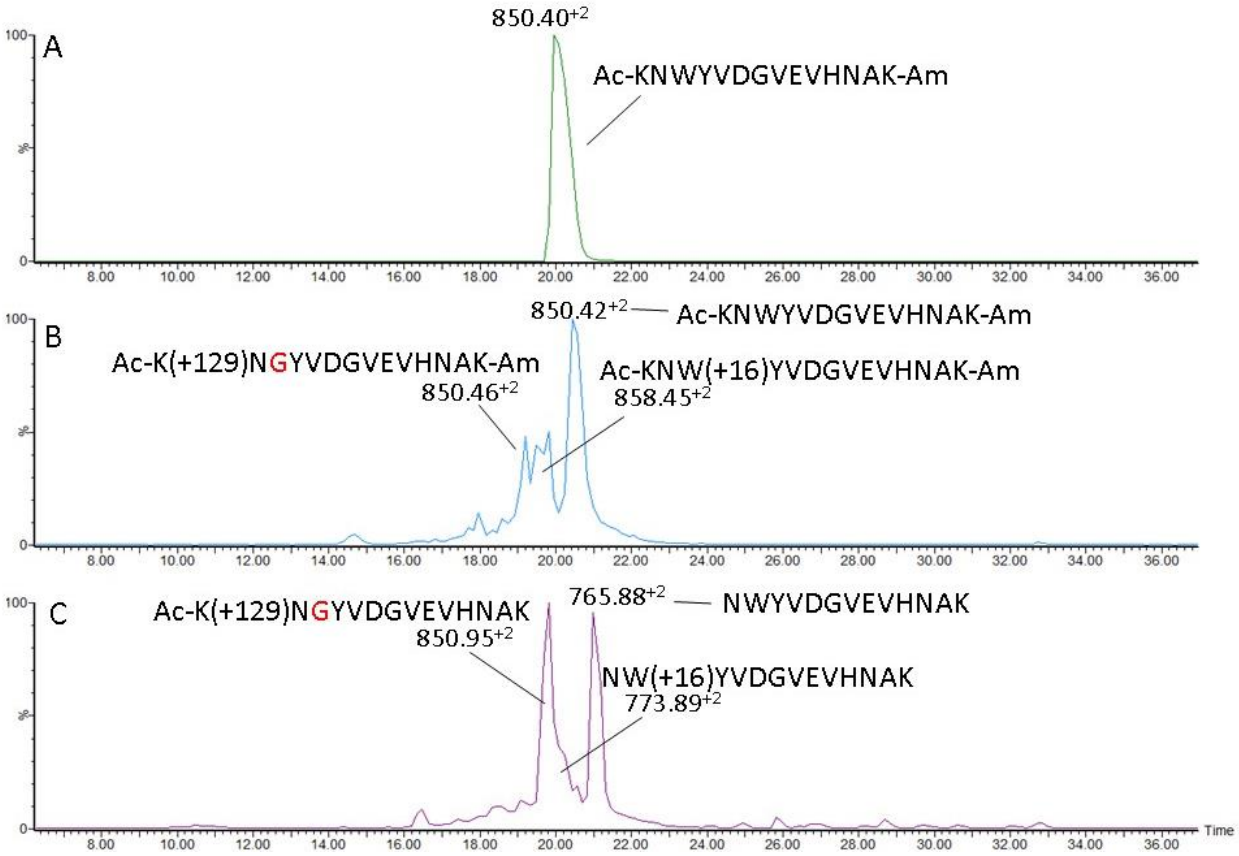

Figure 4.8. LC-MS chromatogram of the H293W peptide (A) control; (B) irradiated sample; (C) irradiated sample after tryptic digestion.

although the MS/MS spectrum is identical to that of the control. In addition, three new peaks elute at 19.2, 19.5, and 19.8 minutes. The peak at 19.2 minutes corresponds to product **1**, and the peaks at 19.5 and 19.8 minutes correspond to Trp mono-oxidation products. Figure 4.8C shows the LC-chromatogram after trypsin digestion, where there are no longer any isobaric products observed. Now, there are only two major peaks, and a shoulder on the first peak. The first peak elutes at 19.8 minutes with a m/z 850.95^{+2}, a gain of 1 Da compared to the native H293W peptide, corresponding to deamidation of the amidated C-terminal. The shoulder on the first peak contains ions with m/z 773.89^{+2}, corresponding to the mono-oxidation of the Trp residue, cleavage of the N-terminal Lys, and deamidation. The second peak, eluting at 21.2 minutes, contains a product with a m/z of 765.88^{+2}. This m/z value corresponds to the cleavage of the N-

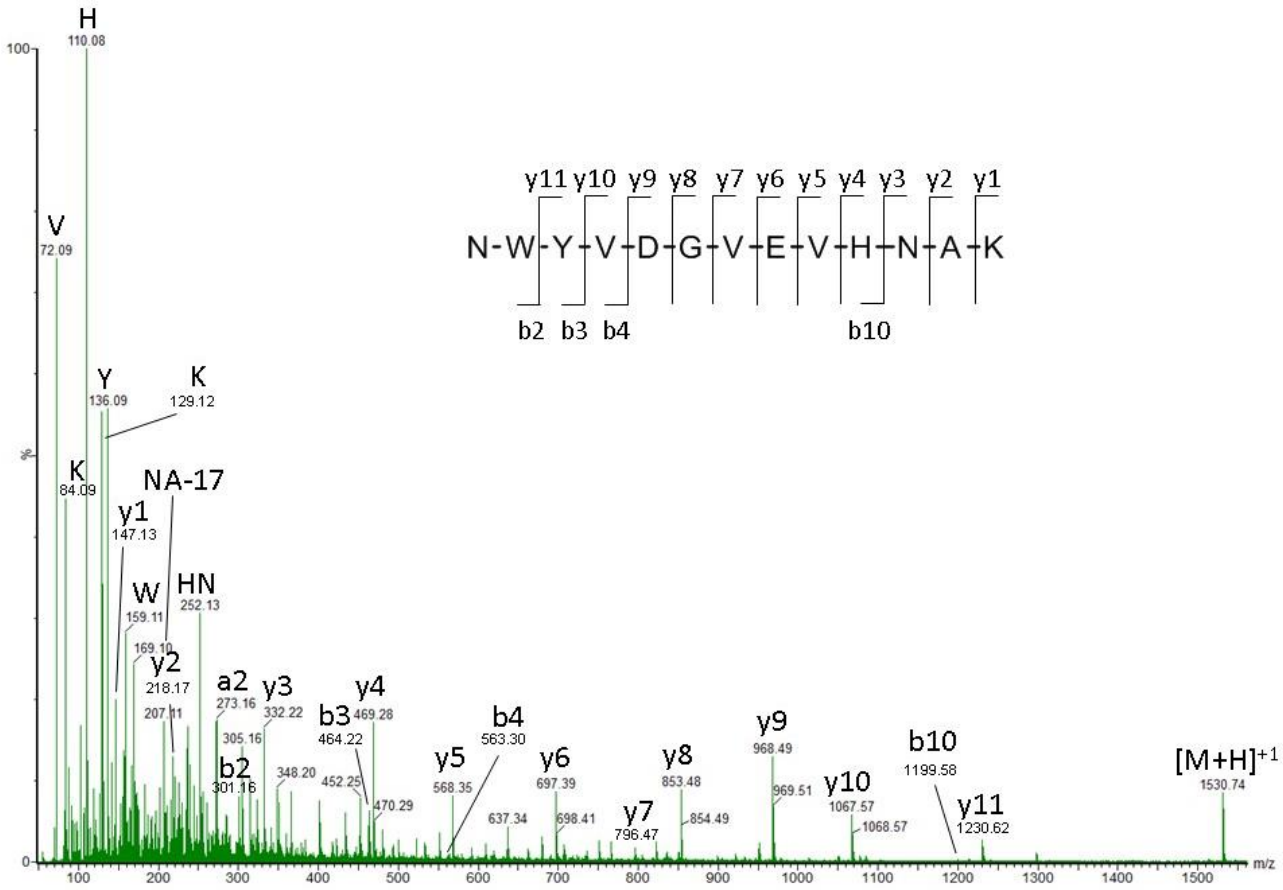

Figure 4.9. MS/MS spectrum of the m/z 765.88^{+2} peak observed after the digest of the irradiated H293W peptide, and corresponding to the native H293W peptide.

terminal Lys and deamidation of the native H293W peptide. The MS/MS spectrum of the m/z 765.88^{+2} product eluting at 21.2 minutes is displayed in Figure 4.9. The fragmentation ions are indicative of an unmodified H293W peptide with no N-terminal Lys or C-terminal amine group, the product expected from a tryptic digest. Although no b1 ion is observed, the Trp immonium ion is detected (m/z 159.11), as observed in the control H293W peptide spectrum in Figure 4.6. The MS/MS spectrum of the m/z 850.95^{+2} product eluting at 19.8 minutes is displayed in Figure 4.10. Importantly, the observed b1 ion (m/z 300.13) matches the predicted m/z value of a Lys residue attached to 3-methyleneindolenine (3-MEI), i.e. the Lys attached to the Trp side chain, as is the predicted structure of product **1**. The rest of the fragment ions match closely to the MS/MS spectrum observed in non-digested product **1** (Figure 4.7), except with the addition of 1 Da to all

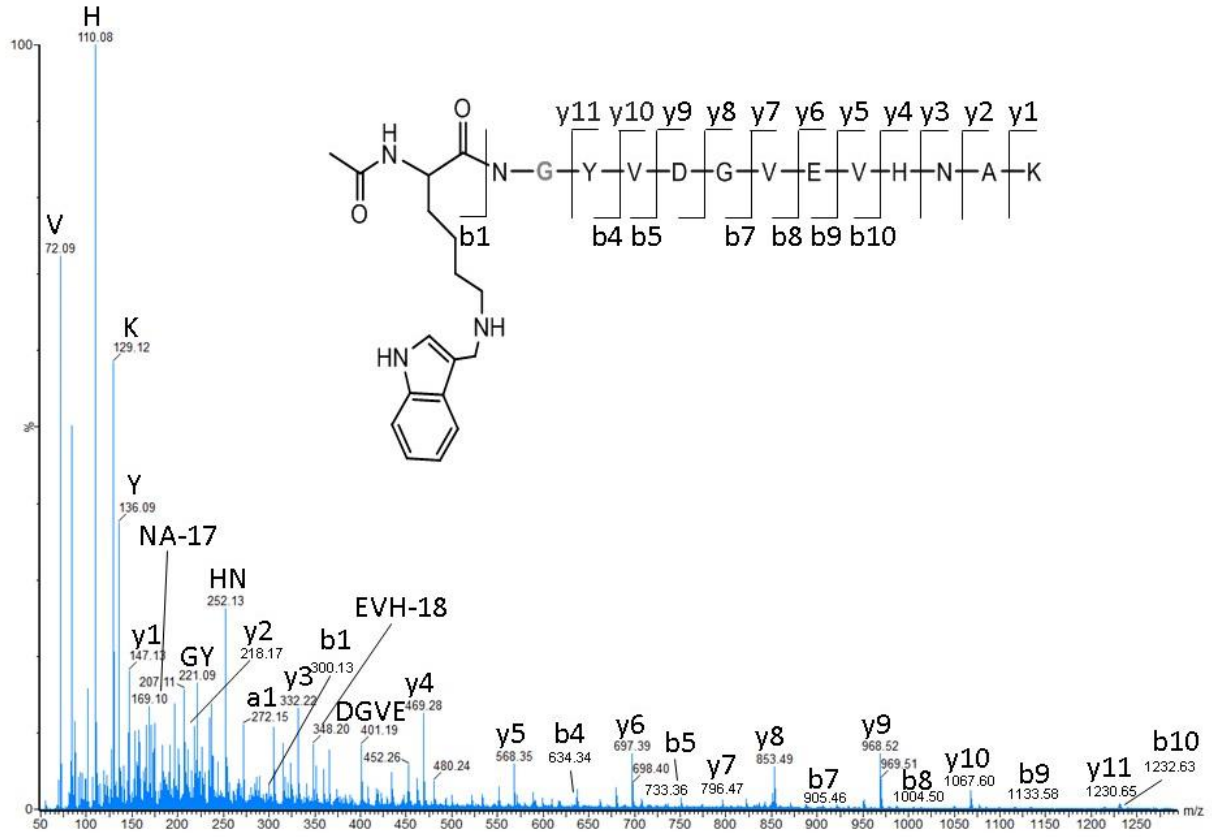

Figure 4.10. MS/MS spectrum of the m/z 850.95^{+2} peak observed after the digest of the irradiated H293W peptide, and corresponding to the tryptic digest of product **1**.

the y-ions because of the C-terminal deamidation. The inability of the trypsin to digest the isobaric product, along with the b1 ion corresponding to Lys attached to 3-MEI was enough evidence to conclude that during the photo-oxidation of H293W, the Trp side chain was cleaved and trapped with the N-terminal Lys residue in product **1**. The tryptic digest using the Sigma-Aldrich trypsin showed similar results, except many other chymotryptic fragments were observed, so it is presented and explained in Figure C.5.

iv. Trapping 3-methyleneindolenine (3-MEI) with Oxidized L-glutathione (GSSG). To trap the resultant Trp side chain, 3-MEI, before the Lys amine can react with it and form product **1**, oxidized L-glutathione (GSSG) was added to the H293W sample prior to irradiation at λ = 254 nm. 100 µM oxidized glutathione was added in a 1:1 ratio with the H293W peptide. The

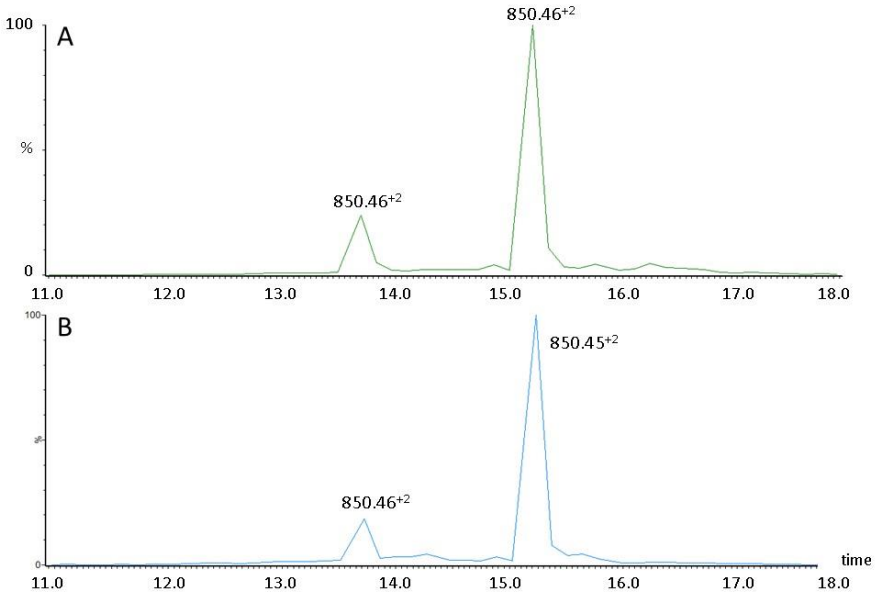

Figure 4.11. Extracted ion chromatograms (XIC) from H293W peptides (A) after irradiation at λ = 254 nm in water at pH 7.0 and (B) after irradiation with GSSG at λ = 254 nm in water at pH 7.0.

sample was then saturated with oxygen, irradiated at pH 7.0 in water for twenty minutes, and then frozen at -20 °C until mass spectrometry analysis. The sample was irradiated at pH 7.0 so the equilibrium was shifted towards the nucleophilic thiolate species. Figure 4.11 shows the XIC of the products with m/z 850.46^{+2}, i.e. the native H293W peptide and product **1**. Figure 4.11A displays the H293W peptide after irradiation, and Figure 4.11B displays the H293W peptide after irradiation with GSSG. Both XIC chromatograms look nearly identical, and there was no trace of m/z 437.4, the m/z value corresponding to the 3-MEI trapped with reduced L-glutathione, as was observed in experiments in Chapter 3, Section 3.3. Since this trapping experiment was unsuccessful, we assumed that the *intra*molecular isobaric product formation was much quicker than an *inter*molecular reaction. Another possible reason this trapping experiment was not successful is due to the presence of O_2 during the photolytic reaction. The reaction should have been done in Ar so O_2 would not react with the photolytically generated thiyl radicals and Trp radical cations, inhibiting the formation and reaction of 3-MEI with glutathione.

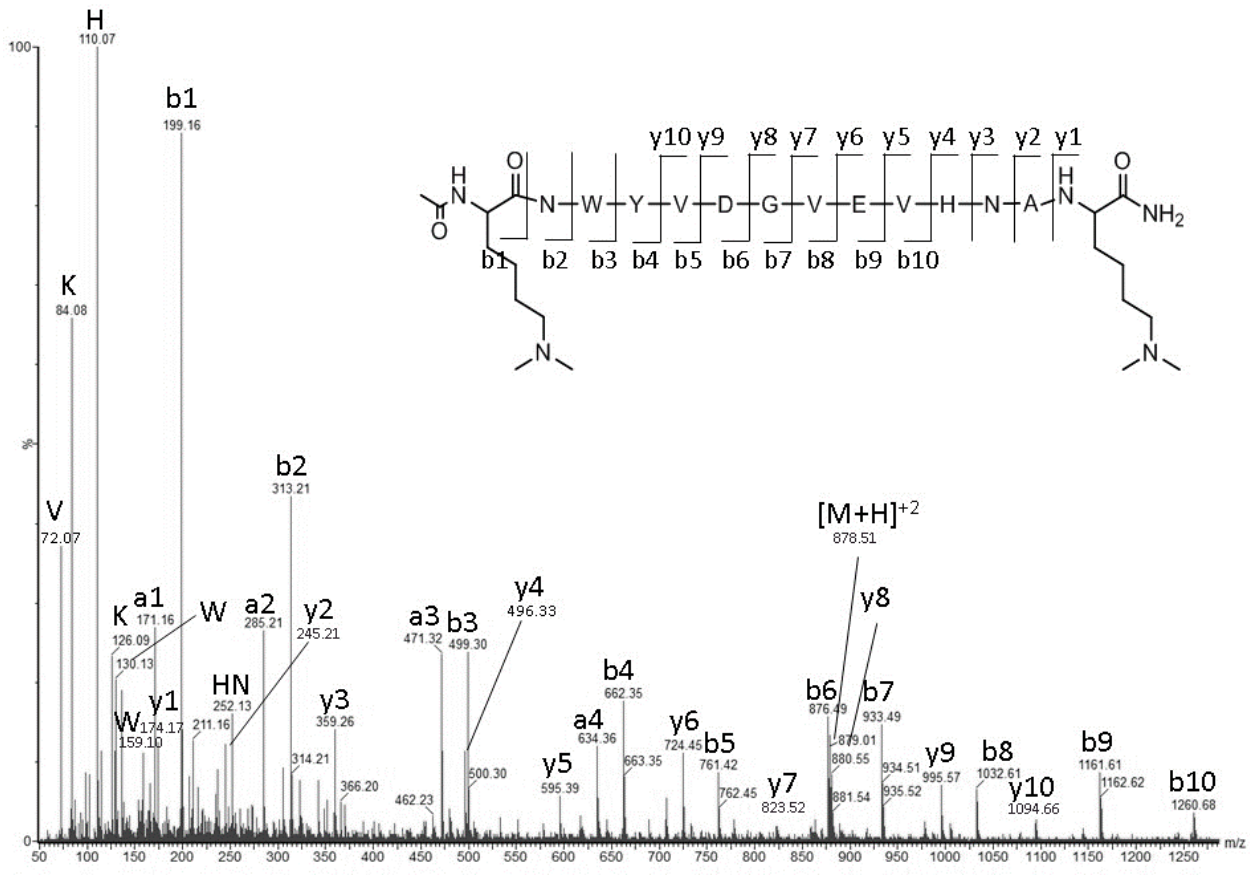

Figure 4.12. MS/MS spectrum of the control H293W$_K$ peptide.

v. Blocking the H293W Lys Amine Reactivity by Methylation. To inhibit the formation of product **1,** the Lys amines were di-methylated to block their nucleophilic propensity. In separate experiments, following the photolysis of H293W and subsequent formation of product **1**, the samples were also methylated. In this case, methylation of the N-terminal amine in product **1** was unexpected, as the 3-MEI group on the N-terminal Lys should inhibit the Lys group from reacting with the methylation reagents.

Both Lys residues in the H293W peptide were di-methylated prior to irradiation using a reductive alkylation method with formaldehyde and sodium borohydride, thus increasing the molecular weight of the peptide by 56 Da. This H293W peptide derivative will be labeled as H293W$_K$ in the following sections. Figure 4.12 shows the MS/MS spectrum of the control H293W$_K$ peptide, with m/z 1755.96^{+1}/878.48^{+2}. The b1 ion now shows an increase in 28 Da

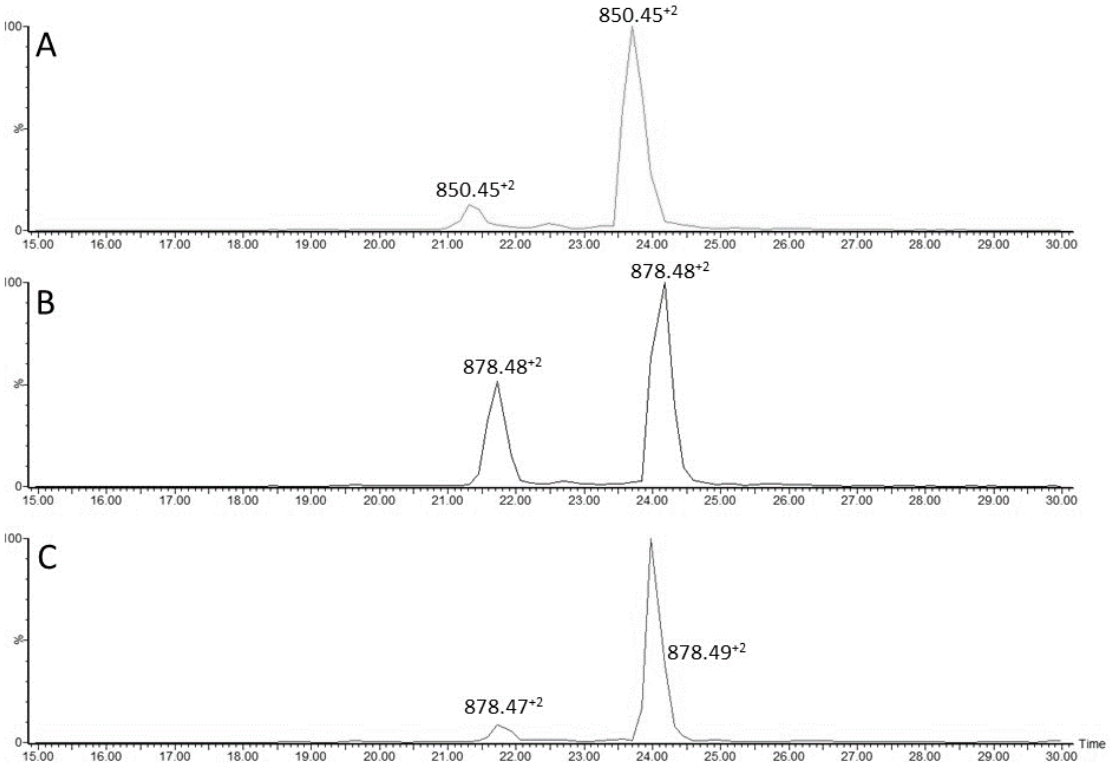

Figure 4.13. Extracted ion chromatograms (XIC) from (A) H293W after irradiation; (B) $H293W_K$ after irradiation and (C) H293W after irradiation, then methylation.

compared to the original b1 ion in the H293W peptide (Figure 4.6), confirming methylation on the N-terminal Lys residue. Likewise, the m/z value of the y1 ion also corresponds to an increase of 28 Da compared to the b1 ion of the unmodified C-terminal Lys in H293W. The rest of the b and y ions in $H293W_K$ are consistent with unmodified residues on the interior of the peptide.

The $H293W_K$ peptide and the H293W peptide were dissolved in water to a concentration of 100 μM at pH 4.0, saturated with O_2, and irradiated at $\lambda = 254$ for 20 minutes. Then, after irradiation, an aliquot of the H293W sample was methylated under the same methylation conditions as mentioned above. The resultant products were then analyzed by LC-MS/MS using the Q-tof Premier.

Figure 4.13 shows the XIC of m/z 850.5^{+2} for the H293W peptide after irradiation (Figure 4.13A), the XIC of m/z 878.5^{+2} for the $H293W_K$ peptide after irradiation (Figure 4.13B),

Peptide	Product	Proposed product structure	MS/MS
$H293W_K$	Product **2a**	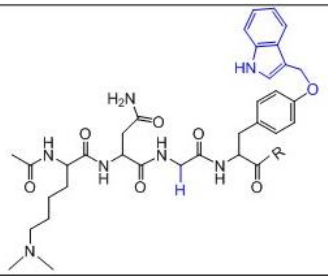	Figure 4.14
$H293W_K$	Product **2b**	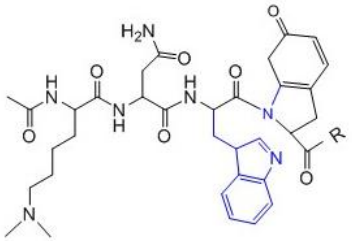	Figure 4.14

Table 4.3. Proposed structures of product **2a** and **2b**. R = VDGVEVHNAK-NH_2.

and the XIC of m/z 878.5^{+2} for the H293W peptide after irradiation, then methylation (Figure 4.13C). In all the spectra, the native, unmodified peak elutes at ca. 24 minutes, and an isobaric product elutes ca. 2 minutes earlier, at 22 minutes. We expected product **1** to appear during the irradiation of the H293W peptide, but it was unexpected to see an isobaric product, from here on notated as product **2a/2b**, in Figure 4.13B, when the Lys residues were methylated before irradiation. Table 4.3 shows the proposed structures of products **2a** and **2b**. Furthermore, the peak area of product **2a/2b** in Figure 4.13B was three times more (ca. 30%) than the peak area of product **1** (ca. 10%) in Figure 4.13A, although the samples were irradiated for the same amount of time at similar concentrations. Interestingly, when the H293W peptide was first irradiated, forming product **1**, followed by methylation (Figure 4.13C), product **2a/2b** (m/z 878.47^{+2}) was detected, not product **1** (m/z 850.45^{+2}). We expected the 3-MEI attached to the N-terminal Lys in product **1** to inhibit the reactivity of the methylation reagents towards the N-terminal Lys, however, this was not observed. When the MS/MS spectra of product **2a/2b** from both Figure

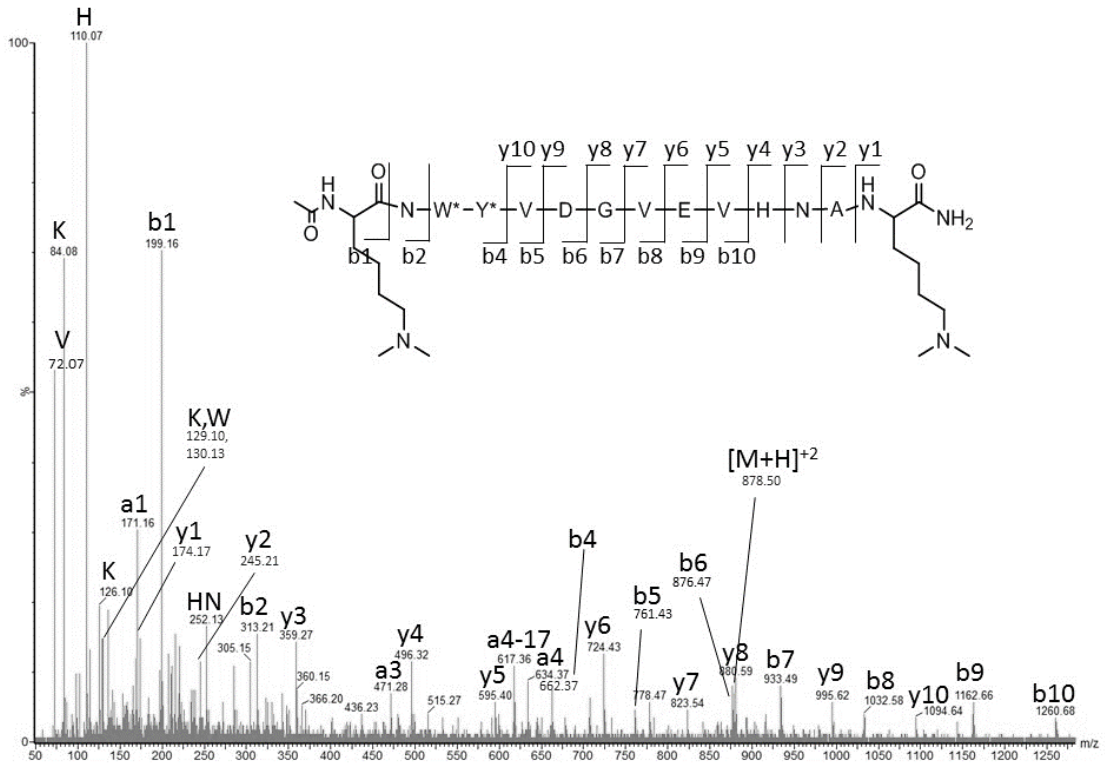

Figure 4.14. MS/MS spectrum of product **2a/2b**. The W* and Y* represent modified Trp and Tyr residues consistent with either product **2a** or **2b**.

4.13B and Figure 4.13C were compared to each other and to the control H293W$_K$ peptide (Figure 4.12), the MS/MS spectra of product **2a/2b** was similar between the two experiments, and dissimilar to the control H293W$_K$ peptide. Figure 4.14 shows the MS/MS spectrum of the product **2a/2b** generated after the irradiation of the H293W$_K$ peptide. The y fragmentation (through y10) is identical to that of the native, unmodified peptide (Figure 4.18), and the b1 and b2 ions are consistent with no 3-MEI addition to the Lys, but there is one ion missing from the b ion fragmentation: the b3 ion. The lack of the b3 ion suggests that either the Tyr hydroxyl group abstracted the Trp side chain (product **2a**) or a crosslink between the Trp and Tyr residues has formed (product **2b**), however, we cannot distinguish between the two structures in this experiment, so both structures are presented. The presence of product **2a/2b** after the Lys amines were blocked suggests that the Trp side chain is still cleaved, but since it cannot be trapped by

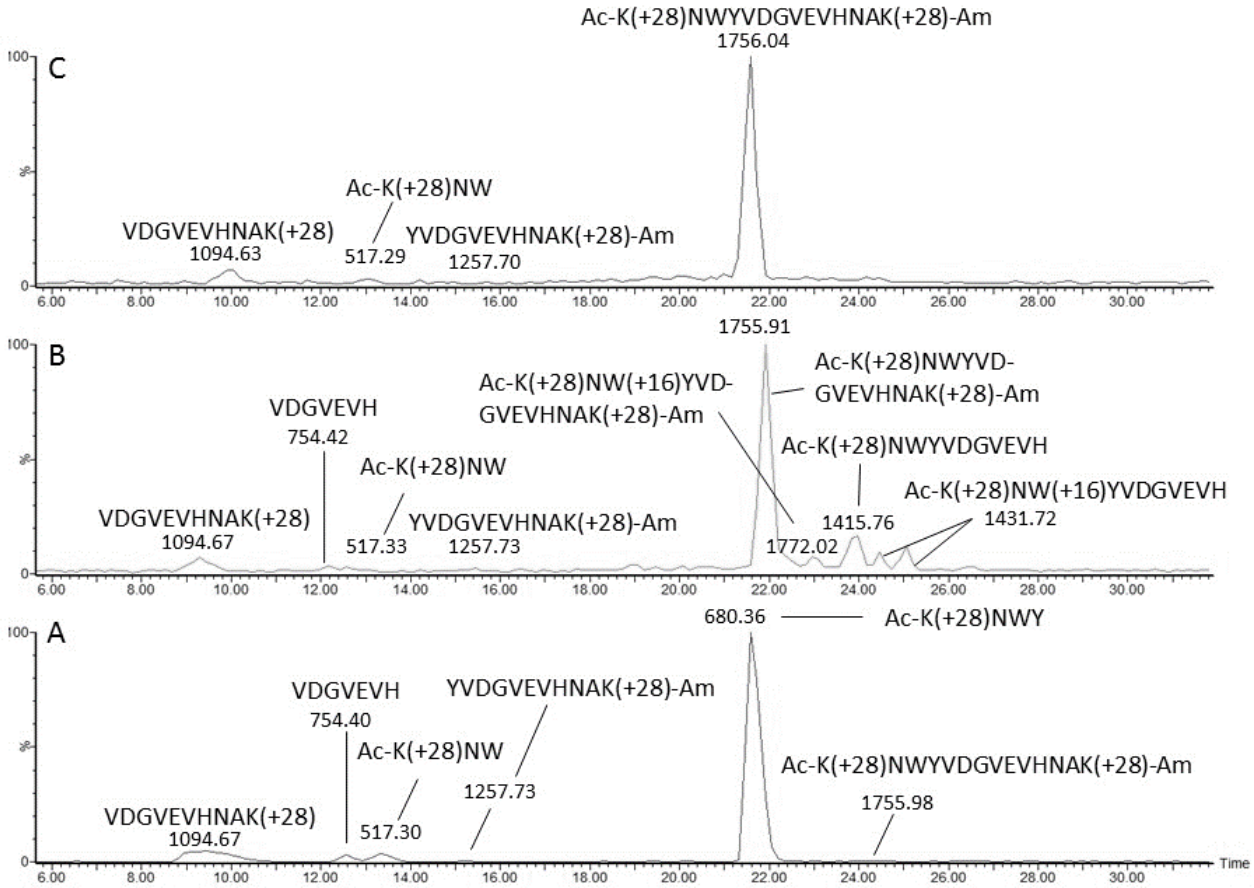

Figure 4.15. LC-MS of the tryptic/chymotryptic digest for the (A) $H293W_K$ control (non-irradiated); (B) irradiated $H293W_K$; and (C) irradiated H293W, followed by methylation.

the Lys side chain, another pathway is favored. This second pathway forming product **2a/2b** was always a possibility, as evidenced by the fact that we observed product **2a/2b** when the H293W peptide was first irradiated, then reductively alkylated (Figure 4.13C), however the Lys amine is a better nucleophile than the Tyr hydroxyl group, so product **1** is favored when the Lys is freely available.

vi. Chymotryptic Digestion of $H293W_K$. To confirm the involvement of the Tyr residue in product **2a/2b**, the irradiated $H293W_K$ peptide was digested with the Sigma-Aldrich trypsin that contained chymotryptic activity. Therefore, if the photolytically cleaved Trp side chain is connected to the Tyr hydroxyl group or if there is a crosslink between the Trp and Tyr, the chymotrypsin will most likely not recognize the modified Tyr as a substrate and no C-terminal

Tyr cleavage will occur. Conversely, if the Tyr is not involved, (like the control, non-irradiated peptide) the C-terminal cleavage of the Tyr group in product **2a/2b** will occur during the digestion.

The control H293W_K peptide, irradiated H293W_K sample, and the irradiated H293W sample followed by methylation were all digested with chymotrypsin. First, the pH of the samples was adjusted to pH 7.8 with ammonium bicarbonate buffer, then trypsin was added to the samples in a 1:20 enzyme to protein ratio and incubated at 37 °C for four hours.

Figure 4.15 shows the LC-MS of the chymotryptic digest for the control H293W_K peptide (Figure 4.15A), the irradiated H293W_K sample (Figure 4.15B), and the irradiated H293W peptide followed by Lys methylation (Figure 4.15C). No tryptic peptides were observed, just chymotryptic peptides, since the Lys residues were methylated, and the enzyme did not recognize the modified Lys residues as substrates. This lack of tryptic digestion is further evidence for the product **1** structure to contain the Lys-3-methyleneindolenine crosslink proposed in Table 4.2. The largest peak in the LC-MS for the control H293W_K peptide (Figure 4.15A) was the Ac-K(+28)NWY peptide peak, m/z 680.36, where the '+28' indicates the double methylation of the Lys residues. The other chymotryptic peaks present in Figure 4.15A were VDGVEVHNAK(+28) (m/z 1094.67), VDGVEVH (m/z 754.40), Ac-K(+28)NW (m/z 517.30), and YVDGVEVHNAK(+28)-Am (m/z 1257.73). There was also a trace of the undigested control H293W_K peptide at 24.2 minutes, where it eluted in the non-digested control (Figure 4.13B and C). Following the digest of the irradiated H293W_K sample (Figure 4.15B), and the irradiated H293W peptide followed by irradiation (Figure 4.15C), the largest peaks in the chromatogram were again at 21.5 minutes, but the MS/MS spectra did not match that of Ac-K(+28)NWY (m/z 680.36). Instead, the main fragment ions in the chromatogram for Figure

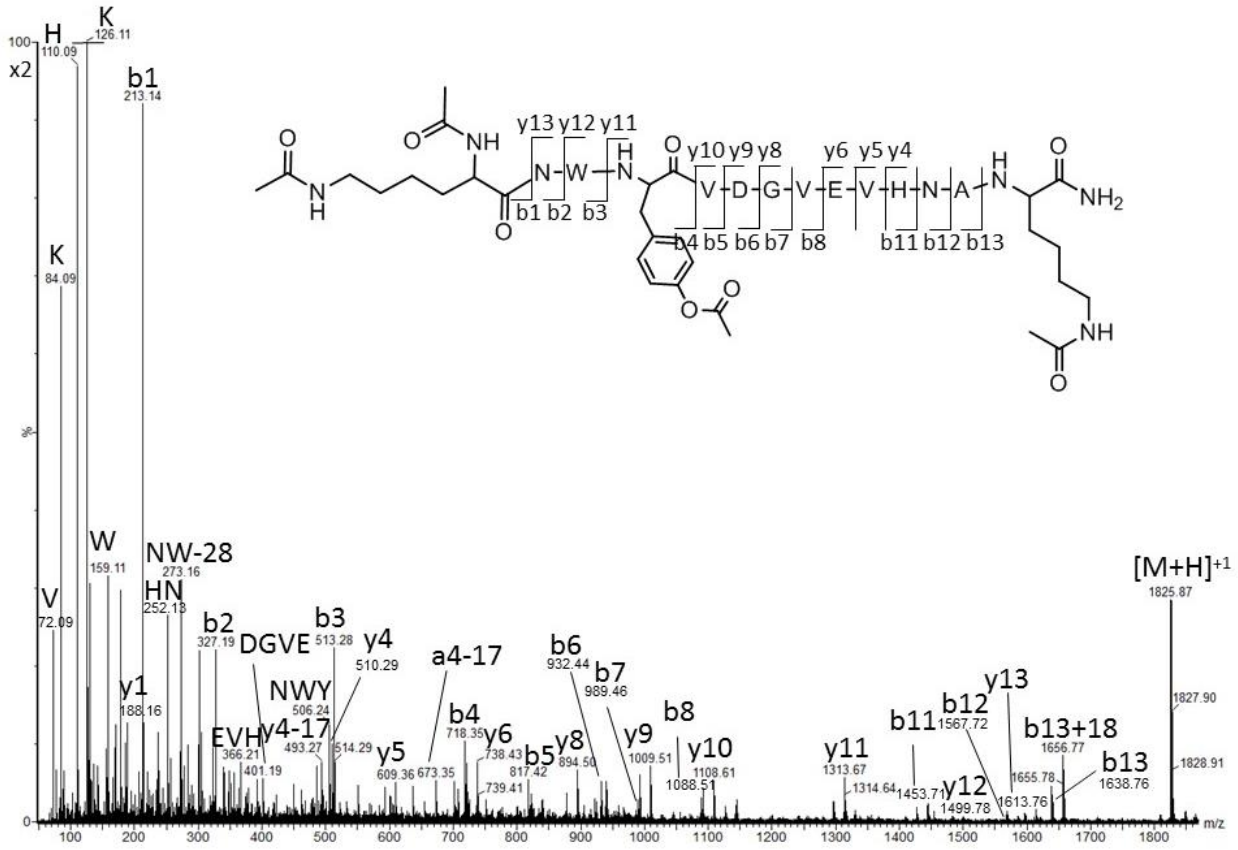

Figure 4.16. MS/MS spectrum of the control H293W_{KY} peptide.

4.21B and C were m/z 1755.91 and m/z 1756.04, respectively. Furthermore, both MS/MS fragmentation patterns matched that of the control H293W_K peptide, although the control H293W_K peptide elutes at 24.5 minutes and product **2a/2b** elutes at 22 minutes. The absence of m/z 680.36 in the irradiated, methylated samples (Figure 4.15B and C) indicates that chymotrypsin did not recognize the Tyr as a substrate like it did in the control (Figure 4.15A), thereby not cleaving the peptide C-terminal to the Tyr residue: Ac-K(+28)NWY. However, the other chymotryptic peaks (m/z 1094.6, m/z 754.4, m/z 517.3, and m/z 1257.7) observed in the control were also observed after irradiation. In addition, peaks corresponding to the oxidation of the Trp residue were also observed in Figure 4.15B (m/z 1772.02 and m/z 1431.72), along with chymotryptic cleavage C-terminal to the His residue (m/z 1415.76).

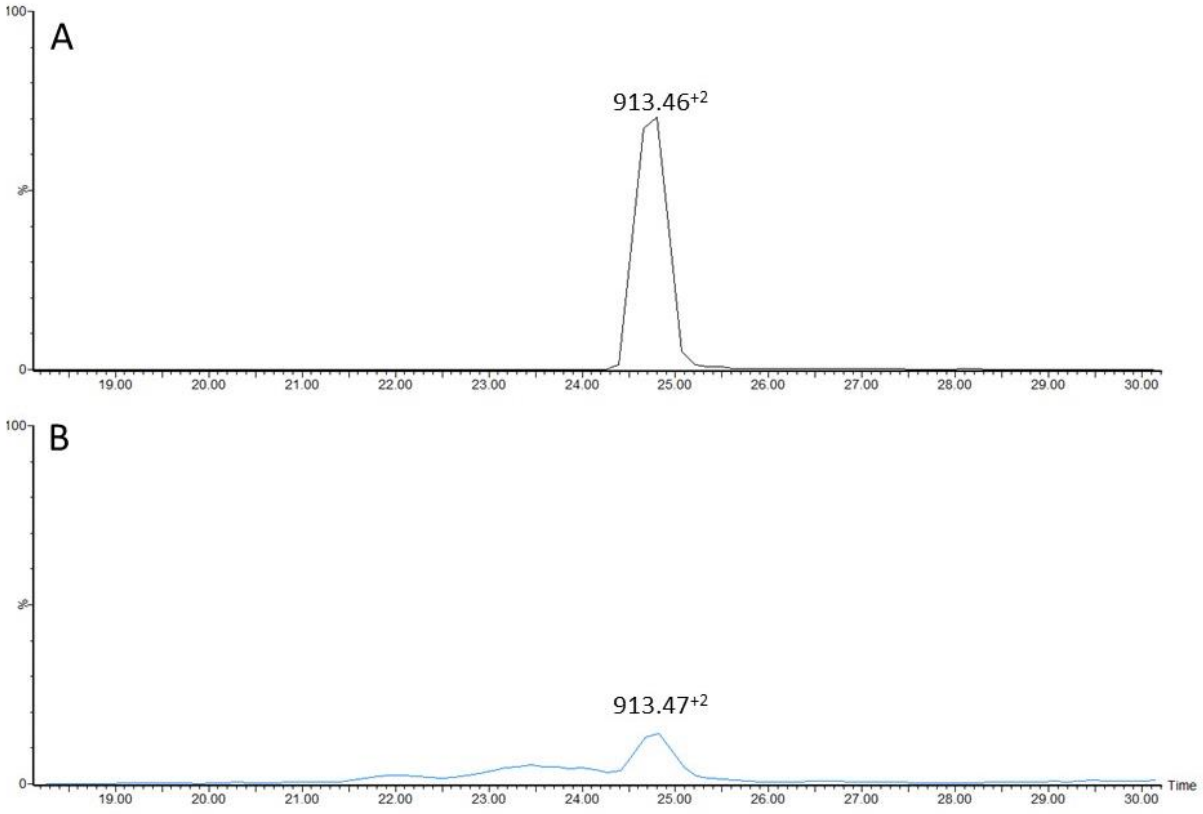

Figure 4.17. Extracted ion chromatograms (XIC) from (A) control H293W$_{KY}$ and (B) H293W$_{KY}$ after irradiation.

vii. Blocking the H293W Lys Amine and Tyr Hydroxyl group Reactivity by Acetylation.

To further confirm the Tyr involvement in product **2a/2b** after irradiation of H293W$_{K}$, we decided to acetylate both the Tyr and Lys reactive sites to inhibit formation of both product **1** and **2a/2b**. N-succinimidyl acetate was added to the H293W peptide in pH 9.0 phosphate buffer, and reacted at room temperature for 15 minutes, generating an acetylated peptide with an increase in molecular weight of 126 Da relative to the H293W peptide (a 42 Da increase on each Lys and the Tyr), with an m/z of 1825.87^{+1}/913.44^{+2}. This peptide will be notated as H293W$_{KY.}$ This peptide was purified by HPLC prior to use, and analyzed by LC-MS/MS on the Q-tof Premier. The MS/MS of peptide H293W$_{KY}$ is shown in Figure 4.16. The b1 ion has increased 42 Da compared to the original b1 ion in the H293W peptide (Figure 4.6), confirming acetylation on the N-terminal Lys residue. Likewise, the b3, b4, y10, and y11 ions confirm the acetylation of the Tyr residue, and the b13 ion confirms the acetylation of the C-terminal Lys.

The $H293W_{KY}$ peptide was dissolved in water to a concentration of 100 μM at pH 4.0, saturated with O_2, and irradiated at $\lambda = 254$ for 20 minutes. The resultant products were then analyzed by LC-MS/MS using the Q-tof Premier. Figure 4.17 shows the XIC of m/z 1825.87 for the control (Figure 4.17A) and irradiated sample (4.17B). Both chromatograms show the peak for the native peptide at 24.8 minutes. In the irradiated sample, the intensity of the native peak is reduced, but importantly, no isobaric product is observed. Clearly, the Tyr residue was involved in the formation of product **2a/2b**.

4.4 Discussion

In recent photo-oxidation studies, detection of double and triple His oxidation in the Fc region of IgG1 molecules was observed, motivating us to study the mechanism of such His oxidation using model peptides.[16] A common thread between the His oxidation products was the close proximity in primary sequence to a Trp residue. Since Trp is the most sensitive amino acid towards photodegradation,[26] we hypothesized that nearby Trp residues mediated the His oxidation via catalytic oxidation of water and generation of hydrogen peroxide.[27,28] Model peptides for His[293, HC] and His[318, HC] were synthesized to test this hypothesis. Synthesis of mutant model peptides with Ala residues instead of Trp residues were also studied. However, when the model peptides were irradiated, little His oxidation was detected on any of the model peptides. Only H318A, an Ala-containing model peptide was triply oxidized at the His residue. Interestingly, the H318A peptide contained no aromatic residues, whereas the H293A, H293W, and H318W peptides contained Tyr, Tyr and Trp, and Trp, respectively. In the model peptides H318W and H293W, the major oxidation products were Trp oxidation products. Since the only model peptide that was triply oxidized was an Ala-containing one, we cannot say that Trp was involved in the formation of the oxidized His in the model peptides, and most likely not involved

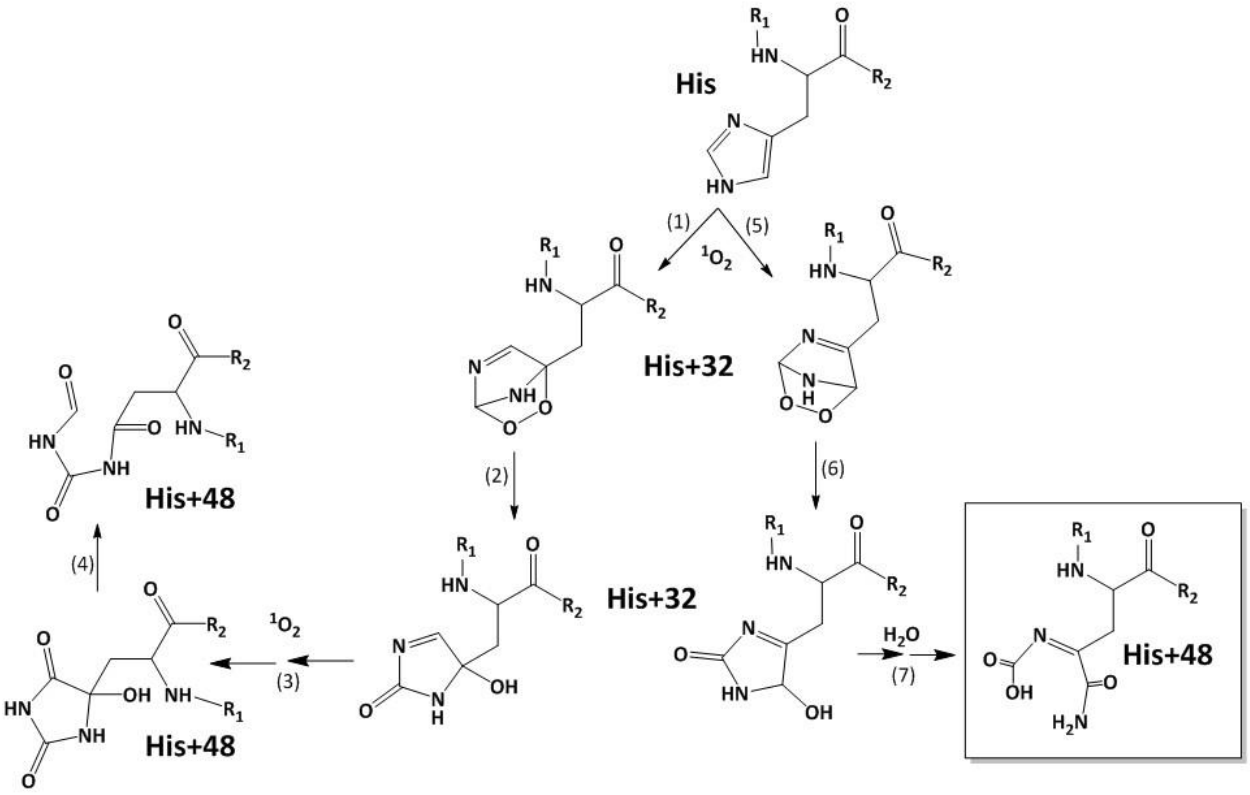

Scheme 4.2. Proposed mechanism for His oxidation products.

in mAb A either. Of course, the conformation of an antibody is much different than that of a model peptide. Most of the residues in small peptides are solvent exposed, whereas in a protein, residues can be buried and inert to oxidizing agents and light. In a protein, there are also many other residues that can quench the Trp excited state, such as Tyr, Phe, and the disulfide bond.[4,29,30] Since the Trp residues are exposed in the model peptides, Trp absorbs almost all of the light, generating most of the photoproducts so mechanistically, these model peptides were not appropriate to determine the mechanism of His oxidation in proteins. However, the MS/MS data of the oxidized H318A model peptide was helpful in determining the possible structure for the triply oxidized His products. The major ion in each spectrum was neither a b or y ion, but a doubly charged molecular ion with a neutral loss of water or ammonia. Another interesting observation in these spectra was the abundance of neutral losses on the y and b ions when the

oxidized His residue was contained in the sequence. These fragmentation patterns are indicative of free amines and carboxylic acids, generating more charged residues on the peptide. These two peptides do contain charged amino acids at pH 4.0 (K, D, E, H), but the non-oxidized peptides do not show many neutral fragments. Therefore, the oxidation of His must open up the imidazole ring, exposing free amines and carboxylic acids that are easily fragmented through gas-phase chemistry. In Scheme 4.2, a proposed photo-oxidative mechanism and structure of triply oxidized His is presented. Singlet oxygen initiates the oxidation of His, generating isomeric endo-peroxides on the imidazole ring (reactions 1 and 5).[22] These intermediates lead to the formation of a pair of hydroxylated imidazolones (reactions 2 and 6). In one pathway, water can then hydrolyze the amide bond on the hydroxyl imidazolone ring, cleaving it to yield a product with carboxylic and amide functions and an increase in molecular weight of 48 Da (reaction 7). This structure is a good candidate for the triply oxidized His product observed in our studies because both water or ammonia can easily be cleaved from the structure during gas phase MS fragmentation. Another pathway involves the oxidation of the hydroxyl imidazolone ring, generating a triply oxidized His with an intact ring (reaction 3). The hydroxyl group on the His $^{\gamma}$C will oxidize, opening the ring, yielding a ketone and free aldehyde on the triply oxidized His residue (reaction 4). The triply oxidized His resides generated from reactions 3 and 4 would not likely show neutral losses of ammonia or water, but likely losses of 28 Da from CO.

The highest yielding photoproduct observed in the H293W peptide, product **1**, was an isobaric product with the same m/z value as the native peptide, but eluting ca. 2 minutes ahead of the native, non-modified peptide in a separate peak (Figure 4.4A and 4.4B). The MS/MS of product **1** (Figure 4.7) was nearly identical to the MS/MS of the native peptide (Figure 4.6), except for the absence of the b1, b2, and b3 ions. Further structural characterization of product **1**

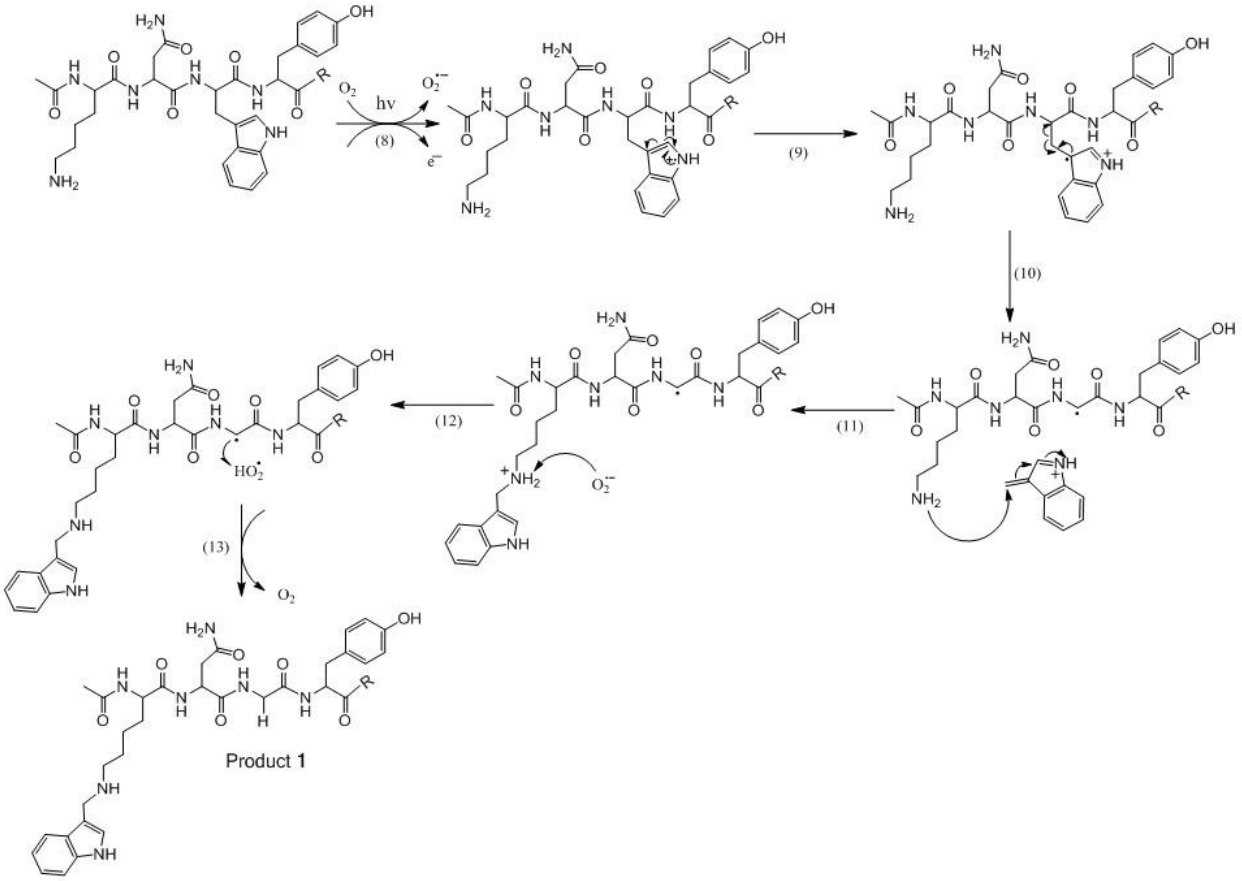

Scheme 4.3. Proposed mechanism for product **1** formation. 'R' represents the remaining amino acid sequence VDGVEVHNAK-Am.

was consistent with Trp side chain cleavage and abstraction of the resultant 3-methyleneindolenine (3-MEI) by the N-terminal Lys. Similar Trp side chain cleavages have been observed in IgG1[18] and the octreotide peptide, in which the 3-MEI was abstracted by a nearby Lys residue as well.[19] Alternative structures we explored for product **1** included the transformation of L- to D-Trp and the oxidation of Trp to Ky in addition to two crosslinks between the Ac-KNW region of the peptide. These structures were rejected after we observed the inability of trypsin to cleave the N-terminal Lys in product **1**, confirming the modification of both the Lys and Trp groups through the transformation of Trp to Gly and the abstraction of 3-MEI on the Lys amine (Figure 4.8). The proposed mechanism of product **1** generated through the photo-oxidation of the H293W peptide is presented in Scheme 4.3. Initially, upon photo-

oxidation, the Trp is photoionized to a Trp radical cation ($TrpNH^{+\bullet}$) while releasing an electron from its shell, which is quickly solvated by water (reaction 8). Ground state triplet oxygen is also reduced to a superoxide radical. The Trp radical then migrates to the $^{\gamma}C$ of the Trp residue (reaction 9), and further radical migration cleaves the $^{\alpha}C$-$^{\beta}C$ bond of the Trp residue, yielding a Glycyl radical and the free Trp side chain, i.e. 3-MEI (reaction 10). Due to its electrophilic nature, 3-MEI, is quickly abstracted by the nearby N-terminal Lys amine (reaction 11). The amine group is neutralized when the superoxide anion abstracts a proton from the Lys amine group (reaction 12), then the Glycyl radical is neutralized with the hydroperoxyl group (reaction 13), yielding the final product.

To inhibit the reaction of the N-terminal Lys with 3-MEI during irradiation, the reactivity of Lys was blocked by the addition of methyl groups on the Lys amines the $H293W_K$ peptide. The Lys groups were also methylated after irradiation of the H293W peptide to distinguish the m/z of product **1** with the methylated $H293W_K$ peptide since the N-terminal Lys in product **1** would be unable to react with the methylation reagents. Interestingly, in both sets of methylation experiments, isobaric products to the $H293W_K$ peptide were observed, product **2a/2b** (Figure 4.13). The MS/MS spectra of product **2a/2b** formed after irradiation of $H293W_K$ and irradiation of H293W followed by methylation were identical, hinting toward the Trp to Gly conversion product and Tyr abstraction of the resultant 3-MEI group (product **2a**) or a crosslink between the Trp and Tyr residues (product **2b**). However, from the MS/MS data for product **2a/2b**, we could not confirm the exact structure of the isobaric product. Until further experimentation is done, both possible structures for the Tyr involvement in product **2a/2b** have been presented, although there could be other possibilities. It was interesting that the product **2a/2b**, and not product **1**, was observed after irradiation of H293W, followed by methylation, because the N-terminal Lys-

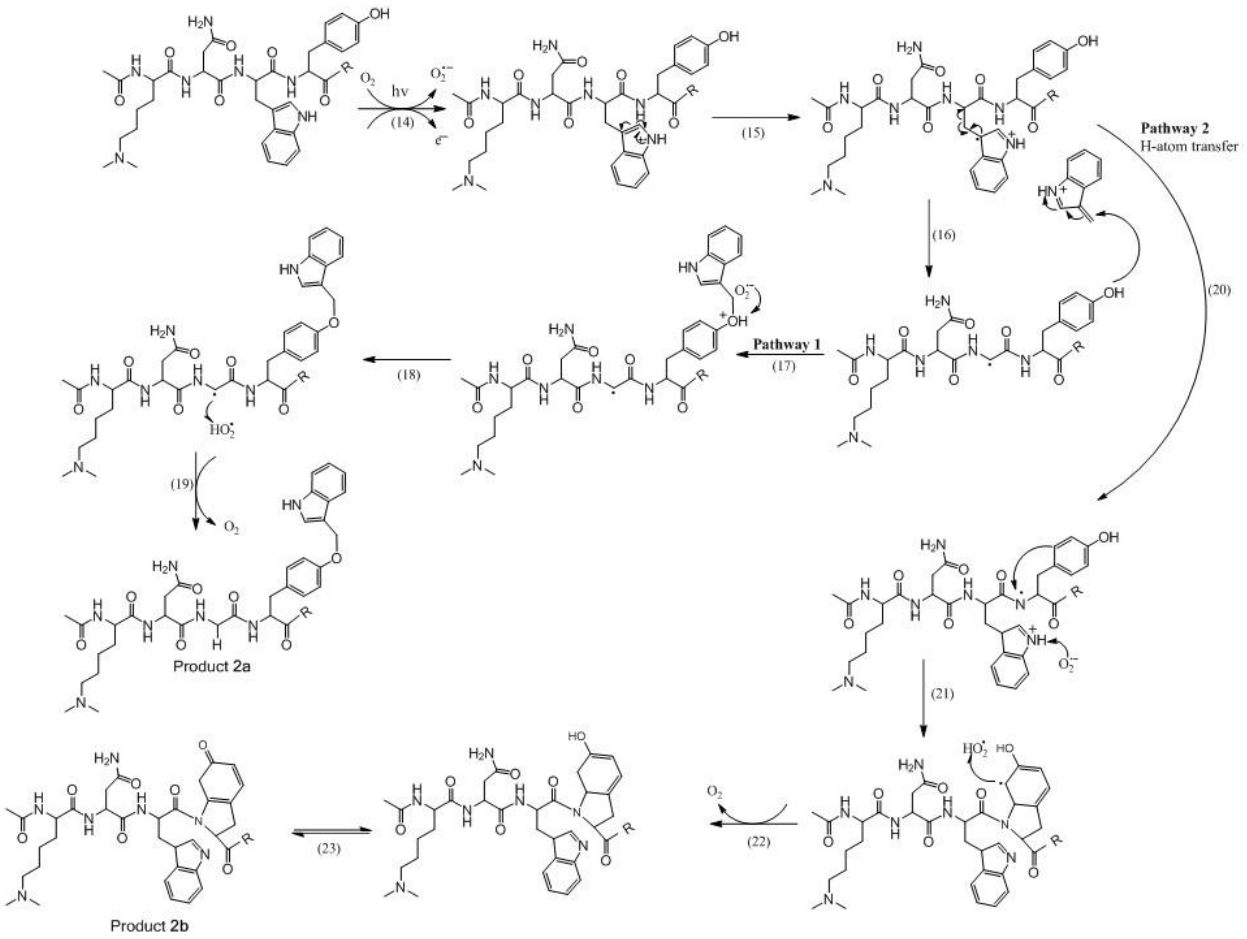

Scheme 4.4. Proposed mechanism for product **2a** and **2b** formation. 'R' represents the remaining amino acid sequence VDGVEVHNAK-Am.

3-MEI crosslink in product **1** should have rendered the Lys unavailable for methylation. One explanation for the absence of product **1** following the methylation of H293W after irradiation is that product **1** degraded during the reductive environment of the methylation process, whereas product **2a/2b** did not. Chymotryptic digest of product **2a/2b** confirmed the Tyr involvement in the product because the enzyme did not recognize the Tyr, thereby not cleaving C-terminal to the Tyr residue like it had in the control H293W$_K$ peptide (Figure 4.15).

In Scheme 4.4, the proposed reaction mechanisms of product **2a** and **2b** are shown. In Pathway 1, the mechanism for the Tyr-Trp side chain product is presented, product **2a**, and in Pathway 2, the mechanism for a Tyr side chain-backbone cyclization product, product **2b** is

presented. Both pathways are initiated in the same way as product **1** formation as shown in Scheme 4.3: Trp photoionization (reaction 14) and radical migration to the $^{\gamma}$C of the Trp residue (reaction 15). From there, Pathway 1 shows the cleavage of the $^{\alpha}$C-$^{\beta}$C bond of the Trp residue, yielding a Glycyl radical and the free Trp side chain, 3-MEI (reaction 16). However, instead of the N-terminal Lys abstracting 3-MEI as was the case in product **1**, the Tyr hydroxyl group reacts with it (reaction 17). The newly formed ether bond with the Tyr hydroxyl group is neutralized when the superoxide anion abstracted the extra proton (reaction 18), then the Glycyl radical is neutralized with the hydroperoxyl group (reaction 19), yielding product **2a**, a Tyr-3-MEI crosslink. In Pathway 2, the Trp side chain is not cleaved, but following the radical migration of the radical to the $^{\gamma}$C of the Trp residue (reaction 15), the Tyr amide nitrogen abstracts the C-centered radical from the Trp (reaction 20). Then, a crosslink between hydroxyphenyl side chain and the nitrogen forms, creating an indole heterocycle and C-centered radical on the hydroxyphenyl ring (reaction 21) that is stabilized through resonance with the hydroxyl group (not shown). The superoxide anion also abstracts the proton from the Trp cation to form the hydroperoxyl radical and neutralize the Trp residue. The C-centered radical abstracts an H-atom from the hydroperoxyl radical (reaction 22), creating product **2b**, which can isomerize from the enol to keto form (reaction 23).

Interestingly, the formation of products **1**, **2a** and **2b** all rely on reactive oxygen species (superoxide and hydroperoxyl radicals) as reducing agents, but Trp to Gly hydroperoxide was not detected. These Trp side chain cleavage products were only observed in one Trp-containing peptide, H293W, and not H318W, highlighting the importance of protein conformation on protein stability and photoproduct formation. The H293W peptide contained nucleophilic Lys

and Tyr residues in close proximity to the Trp residue, whereas the H318W peptide did not contain any nucleophilic amino acids in close proximity.

4.5 Conclusion

A triply oxidized His residue was detected after photo-oxidation studies in an Ala-containing peptide modeled after a tryptic peptide found in the Fc region of IgG1 molecules. Although the oxidation of His is a small degradation product, the oxidation could affect the overall stability and efficacy of the IgG1, and if the His ring is opened upon oxidation, nucleophilic residues are exposed for protein aggregation. Interestingly, in a Trp-containing peptide, the Trp side chain was photolytically cleaved and trapped by a neighboring Lys residue, and when the Lys residue was methylated to block reactivity, the neighboring Tyr residue was involved in the reaction. If the Trp side chains in proteins are cleaved, there are many possible nucleophilic amino acids nearby that could trap the side chain. This could lead to protein instability or lowered efficacy if the Trp or the Trp side chain trapping residue is involved in antigen binding or receptor recognition. This work also highlights the significant conformational differences between model peptides and proteins, and the importance of light stress studies in both systems to understand protein stability and mechanistic details.

4.6 References

1. Davies, M. J., The oxidative environment and protein damage. *Biochim Biophys Acta* **2005,** *1703* (2), 93-109.
2. Li, S.; Schöneich, C.; Borchardt, R. T., Chemical instability of protein pharmaceuticals: Mechanisms of oxidation and strategies for stabilization. *Biotechnol Bioeng* **1995,** *48* (5), 490- 500.
3. Manning, M. C.; Patel, K.; Borchardt, R. T., Stability of protein pharmaceuticals. *Pharm Res* **1989,** *6* (11), 903-18.
4. Kerwin, B. A.; Remmele, R. L., Jr., Protect from light: photodegradation and protein biologics. *J Pharm Sci* **2007,** *96* (6), 1468-79.
5. Agon, V. V.; Bubb, W. A.; Wright, A.; Hawkins, C. L.; Davies, M. J., Sensitizer-mediated photooxidation of histidine residues: evidence for the formation of reactive side-chain peroxides. *Free Radic Biol Med* **2006,** *40* (4), 698-710.
6. Beck, A.; Wagner-Rousset, E.; Ayoub, D.; Van Dorsselaer, A.; Sanglier-Cianferani, S., Characterization of therapeutic antibodies and related products. *Anal Chem* **2013,** *85* (2), 715-36.
7. Wei, Z.; Feng, J.; Lin, H. Y.; Mullapudi, S.; Bishop, E.; Tous, G. I.; Casas-Finet, J.; Hakki, F.; Strouse, R.; Schenerman, M. A., Identification of a single tryptophan residue as critical for binding activity in a humanized monoclonal antibody against respiratory syncytial virus. *Anal Chem* **2007,** *79* (7), 2797-805.
8. Chumsae, C.; Gaza-Bulseco, G.; Sun, J.; Liu, H., Comparison of methionine oxidation in thermal stability and chemically stressed samples of a fully human monoclonal antibody. *J Chromatogr B Analyt Technol Biomed Life Sci* **2007,** *850* (1-2), 285-94.

9. Qi, P.; Volkin, D. B.; Zhao, H.; Nedved, M. L.; Hughes, R.; Bass, R.; Yi, S. C.; Panek, M. E.; Wang, D.; Dalmonte, P.; Bond, M. D., Characterization of the photodegradation of a human IgG1 monoclonal antibody formulated as a high-concentration liquid dosage form. *J Pharm Sci* **2009,** *98* (9), 3117-30.

10. Wang, W.; Vlasak, J.; Li, Y.; Pristatsky, P.; Fang, Y.; Pittman, T.; Roman, J.; Wang, Y.; Prueksaritanont, T.; Ionescu, R., Impact of methionine oxidation in human IgG1 Fc on serum half-life of monoclonal antibodies. *Mol Immunol* **2011,** *48* (6-7), 860-6.

11. Bertolotti-Ciarlet, A.; Wang, W.; Lownes, R.; Pristatsky, P.; Fang, Y.; McKelvey, T.; Li, Y.; Drummond, J.; Prueksaritanont, T.; Vlasak, J., Impact of methionine oxidation on the binding of human IgG1 to Fc Rn and Fc gamma receptors. *Mol Immunol* **2009,** *46* (8-9), 1878-82.

12. Luo, Q.; Joubert, M. K.; Stevenson, R.; Ketchem, R. R.; Narhi, L. O.; Wypych, J., Chemical modifications in therapeutic protein aggregates generated under different stress conditions. *J Biol Chem* **2011,** *286* (28), 25134-44.

13. Chang, S. H.; Teshima, G. M.; Milby, T.; Gillece-Castro, B.; Canova-Davis, E., Metal-catalyzed photooxidation of histidine in human growth hormone. *Anal Biochem* **1997,** *244* (2), 221-27.

14. Hovorka, S. W.; Hong, J.; Cleland, J. L.; Schöneich, C., Metal-catalyzed oxidation of human growth hormone: modulation by solvent-induced changes of protein conformation. *J Pharm Sci* **2001,** *90* (1), 58-69.

15. Zhao, F.; Ghezzo-Schöneich, E.; Aced, G. I.; Hong, J.; Milby, T.; Schöneich, C., Metal-catalyzed oxidation of histidine in human growth hormone. Mechanism, isotope effects, and inhibition by a mild denaturing alcohol. *J Biol Chem* **1997,** *272* (14), 9019-29.

16. Amano, M.; Kobayashi, N.; Yabuta, M.; Uchiyama, S.; Fukui, K., Detection of histidine oxidation in a monoclonal immunoglobulin gamma (IgG) 1 antibody. *Anal Chem* **2014,** *86* (15), 7536-43.

17. Liu, M.; Zhang, Z.; Cheetham, J.; Ren, D.; Zhou, Z. S., Discovery and characterization of a novel photo-oxidative histidine-histidine crosslink in IgG1 antibody utilizing ^{18}O-labeling and mass spectrometry. *Anal Chem* **2014**.

18. Haywood, J.; Mozziconacci, O.; Allegre, K. M.; Kerwin, B. A.; Schöneich, C., Light-induced conversion of Trp to Gly and Gly hydroperoxide in IgG1. *Mol Pharm* **2013,** *10* (3), 1146-50.

19. Mozziconacci, O.; Schöneich, C., Effect of conformation on the photodegradation of Trp- and cystine-containing cyclic peptides: octreotide and somatostatin. *Mol Pharm* **2014,** *11* (10), 3537-46.

20. Rayment, I., Reductive alkylation of lysine residues to alter crystallization properties of proteins. *Methods Enzymol* **1997,** *276*, 171-179.

21. Abello, N.; Kerstjens, H. A.; Postma, D. S.; Bischoff, R., Selective acylation of primary amines in peptides and proteins. *J Proteome Res* **2007,** *6* (12), 4770-6.

22. Tomita, M.; Irie, M.; Ukita, T., Sensitized photooxidation of histidine and its derivatives. Products and mechanism of the reaction. *Biochemistry* **1969,** *8* (12), 5149-60.

23. Ranganathan, S.; Ranganathan, D.; Bhattacharyya, D., The transformation of tryptophan to aspartic acid in peptides. *Journal of the Chemical Society, Chemical Communications* **1987,** (14), 1085-1086.

24. Murray Kermit, K.; Boyd Robert, K.; Eberlin Marcos, N.; Langley, G. J.; Li, L.; Naito, Y., Definitions of terms relating to mass spectrometry (IUPAC Recommendations 2013). In *Pure and Applied Chemistry*, 2013; Vol. 85, p 1515.

25. Gross, J. H., *Mass Spectrometry: A Textbook*. 1st ed.; Springer-Verlag: Berlin, 2004.

26. Creed, D., The photophysics and photochemistry of the near-UV absorbing amino-acids .I. Tryptophan and its simple derivatives. *Photochem Photobiol* **1984,** *39* (4), 537-562.

27. Wentworth, P., Jr.; Jones, L. H.; Wentworth, A. D.; Zhu, X.; Larsen, N. A.; Wilson, I. A.; Xu, X.; Goddard, W. A., 3rd; Janda, K. D.; Eschenmoser, A.; Lerner, R. A., Antibody catalysis of the oxidation of water. *Science* **2001,** *293* (5536), 1806-11.

28. Sreedhara, A.; Lau, K.; Li, C.; Hosken, B.; Macchi, F.; Zhan, D.; Shen, A.; Steinmann, D.; Schöneich, C.; Lentz, Y., Role of surface exposed tryptophan as substrate generators for the antibody catalyzed water oxidation pathway. *Mol Pharm* **2013,** *10* (1), 278-88.

29. Prompers, J. J.; Hilbers, C. W.; Pepermans, H. A., Tryptophan mediated photoreduction of disulfide bond causes unusual fluorescence behaviour of Fusarium solani pisi cutinase. *FEBS Lett* **1999,** *456* (3), 409-16.

30. Vanhooren, A.; Devreese, B.; Vanhee, K.; Van Beeumen, J.; Hanssens, I., Photoexcitation of tryptophan groups induces reduction of two disulfide bonds in goat alpha-lactalbumin. *Biochemistry* **2002,** *41* (36), 11035-43.

4.7 Appendix C

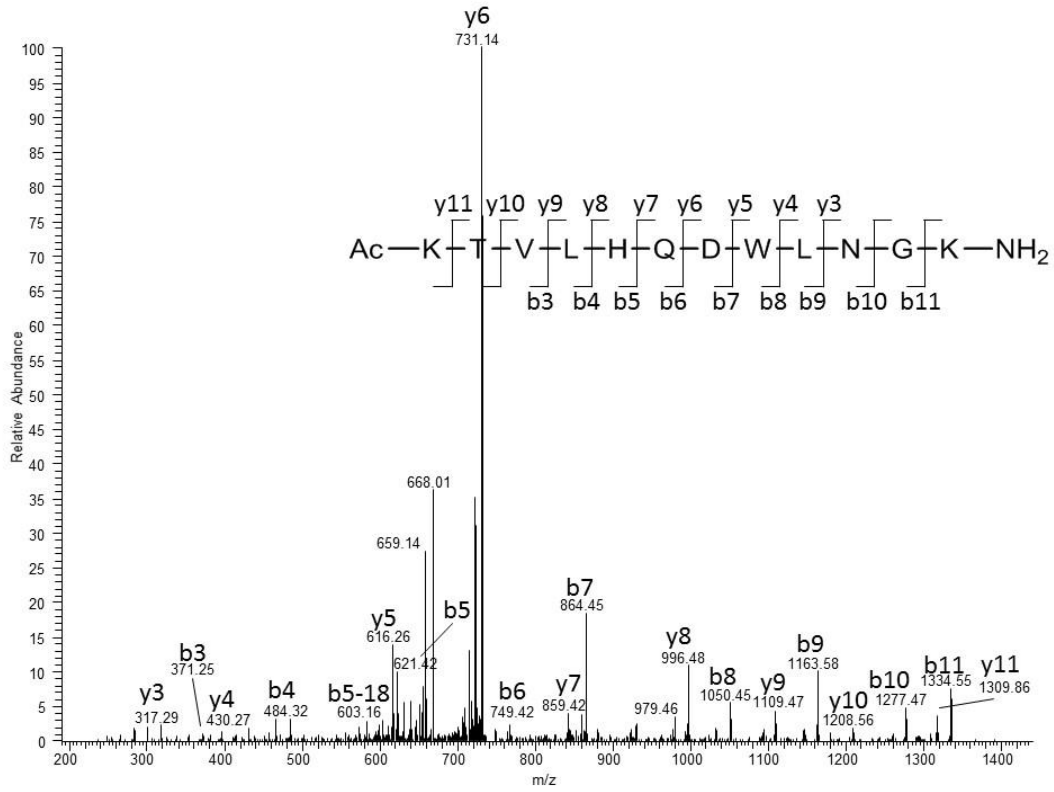

Figure C.1. MS/MS of the control H318W model peptide.

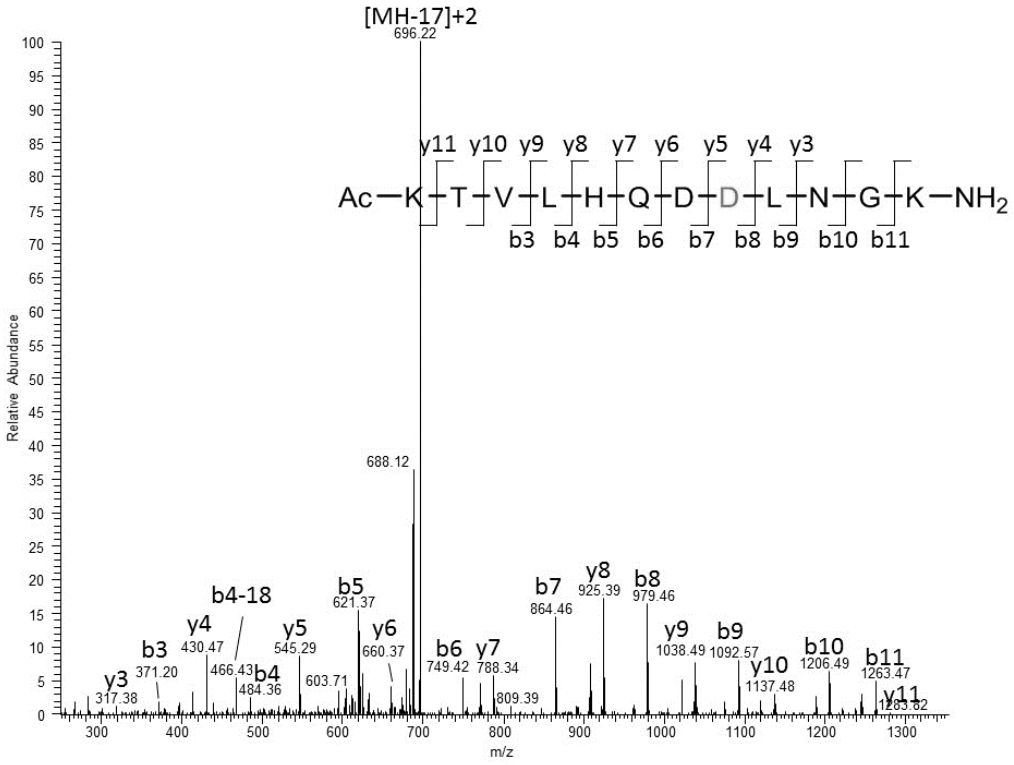

Figure C.2. MS/MS of the Trp to Asp conversion product after irradiation of the H318W model peptide at λ = 254 nm in water at pH 4.0.

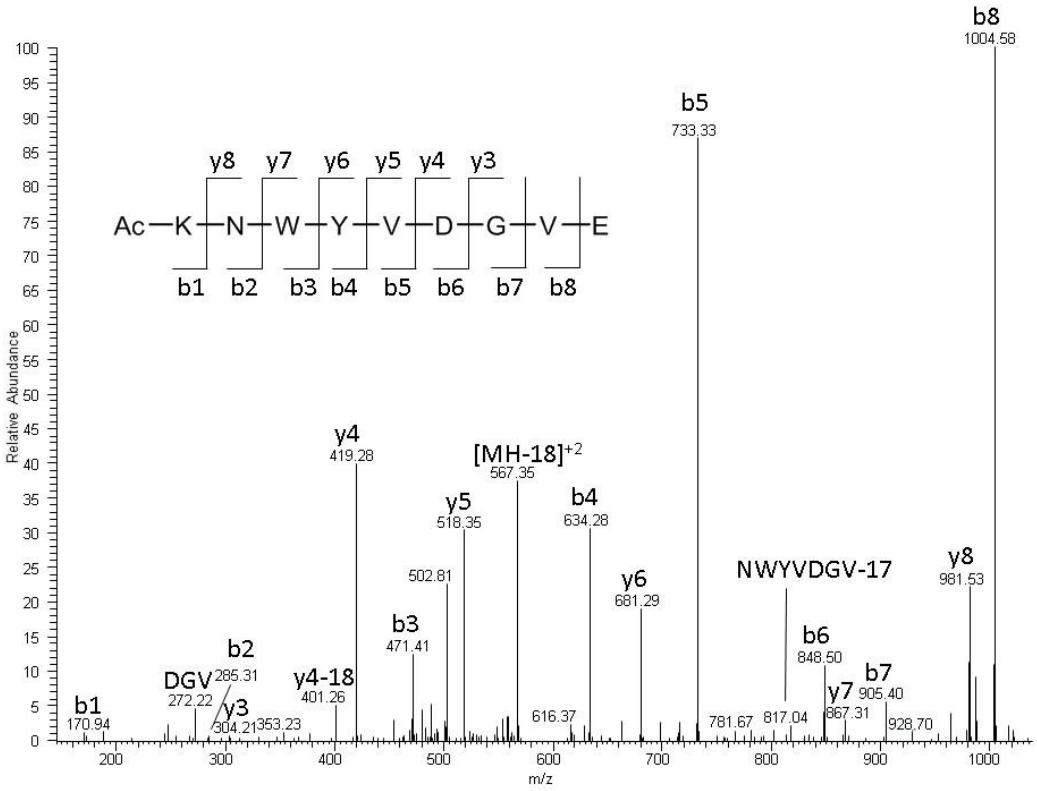

Figure C.3. MS/MS of the control H293W model peptide after Glu-C digestion.

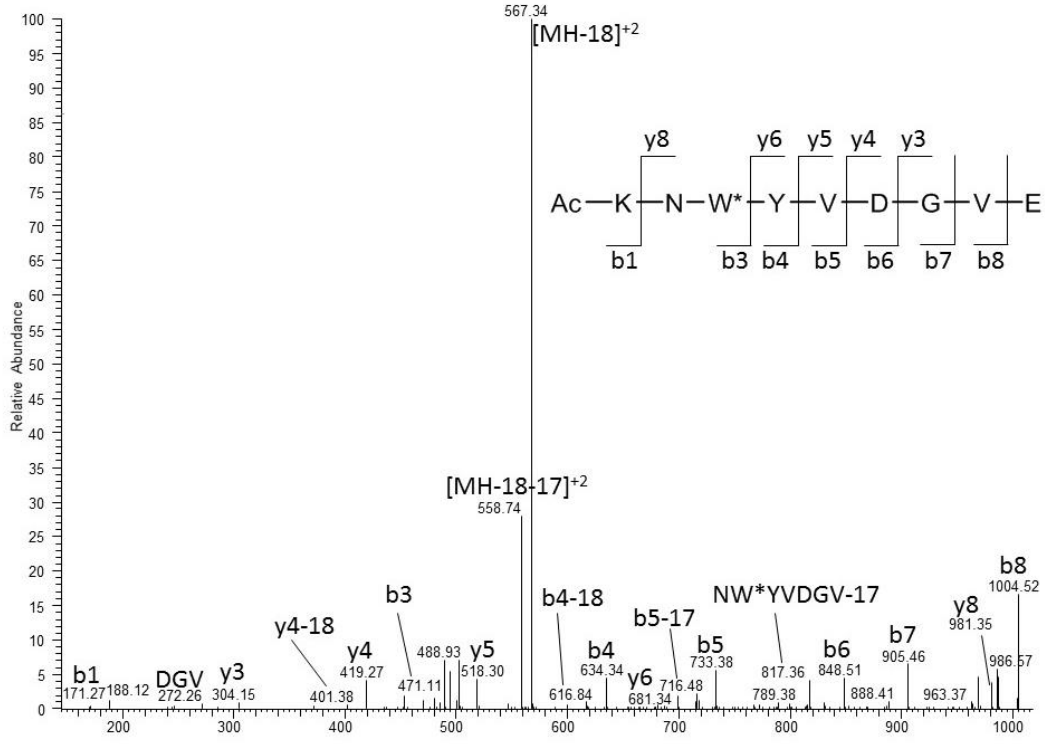

Figure C.4. MS/MS of the isobaric product, product **1**, after Glu-C digestion. This product was formed during the irradiation of the H293W model peptide at λ = 254 nm in water at pH 4.0.

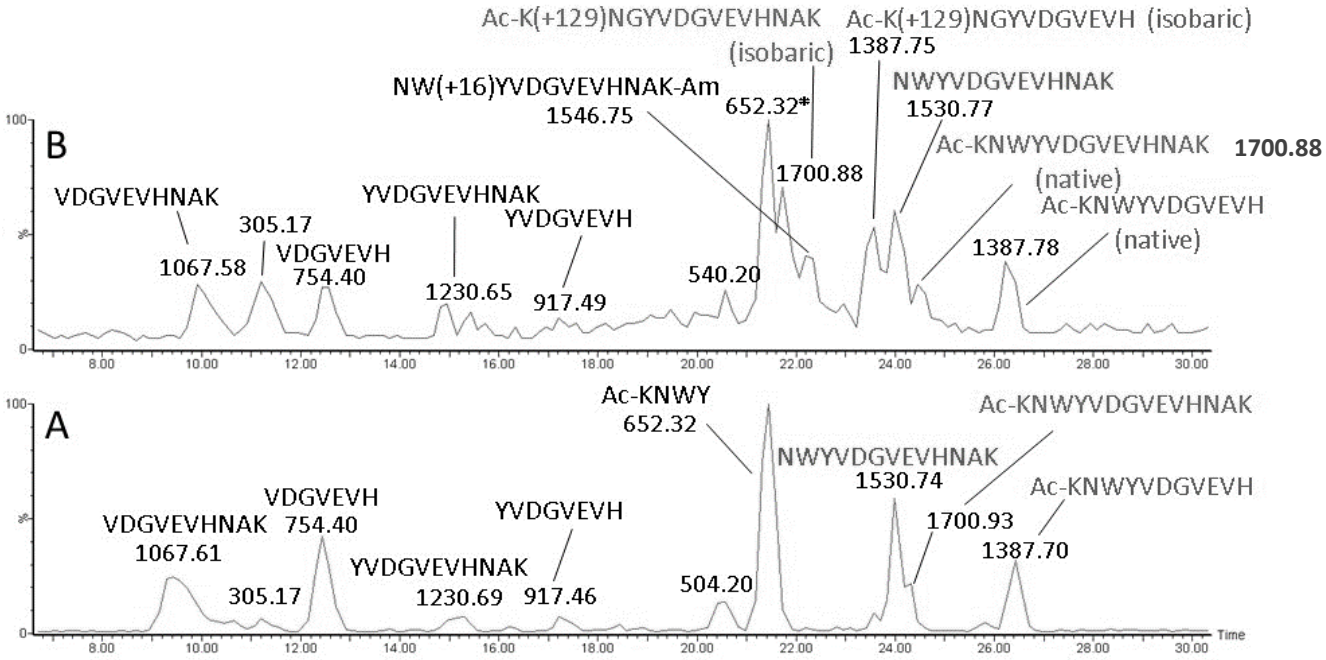

Figure C.5. LC-MS of the H293W tryptic digest (using the Sigma -Aldrich trypsin) in the (A) control (non-irradiated) and (B) irradiated samples after irradiation of 100 μM H293W at λ = 254 nm in water at pH 4.0.

Surprisingly, along with tryptic peptides, many chymotryptic peptides were also observed during the tryptic digest using the Sigma-Aldrich trypsin. The two tryptic peptides observed in the control H293W peptide (Figure C.5A) were the single (24.5 minutes) and double (21.5 minutes) C-terminal cleavage of the Lys residue: Ac-KNWYVDGVEVHNAK and NWYVDGVEVHNAK, respectively. The rest of the peptides observed in the chromatogram were chymotryptic peptides, created by the C-terminal cleavage of the Trp, Tyr, and His residues. In fact, the largest peak in the chromatogram was the chymotryptic peptide Ac-KNWY, eluting at 21.5 minutes. The tryptic digest of the irradiated H293W sample contained new peaks, in addition to those observed in the control (Figure C.5B). For instance, the tryptic fragment of the oxidized Trp residue was observed at 22.5 minutes, but was not present in the control. Two peaks with the same m/z value appeared in the irradiated sample: m/z 1700.88 at 21.5 minutes and 24.5 minutes and m/z 1387.78 at 23.5 minutes and 26.5 minutes. The peaks at 24.5 and 26.5 minutes were observed in the control, however, the other two peaks were not, and therefore, were related to the digest of the isobaric product, product **1**. Interestingly, the tryptic digest peak observed at 24.5 minutes in the control that did not contain the N-terminal Lys (NWYVDGVEVHNAK) was observed in the irradiated sample only once, not twice. The absence of the second NWYVDGVEVHNAK peak belonging to the isobaric peptide **1** provides evidence that in the isobaric product, the Lys amine group is attached to the Trp side chain, and trypsin was unable to recognize this Lys as a substrate. Unfortunately, the N**G**YVDGVEVHNAK peptide was not observed in this LC-MS. Another interesting product in Figure C.5B eluted at 21.5 minutes, and just like the peak in Figure C.5A, contained the m/z value 652.32 matching the Ac-KNWY peptide. However, the MS/MS fragmentation of this product did not match that of Ac-KNWY, but contained the y fragment ions from the peptide YVDGVEVHNAK, but no b ions. We suspect this peak may contain multiple products, but since the MS^E method was used, it was difficult to distinguish the fragmentation ions between multiple products.

Chapter 5. Conclusions and future directions

5.1 Summary and conclusions

Protein therapeutics are often more effective against a variety of diseases than small molecule drugs because of their superior efficiency and affinity toward their targets.[1,2] However, proteins such as monoclonal antibodies are still sensitive to a number of chemical and physical instabilities such as oxidation and photochemical degradation that hinders their ability to be used as commercial drugs for safety and efficacy concerns.[3] These degradation pathways could enhance immunogenicity or cause inactivation.[4,5] Therefore, to increase the stability of these antibodies, an understanding of their mechanisms of degradation is necessary. In proteins, two of the most light-sensitive amino acids are Trp and the disulfide bond, and proteins, such as monoclonal antibodies, contain multiple disulfides and Trp residues important in maintaining their structure and function.[6] Therefore, the aim of this dissertation project was to further investigate protein stability in proteins and model peptides containing Trp and/or disulfide bonds to help elucidate novel mechanisms of protein degradation to lead to a greater understanding of protein stability.

Chapter 2 details the reactions of the disulfide-containing peptides (LG**V**C**V**GL)$_2$, in which the Val residues displayed natural C-isotope distribution or were uniformly ^{13}C labeled at either the i+1 or i-1 position. Our results demonstrated that the photolytically or radically initiated thiyl radicals reacted with the Val residues as had been observed in previous model peptides such as (GGCGGL)$_2$ and (LGACAGL)$_2$ to form dehydroamino acids. Interestingly, thiyl radicals also entered a new pathway not observed before, forming an isothiazole-3(2H)-one product in a 90% yield after 1 minute of irradiation. The formation of this product is likely the result of steric

constraints from the bulky Val residues, disfavoring *inter*molecular reactions for *intra*molecular reactions with thiyl radicals.

Chapter 3 elucidates a mechanism for the photolytic Trp side chain cleavage and transformation of Trp into Gly and/or Gly hydroperoxide. These reaction products were observed in three locations on the IgG1 molecule studied and three Trp and disulfide-containing model peptide systems. In the IgG1, each affected Trp residue was in close proximity to a disulfide bond, highlighting the importance of Trp and disulfide interactions to form this modification. The reaction mechanism was proposed to be initiated by Trp radical cation formation, followed by $^{\alpha}C$-$^{\beta}C$ cleavage of the Trp side chain, resulting in a glycyl radical reduced to Gly by H-atom transfer from thiol residues or Gly hydroperoxide by oxygen.

Chapter 4 identifies a novel triply oxidized His residue in an IgG1 molecule and a model peptide, and characterizes the photo-oxidative Trp side chain cleavage in the absence of a disulfide in a Trp-containing model peptide. Chapter 3 hypothesizes that H-atom transfer from Cys thiol residues is important in reducing the Trp to Gly, however, in a Trp-containing model peptide with no Cys residues, the Trp side chain was cleaved, and a nearby Lys residue abstracted it. Interestingly, another reaction pathway was also observed when the Lys residues were methylated, where the Tyr residue abstracted the Trp side chain.

The Cys crosslinks and Trp cleavage products highlight the damage light exposure can have by not only inducing significant amino acid modifications, but also modifications that could lead to protein aggregation or amino acid hydroperoxides that have the potential to induce

additional protein oxidation. The products identified and reaction schemes proposed have given us greater understanding of protein stability towards reactive thiyl and Trp radical cations generated photolytically.

5.2 Future directions

For the photolytically generated reaction products we observed in IgG1 and the model peptides, it would be interesting to examine their biological activity and effect on protein efficacy and/or safety, since that is what is ultimately important in the pharmaceutical industry. If we did see lowered biological activity or increased immunogenicity in IgG1, it would be difficult to deduce which protein modifications were the root cause. However, with peptides, we can easily collect and purify the modified peptides for biological testing.

Interestingly, some of our photoproducts contained dehydroamino acids and heterocycles, such as the isothiazol-3(2H)-one. Many antimicrobial peptides and peptide derivatives have unique modifications that increase their potency and activity, such as dehydroamino acids, D-amino acids, and heterocyclic moieties, and it is reported that peptide backbones can cyclize to heterocycles via synthetic pathways.[7] For example, penicillin and cephalosporin, common small molecule drugs with peptide characteristics, are both comprised of sulfur-containing heterocycles. Our work to discover novel protein modifications via photolysis could fill the niche as a simple and efficient method to modify amino acids to be used as starting materials for antimicrobial peptides. Importantly, the development of new antimicrobial peptides is vital because bacterial resistance has become a widespread problem.

5.3 References

1. Dingermann, T., Recombinant therapeutic proteins: production platforms and challenges. *Biotechnol J* **2008,** *3* (1), 90-7.
2. Carter, P. J., Introduction to current and future protein therapeutics: a protein engineering perspective. *Exp Cell Res* **2011,** *317* (9), 1261-9.
3. Wang, W.; Singh, S.; Zeng, D. L.; King, K.; Nema, S., Antibody structure, instability, and formulation. *J Pharm Sci* **2007,** *96* (1), 1-26.
4. Wei, Z.; Feng, J.; Lin, H. Y.; Mullapudi, S.; Bishop, E.; Tous, G. I.; Casas-Finet, J.; Hakki, F.; Strouse, R.; Schenerman, M. A., Identification of a single tryptophan residue as critical for binding activity in a humanized monoclonal antibody against respiratory syncytial virus. *Anal Chem* **2007,** *79* (7), 2797-805.
5. Jiskoot, W.; Randolph, T. W.; Volkin, D. B.; Middaugh, C. R.; Schöneich, C.; Winter, G.; Friess, W.; Crommelin, D. J.; Carpenter, J. F., Protein instability and immunogenicity: roadblocks to clinical application of injectable protein delivery systems for sustained release. *J Pharm Sci* **2012,** *101* (3), 946-54.
6. Kerwin, B. A.; Remmele, R. L., Jr., Protect from light: photodegradation and protein biologics. *J Pharm Sci* **2007,** *96* (6), 1468-79.
7. Walsh, C. T.; Nolan, E. M., Morphing peptide backbones into heterocycles. *Proc Natl Acad Sci U S A* **2008,** *105* (15), 5655-6.